Polymer Support Fluids in Deep Foundations

Daniel P. McNamara

Hertford College

Department of Engineering Science



A thesis submitted for the degree of

Doctor of Philosophy

Michaelmas 2025

This thesis is dedicated to my parents who inspire me every day,

my brothers who regale me always,

and Dena who offered unwavering support throughout.

Abstract

In the mid-20th century, engineers began using clay slurries to support unstable soils during excavation, with bentonite quickly becoming the industry standard. Despite the drawbacks of bentonite use, such as being an over-exploited resource and a threat to marine life, polymer fluids experienced only sporadic use due to associated failures. These failures can be largely attributed to the intrinsic differences in flow mechanisms between the fluids, combined with a conservation of management methods between them. Growing interest in alternatives has led contractors to reconsider polymer fluids. This research aims to improve the management of these fluids and advance the understanding of the processes in soils that occur when polymer fluids are used for excavation support.

To improve fluid management, two test procedures were developed. The American Petroleum Institute (API) filter press test highlighted flow behaviour differences between bentonite and polymer fluids, revealing its potential as a rapid indicator of fluid flow behaviour in soils. A second test, using a simple falling-ball apparatus, examined viscosity heterogeneity, showing that polymer molecules form localised high-viscosity networks that significantly influence the bulk characteristics of the fluid. These findings led to recommendations for managing polymer fluids on-site and in the laboratory.

To understand flow processes in soils, a bespoke permeameter was designed and developed to investigate the flow of polymer fluids in sands. The tests confirmed a clogging mechanism with some polymer systems and provided insights into how the behaviour of the fluid changes with key parameters such as polymer type, sand grading, and the influence of additives. This investigation establishes a comprehensive understanding of the flow mechanics of polymer fluids in sands, creating a significant database for numerical modelling.

Finally, oedometer and direct shear testing were undertaken to advance understanding of soil-polymer fluid interactions. Contrary to on-site observations of reduced soil softening with polymer fluid exposure, the oedometer tests indicated that exposure to these fluids caused greater absorption than exposure to water. This suggests that the polymer molecules may be acting as a binder.

Shear testing indicated that polymers can significantly increase the shear strength of nor-

mally consolidated clays in comparison to exposure to water. In over-consolidated clays, however, the choice of fluid was less critical, with comparable shear strengths across water, bentonite, and polymer.

The results of this project have improved the management capabilities of the fluid, uncovered unknown behaviours of the fluid, and provided an extensive dataset to inform design of foundations formed with polymer fluids.

Acknowledgements

Firstly, a thank you to Professor Brian Sheil. Brian brought me to Oxford to undertake research alongside some of the world's most brilliant engineers and people. His dynamic enthusiasm was crucial to the success of the project. The project greatly benefited from his driven and goal-oriented nature, from his ability to fix persistent LabVIEW issues, to his unrivalled rate of digestion and review of all written work. Cambridge has gained an incredible engineer and mentor.

Every conversation with Professor Stephan Jefferis provided new knowledge both on and off the topic of my research, and clarified the necessities of the current problem I faced. Stephan's generosity in time and shared expertise are gifts I can never repay. His guidance has been completely invaluable, and I am extraordinarily grateful for the opportunity to work with him. Amidst the many challenges of a doctoral project, I could always rely on Stephan as a source of sage advice and moral support. I am eternally grateful for his support over the past few years.

I thank Arup for their financial and technical support of this project. In particular, I want to thank Chris Barker and Duncan Nicholson. Their enthusiasm and interest, along with the arrangement of site visits and sample collections, ensured the project successfully bridged the gap between academia and industry. This collaboration enabled the work to impact industry practice and prevented it from being lost on the many shelves of Oxford.

I also thank the Department of Engineering Science and Hertford College for their technical and welfare support. Additionally, I thank Professor Chris Martin for facilitating the project's continuation following Brian's departure. Thanks also go to Professor Orestis Adamidis and Professor Chris MacMinn for their input and assessment of the research.

A special thank you goes to Dr Alex Swallow for his camaraderie and the friendly competition he provided in the lab over the years. The conferences to Cambridge and Vietnam are cherished memories, and I am sure the regular pub trips will continue for many years to come. I thank Bryn Phillips for welcoming me into the lab, offering advice, and providing guidance on the permeameter and filter press testing. I am grateful to Clive Baker for his outstanding effort in the lab; his attention to detail and high standards of workmanship were invaluable. I also thank Alison May, who ensured prompt arrangement of all necessary materials, travel,

and administration.

Thank you to all my colleagues in the engineering department. Rachel Keane always offered moral support, advice, and the effortless ability to foster a sense of community. Thomas and Tim, whose humorous antics and conversation over tea and crumpets provided much-needed respite from data analysis and writing. Thank you also to the rest of the Fun Lunch crew, who brought joy to every day in the office. I thank the Hertford Gang (Daniel, Drew, Gerwin, Julia, Marie, Pip, and Renee) for all their support and friendship over the years. These are friendships I will hold dear forever. I am grateful to my friends back in London, the CBs, who kept me entertained from a distance and always welcomed me back with open arms.

Finally, and most significantly, thank you to my immediate family (Andrew, Lorraine, Sam McNamara, Robert Purnell, and Dena Severo) and my extended family. A support network as robust as mine made this project possible; thank you for always being there for me.

Contents

1 Introduction **16**

1.1 Background . . . 16

1.2 Problem statement . . . 18

1.3 Research question and objectives . . . 19

1.4 Research dissemination . . . 20

1.5 Thesis structure . . . 21

2 Literature review **22**

2.1 Introduction . . . 22

2.2 Chemistry . . . 24

2.3 Rheology . . . 26

2.3.1 The power law model . . . 28

2.3.2 The Carreau model . . . 28

2.4 Sorption . . . 29

2.5 Laboratory investigations . . . 30

2.6 Filtration behaviour . . . 30

2.7 Shear resistance and excavation face . . . 33

2.8 Summary and gaps in knowledge . . . 35

3 An investigation of the behaviour of polymer fluids in the American Petroleum Institute filter press **37**

3.1 Introduction . . . 37

3.2 Materials and methods . . . 38

3.2.1 API test apparatus and procedure . . . 38

3.2.2 Tested polymers . . . 39

3.2.3 Polymer fluid preparation . . . 40

3.2.4 Bentonite slurry benchmarking . . . 41

3.2.5 Viscosity measurement . . . 41

3.2.6 Scope of testing . . . 41

3.3 Results . . . 44
3.3.1 Exemplar results and comparisons to bentonite behaviour . . . 44
3.3.2 Utility of the API filter press for the assessment of polymer fluids . . . 45
3.4 Parametric study . . . 48
3.4.1 Influence of polymer type . . . 48
3.4.2 Xanthan testing . . . 49
3.4.3 Influence of concentration . . . 50
3.4.4 Repeated passing through a filter paper . . . 51
3.4.5 Viscosity measurement with the IKA and Fann viscometers . . . 52
3.4.6 Effect of filter paper pore size . . . 53
3.4.7 Effect of applied pressure . . . 54
3.5 Apparent viscosity and shear rate . . . 56
3.6 Pore diameter from intrinsic permeability . . . 58
3.7 Implications for current practice . . . 60
3.8 Summary . . . 61

4 An investigation of heterogeneity in polymer fluids and its impact on civil engineering applications 63

4.1 Introduction . . . 63
4.2 Theory and method . . . 64
4.2.1 Theoretical overview . . . 64
4.2.2 Polymer fluid preparation . . . 65
4.2.3 Testing programme . . . 66
4.2.4 Experimental setup . . . 67
4.3 Investigation of heterogeneity within a column of polymer fluid . . . 68
4.3.1 Specimen test results . . . 68
4.3.2 Verification testing . . . 69
4.3.3 Lateral movement . . . 70
4.3.4 Drop height . . . 71
4.3.5 Polymer dissolution . . . 71
4.3.6 The effect of standing time on viscosity development . . . 72

4.3.7 Rotational viscometry . . . 73
4.3.8 Influence of de-airing on viscosity development . . . 75
4.3.9 Effect of mechanical shear on polymer viscosity . . . 77
4.3.10 Influence of polymer concentration . . . 80
4.3.11 Concentration and polymer molecular interaction . . . 81
4.4 Possible causes of heterogeneity . . . 82
4.4.1 Phase separation investigation . . . 82
4.5 Parametric study on factors influencing viscosity and network development . . . 86
4.5.1 Influence of polymer type . . . 86
4.5.2 Influence of site mixing method . . . 87
4.5.3 Influence of salt content . . . 88
4.5.4 Influence of temperature on the development of networks . . . 89
4.6 Parametric study of environmental factors . . . 90
4.6.1 Influence of photodegradation . . . 90
4.6.2 Influence of temperature . . . 92
4.7 Summary . . . 93

5 Laboratory investigation of polymer fluid flow in sands 95

5.1 Introduction . . . 95
5.2 Materials and methods . . . 95
5.2.1 Permeameter test apparatus . . . 95
5.2.2 Permeameter test procedure . . . 98
5.2.3 Additive mixing . . . 100
5.2.4 Sand grading . . . 100
5.2.5 Scope of testing . . . 101
5.3 Results . . . 102
5.3.1 Exemplar results . . . 104
5.3.2 Hold periods . . . 109
5.3.3 Polymer product analysis . . . 110
5.3.4 Applied pressure analysis . . . 119
5.3.5 Concentration analysis . . . 120

5.3.6 Sand grading analysis . . . 126
5.3.7 Additive analysis . . . 131
5.4 Summary . . . 136

6 Investigation of polymer fluid-soil interaction 138
6.1 Introduction . . . 138
6.2 Materials and methods . . . 140
6.2.1 Clay preparation . . . 140
6.2.2 Polymer preparation . . . 141
6.2.3 Oedometer test apparatus . . . 142
6.2.4 Clay mass loss during tests . . . 143
6.2.5 Oedometer test procedure . . . 145
6.2.6 Direct shear apparatus . . . 146
6.2.7 Concrete . . . 147
6.2.8 Direct shear test procedure . . . 147
6.2.9 Scope of testing . . . 150
6.3 Results . . . 151
6.3.1 Moisture content tests . . . 151
6.3.2 Oedometer testing - void ratio and fluid type . . . 153
6.3.3 Oedometer testing - influence of fluid type on swelling rate . . . 155
6.3.4 Shear testing - kaolin clay tests . . . 157
6.3.5 Shear testing - Lambeth Clay tests . . . 160
6.4 Summary . . . 161

7 Conclusions and recommendations for further research 165
7.1 Introduction . . . 165
7.2 Key contributions . . . 165
7.2.1 Qualitative testing of polymer fluids on site . . . 165
7.2.2 Polymer fluid heterogeneity . . . 166
7.2.3 Polymer fluid flow in sands . . . 167
7.2.4 The influence of polymer fluid on clay swelling . . . 170

7.2.5 The influence of polymer fluid on clay shear strength 170
7.3 Recommendations for future research 171
7.3.1 Chemistry 171
7.3.2 Mixing procedure 172
7.3.3 Influence on shear resistance 173
7.3.4 Embodied carbon 173
7.3.5 Naturally derived polymers 173
7.3.6 Suitability for other applications 174
7.4 Concluding remarks 174

A Site Guide to Polymer Support Fluids **176**

Notation

API	American Petroleum Institute
BP	Baroid paper (filter paper brand)
BS	British Standard
CFA	Continuous Flight Auger
CRU	Constitutional Repeating Unit (for polymers)
DFI	Deep Foundations Institute (US)
DIN	Deutsches Institut für Normung (German standards)
EFFC	European Federation of Foundation Contractors
EN	European Norm (standard)
FG	Fisher Grade (filter paper brand)
GGBS	Ground Granulated Blast Furnace Slag
HPAM	Partially Hydrolysed Polyacrylamide
ICE	Institution of Civil Engineers
ISSMGE	International Society for Soil Mechanics and Geotechnical Engineering
IPA	Isopropyl Alcohol
LB	Leigthon Buzzard sand
PHPA	Partially Hydrolysed Polyacrylamide (alternative to HPAM, used in civil engineering)
PPT	Pore pressure transducer
PVC	Polyvinyl chloride
RP	Recommended Practice
SEM	Scanning Electron Microscopy
UV	Ultraviolet
WG	Whatman Grade (filter paper brand)

a	Flow rate difference
A	Area
B_{pp}	Flow decay rate coefficient for polymer-polymer flow
B_{pw}	Flow decay rate coefficient for polymer-water flow
c	Concentration
c_v	Coefficient of consolidation
c^e	Entanglement concentration
c^*	Overlap concentration
c^{**}	Interpenetration concentration
CV	Coefficient of Variance
C_c	Compression index
C_s	Swelling index
d	Diameter
d_s	Pore diameter
d_{10}	Maximum grain diameter of the smallest 10% of soil particles in a sample
d_{50}	The median grain diameter of soil particles in a sample
F	Force
g	Acceleration due to gravity
h	height
i_h	hydraulic gradient
j	swell limit coefficient
k_p	Polymer conductivity
k_w	Hydraulic conductivity
K	Intrinsic permeability
L	Length
m	Consisistency coefficient
n	Power law index

n_c	Curve fitting parameter for Carreau model
n_p	Flow behaviour index
N_{ads}	Number of adsorbate atoms per unit area
N_s	Number of surface atoms per unit area
P	Pressure
P_f	Pressure fraction
P_T	Total pressure drop
P_z	Pressure at a given height
PSD	Particle size distribution
PV	Pore volume
q	Filtration rate
Q	Flow
r	Radius
Re	Reynolds number
s	Swelling rate coefficient
S_u	Undrained shear strength
SD	Standard deviation
t	Spacing thickness
u	Pore water pressure
U	Relative velocity
v	Velocity
$\bar{v}$	Average velocity
$\dot{\gamma}$	Shear rate
η	Apparent viscosity
η_{before}	Viscosity before permeation
η_{frac}	Viscosity fraction
η_t	Apparent viscosity at a given time

η_t	Viscosity at a given shear rate
η_x	Viscosity gain factor
η_z	Apparent viscosity at a given height
η_0	Zero shear viscosity
η_∞	Viscosity as shear approaches infinity
θ'	Coverage of adsorbate on a surface
λ	Time constant (curve fitting parameter for Carreau model)
μ	Mean average
ρ	Density
ρ_b	Ball density
ρ_f	Fluid density
ρ_w	Water density
σ	Total stress
σ'	Effective stress
σ_n	Normal stress
τ	Shear stress
$\tau_{control\ peak}$	Maximum shear stress in a control test
τ_{frac}	Shear stress fraction
τ_n	Shear stress at any given time

1 Introduction

1.1 Background

Civil engineering support fluids are used to maintain the stability of open excavations during construction. Support fluids are designed so that they are resistant to permeation into the surrounding soil such that when they are placed into an excavation they exert a stabilising, hydrostatic pressure on excavation walls. To prevent groundwater from entering, the stabilising pressure of the support fluid must exceed the free-field pore water pressure at all depths (Lam and Jefferis, 2018); it must counteract the destabilising force of the groundwater, the soil pressure, and any surcharge loads. The hydrostatic pressure should act at the fluid-soil interface or close to it, otherwise, there will be a risk of the soil 'sloughing' backwards from the excavation face (EFFC/DFI Support Fluids Task Group, 2019). As the support fluid exerts pressure on the excavation faces, it tends to flow into the surrounding soil, leading to a drop in pressure into the soil. Owing to losses into the surrounding ground, the fluid level in the excavation must be periodically topped-up to maintain sufficient support (Lam and Jefferis, 2018). Figure 1.1 shows the basic interactions between the fluid and the pressures in the ground.

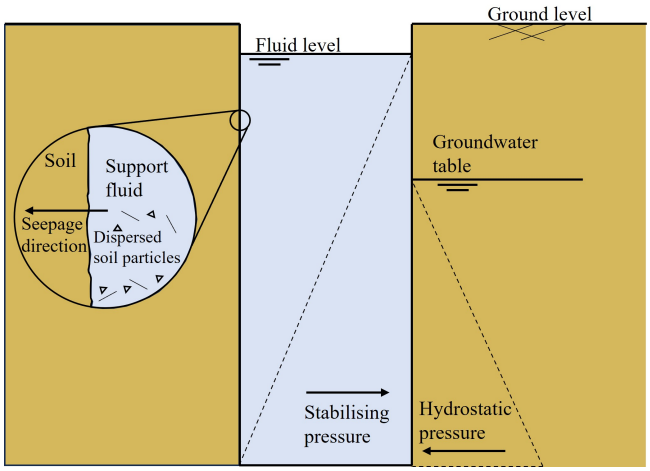


Figure 1.1: A schematic diagram of a fluid-supported excavation. Adapted from Lam and Jefferis (2018)

Traditionally, bentonite slurries have been the preferred fluid for excavation support. However, bentonite slurries have their drawbacks, including declining reserves of the mineral,

the requirement for vigorous mixing and long hydration times, the need for separation plant, and the disposal and environmental costs (Lam and Jefferis, 2018). Polymer support fluids are an increasingly popular alternative for their overall lower cost, potential lower carbon footprint, and performance, despite initial hesitance arising from early failures. Over the past decade, there has been a large uptake of polymer fluids on major construction sites. They have been used as the sole support fluid on billion-pound projects such as the Silvertown Tunnel and are being used extensively to construct the piles on The Line Project in Neom, which will require 30,000 piles for completion (NEOM Newsroom, 2024). In contrast, understanding of the behaviour of polymer fluids as support fluids has not kept pace and substantial work is still needed for a comprehensive understanding that will ensure consistent and stable use in industry.

Bentonite slurries limit seepage as a result of the plate-like geometry of bentonite clay particles, which form a low-permittivity filter cake on the exposed excavation faces. In contrast, polymer fluids rely on a different mechanism: the frictional drag exerted by the long chain-like polymer molecules on the soil particles limits seepage by increasing the fluid viscosity. By way of example, Figure 1.2 illustrates these distinct mechanisms in the context of fluid flow through a filter paper, as occurs in an API filter press test. A key difference between bentonite slurries and polymer fluids lies in the development of a filter cake on the excavation walls. Solutions of synthetic polymer are not expected to form a filter cake. The absence of a filter cake can significantly improve the shear resistance between the concrete and soil. Without a filter cake, the concrete is in direct contact with the soil, potentially resulting in a higher load capacity for piles formed under synthetic polymer fluids compared to those formed under bentonite slurry.

Polymer products have been commercially available since the 1970s, with Telmarch being among the earliest companies to offer a polymer fluid system for use in diaphragm walling. However, a significant breakthrough occurred in the 1990s when several companies began promoting partially hydrolysed polyacrylamide (HPAM, also referred to as PHPA) products for use in construction. It is important to note that other polymers have also been explored, and some continue to be used, such as carboxymethyl and hydroxyethyl celluloses, as well as xanthan and guar gums. These alternatives, derived from natural sources, are often referred

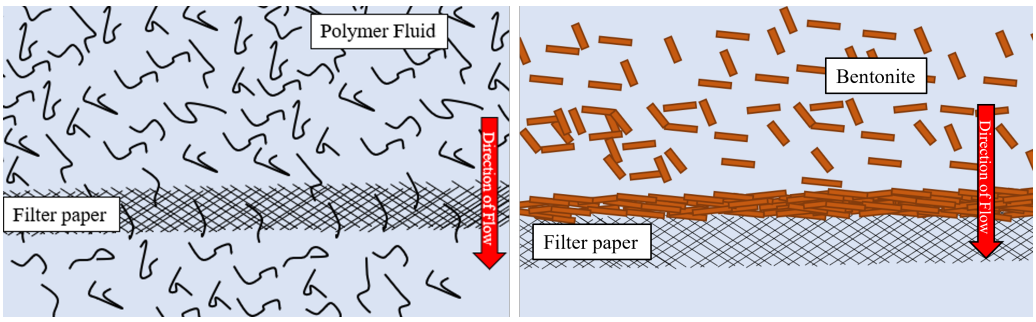


Figure 1.2: Schematic illustrations (not to scale) of: (a) Polymer fluid flowing through a filter paper during an API filter press test. The interaction of the polymer chains results in a viscous fluid resisting flow through the paper. (b) Bentonite particles retain on the filter paper and form a low permittivity barrier on the filter paper, slowing the flow of pore fluid through the system.

to as "natural gums" to distinguish them from HPAMs, which are synthetic. In this report, the term "polymer" specifically refers to HPAM polymer unless otherwise indicated.

1.2 Problem statement

The use of HPAMs in civil engineering has grown in popularity, yet their application has been hindered by challenges such as excavation collapses, voids, and inclusions in final concrete elements (Lam and Jefferis, 2018). A primary reason for these failures was the poor understanding of the behaviour of HPAMs and their management on site. In many cases, polymer fluids were, and on occasions still are, managed as if they were bentonite-based slurries, despite significant differences in their properties and necessary management procedures. Over recent years, the industry has developed reasonably successful management procedures for HPAM fluids; however, a lack of comprehensive understanding means that problems arising under certain conditions cannot be effectively addressed. Previous research has significantly contributed to the knowledge base for polymer fluids in civil engineering, including studies on polymer flow through porous media, their effect on the shear resistance of sands, and their potential to form low-permeability barriers. These studies have also included insights derived from site observations and practice. Although such work has positioned HPAMs as a viable and increasingly popular option for contractors, important knowledge gaps remain. These gaps include (i) the detailed mechanisms of polymer-soil interaction, (ii) the swelling behaviour of soils exposed to polymer fluids, (iii) the impact of the fluid on the interface shear resistance between foundation concrete and clays, (iv) the effects of fluid heterogeneity and (v) soil and site conditions when polymer fluids should not be used.

Currently, industry practices often adapt methods developed for bentonite, alongside site experience, to manage polymer fluids. However, given the unique characteristics of HPAMs, a more rigorous and scientific approach is necessary to optimise their use. This research aims to address these knowledge gaps by enhancing the understanding of polymer fluid interactions with soils, thereby enabling more effective excavation stability analysis and the design of permanent geotechnical elements. Achieving this will help unlock the full potential of polymer fluids, with potential benefits including shorter pile lengths, reduced carbon emissions, lower costs, and shorter project durations.

1.3 Research question and objectives

The research question this research seeks to address is: How do polymer fluids interact with various soil types, and what are the implications for soil shear resistance, swelling behaviour, excavation stability, and industry practice for polymer fluid management?
To address this question the research project is split into three objectives:

1. **Enhance industry practice and management:** Improve the management of polymer fluids to unlock their potential benefits for the industry.

2. **Develop the understanding of flow processes:** Develop the understanding of polymer fluid flow in soils and how this affects excavation stability.

3. **Advance understanding of polymer-soil interactions:** Deepen the knowledge of how polymer fluids interact with soil, with implications for design practice.

To address each objective, laboratory testing was conducted to investigate various aspects of polymer fluids related to the specific aims. The following tests were conducted:

API Filter Press Testing (Objective 1)
This testing evaluates whether the API filter press, typically used for bentonite fluids, is suitable for polymer fluid assessment and can be effectively used to inform polymer fluid management.
Novel Drop Test Method (Objective 1)

The drop test method provides insight into the intrinsic behaviours of polymer fluids and their implications for industry practice and fluid management. This testing helps clarify how polymer fluids behave under different conditions, informing better handling and use on-site.

Permeameter Testing (Objective 2)

Testing with a permeameter apparatus aims to improve the understanding of polymer fluid flow through sands, a soil type that presents challenges for polymer fluid use. This testing will provide a significant database to facilitate more comprehensive numerical modelling of polymer fluid flow. The results are crucial for developing strategies to maintain excavation stability when polymer support fluids are employed.

Oedometer and Direct Shear Testing (Objective 3)

The oedometer tests investigate the effects of polymer fluids on the swelling and softening behaviour of clays, which are key factors influencing aggregate penetration from concrete into excavation walls. Subsequently, the direct shear tests explore how exposure to polymer fluids impacts the shear resistance of clays.

1.4 Research dissemination

The research conducted in this doctoral project has produced two initial journal papers, one conference paper, and one industry guide:

Journal paper 1: McNamara, D., Sheil, B., Jefferis, S., Barker, C., Nicholson, D., 2024. "An investigation of the behaviour of polymer fluids in the American Petroleum Institute Filter Press". Géotechnique. (published Oct 2024 https://doi.org/10.1680/jgeot.23.00209)

Journal paper 2: McNamara, D., Sheil, B., Jefferis, S., Barker, C., Nicholson, D., "An investigation into the impact of heterogeneous viscosity development in polymer fluids on civil engineering applications" (submitted).

Conference paper: McNamara, D., Sheil, B., Jefferis, S., Barker, C., 2023. "Analysing the suitability of the American Petroleum Institute filter press test for polymer support fluids". Proceedings of the 5th International Conference on Geotechnics for Sustainable Infrastructure Development. GEOTEC 2023.

Industry guide: McNamara, D. "A Guide to Polymer Support Fluids for the Site Team" 2024. Self-published and distributed to technical staff during site visits.

1.5 Thesis structure

Figure 1.3 presents an overview of how the research questions are explored, with each chapter focusing on a different experimental investigation. Chapter 2, the literature review, covers a background of support fluids, chemistry, rheology, sorption, and previous work, and provides a summary of the current knowledge gaps. Chapter 3 covers the API investigation that aims to address Research Objective 1, along with Chapter 4, which focuses on an investigation of the development of heterogeneity in bulk polymer fluids. These chapters aim to provide actionable insights into polymer management to enable the optimal use of polymer fluids for excavation support. Chapter 5 focuses on the permeameter investigation undertaken, in turn addressing Research Objective 2. This chapter aims to develop the understanding of the flow behaviour of the fluids in sands, one of the most problematic soil types for support fluids. Chapters 6 and 7 focus on the oedometer and direct shear testing that addresses Research Objective 3. The chapters present the research on polymer-soil interactions and what these mean for excavation support capabilities and the final foundation design.

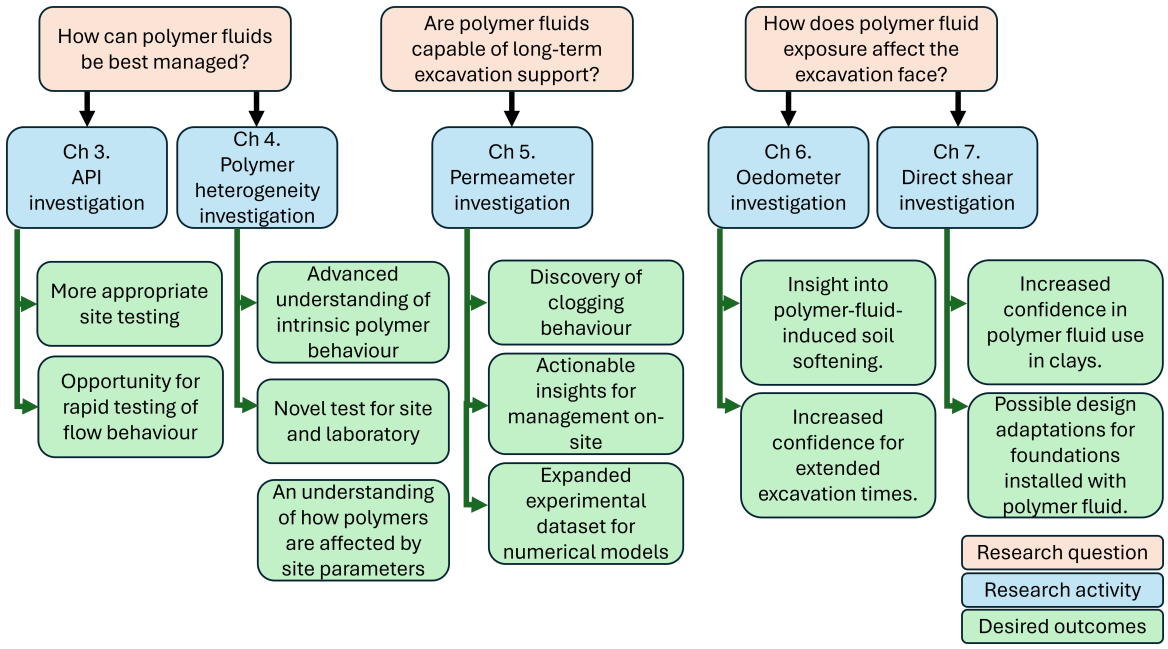


Figure 1.3: A diagram to detail the structure of the thesis in relation to the original research questions, the experimental investigations undertaken to address these, and the outcomes.

2 Literature review

2.1 Introduction

Support fluids are crucial for the temporary stabilisation of excavations across a range of geotechnical and civil engineering applications. These include bored piles, diaphragm walls, slurry tunnelling, horizontal directional drilling, water and oil well drilling, site investigation boreholes, and the formation of permeable reactive barriers and deep drainage walls (Lam and Jefferis, 2018). Pile foundations are essential structural elements that transfer loads from superstructures to the soil by friction along their depth and by a normal contact force from more competent soil or rock strata at depth. These foundations are typically constructed using steel or reinforced concrete. The load-carrying capacity of piles is derived from a combination of shaft resistance, generated along the pile-soil interface, and base resistance, provided by the soil at the pile tip. Piles are commonly installed either by driving (for steel, timber, or precast concrete piles) or by boring and constructing the pile in situ. Bored piles are often preferred in situations where (i) large diameter or deep foundations are required, (ii) the excavations are in harder ground conditions, and/or (iii) where minimising vibration and disturbance to the surrounding environment is critical. This last point is particularly important in urban environments, where reducing disruption can be a primary reason for selecting bored piling. The construction of a foundation element using a support fluid begins with the excavation of the void, with the fluid providing temporary support to the excavation. Support fluids are typically prepared by mixing appropriate materials with water. Their primary function is to maintain the stability of open excavations until they are backfilled with structural materials, such as concrete. Crucially, the fluid level within the excavation is maintained above the surrounding groundwater table. Support is achieved through the pressure differential across the fluid-soil interface, which also promotes a slow infiltration of the fluid into the surrounding soil (see Figure 2.1).

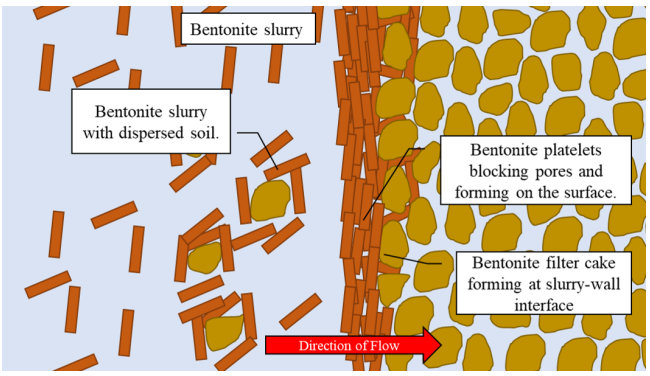


Figure 2.1: Formation of bentonite filter cake on bore wall. Adapted from EFFC/DFI Support Fluids Task Group (2019).

The two most widely used support fluids are bentonite clay slurries and polymer support fluids. Bentonite clay slurries have been in widespread use since the 1950s. Bentonite is an off-white montmorillonite clay formed from altered volcanic ash. Sodium-rich bentonites are particularly effective as they can absorb up to ten times their own weight in water and swell to occupy eighteen or more times their dry volume (Sigurdsson et al., 2015). This property makes bentonite an ideal material for forming slurries, as a compact material can create a large volume of slurry, and its particles have the capacity to block pores within the soil, thereby forming a low-permeability filter cake. The concept of using bentonite as a support fluid for deep foundation construction was first conceived by Christian Veder in the 1930s (as documented by Glossop (1964); Xanthakos (1979)). Despite its widespread use, bentonite has several practical constraints. It requires specialist plant for optimal performance, and the mixing and hydration processes are time-consuming. Excavated soil solids can also accumulate in the slurry, necessitating soil-slurry separation plant to prevent quality issues. Furthermore, there are significant disposal (Uchiyama and Horiuchi, 1994) and environmental issues associated with bentonite waste (Thasnanipan et al., 2002). Concerns regarding the reserves of high-quality Wyoming bentonite in the late 1970s, coupled with the rising costs of liquid waste disposal, spurred the search for alternative support fluid materials (Lam and Jefferis, 2018).

The earliest reported use of polymer support fluids dates back to the 1970s with the product 'Telmarch' for diaphragm wall construction; however, its use was short-lived for unspecified reasons. From the 1970s to the 1990s, natural polymers such as carboxymethyl cellulose, guar gum, and xanthan gum were used, but they had limited industry impact due to their rapid

biodegradability. The addition of biocides to counteract biodegradation led to further environmental concerns (Lam and Jefferis, 2018). A significant breakthrough occurred in the early 1990s with the introduction of synthetic partially hydrolysed polyacrylamides (HPAMs) in geotechnical engineering (Lam and Jefferis, 2018). Developed in the USA, HPAMs have progressively become a globally viable option in construction due to their efficacy and their suitability for large-scale manufacturing. The development of additives, such as soil settlement enhancers (loosely referred to as flocculants), which can be used in conjunction with HPAMs, has further enhanced their versatility.

2.2 Chemistry

Polymers are large molecules, also known as macromolecules, which are composed of smaller, repeating units called monomers (Painter and Coleman, 1997). Synthetic polymers are created through the replication of a constitutional repeating unit (CRU), where each CRU is joined to its neighbours by covalent bonds. Polymers can be categorised in various ways, one such classification being whether they are synthetic or natural. Synthetic polymers are from petroleum oil, including Nylon, Teflon, and PVC, while natural polymers occur solely in nature, such as wool, cellulose, and silk (Lam and Jefferis, 2018). Although biodegradability might commonly be assumed to imply a material is natural, it is important to note that some synthetic polymers are specifically designed to be biodegradable (Lam and Jefferis, 2018). Polymers can be classified by their chemical structure, which depends on the repeated monomer(s) and their structural pattern. Polymers with one repeating unit are known as homopolymers, whilst those with two or more repeating units are termed co-polymers (see Figure 2.2).

Homopolymer:	– A – A – A – A – A – A – A – A – A – A
Copolymer (alternating):	– A – B – A – B – A – B – A – B– A – B
Copolymer (random):	– A – B – B – A – B – A – A – B– A – A

Figure 2.2: Classification of polymers depending on chemical structure, where A and B represent monomers with the polymer (adapted from Lam and Jefferis (2018)).

Popular polymers used as support fluids include HPAMs, polyacrylates, cellulose, xanthan gum, and guar gum, with HPAMs arguably being the most commonly employed in

construction. HPAM and polyacrylate are synthetic polymers, whereas cellulose, xanthan gum, and guar gum are natural, though they they typically receive some processing prior to use.

Polyacrylamide, as distinct from HPAM, possesses the chemical structure $(C_3H_5NO)_n$, where 'n' represents any number greater than 1. Polyacrylamide itself is non-ionic and does not carry any charges; it lacks functionality as a support fluid (Lam and Jefferis, 2018). The absence of functionality in the polyacrylamide form necessitates the use of its partially hydrolysed counterpart. This involves substituting some acrylamide units with acrylate units to create an anionic copolymer. The partially hydrolysed form has the chemical formula $(C_3H_5NO)_x - (C_3H_3O_2A)_y$, where 'A' is a positive ion, and 'x' and 'y' are dependent on the degree of hydrolysis (Lam and Jefferis, 2018). Figure 2.3 illustrates the structural differences between polyacrylamide and partially hydrolysed polyacrylamide.

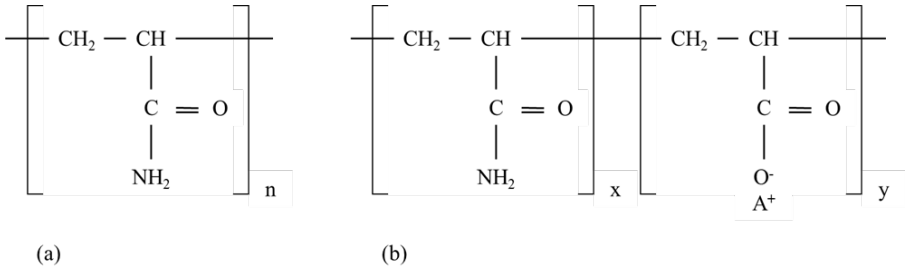


Figure 2.3: Chemical structures of (a) polyacrylamide and (b) its partially hydrolysed form. Adapted from (Lam and Jefferis, 2018).

It should be noted that if a polyacrylamide is fully hydrolysed (i.e. x=0 and y=1, in reference to Figure 2.3), then the product is a polyacrylate. As any hydrolysis short of full hydrolysis to polyacrylate is partial, some authors prefer the term HPAM to PHPA. The degree to which a polyacrylamide is hydrolysed has a direct influence on the viscosity of the resultant mixed fluid and its significance is dependent on the chemistry of the mix water. For example, a degree of hydrolysis of 25%-35% achieves maximum viscosity when mixed with fresh water and sodium chloride brines, whereas 15% hydrolysis achieves a maximum viscosity with calcium chloride brines (Martin, 1975). An increase in the degree of hydrolysis causes water solubility to increase but the viscosity of the polymer at a given concentration decreases (Lam and Jefferis, 2018). For the polymer to achieve a uniform viscosity, it must be able to dissolve in the mixing fluid. It may be noted that polyacrylates have been used as support fluids, but because of their lower solution viscosities, higher concentrations are required than for HPAMs.

Most HPAMs supplied to the construction industry have sodium as the ion to balance the negative charge of the acrylate units. The backbone of these HPAM polymers is formed from carbon-carbon single bonds. These bonds are flexible, so the chains can take up random and ever-changing configurations. However, the negative charges distributed along the polymer chain tend to repel each other, causing the chains to stretch out. This is significant because the greater the effective length of the polymer molecules in solution, the greater the viscosity of the solution. However, if the mix water contains dissolved salts, then the range of effect of the ions on the polymer chain is reduced, and the molecules can tend to curl up, thus reducing the solution viscosity.

2.3 Rheology

Rheology is the study of the deformation and flow of matter. Isaac Newton described rheological behaviour as "the resistance which arises from the lack of slipperiness of the parts of the liquid, other things being equal, is proportional to the velocity with which the parts of the liquid are separated from one another" (Newton, 1833). The "lack of slipperiness" is now referred to as 'viscosity' and is both synonymous with internal fluid friction and a measure of resistance to flow (Barnes et al., 1989). Figure 2.4 depicts Newton's derivation of the shearing mechanism in fluids.

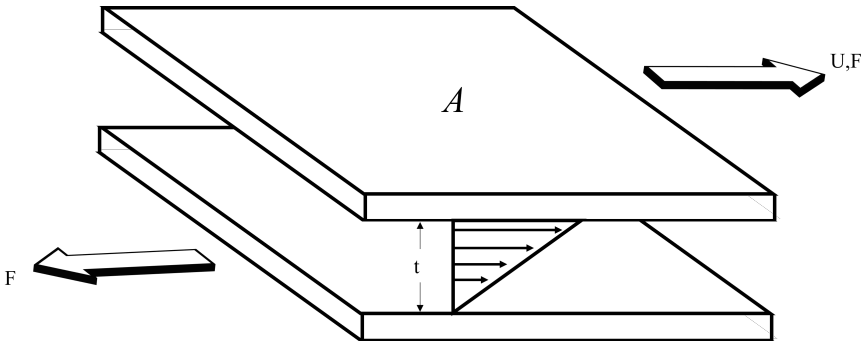


Figure 2.4: Newton's viscosity model. Two parallel planes, each of area A, at y=0 and y=t respectively, the space in between is filled with sheared fluid. The upper plane moves with relative velocity, U, and the length of the arrows between planes is proportional to the local velocity in the liquid (adapted from Barnes et al. (1989)).

The shear force, F, applied over a given area, A, to achieve a relative velocity, U, is directly proportional to the shear rate, $\dot{\gamma}$ (where $\dot{\gamma} = U/t$). The applied shear stress $\tau(= F/A)$ is dependent on the coefficient of viscosity, η, as follows:

$$\tau = \eta \cdot \dot{\gamma} \tag{2.1}$$

While Newton's linear law is useful to describe the rheological behaviour of many different materials (e.g. water, corn oil, glycerol), polymer fluids cannot be described by constant η and are therefore considered 'non-Newtonian'. The viscosity of non-Newtonian fluids is dependent on the applied shear rate and for some fluids, such as bentonite slurries, the shear history. Figure 2.5 shows Newtonian and a variety of non-Newtonian fluid behaviours on a plot of shear stress against shear rate. The slope of a tangent to the plots is defined as the shear viscosity (or plastic viscosity), and the slope of a line joining any point on the plots to the origin is known as the apparent viscosity. For non-Newtonian fluids, both these viscosities will be a function of the shear rate at which they are determined. Figure 2.5 also shows relationships for fluids that will shear only when the shear stress exceeds a certain yield stress (such as the Bingham plastic and the yield pseudo-plastic materials). Fluids showing this behaviour include bentonite slurries, cement grouts and many food products such as mayonnaise.

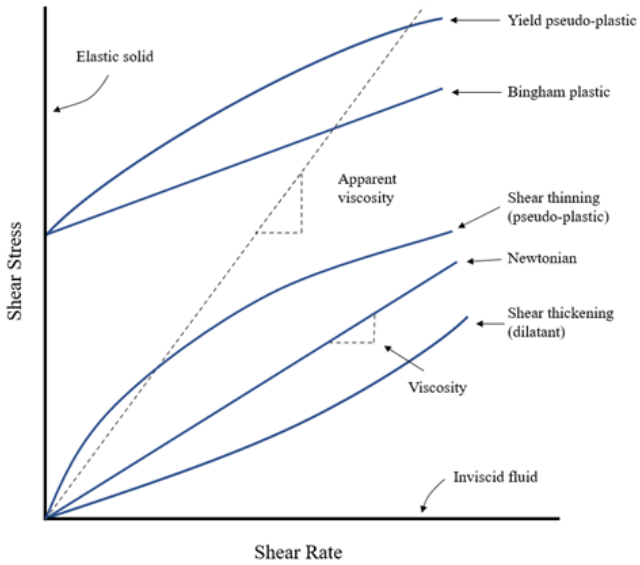


Figure 2.5: Various fluid behaviours modelled over a range of shear rates (Lam and Jefferis, 2018).

Polymer fluids exhibit shear-thinning behaviour, meaning their apparent viscosity decreases as the shear rate increases. At high shear rates, their viscosity tends towards that of the solvent (which is water for support fluids). Various models have been proposed in the literature to describe the rheological behaviour of polymers. Among these, the power-law and

Carreau models have been identified as the most suitable for HPAM support fluids (Lam and Jefferis, 2018).

2.3.1 The power law model

The simplest model used to describe shear thinning and thickening behaviour is the power-law model (Waele, 1923; Ostwald and Auerbach, 1926), defined as:

$$\tau = m\dot{\gamma}^{n_p} \tag{2.2}$$

Where m is the flow consistency index and n_p is the flow behaviour index; values of $n_p < 1$ and $n_p > 1$ yield shear thinning and shear thickening behaviour respectively whereas Newtonian viscosity is recovered for $n_p = 1$ (Lam and Jefferis, 2018). Substituting the power-law model into the Equation 2.1 gives the apparent viscosity of the fluid at shear rate $\dot{\gamma}$:

$$\eta = m\dot{\gamma}^{n_p-1} \tag{2.3}$$

2.3.2 The Carreau model

For the more commonly encountered partially hydrolysed polyacrylamide, the power-law model provides poor predictions at both very high and very low shear rates. This is because real behaviour approaches limiting viscosity values at these shear rates, whereas the power-law model predicts a straight line in log-log space. The constant viscosity observed at extremely low shear rates is referred to as the 'upper Newtonian plateau', i.e. highest viscosity, and similarly, the constant viscosity at high shear rates is known as the 'lower Newtonian plateau' i.e. lowest viscosity (Lam and Jefferis, 2018). To better model this behaviour, the Carreau model introduces additional parameters:

$$\frac{\eta - \eta_\infty}{\eta_0 - \eta_\infty} = \left[1 + (\lambda\dot{\gamma})^2\right]^{\frac{n_c-1}{2}} \tag{2.4}$$

Where, η_∞ and η_0 represent the limiting viscosity at very high and very low shear rates, respectively. λ and n_c are curve-fitting parameters. To ensure dimensional consistency, λ has units of time and is therefore referred to as the time constant. In the model, λ controls the transition between the lower Newtonian plateau and the lower bound of the shear-thinning

region (Lam and Jefferis, 2018).

2.4 Sorption

While polymer support fluids primarily rely on viscous drag to maintain a constant pressure head, sorption represents another mechanism that influences the filtration mechanics of a fluid. Polymer sorption onto a soil surface will retard the advance of the polymer front relative to the velocity of the fluid.

Sorption is a general term encompassing various processes. Adsorption describes the process where a molecule (an adsorbate) forms a bond to a surface (an adsorbent) (Attard and Barnes, 1998). This is distinct from 'absorption', which refers to molecules entering into the bulk of a substrate. When a molecule collides with a surface, it may either rebound or be retained on the surface. A retained molecule will interact with the surface through either physical adsorption (physisorption) or by forming chemical bonds with the surface, resulting in chemical adsorption (chemisorption) (McCash, 2023). The coverage, θ', of the adsorbate on a surface is given as:

$$\theta' = \frac{N_{ads}}{N_s} \tag{2.5}$$

Where, N_{ads} represents the number of adsorbate atoms per unit area, and N_s is the number of surface atoms per unit area. Physisorption involves the delicate balance of a weak attractive force, such as a Van der Waals force, between the surface and the adsorbate (McCash, 2023). Generally, physisorption is a non-specific process that can occur between any molecule and surface under appropriate experimental conditions, including temperature and heat (McCash, 2023). In contrast, chemisorption is a process where a strong chemical bond forms between the surface and the adsorbate, involving the exchange of electrons. These bonds can be either ionic or covalent.

The capacity to adsorb onto surfaces is a fundamental requirement for polymers employed as flocculants across numerous industries (Gregory and Barany, 2011). Flocculants facilitate the coalescence of solid particles within a suspension, leading to the formation of larger flocs or more densely packed aggregates. These larger structures can then be easily separated by physical means, such as settlement. Polymer adsorption can involve the attachment of various

lengths, or 'trains', of the polymer to the surface, as illustrated in Figure 2.6. Because multiple segments are capable of bonding with the surface, the adsorption affinity per segment does not need to be high for an entire polymer chain to be adsorbed to a surface (Gregory and Barany, 2011).

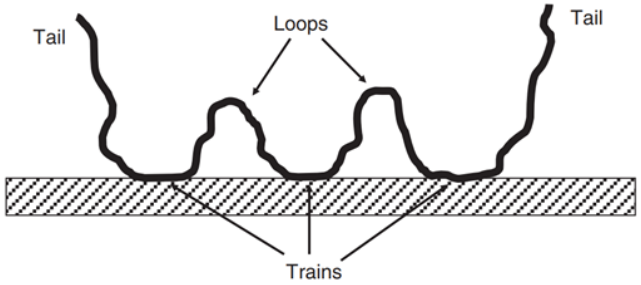


Figure 2.6: Model depicting a polymer chain adsorbed to a surface (Gregory and Barany, 2011).

It should be noted that the HPAMs utilised as support fluids typically possess a very high molecular weight, with some products weighing over 20 million Daltons (3.32E-17 g). In contrast, HPAMs used as flocculants generally have a low molecular weight. While flocculation may not occur with polymer support fluids, the soil-polymer interaction, and particularly the ability of the polymers to inhibit the dispersion of the formation soil, offers numerous advantages, such as preventing soil build-up in the fluid.

2.5 Laboratory investigations

2.6 Filtration behaviour

To provide support to an excavation, the support fluid pressure head must exceed the highest pore water pressure within the ground being excavated. This pressure differential can support the face of the excavation, but it must be exerted directly at the face or over a very limited distance behind it. If the fluid pressure drops over too great a distance, the soil face may slough into the excavation, leading to progressive collapse. The penetration of the support fluid can be limited either by cake formation, as is characteristic of bentonite slurries, or primarily by the fluid viscosity, which is the main process for polymer fluids, or indeed by a combination of both mechanisms.

In both the oil and construction industries, filtration characteristics are commonly investigated using an American Petroleum Institute (API) filter press or a permeameter,

schematics of which are presented in Figure 2.7(a) and Figure 2.7(b), respectively.

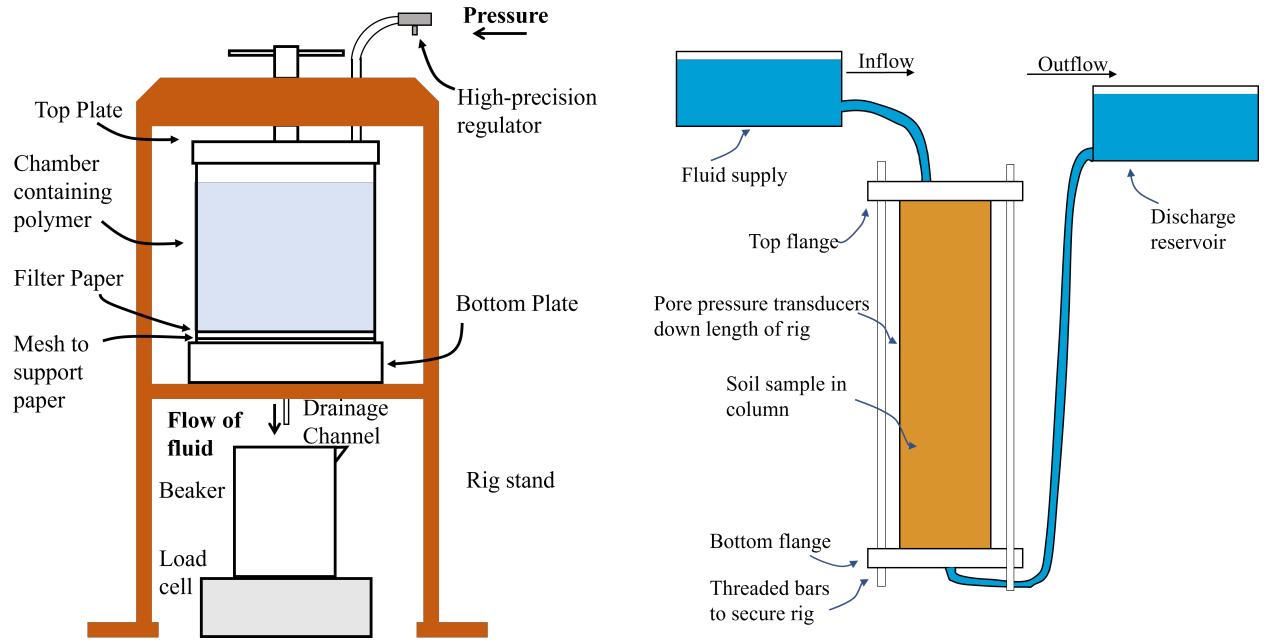


Figure 2.7: (a) API Filter Press schematic, the fluid under test is pressurised against a permeable membrane enabling determination of the filtration rate (filter loss) and filter cake development. (b) Permeameter schematic, the rig is designed to measure the difference in pore pressure as the fluid flows through the chamber.

Ejezie (2018) employed a permeameter to investigate the flow characteristics of polymer fluids in coarse sands. Their research explored the influence of grain size and applied head on flow behaviour, utilising a combination of freeze-drying and scanning electron microscopy (SEM) to inspect the permeated sand post-permeation. The SEM imaging revealed that individual polymer chains stretched out and became intertwined during penetration. This stretching was attributed to the repulsion of like charges along the polymer chain, forcing them apart while remaining constrained within the overall chain structure. The permeameter results further indicated that the polymer flow front penetrated the soil as a relatively uniform barrier. However, the pressure gradient at the soil face progressively decreased as fluid penetration advanced, with the timescale for this being governed by the viscosity of the fluid at the in-pore shear rate and any subsequent clogging of the sand. Ejezie (2018) provided an example of a hydraulic conductivity reduction factor of 1000 (hydraulic conductivity / polymer conductivity) in 1.7 – 4 mm graded coarse sand to fine gravel, implying that the pressure gradient at the excavation face should be adequate for stability for several days. Ejezie (2018) also utilised the API filter press to investigate the occurrence of pore blocking in porous media. From these tests, the author concluded that the silt and sands suspended

within the polymer fluids led to two competing effects: firstly, a detrimental decrease in fluid viscosity due to polymer loss via sorption onto the soil, and secondly, a beneficial increase in flow resistance resulting from the clogging of pores in the filter paper.

Sims (2020) investigated the effect of several parameters on the filtration behaviour of polymer fluid using an API filter press. Their research examined the influence of pressure, concentration, age, and pore size on filtration. Their results indicated that the filtration rate increased non-linearly with pressure. Regarding concentration, the author found that filtration mechanisms differed at low and high concentrations; a fluid with half the standard concentration exhibited a filtration rate double that of the standard, although a mix with double the concentration did not follow this trend, showing only a slightly lower filtration rate than the standard. From the ageing tests, it was observed that the rate of polymer filtration increased with age, leading the author to infer that the fluid becomes less capable of producing a membrane to slow filtration as it ages. The investigation into the effect of pore size revealed that the filtration rate increased and decreased at certain points during each test. It was concluded that the fluid indeed developed a membrane on the filter paper, but at different stages of the test. However, for larger pore sizes, there was an indeterminate length of time required for a membrane to form. As anticipated, the author found that the filtration rate increased with pore size. It is important to note that the standard mix used in these tests included the proprietary additives designed by the polymer supplier to encourage membrane formation.

Verst et al. (2022b) investigated the rate of penetration of polymer solutions into sand and glass beads using a permeameter apparatus. The author analysed the data using a capillary bundle model, coupled with standard equations for the flow of power-law fluids in tubes. The author explored the influence of the polymer molar mass (serving as a surrogate for chain length) and concentration on the flow behaviours of the polymer fluids. The author found that the capillary bundle model was capable of providing a qualitative indication of the slope of the capillary velocity (fluid velocity in a pore) against hydraulic gradient plot for velocities greater than 5×10^{-7} m/s. Verst (2021) employed four distinct experimental methods to investigate the penetration rate-pressure relationship for polymer fluids in soils: vertical soil penetration, small-scale vertical soil penetration, uni-directional horizontal soil penetration,

and radial horizontal soil penetration. Verst (2021) also used polymers with mineral additives, specifically quartz powder and bentonite, alongside 'clean' polymer, to gain a deeper understanding of the process of soil clogging with fines (sometimes referred to as deep filtration or colmation) and how this limits the polymer fluid flow rate in soils. Subsequently, the author developed stability rules based on DIN 4126 for the stability of excavations under support fluids, applicable to both clean fluids and those with added minerals. It should be noted that DIN 4126 adopts a traditional sliding wedge approach for stability assessments and assumes that the stabilising pressure is uniformly distributed along the distance the fluid has penetrated into the ground, with only pressure dropped within the sliding wedge contributing to stability. Typical polymer fluids do not gel and will therefore continue to penetrate the soil unless clogging occurs.

2.7 Shear resistance and excavation face

A pivotal area of research concerning the application of polymer fluids in deep excavations is their potential influence on the shear resistance at the interface between concrete and excavation walls. To investigate this effect, the shear box apparatus has been commonly employed. Figure 2.8 illustrates the experimental setup used by Lam et al. (2014) for such investigations. More recently, Verst et al. (2022a) also utilised a shear box, incorporating the additional feature that concrete (with a maximum aggregate size of 2 mm) could be pumped directly into the shear box.

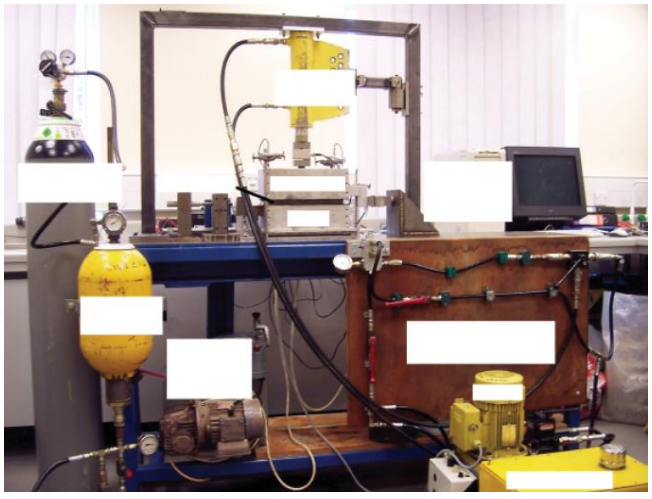


Figure 2.8: Apparatus used to investigate the effect that polymer fluids have on the shear resistance of soil (Lam et al., 2014).

In each instance, soil samples were exposed to pressurised polymer fluids for a predetermined period before being displaced by concrete, which was then allowed to cure. The hardened concrete-soil interface was subsequently subjected to shearing. For the testing conducted by Lam et al. (2014), each soil sample was exposed to the polymer for 7.5 hours. The concrete was permitted to cure for 3 days in one test and 7 days in another. While this is a valuable parameter to investigate, extending the polymer exposure time would allow for a more comprehensive study of problematic excavations that exceed their planned open duration. Figure 2.9 illustrates the shear stress-displacement plots for the polymer tests and a control test performed with water-saturated sand. The test conducted with water exhibited a higher initial stiffness, which was attributed to its greater initial dry density. Despite variations in concrete curing time, the three tests yielded similar peak shear stresses. The authors attributed this behaviour to the substantial aggregate protrusion into the sand. This protrusion caused the failure plane to consistently occur within the sand sample, therefore, similar shear stresses were required to form the failure plane.

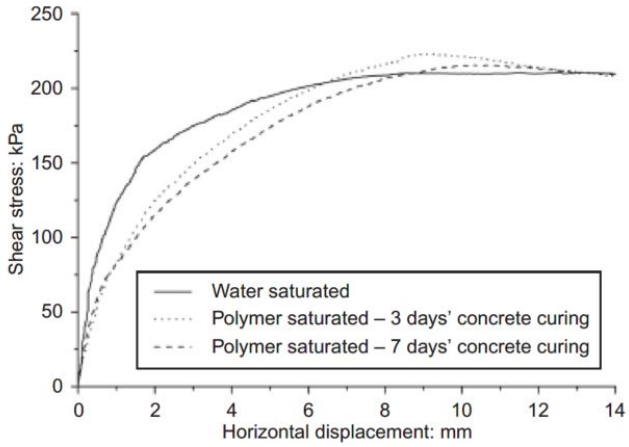


Figure 2.9: Three shear-displacement curves for sand samples exposed to fluids (1 water, 2 polymer fluid) then sheared (Lam et al., 2014).

The findings of Lam et al. (2014) are summarised in Figure 2.10 in the original text, which presents a comparison of peak shear stresses from all tests involving water, polymer fluid, and bentonite. The peak shear stresses mobilised by the samples exposed to polymer were significantly greater than those with bentonite cakes, and were either comparable to or greater than those achieved with water. These results suggest that the industrial application of polymer fluids in excavations could lead to enhanced shear resistance, and for piling, potentially shorter piles, resulting in reduced excavation, concrete consumption, lower overall

costs, and less pollution.

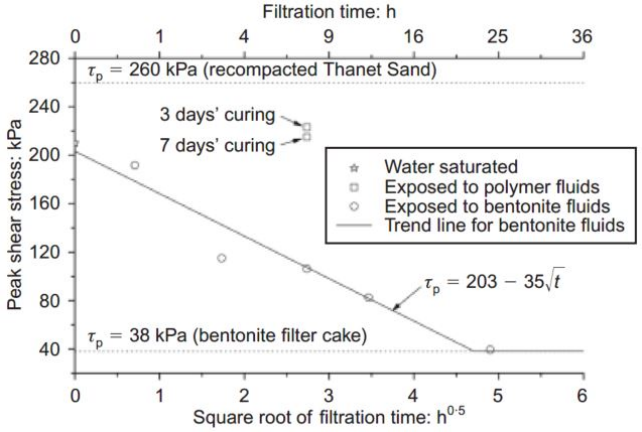


Figure 2.10: Peak shear stress activated by samples exposed to various fluids against the filtration times (Lam et al., 2014).

The testing conducted by Verst et al. (2022a) employed essentially the same methodology as previous studies, but with an expanded number of polymer tests, including both HPAM and cellulosic polymers. A notable added feature was that, since the polymers did not stagnate (i.e. flow did not stop) in the sample, a charge of either bentonite slurry or quartz powder was added to the polymer sample prior to use. The objective of this testing was to derive shear resistance values for the soil samples after exposure to the support fluids.

The derived shear resistance from testing soil exposed to polymer fluids were generally higher than those for samples exposed to bentonite. The results from Verst et al. (2022a) therefore support and extend the findings produced by Lam et al. (2014). This later work expanded on the earlier research by incorporating tests on cakes derived from bentonite slurries that contained excavation soil. Verst demonstrated that the presence of this soil increased the shear resistance compared to the results for pure bentonite obtained by Lam et al. (2014). Verst does note that in two of their tests, the shear plane did not occur at the concrete-soil interface, which renders these specific results relatively unreliable.

2.8 Summary and gaps in knowledge

The body of literature concerning the use of polymer fluids in civil engineering is still in its developing stages. Prior work has encompassed several laboratory studies focusing on polymer fluid flow in porous media, the influence of the fluid exposure on shear resistance, and various on-site studies. The research completed to date has enabled the industry to

effectively utilise these fluids; however, a comprehensive understanding of the properties of the fluid and how to fully realise its potential remains in progress.

Regarding industry practice and management, optimal on-site processes for polymer fluid implementation and qualitative testing have yet to be established. Frequently, polymer fluids are treated interchangeably with bentonite, leading to damage or ineffective treatment. Further studies are required to fully comprehend each stage of the fluid use, from mixing and testing to eventual re-use.

These polymer fluids continue to present researchers with unexpected behavioural quirks. The sustained study of these fluids will enable the civil engineering industry to fully grasp their behaviour and determine how best to harness them for desired purposes.

Understanding the flow dynamics of polymer fluids into the surrounding excavation is crucial for maintaining excavations with these fluids. Significant insights have already been gained from the work of several researchers. However, previous work has often been conducted with a narrow range of parameters and has primarily focused on polymer fluid displacing polymer fluid. To achieve a comprehensive understanding of flow in porous media that will enable the prediction of polymer fluid advance rate into an excavation face, testing is required for polymer displacing water, and across a broad range of parameters, including different polymer types, sand grading, and more.

A key consideration for the use of polymer fluids in excavation support is their effect on the shear resistance of soils once exposed to the fluid. Previous laboratory and site testing has indicated that the use of polymer fluids has a less adverse effect on the shear resistance at the soil concrete interface than excavation under bentonite. The laboratory testing completed to date has primarily focused on sand-concrete interfaces, with no studies yet conducted on clays. Furthermore, many other parameters, such as exposure time, polymer concentration, and soil type require study.

3 An investigation of the behaviour of polymer fluids in the American Petroleum Institute filter press

3.1 Introduction

The four primary tests currently used to manage polymer support fluids are identical to those used for bentonite slurries which, in turn, were imported from the oil well drilling industry. These are density (by mud balance), Marsh funnel flow time (used as a surrogate for polymer concentration), sand content, and American Petroleum Institute (API) filter press testing (Institution of Civil Engineers, 2016). While research has refined procedures for the testing of density and viscosity for polymer fluids (Lam and Jefferis, 2018) there remains significant uncertainty about the reliability, utility, and appropriateness of the API filter press test for managing polymer fluid quality. API filter press testing of bentonite slurries is well-established, widely accepted, practical for use on site (EFFC/DFI Support Fluids Task Group, 2019), and indeed advised by the Institution of Civil Engineers (2016). For bentonite slurries, because the hydraulic resistance of the developing filter cake (the filtered bentonite solids) rapidly becomes much greater than that of typical filter papers, the filtration rate is controlled by the filter cake rather than the filter paper (the filtrate flow rate is referred to as the filtration rate and for the tests in the API filter press this is the rate of flow from the test cell in ml/s or g/s as the density of the filtrate will be effectively 1 g/ml). The cake also protects the filter paper from mechanical damage from the applied test pressure. However, the flow mechanics of polymer fluids are quite different: polymer materials can fully dissolve in water (Lam and Jefferis, 2018) and will flow through a filter paper without cake formation. However, some molecules will adsorb or become entrapped when passing the filter paper; there can also be very small amounts of undissolved solids and gelatinous globules in the fluid. For polymer fluids, the filter paper itself is the controlling element. This difference in behaviour is recognised in Institution of Civil Engineers (2016) which shows the filter press

test as mandatory for bentonite slurry but for polymer fluids it is noted "if required in project specification". It is described as "not applicable" for polymer fluid management in EFFC/DFI Support Fluids Task Group (2019).

Given this difference in behaviour, this chapter explores the utility of the API test for clean polymer support fluids and then develops an analysis of the flow behaviour of the polymer fluids through filter papers building on the work presented in Ejezie et al. (2021). The behaviour of ten different filter papers is investigated in conjunction with five polymer support fluids commonly used in industry. A parametric study is subsequently performed to explore the influence of applied pressure, polymer concentration and possible polymer degradation by shearing in the pores of the filter paper. From an analysis of polymer fluid flow in filter papers with a range of pore sizes and over a range of pressures it is found that the API test may be used as a rapid indicator of the apparent viscosity of polymer fluids flowing in porous media such as soils at the high shear rates that may occur in high hydraulic conductivity soils. The principle findings from this work have been published in McNamara et al. (2024b) and McNamara et al. (2024a).

3.2 Materials and methods

3.2.1 API test apparatus and procedure

Figure 3.1 shows a schematic illustration of the standard API test apparatus. A sample of polymer fluid is poured into the test chamber which is then pressurised using the laboratory air supply. The desired pressure is maintained using a precision regulator and monitored using an electronic pressure transducer. The applied pressure causes a flow of polymer through the filter paper (of area 45.8+/-0.6 cm^2 (American Petroleum Institute, 2009)), which is in turn supported on a fine mesh; the resulting filtrate mass is measured using a low-capacity load cell. The pressure transducer and load cell are logged at a rate of 1 Hz using a data acquisition system. The test is stopped once 250 g of filtrate is obtained (the maximum capacity of the API cell is about 450 ml). Modifications to the apparatus were avoided to ensure the current industry practice.

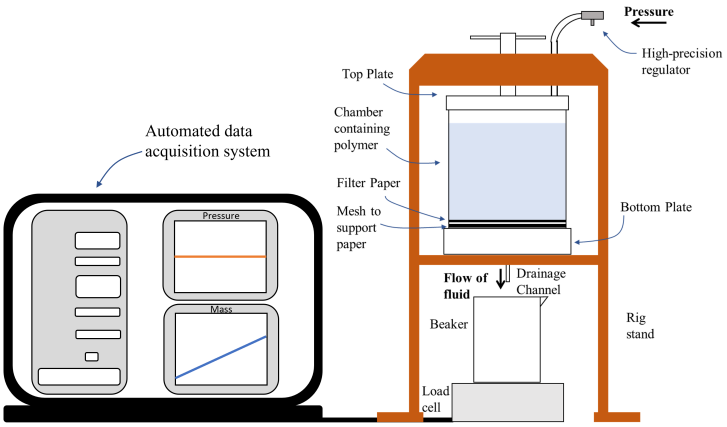


Figure 3.1: Schematic of the API filter press test set-up, instrumentation, and data acquisition system.

3.2.2 Tested polymers

Since procuring a pure HPAM with a known degree of hydrolysis and molecular weight is difficult, the polymers tested throughout the project were commercial products encountered on-site. This enables the research to be directly attributed to real-world methods and observations. Similarly, the solutions were prepared with treated tap water, rather than deionised or distilled water, which are unlikely to be used for mixing purposes on-site. The following subsection provides details on each polymer product used, its supplier, and a brief description.

- **SlurryPRO CDP, KB** - The primary KB product, an HPAM, that has been used successfully on UK projects for several years. According to its supplier, it is suitable for a variety of soil and water chemistries and is capable of forming a synthetic membrane at excavation walls.

- **SlurryPRO CDP PA, KB** - A KB product that is not listed on the company website, but was used on the Silvertown Tunnel Project, London. The only synthetic polymer not labelled as an HPAM. Instead, it is labelled as a polyacrylate. It has a lower molecular weight than HPAM, and a shorter chain length.

- **Shore Pac, Cetco** - Thought to be a purer chemical product, the supplier describes Shore Pac as suitable for a variety of drilling, trenching, and walling applications.

- **Super Mud, PDS Co** - An HPAM polymer, used in drilled shafts (bored piling), diaphragm wall construction, and slurry trenching.
- **LTP 709, Bauer** - This product was supplied directly to the project under this label, though there is limited mention of it available online. The product is an HPAM used in piling and diaphragm wall operations.
- **EZ Mud, Baroid** - This product is the only polymer product in the investigation that was an emulsion. The product is used primarily as a borehole stabiliser and added to drilling fluids to increase lubricity and fluid viscosity.

3.2.3 Polymer fluid preparation

The polymer fluids were prepared using Oxford City tap water pre-treated with sodium hydroxide to pH 10.6 to precipitate calcium (as calcium carbonate, the carbonate ion being derived from the bicarbonate ion naturally present in the tap water which is converted to carbonate on raising the pH) and magnesium ions (as magnesium hydroxide). These ions are present in the tap water prior to treatment at mean values 89.8 mg/l and 5.1 mg/l for calcium and magnesium respectively (data obtained from Thames Water, the water undertaker). At pH10.6 the calcium ion concentration should be reduced to <1 mg/l and the magnesium to <3 mg/l. The magnesium ion concentration could be further reduced by increasing the pH but 10.6 was adopted as reasonably typical of site practice. Both calcium and magnesium ions can inhibit 'stretching' of the polymer chains, and the development of polymer fluid viscosity. A pH of 10.6 also helps to inhibit microbial degradation of the polymer (Mohanan et al., 2020). Twenty litres of the treated water are pumped into a 'mixing tank' and agitated using a bespoke aeration system with tuneable vigour. The polymer is carefully sifted into the agitated water to minimise the risk of agglomerates of undissolved polymer remaining in the mix. The mix is stored in opaque 'storage tanks' to minimise photodegradation and allowed to stand for at least 24 hours for polymer dissolution. The polymer fluid used for the tests was thus a clean fluid as distinct from an in-use site fluid which may contain some suspended soil.

3.2.4 Bentonite slurry benchmarking

Benchmark bentonite slurries were prepared at 40 kg/m^3 by sifting Tunnel-Gel Plus bentonite into Oxford City tap water and mixing with a propeller mixer at 380 rpm rising to 2080 rpm to ensure effective dispersion. The mix was allowed to hydrate for at least 24 hours prior to testing.

3.2.5 Viscosity measurement

The viscosity of the polymer fluids was measured using two coaxial cylinder viscometers: a direct indicating Fann viscometer (used as standard in the construction and oil industries) and a ROTAVISC lo-vi viscometer from IKA. For the Fann viscometer the shear stress, τ, on the bob can be measured at six shear rates, over the range 5.11 to 1021 s^{-1}. For the IKA viscometer τ (Pa) was also measured at six shear rates, $\dot{\gamma}$, but over the range of 0.05 to 264 s^{-1}. For both instruments the apparent viscosity, η (Pa.s) of the fluid at any shear rate, $\dot{\gamma}$ is then determined from the shear stress, τ as follows:

$$\eta = \frac{\tau}{\dot{\gamma}} \tag{3.1}$$

3.2.6 Scope of testing

The base case parameters adopted for the study are presented in Table 3.1. The base case polymer used in the testing was SlurryPRO CDP (a polymer system based on partially hydrolysed polyacrylamide) from KB International at a concentration of 1.2 kg/m^3 which is a typical concentration for excavations in coarser soils. The names of the polymer products are provided to distinguish between them as their chemical formulations are proprietary to the manufacturers. The resulting polymer fluid has a specific gravity of 1.00, which was determined with a fixed volume container with a volume of about 700 ml and an electronic balance with a resolution of 0.1 g. The base case testing focuses on the behaviour of the filter paper. To this end, ten different filter papers are investigated with each paper type subjected to six repeat tests to obtain a measure of repeatability within a paper type. The specifications for the filter papers, as provided by their suppliers, are shown in Table 3.2. After each test, the filter papers were inspected using an Alicona InfiniteFocus microscope. The scope of the

subsequent parametric study is summarised in Table 3.3. Resilience (sensitivity of the fluid itself to degradation and loss of performance) is explored by repeatedly passing the collected polymer filtrate through fresh filter papers for a number of 'passings'.

Table 3.1: Adopted base case parameters.

Parameter	**Type/Value**
Polymer type	SlurryPRO CDP
Polymer concentration, c (kg/m^3)	1.2
API test pressure, P (kPa)	300
Polymer fluid mix age (hours)	$\geq$24

Table 3.2: Descriptions and properties of the adopted filter papers, and mean filtration rate and coefficient of variation for tests with the base case parameter set.

Paper	**Mass (g/m^2)**	**Thickness (µm)**	**Pore size (µm)**	**Supplier's description**	**Mean filtration rate (g/s)**	**Filtration rate coefficient of variation (%)**
Whatman Grade 1 (WG1)	87	180	11	Qualitative	0.217	39.6
Whatman Grade 2 (WG2)	97	190	8	Qualitative	0.416	19.6
Whatman Grade 4 (WG4)	92	205	20-25	Qualitative	3.908	75.0
Fisher Grade 111 (FG111)	84	200	12-15	Qualitative	0.208	46.9
Fisher Grade 113 (FG113)	75	290	8	Qualitative	0.123	39.6
Fisher Grade 114 (FG114)	90	140	3-5	Qualitative	0.036	36.4
Baroid (BP)	98	122	2-5*	Assumed Quantitative, Hardened	0.099	18.7
Whatman Grade 50 (WG50)	97	121	2.7	Quantitative	0.019	38.1
Whatman Grade 52 (WG52)	96	175	7	Quantitative, Hardened	0.935	54.1
Whatman Grade 54 (WG54)	92	185	22	Quantitative, Hardened	2.023	17.3

** Pore size implied from API RP 13B. Hardened papers can be expected to have higher wet strength. Quantitative papers have a low ash weight when ignited, a procedure used in quantitative chemistry. The distinction qualitative/quantitative is of no significance for the fluid loss testing.*

Table 3.3: Parameters investigated in the parametric study.

Parameter	Variation
Polymer type	SlurryPRO CDP, SlurryPRO CDP-PA, SuperMud, EZ-Mud emulsion, Shore Pac
Pressure, P (kPa)	50, 100, 150, 200, 250, 300, 500
Polymer concentration, c (kg/m^3)	0.6, 1.0, 1.2, 1.4, 2.4
Polymer resilience	1, 2, 3, 4 (passings)

3.3 Results

3.3.1 Exemplar results and comparisons to bentonite behaviour

To explore differences in behaviour between polymer and bentonite fluids, API results for the base SlurryPRO CDP polymer are compared with those for the Tunnel-Gel Plus bentonite slurry benchmark. Results using two different filter papers from the same supplier are selected for illustrative purposes: Whatman WG1 and WG54, to cover different paper types (not hardened/hardened) and pore sizes. The measured filtrate mass-time histories are presented in Figure 3.2. The bentonite results show the expected very similar behaviour for both papers, even though the pore sizes differ by a factor of 2, confirming that the flow is dominated by the development of a low-permittivity filter cake. In contrast, there is a marked difference for the SlurryPRO CDP with WG54 yielding a filtration rate 25 times higher than that for WG1 within this tranche of testing. The results demonstrate that API test results for polymer fluids are highly dependent on the particular filter paper used.

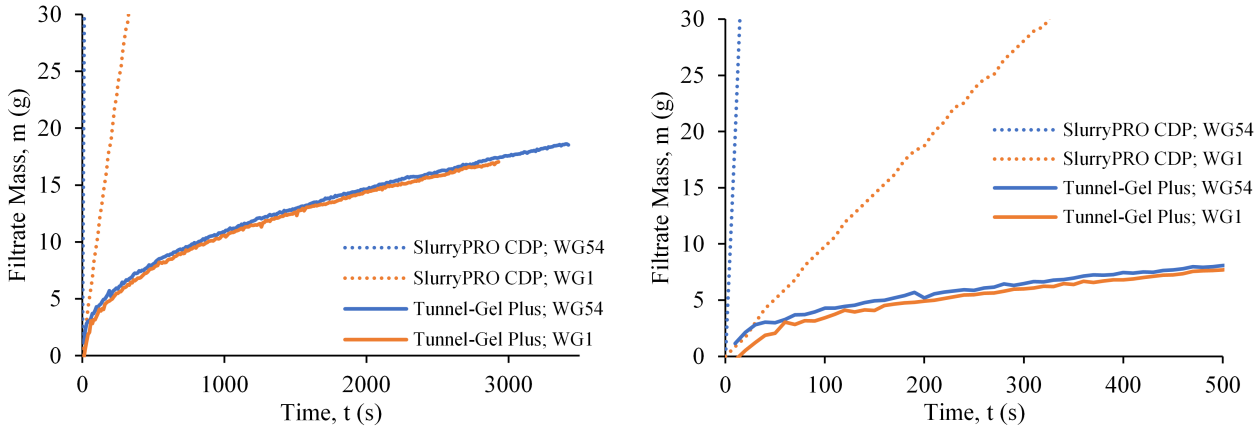


Figure 3.2: Exemplar filtrate mass-time histories for the base case polymer obtained using two different filter papers compared to the bentonite benchmark. N.B. the SlurryPRO CDP; WG54 plot is close to the y-axis. Graph 3.2(b) is as Graph 3.2(a) but with the time axis reduced to 500s to permit the SlurryPRO CDP; WG54 plot to be distinguished from the y-axis. The tests were conducted with the benchmark parameters.

3.3.2 Utility of the API filter press for the assessment of polymer fluids

The reliability of the API filter press for polymer fluids is assessed using repeatability as a proxy, quantified using the coefficient of variation (CV) of the calculated filtration rates, q:

$$\text{CV} = \frac{SD}{\mu} \tag{3.2}$$

Where SD and μ are the standard deviation and mean (respectively) of the filtration rate, q, which is determined from the best-fit line to the complete dataset for a given test (in units of g/s). Examples of repeatability tests are plotted in Figure 3.3 for the SlurryPRO CDP base case parameters as shown in Table 3.1 with the WG1 filter paper. There are significant differences in the calculated filtration rate, q, reflected in a CV of 39.6%. The results also reveal two noteworthy behaviours: (i) 'damage', indicated by a sharp increase in filtration rate (e.g. Test 2) and (ii) 'clogging', indicated by a gradual reduction in the filtration rate due to possible blocking of the pores or swelling of the filter paper fibres (reduction in filtration rate was seen in some tests with just water, see later discussion). The absence of a filter cake leads to full test pressure being applied across the filter paper alone. This resulted in several distinct 'pinprick' penetrations, which were not seen in visual inspections prior to the tests but were confirmed by microscope imaging of the paper after the tests, as shown in Figure 3.4. These papers were typically damaged near the location of the discharge point (near the centre of the cell) and so any damage was relatively easy to identify. The pinpricks explain

the sharp increases in filtration rate observed in Tests 2, 3 and 6. Note, the tests were run at 300 kPa; had the API standard test pressure of 100 psi (689 kPa) been applied then more damage would likely have occurred.

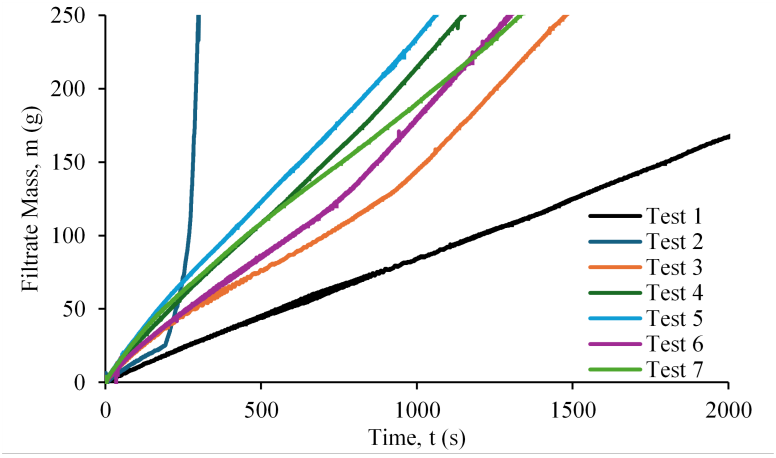


Figure 3.3: Repeatability testing using SlurryPRO CDP: filtrate mass-time histories for WG1 filter paper using the base case parameter set. N.B. there is early slowing around 100s in the tests 3-7, the only plot that seems to keep to this trend is test 7.

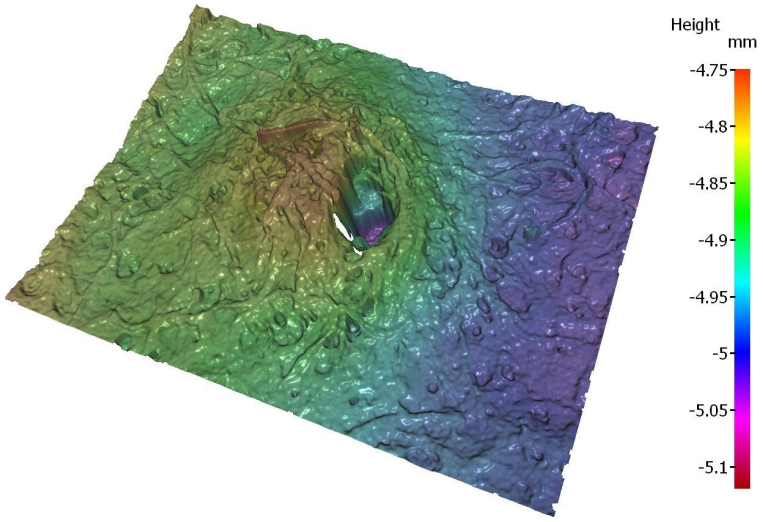


Figure 3.4: Optical microscope image of a 1.43 mm × 1.09 mm patch of Baroid filter paper following testing conducted at 300 kPa showing a clear perforation caused by polymer filtration.

To further explore the influence of the filter paper type, results for all ten filter papers are compared in Figure 3.5. The results show the key dependence of the filtration rates on the type of filter paper used with differences by a factor of 233 obtained for identical polymer samples. In all cases, tests that showed a sharp increase in filtration rate were confirmed as having experienced damage to the filter paper using microscope imaging. These tests highlight the role of the filter paper and the importance of linking API test results to the

exact paper used. The repeatability study identified WG54 as having the lowest CV (17.3%) which is closely followed by WG2 (18.8%) and Baroid (18.7%) papers. It is noteworthy that WG50, a paper noted in the API 13B standard as an 'example of a suitable product available commercially', showed a high CV of 38.1% which would be wholly unacceptable for on-site quality control of polymer fluids. The WG54 flow plots are shown in Figure 3.6. There is good linearity of the mass-time plots (i.e. no evidence of clogging perhaps because of the large pore size) and no evidence of damage.

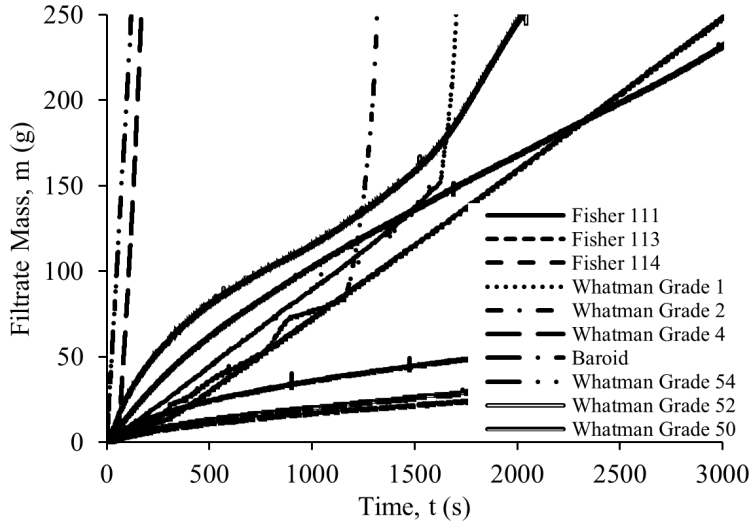


Figure 3.5: Influence of filter paper type on filtrate mass - time histories using the base case parameter set (see Table 3.1) and polymer fluid.

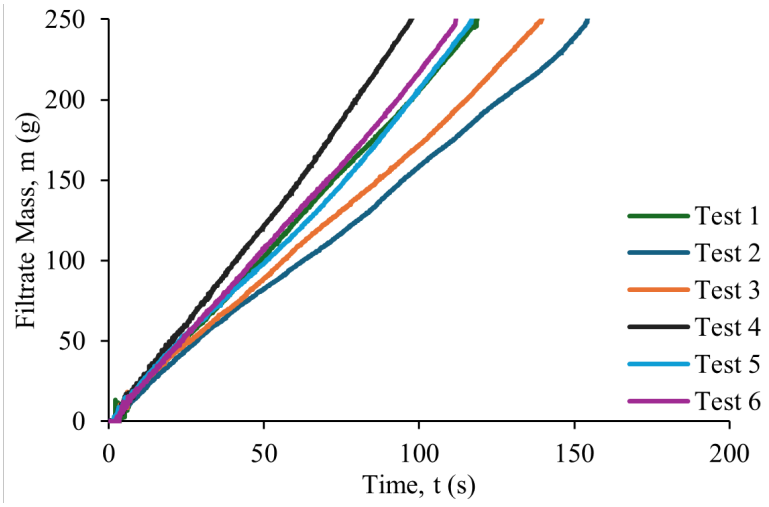


Figure 3.6: Repeatability testing: filtrate mass - time histories for WG54 filter paper using the base case parameter set and polymer fluid.

3.4 Parametric study

3.4.1 Influence of polymer type

A parametric analysis is used to explore whether the API test, using an appropriate filter paper (WG54 in this case), is a useful discriminator of polymer behaviour. The influence of polymer type on the filtration rate, q is shown in Figure 3.7. The polymer types tested are as shown in Table 3.3. The HPAMs (KB SlurryPRO CDP, Shore Pac, Super Mud) showed the lowest filtration rates, implying the highest fluid viscosities at a polymer concentration of 1.2 kg/m^3. The higher filtration rate measured for EZ-Mud is because it is an emulsion, and not all the emulsion mass will be active polymer. The KB SlurryPRO CDP-PA is a polyacrylate for which the manufacturer recommends a higher in-use concentration of 2-3 kg/m^3 rather than 1.2 kg/m^3 recommended for KB SlurryPRO CDP in coarse soils.

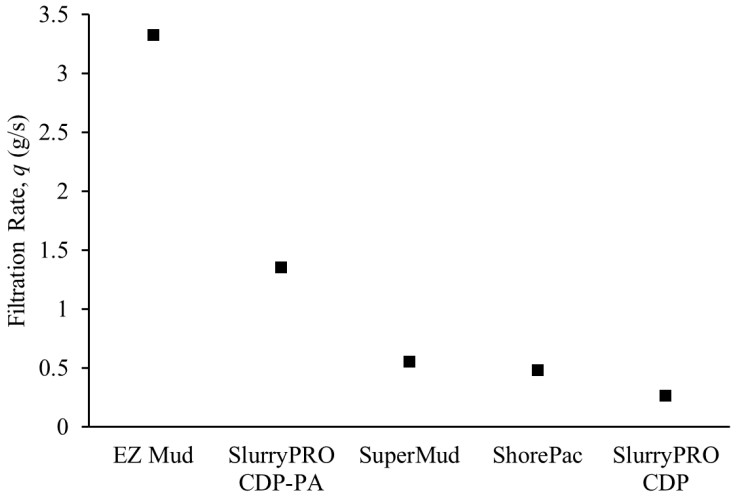


Figure 3.7: Influence of polymer type on the measured API filtration rate, conducted with WG54; c = 1.2 kg/m^3, P = 300 kPa.

The apparent viscosity of each of the polymer fluids at a concentration of 1.2 kg/m^3 was determined using the Fann viscometer over its full range of shear rates: 5.11 to 1021 s^{-1}, the results are presented in Figure 3.8 as log-log plots which show the expected linear behaviour of shear thinning power law fluids. Comparing Figures 3.7 and 3.8, the high viscosity of the SlurryPRO CDP is reflected in a low API filtration rate with the low viscosity EZ Mud showing the highest filtration rate though this behaviour was not consistent across all the polymers; the polyacrylate SlurryPRO CDP-PA had a greater filtration rate than the SuperMud and Shore Pac polymers but a viscosity intermediate between these two products.

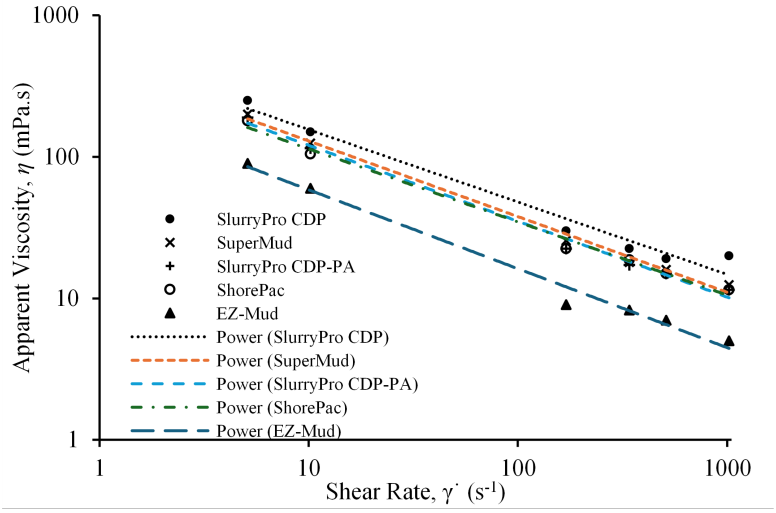


Figure 3.8: Apparent viscosity test results for the series of polymer types tested in the parametric study; $c = 1.2\ kg/m^3$.

3.4.2 Xanthan testing

In addition to the testing of bentonite and synthetic polymer fluids, a brief investigation of the behaviour of a naturally derived polymer, xanthan, was undertaken using the API filter press. This was to investigate whether there was different behaviour between synthetic and naturally derived polymers. As shown in Figure 3.3, the synthetic polymer solutions typically showed a constant flow rate through the filter papers (in the absence of damage) whereas the xanthan solution showed significant clogging behaviour as shown in Figure 3.9. Research on xanthan identified that its production via bio-fermentation often results in the presence of cells and cell debris. As Yang et al. (1998) noted, this contamination lowers the filterability of the xanthan solution and limits its industrial applications. Whilst this is problematic in enhanced oil recovery, which was one of the applications considered by Yang et al. (1998), reduced filterability can be advantageous for geotechnical excavation support fluids. To test the significance of debris clogging in the API test a sample of the xanthan fluid was centrifuged for 10 minutes at 3800 g and then tested. The resulting flow plot has a constant filtration rate, similar in behaviour to the synthetic polymer fluids.

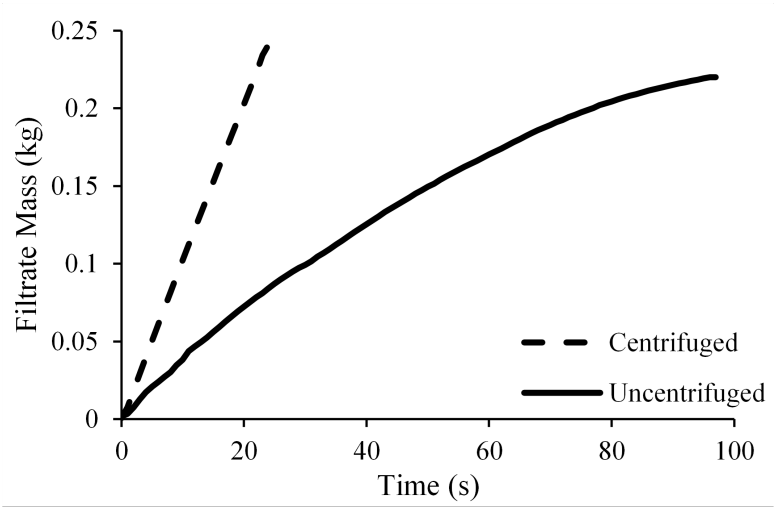


Figure 3.9: Filtration mass against time for two samples of xanthan fluid, one sample has been centrifuged to remove debris from the fluid, the other has not. It is clear from these plots the effect the particles clogging have on the performance of the fluid. These tests were performed with a xanthan fluid mixed in distilled water at a concentration of 1.2 g/l, 1 hour after mixing, the pressure applied was 300kPa, and WG52 papers were used.

3.4.3 Influence of concentration

The influence of polymer concentration on filtration rate was investigated for the base case SlurryPRO CDP; the results are presented in Figure 3.10. An increase in polymer concentration causes an apparently logarithmic decreasing trend in filtration rate reflecting the increase in viscosity. The greater concentration of polymer led to a greater fluid viscosity and so a decreasing filtration rate. The logarithmic trend shows that adding more polymer to a fluid brings diminishing benefit in reducing filtration rate.

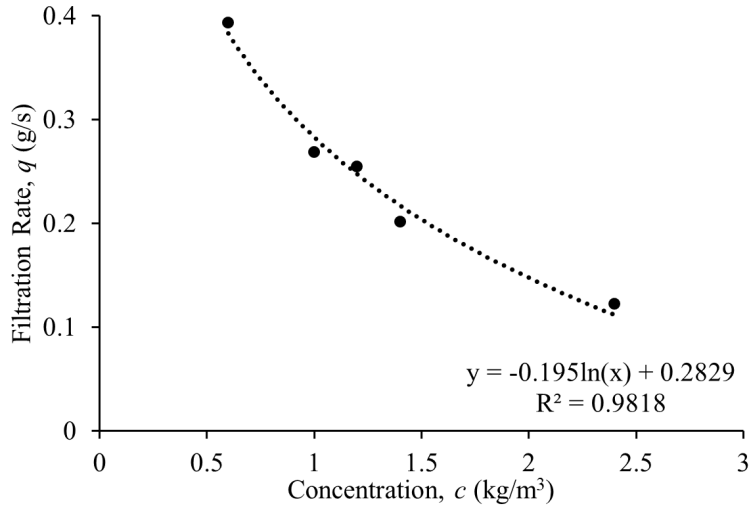


Figure 3.10: Influence of polymer concentration on the filtration rates for the base case polymer fluid; SlurryPRO CDP, P = 300 kPa.

3.4.4 Repeated passing through a filter paper

Figure 3.11 presents the results of repeated passes of the polymer fluids through a single type of filter paper. The first pass using fresh polymer fluid and subsequent passes using the filtrate from the previous pass. For each polymer type, the measured filtration rate, q, for each pass is normalised by the value for the first pass, q_1. The polymer with the most resilient performance in this test is the SlurryPRO CDP, whereas EZ Mud exhibits a significant drop in performance. At the end of the first pass, globules of hydrolysed polymer were observed to partially cover the filter paper post-test for all polymers, except for the emulsion EZ-Mud, with the potential to block some of the pores in the paper (an emulsion polymer can be expected to dissolve more rapidly and fully). As most of the globules would be expected to be filtered out at the first pass (indeed none were visible to the naked eye in later passes), an increasing number of passes should significantly reduce the quantity of globules and therefore their impact. The increase in filtration rate shown in Figure 3.11 might be attributed to removal of globules. However, for EZ-Mud which had the lowest resilience to repeat testing there were no visible globules at any stage. The behaviour of the polymers in these tests might be ascribed to shear degradation of the polymer chains but should not be taken as evidence that polymer degradation is occurring without confirmatory evidence. Other factors which require consideration are: sorption of polymer onto the filter paper (the weight of polymer in the fluid passed through the paper will be comparable to the dry weight of the paper itself) and mechanical entrapment of polymer molecules which may preferentially remove longer chain molecules which impart higher low-shear viscosity.

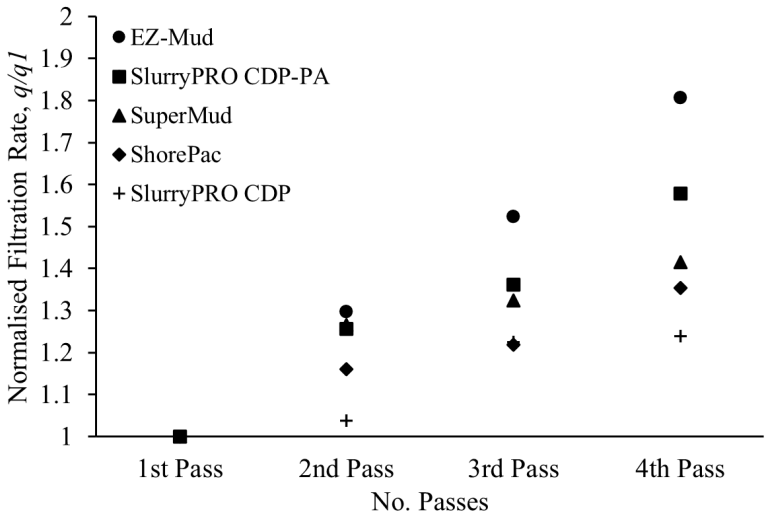


Figure 3.11: Influence of polymer type on the development of the normalised filtration rate with the number of passings through the API filter press; c = 1.2 kg/m^3, P = 300 kPa.

3.4.5 Viscosity measurement with the IKA and Fann viscometers

Figure 3.12 presents apparent viscosity of the polymer fluid, η, against shear rate results for SlurryPRO CDP at a concentration of 1.2 kg/m^3. The tests were performed using both the IKA and Fann viscometers. As previously noted, the IKA can provide apparent viscosity data at shear rates much below those of the Fann viscometer which can provide data at higher shear rates. For shear rates below 100 s^{-1}, the two instruments gave closely aligned results. Above 100 s^{-1} there is more uncertainty, with the Fann viscometer data suggesting that the lower Newtonian plateau may have been reached by about 200 s^{-1} whereas the IKA data suggest that the power law behaviour persists to higher shear rates. Figure 3.12 will be used as the basis for the analysis of the effects of pore size and applied pressure on the filter loss as discussed below.

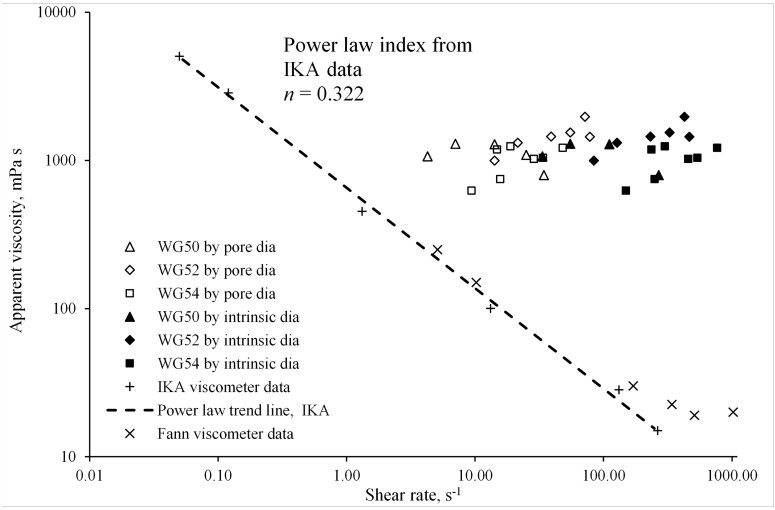


Figure 3.12: Apparent viscosity – shear rate data from rotational viscometry and flow through filter papers for the base case polymer. N.B. The added data for apparent viscosity and shear rate in the filter papers is discussed in pages 56-59.

3.4.6 Effect of filter paper pore size

Figure 3.13 presents a plot of log(mean pore velocity i.e. filtration rate divided by the total open area of pores) against log(supplier's pore size) for each of the filter papers tested using SlurryPRO CDP polymer at 1.2 kg/m^3. The theoretical exponent for diameter, d, for a power law fluid flowing in a capillary is $(n+1)/n$ as shown in Equation 3.3 (see, for example, Chhabra and Richardson (1999) for the derivation of this standard equation):

$$\bar{v} = \frac{n}{3n+1}\left(\frac{\Delta P}{2mL}\right)^{1/n}\left(\frac{d}{2}\right)^{(n+1)/n} \tag{3.3}$$

where n is the power law index for the fluid, m its consistency coefficient (for Newtonian fluids this is its viscosity), $\bar{v}$ is the average fluid velocity over the cross-section of the capillary, and p is the pressure drop over length L of the capillary. For Newtonian fluids which have a power law index $n = 1$, Equation 3.3 reduces to the Hagen-Poiseuille equation:

$$\bar{v} = \frac{\Delta P d^2}{32\eta L} \tag{3.4}$$

From the data shown in Figure 3.12, the n value for the KB SlurryPro CDP from the IKA viscometer is 0.322 (noting that the slope of the line in Figure 3.12 is (n-1)) and thus the theoretical exponent for the pore diameter in Figure 3.12 should be $1.322/0.322 = 4.1$ if the flow in the filter papers behaves as flow in a capillary which might seem reasonable given that

the thickness of the papers is at least 8 times the largest pore diameter (see Table 3.4). However, the best fit line to the data in Figure 3.13 has an exponent of 1.99 (though the coefficient of correlation is very poor at 0.75). From Equation 3.3 the diameter exponent for a Newtonian fluid ($n = 1$) is 2. It therefore seems that polymer fluid is behaving as a Newtonian fluid in the filter papers rather than the power law behaviour shown in the rotational viscometers.

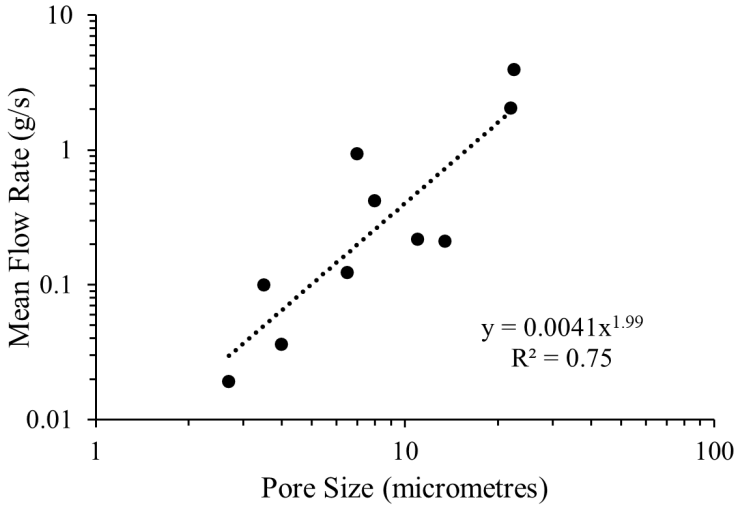


Figure 3.13: Mean filtration velocity as a function of filter paper pore diameter at P = 300 kPa for the base case polymer.

3.4.7 Effect of applied pressure

To further investigate the apparent Newtonian behaviour of the polymer fluids in the filter papers, the relationship between filtration rate and applied pressure was investigated for three filter papers, Whatman WG50, WG52 and WG54 which have pore sizes of 2.7, 7 and 22 microns respectively (see Tables 3.2 and 3.4) and so span the range of pore sizes of the papers used in this investigation. The polymer fluid used for this investigation was that used for the base case, SlurryPRO CDP at a concentration of 1.2 kg/m^3.

Table 3.4: Experimental filter paper properties and derived parameters.

Paper	**Porosity (%)**	**Thickness (μm)**	**Pore Size (μm)**	**Thickness/ Pore Diameter**	**Hydraulic Conductivity (m/s)**	**Intrinsic Permeability (m^2)**	**Calculated Pore Diameter (μm)**	**(Supplier's pore diameter)/(intrinsic pore diameter)**
Whatman Grade 50 (WG50)	49.3	121	2.7	44.8	1.80E-08	1.83E-15	0.35	7.8
Whatman Grade 52 (WG52)	65.3	175	7	25.0	2.77E-07	2.82E-14	1.18	5.9
Whatman Grade 54 (WG54)	68.5	185	22	8.4	4.02E-07	4.10E-14	1.38	15.9

Figure 3.14 shows a log-log plot of mean pore velocity as a function of applied pressure. For the Whatman WG50 paper (the finest of the three papers) there was evidence of damage to the paper at pressures over 200 kPa and so results at higher pressures are not presented. For the coarser paper, Whatman 54, there was no evidence of damage up to the highest pressure used for these tests, 500 kPa. For the WG50 and WG52 papers there was a reduction of filtration rate with volume of filtrate perhaps as a result of some pore blocking so the initial fluid velocities have been used to prepare Figure 3.14 (velocities for a flow of 10 ml corresponding to 2.2 mm of flow over the area of the paper). For the coarser Whatman 54 paper there was no significant reduction in filtration rate with time or flow volume.

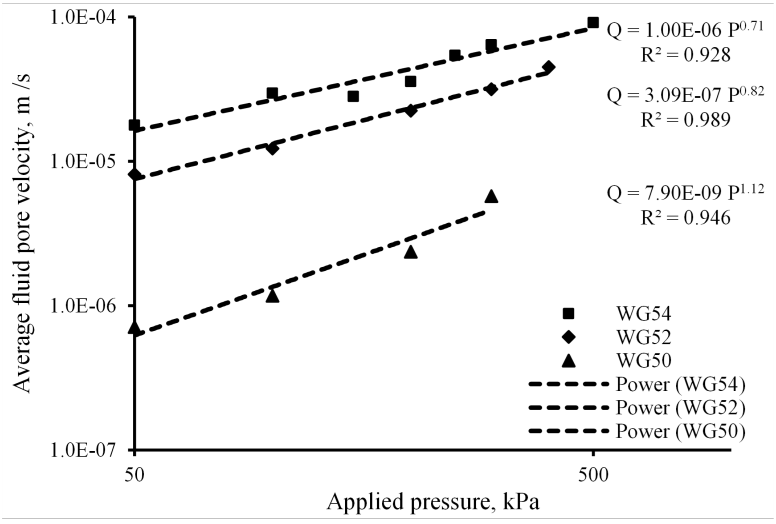


Figure 3.14: Mean filtration rate as a function of filter paper pore diameter at P = 300 kPa for the base case polymer.

From Equation 3.3, if the flow of the polymer fluids in the filter papers can be approximated as the flow in a capillary, then the mean interstitial velocity should be a function of pressure gradient to the power (1/n) or, if L is constant, the applied pressure to the power (1/n). From Figure 3.14, it can be seen that the power law exponents for the WG52 and WG54 papers are 0.82 and 0.71 respectively i.e. slightly sublinear (<1) whereas a trend with $P^{1/n} = \frac{1}{0.322} = 3.1$ would be expected for power law behaviour (see Equation 3.3). The shear rates based on the supplier's pore size data were <100 s^{-1} (see Figure 3.12) and thus from Figure 3.14 were significantly less than the lower Newtonian threshold suggested by rotational viscometry and so power law behaviour would have been expected. The slightly sublinear exponent suggests that the flow may have been tending towards turbulent. However, the Reynolds numbers based on the supplier's pore diameters were all <2x10^{-6} so this seems improbable as the transition to laminar flow in a pipe or capillary would be expected to be >2000 and for flow in a soil greater than about 1. The exponent for the WG50 paper – a paper with a significantly smaller pore size and hence much lower flow rates than for the WG52 and WG54 papers – was 1.12. It can be seen that there is some scatter in the results even on the log-log scale of Figure 3.14, again confirming that the repeatability of flow behaviour between tests with same type of filter paper is limited and thus it would be unwise to draw conclusions from the specific values of the exponents other than that the polymer fluid behaviour in the filter papers appears to have been Newtonian rather than power law.

3.5 Apparent viscosity and shear rate

The initially unexpected Newtonian flow behaviour indicated by both the filter paper pore size and applied pressure data suggested that a different approach was necessary and it was recognised that the flow through the filter papers should be approached as flow in a porous medium and not a flow through a bundle of capillaries.

To further investigate this finding, the hydraulic conductivities (conductivity to water) of the WG50, WG52 and WG54 filter papers were determined. For this it was necessary to use low heads (0.2 and 0.5 m of water) to maintain, as far as practicable, laminar flow in the papers as would be the expected flow condition with the much more viscous polymer fluids and to develop a head - flow calibration for the rig without filter paper so that allowance could be

made for the head loss in the pipework to and from the filter press. The test results showed a slight reduction in flow with time, suggesting the paper might be swelling and reducing pore space. Despite this, a linear line of best fit to the full data set yielded the highest coefficient of determination, and it was used to determine the hydraulic conductivity of the paper. The apparent viscosity of the polymer fluid, η, flowing through the filter paper could then be determined from the relationship:

$$\eta_p = \frac{k_w}{k_p} \cdot \eta_w \tag{3.5}$$

Where k_w is the conductivity of the paper to water (hydraulic conductivity), k_p the polymer conductivity and η_w is the viscosity of water. The polymer conductivity is the equivalent of the hydraulic conductivity when the test fluid is a polymer solution (see Ejezie et al. (2021) for further details). The shear rate at the wall, $\dot{\gamma}$ for a power law fluid flowing in a capillary (Sorbie, 1991) is:

$$\dot{\gamma} = \frac{3n+1}{4n}\frac{8v}{d} \tag{3.6}$$

From the above two relationships (Equations 3.6 and 3.5), the flow velocity – pressure data shown in Figure 3.14 have been converted to apparent viscosity – shear rate data using the supplier's pore diameters given in Table 3.4 as capillary diameters. For the wall shear rate (Equation 3.6), the flow has been assumed to be Newtonian (n=1) as implied by results shown in Figures 3.13 and 3.14 (note for n=0.322, the factor $(3n+1)/4n = 1.53$ so that power law shear rates would be higher by a factor of 1.53). The results have been added to Figure 3.12 as open symbols. From Figure 3.12 it can be seen that the apparent viscosities determined by Equation 3.5 are substantially greater than those found by rotational viscometry over comparable shear rates. This is in line with the findings of Ejezie et al. (2021) for polymer fluid flow in sands who found that for shear rates greater than about 1 s^{-1} the apparent viscosities calculated from polymer conductivities for flow in sand were substantially higher than those from rotational viscometry (see their Figures 8a and b). It also can be seen that the apparent viscosity for the flow in the filter papers is largely independent of shear rate, though with some scatter. This suggests that the lower Newtonian threshold had been reached in the filter papers but as can be seen from Figure 3.12, at much lower shear rates

than in rotational viscometry. Again, this is in line with the findings of Ejezie et al. (2021) – as shown in their Figures 8a and b.

3.6 Pore diameter from intrinsic permeability

The above analysis is based on shear rates determined using the supplier's pore diameters for the filter papers. However, for porous media such as sands only a grain size distribution is available and thus researchers have had to adopt alternative routes for estimating the pore diameter, d_s, to be used in shear rate predictions. To enable comparison of the filter paper data with porous media data, pore sizes for the filter papers have been derived using an approach regularly used for porous media. This approach equates the flow in a porous medium to that through a bundle of capillaries which gives the result (Sorbie (1991), Ejezie et al. (2021)):

$$d_s = 2\sqrt{8K/\phi} \tag{3.7}$$

where K is the intrinsic permeability of the medium and ϕ its porosity. Equation 3.7 is the formulation adopted by Ejezie et al. (2021). Verst et al. (2022b) included a tortuosity factor of (25/12) in the numerator of Equation 3.7 to recognise the tortuous nature flow in porous media. Tortuosity factors other than (25/12) may be adopted, see the discussion by Verst et al. (2022b). Recognising that there is no generally agreed factor and that the effect is modest ($\sqrt{(25/12)} = 1.44$), Ejezie et al. (2021) used Equation 3.7 without added factors. This approach has been adopted in the analysis. The intrinsic permeability can be obtained from the hydraulic conductivity k_w of the medium:

$$K = \frac{\eta_w}{\rho_w g} k_w \tag{3.8}$$

where η_w is the viscosity of water, ρ_w its density and g the acceleration of gravity. The intrinsic permeability of each of three filter papers was determined from their measured hydraulic conductivities. Pore diameters calculated from the intrinsic permeability (herein referred to as intrinsic pore diameters) of the three filter papers have been included in Table 3.4 from which it can be seen that they are all less than the supplier's figures. It also can be

seen that the ratio of the supplier's pore diameter to intrinsic diameter are 7.8, 5.9 and 15.9 for papers WG50 (finest), WG52 and WG54 (coarsest) respectively so that for this, albeit small data set, no single tortuosity factor, nor simple linear function of pore size can achieve equality between the two measures of diameter. As intrinsic pore diameters were lower, it follows that shear rates based on them will be higher than those based on supplier's pore diameters. Shear rates by intrinsic pore diameter have been added to Figure 3.12 as filled data points (the open data points are by supplier's diameters). It should be noted that the apparent viscosities are unaffected by the choice of pore diameter as they are based on hydraulic (water) and polymer conductivities alone. The intrinsic diameter data points in Figure 3.12 can be compared directly with Figures 8a and b of Ejezie et al. (2021), who used the same calculation procedure though it should be noted that they used a different HPAM product (Cetco Shore Pac) prepared with distilled water whereas for the current work treated Oxford tap water was used. Ejezie et al. (2021) found that as shear rates increased beyond 1 s^{-1} the apparent viscosity for flow in sand was about an order of magnitude higher than that from rotational viscometry. For the present tests with filter papers at comparable shear rates (by intrinsic pore diameter) the difference was greater at about 1.5 orders of magnitude. It may be noted that Lam et al. (2015a) estimated the shear rates in soils under field conditions to be in the range 0.8 to 800 for soils with a d_{10} range from 63 μm to 6 mm with hydraulic gradient from 0.1 to 10.

An important new finding from this analysis of flow through filter papers is that the API test, if operated at low pressures to avoid filter paper damage, may provide a rapid field procedure for assessing the apparent viscosity of polymer fluids at high shear rates in porous media (coarse soils). Porous medium apparent viscosities at high shear rates cannot be obtained from rotational viscosity and up until now their determination has had to be via laboratory soil column testing. In excavation practice the apparent viscosity in high hydraulic conductivity soils (perhaps greater than 10^{-3} m/s) is very significant as there is a risk of bulk fluid loss and so the risk of excavation instability when using polymer fluids in these soils.

3.7 Implications for current practice

As a result of this work the following recommendations have been made to the industry regarding the use of the API filter press for polymer fluids (McNamara et al., 2024b).

Test reliability and standards: The testing confirmed that for polymer fluids the key control is the filter paper and importantly it showed that there can be substantial variation in the test results even when papers of the same type are used. The coefficient of variation, CV, a measure of repeatability, was high for all the paper types tested. Indeed it was too high for any of those investigated to be useful for field control of polymer fluids. It may be noted that even the WG50 paper, a paper stated in the API 13B standard to be an "example of a suitable product available commercially" for use in the filter press showed an excessive CV (38.1%). The Whatman Grade 54 was found to provide the most repeatable fluid loss flow rates. The Baroid paper supplied for use with the API press had a comparable coefficient of variation of 18.7% but because of its finer pore size it showed much lower flow rates, rates which can be more easily monitored in a field test.

Filter paper selection: in the absence of a filter cake a paper can be damaged by the applied pressure. Filter paper damage identified by post-test microscopy highlights the importance of using robust, hardened filter papers and low pressures when testing polymer support fluids using the API filter press device.

Use as an indicator of viscosity in coarse soils: the initially unexpected apparently Newtonian behaviour of the polymer fluids when assessed from flow - pore size and flow - pressure data showed that flow in the filter papers must be treated as flow in a porous medium. From this it follows that the API filter press test, if operated at low pressure (to avoid paper damage) could be used to obtain a rapid indication of the lower bound of the apparent viscosity of polymer fluids in porous media at the shear rates induced in the filter papers (4 to 80 s^{-1} by paper pore diameter and 30 to 800 s^{-1} by intrinsic pore diameter and thus from Lam et al. (2015b) representative of flow in coarser soils). This apparent viscosity can be obtained from the ratio of filtration rate with water to that with polymer fluid, as per Equation 3.5 (i.e. the ratio of hydraulic conductivity of the filter paper to its polymer conductivity). For this, it is recommended that a filter paper with a small pore size is used, such as the Baroid paper as flow rates will be lower than with a coarser paper such as the

Whatman 54. Slower flow will allow better resolution of the filtration rate and there will be lower relative head loss in the filter press pipework than across the filter paper. The impact of the poor repeatability of filter paper flow rates could be minimised by first measuring the hydraulic conductivity (water permeability of the paper) and then its polymer conductivity using the same filter paper (i.e. without changing the paper in the press). For research, porous stones of known properties could be used in place of filter papers, but for site testing, costs would be unacceptable as the stones would have to be replaced after each test. This lower bound (lower Newtonian viscosity) for the apparent viscosity in porous media cannot be obtained by rotational viscometry; both Ejezie et al. (2021) and the present author have found this porous media viscosity to be substantially higher than the apparent viscosity from a rotational viscometer at the same shear rates. The much higher viscosity will usefully reduce polymer fluid loss rates in coarse soils where shear rates will be high.

Continued use in industry: If fluid loss tests are used to investigate the behaviour of polymer fluids containing suspended excavation soil, then the fluid loss volume should be recorded as a function of time rather than as a single volume at 30 minutes. The resulting volume - time plot should then be inspected for evidence of cake formation (apparent from a slowing in the filtration rate towards linearity with square root time if the cake build-up controls the flow) or damage (shown by a sharp increase in filtration rate). If the filter press is used to investigate the development of cake thickness for polymer fluids containing suspended soil, then the results should be reported as volume of cake per unit volume of filtrate. Filtration rate data also should be obtained for the clean (no suspended solids) polymer fluid so that the impact of any cake-building by the fluid can be assessed; that is, does the cake significantly impact the filtration rate? It may not.

3.8 Summary

This chapter has described an investigation of the suitability of the API filter press test for the assessment of polymer fluid properties. API test results for a benchmark bentonite slurry were shown to be insensitive to the particular filter paper used as the test result is governed by the permittivity of the filter cake. In contrast, the lack of filter cake formation for ‘clean’ polymers (except perhaps for some globules of swelled but not fully dissolved polymer) means

that API flowrates are controlled by permeation of a viscous fluid rather than filter cake formation. The outcome of the test is therefore controlled by the type of filter paper used. It is shown that tests with different filter papers will yield fundamentally different results due to three key matters: pore size of the filter paper, damage, and clogging (swelling of the filter paper, if it occurs, was minor) and that there will be considerable variability between results even if a single type of paper is used. The API procedure is not suitable as a field control test for polymer fluids. However, the unexpected Newtonian behaviour of polymer fluids suggests that the test, if conducted as suggested in the chapter, could provide a rapid indication of the lower bound of apparent viscosity in porous media. In summary: this chapter has demonstrated that for all ten of the filter papers investigated the coefficient of variation between repeat tests is such that the API test is not suitable for the day-to-day quality control of polymer fluids on-site. However, under laboratory conditions the test can give rapid and valuable insights into polymer fluid behaviour.

4 An investigation of heterogeneity in polymer fluids and its impact on civil engineering applications

4.1 Introduction

Although polymer fluids have distinct physical and chemical properties compared with bentonite, at the site level there can be a tendency to manage the two fluids as if they were the same. There is an unmet need to develop new testing techniques for industry and to put in place the necessary training programmes to utilise them effectively.

As the construction industry continues to adopt and refine the use of polymer fluids, unexpected behaviours and properties continue to be encountered. One such phenomenon involves the development of viscosity variations within a single fluid body, resulting in fluid heterogeneity. This heterogeneity is unexpected and is not a documented or indeed recognised behaviour in civil engineering practice. Its implications are significant, affecting key aspects of industry practice, including fluid mixing, sampling and quality control testing, as well as interactions between the fluid and surrounding soils.

This chapter presents a laboratory investigation employing a novel application of a 'dropping ball' rheometer to examine these poorly understood heterogeneities in polymer support fluids and the implications for field practice. This test provides a method for assessing bulk fluid behaviour, unlike other techniques that can investigate only small sample volumes. It enabled a supplementary study to evaluate the effects of two environmental factors: temperature and UV exposure. The findings from the work will inform best practice for mixing, storing, and testing polymer fluids on-site, so facilitating more effective use of polymer support fluids.

4.2 Theory and method

4.2.1 Theoretical overview

The apparent viscosity of a fluid can be determined from the vertical velocity, v_z, of a ball dropping through a fluid at low Reynolds number, Re (Chhabra and De Kee, 2007). For steady incompressible flow under these conditions, Stokes' Law (1851) can be applied to derive the local apparent viscosity of an equivalent Newtonian fluid at any depth, z in the fluid, $\eta_{(a,z)}$, i.e. the equivalent viscosity of a Newtonian fluid that would give the same fall rate.

$$\eta_{a,z} = \frac{(\rho_b - \rho_f)gd^2}{18v_z} \tag{4.1}$$

Where ρ_b and ρ_f are the density of the ball and fluid respectively, g is acceleration of gravity, and d is the diameter of the ball. Chhabra and De Kee (2007) note that the use of free-falling objects to infer flow properties has been shown to yield reliable results for Newtonian fluids. In contrast, the approach is problematic for non-Newtonian fluids because neither the shear stress nor the shear rate are uniform around the ball. However, most non-Newtonian fluids (except for visco-plastic and time-dependent fluids) approach Newtonian fluid behaviour in the limit of small Reynolds numbers (Chhabra and De Kee, 2007). The Reynolds number for a falling ball can be defined as:

$$Re = \frac{\rho_f v_z d}{\eta_{a,z}} \tag{4.2}$$

For Stokes' law to be valid, Re must be less than 1. Achieving this condition requires selecting a ball with an appropriate density and diameter to ensure a suitably low Reynolds number. However, the large variations in fluid viscosity mean that maintaining Re < 1 is challenging. The chosen material and diameter for the ball enabled tests to be completed within a reasonable time frame while ensuring a reasonably low Re in the least viscous regions.
To evaluate the viscosity distribution with depth, the velocity of the ball was measured over 100 mm depth intervals down the column. The CV of the resulting viscosity measurements was then determined as follows:

$$CV = \frac{SD}{\mu} \tag{4.3}$$

Where SD and μ are the standard deviation and the mean of the determined viscosities for a given drop test, respectively. The CV is used as an indicator of the fluid heterogeneity (viscosity variation). A low CV implies a relatively uniform fluid throughout the depth of the column whereas a high CV indicates the development of discrete viscous regions.

4.2.2 Polymer fluid preparation

The water treatment procedure for this part of the study is identical to that detailed in Section 3.2.3. The treated water was stored in a 120 L storage tank. Treating and storing this quantity of water is beneficial as it provides a consistent mix water over a series of tests.
On construction sites, polymer may be mixed mechanically but the usual practice is to use bubbler bars. In the laboratory, following water treatment, 1.2 kg/m^3 of dry polymer powder was mixed with 8 L of water using either a low-speed planetary mixer or by bubbling. For the planetary mixer, the polymer powder is carefully sifted into the water to minimise the build-up of polymer on the paddle and the mixer bowl. The mix is stirred for 7.5 minutes and a spatula is then used to remove any undissolved polymer adhering to the bowl and paddle. The mix is then stirred for a further 7.5 minutes as the polymer continues to dissolve. For polymer mixing by bubbling, air was introduced through a system of perforated PVC pipes at the bottom of a tank containing the treated water. Dry polymer powder was gradually sifted into the bubbling water. The mix was then bubbled for an additional 15 minutes which was sufficient for visually complete polymer dissolution. In some of the present tests, the fluid was deaired by placing it in a vacuum chamber. The fluid pressure is reduced to and held near -1 bar (0 absolute) until the entrapped air bubbles within the sample have been released.
Some samples of polymer fluid were prepared using isopropyl alcohol (IPA) whereby the polymer powder was 'pre-wetted' with a small amount of IPA. The surface tension of IPA is 23.0 mN m^{-1} at 20 °C, significantly lower than that of water (72.8 mN m^{-1} at 20 °C), mitigating polymer 'clumping' by penetrating between and wetting the polymer particles more effectively. This pre-wetting facilitates a more uniform distribution of the polymer in the water during subsequent mixing. Distilled water was then added gradually to the fluid

whilst it was agitated with a magnetic stirrer. Once 1 L of water had been added to the fluid, the mix was transferred to a larger container where more water was added whilst being bubbled. After 15 minutes of bubbling, the fluid was deaired under a vacuum and then transferred to the column and left quiescent for 24 hours.

4.2.3 Testing programme

The base case parameters considered for this investigation are shown in Table 4.1. The parameters adopted to explore the effects of sunlight and temperature are shown in Table 4.2. These parameters were selected either because of their relevance to industry or because they offer insight into the heterogeneity phenomenon:

- Common commercial polymer products were tested to investigate how each product performs and how its viscosity develops. The polymer products tested (supplier shown in brackets) in this investigation were SlurryPro CDP and SlurryPRO CDP PA (KB), LTP709 (Bauer), SuperMud (PDSCo), EZ-Mud (Baroid), and Shore Pac (Cetco).

- Polymer concentrations of 0.5, 1, and 2 times the base case value were tested to ensure the range covered all values likely to be used on site.

- The drop test also permitted investigation of photodegradation of the bulk fluid. Photodegradation is known to be destructive to polymers. Thus, it is prudent to investigate the extent of damage in the fluid and whether the industry needs to act to prevent such degradation on site.

- As mentioned previously, the polymer fluid is mixed mechanically or by bubbling. It is important to determine whether a particular mixing method may allow contractors to achieve better polymer performance in the field.

- An increase in temperature reduces viscosity; therefore, temperature variations may influence viscosity development and contribute to variability in field test results. Also, temperature variations within a body of fluid will set up convection currents, which may lead to differential movement of more and less viscous regions within the fluid.

Table 4.1: Adopted base case parameters.

Parameter	Type/Value
Polymer type	SlurryPRO CDP
Polymer concentration, c (kg/m^3)	1.2
Polymer fluid standing time after mixing (hours)	24
Ball material	Delrin (polyoxymethylene)
Ball diameter (mm)	8
Ball mass (g)	0.37
Ball density (g/cm^3)	1.384

Table 4.2: Parameters and their ranges explored in this study.

Parameter	Variation
Polymer products	SlurryPRO CDP, SlurryPRO CDP-PA, SuperMud, LTP709, EZ-Mud emulsion, Shore Pac (old product), Shore Pac (new product)*
Concentration, c (kg/m^3)	0.6, 1.0, 1.2, 1.4, 1.6, 2, 2.4
Mixing Method	Bubbling, low-speed mechanical mixing
Photodegradation	Non-exposed/Exposed to UV
Temperature (°C)	10.4, 18.4

** The old Shore Pac product is the same product that was used by Lam and reported in Lam et al. (2014, 2015). While ageing during storage may have influenced its properties, the product serves as a reference point. It is not known whether the formulation of the new product differs significantly from the original.*

4.2.4 Experimental setup

The adopted experimental set-up is shown in Figure 1. Polymer fluid is mixed and poured into a 1 m tall Perspex column. An important consideration is that HPAM molecules are susceptible to degradation when exposed to ultraviolet (UV) radiation from sunlight. UV radiation can be categorised into three types based on wavelength: UVC (100–280 nm), UVB (280–315 nm), and UVA (315–400 nm), the shortest wavelength radiation having the highest energy. Perspex can prevent exposure to UVC and UVB radiation but leaves the fluid susceptible to UVA radiation (Charp, 2017). To prevent this, the column was covered with opaque black plastic to protect it from photodegradation when not being used for tests. The local ambient temperature is recorded with a logger. Following a pre-determined standing time, a ball is dropped into the fluid from a specified height and a camera records the position of the ball at a rate of 60 frames/s. Python programming is used to (i) split the resulting

video into a series of frames, (ii) identify the centre of the ball in each frame, and (iii) track the centre coordinates from frame to frame to determine the velocity. The ball coordinates in pixels can be converted into metric distances by calibrating against the height of the column. The ball is tracked using a discriminative correlation filter with channel and spatial tracking (CSRT) (Lukežič et al., 2018). The method adjusts the filter to focus on the part of the object best suited for tracking, using a spatial reliability map to ensure accuracy. This approach helps create reliable tracking software.

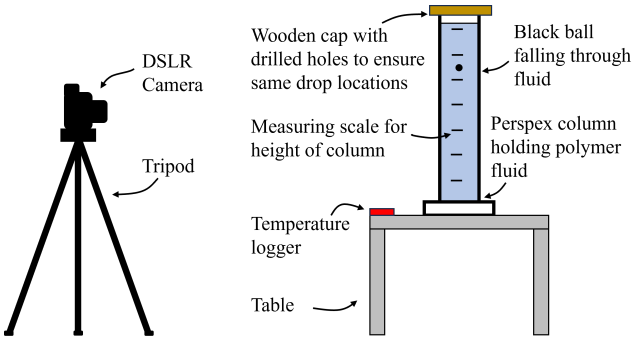


Figure 4.1: Arrangement of the falling-ball test apparatus

Rotational viscometry was also undertaken to obtain baseline viscosity data for the polymer fluid. The viscometer is a ROTAVISC lo-vi from IKA with coaxial cylinders for shearing and a water jacket for temperature control. A narrow gap geometry (inner and outer radii of 17.5 and 19 mm) was used. The resulting shear rate ($\dot{\gamma}$, s^{-1}) can be determined from the radii and rotational speed and the shear stress (τ, Pa) is calculated from the torque applied to the bob. With the chosen geometry, the viscometer was operated over the range of shear rates from 0.05 s^{-1} to 264 s^{-1}. To cover the full range of the apparatus, data are collected at these shear rates and at four intermediate shear rates. The apparent viscosity of the fluid at each shear rate is then determined as per Equation 3.1.

4.3 Investigation of heterogeneity within a column of polymer fluid

4.3.1 Specimen test results

The measured velocity of the ball with depth below the fluid surface and the corresponding inferred apparent viscosity are presented in Figures 4.2(a) and 4.2(b) respectively for an exemplar test using the base case parameters outlined in Table 4.1. Fall velocities were averaged over 100 mm depths and inferred viscosities were calculated using Equation 4.1.

From Figure 4.2(b), regions of high and low viscosity are apparent. In particular, there are markedly high viscosity regions near the surface of the fluid and at a fluid depth of approximately 0.6 m.

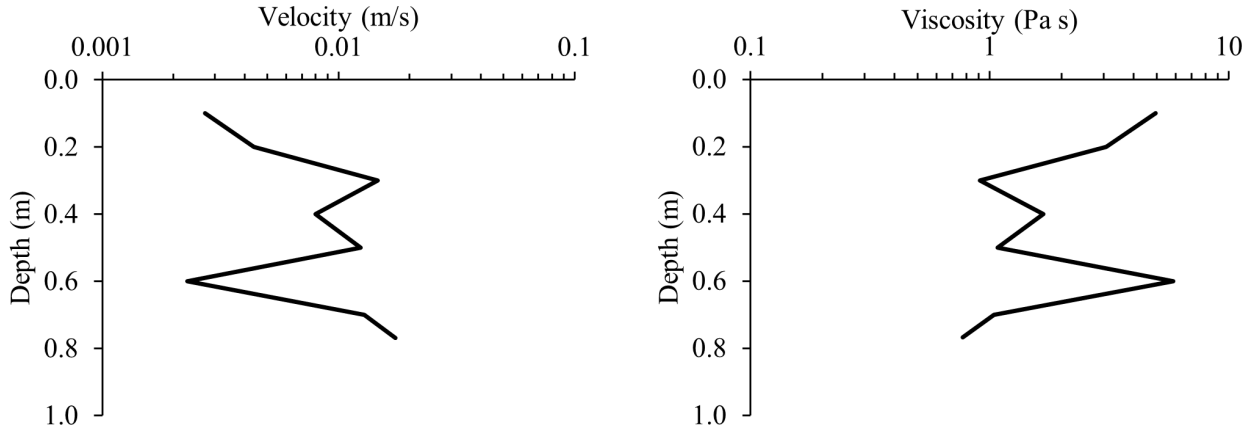


Figure 4.2: (a) Measured velocity of a dropping ball and (b) the corresponding inferred viscosity profile as a function of depth for a polymer fluid using base case parameters (Table 1). Note that the top of the fluid is at the 0.0 m mark, the base of the column in this test is at the 0.8 m mark. However, in later tests a taller column is used and the base is located at the 1.0 m mark.

4.3.2 Verification testing

Initial tests were conducted to assess the reliability, reproducibility, and sensitivity of the proposed drop test to initial conditions. Multiple drop tests were performed on the same fluid sample to evaluate repeatability. Successive drop tests were carried out at the same location within the fluid at 1-minute intervals. Figure 4.3 presents (a) measured velocity and (b) inferred viscosity profiles with depth for eight successive ball drops. It can be seen that there is quite a large variation in viscosity near the surface of the polymer. This variation reduces after the first depth measurement increment, though there is still variation by a factor of half an order of magnitude. There is general repeatability of viscosity trends between tests, if not the absolute values of viscosity, mostly revealing similar regions of high and low viscosity.

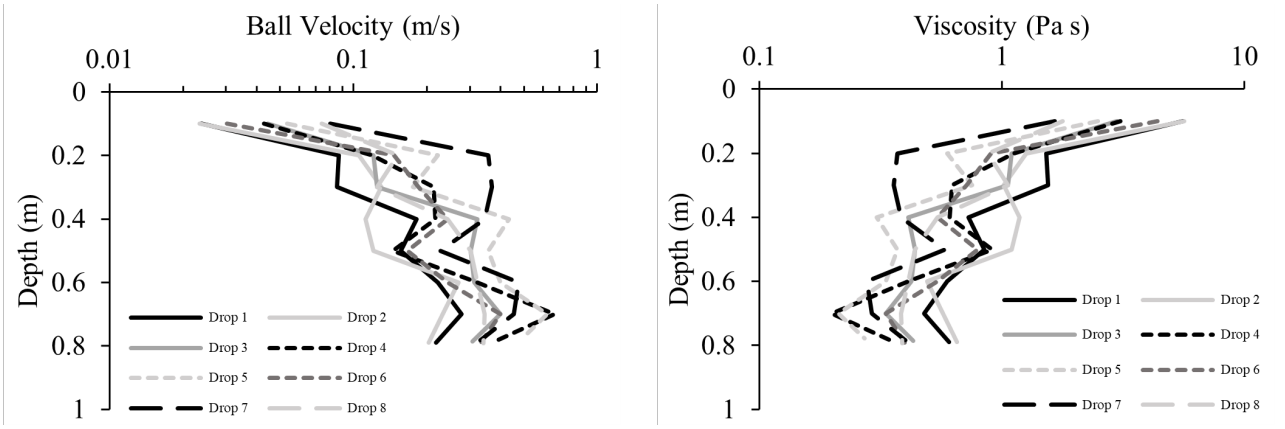


Figure 4.3: (a) Measured ball velocity and (b) inferred viscosity as a function of depth for a polymer fluid subjected to a series of drop tests conducted at 1-minute intervals to determine the repeatability of the testing method using base case parameters, see Table 4.1.

4.3.3 Lateral movement

During these tests the lateral movement of the ball was also recorded. Figure 4.4 plots the lateral (x-axis) movements as a function of depth to determine the extent of the lateral meander through the fluid for successive ball drops. It can be seen that the balls follow relatively similar paths – within about +/- 6 mm of a notional centreline – with limited lateral variation in the paths. There is also no clear correlation between the velocity values and test sequence e.g. a reduction in viscosity with repeated exploitation of a single pathway if preferential paths were being formed through regions of lower viscosity.

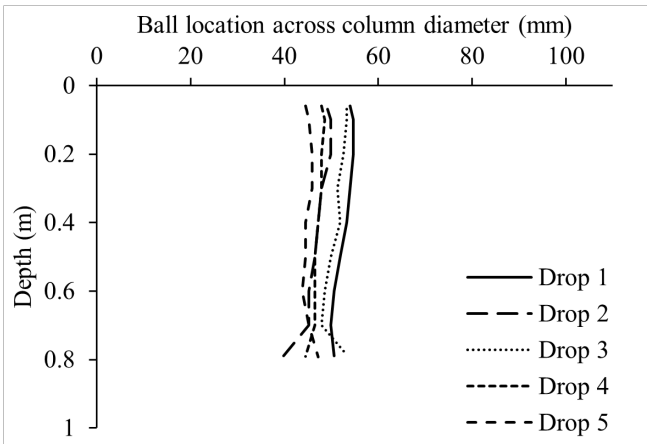


Figure 4.4: The horizontal movements for five individual drop tests conducted for repeatability assessment. The width of the column was 100 mm.

4.3.4 Drop height

To assess the sensitivity of the results to the drop height, a ball was dropped from heights ranging from 50 mm to 200 mm above the fluid surface in increments of 50 mm. The balls were dropped at the same location in the same sample at approximately 5-minute intervals, to allow for a readjustment of the equipment after each drop. Figure 4.5 presents the velocity-depth profile for each of these drops. The drop test results appear insensitive to the initial drop height with good agreement between the four tests. It can be seen that the velocity of the ball after contact with the fluid rapidly becomes controlled by the viscosity of the fluid rather than the velocity of the ball on impact. A drop height of up to 200 mm seems to affect the results to a depth of 10 cm into the fluid, but no further. These results help to validate the legitimacy of the method.

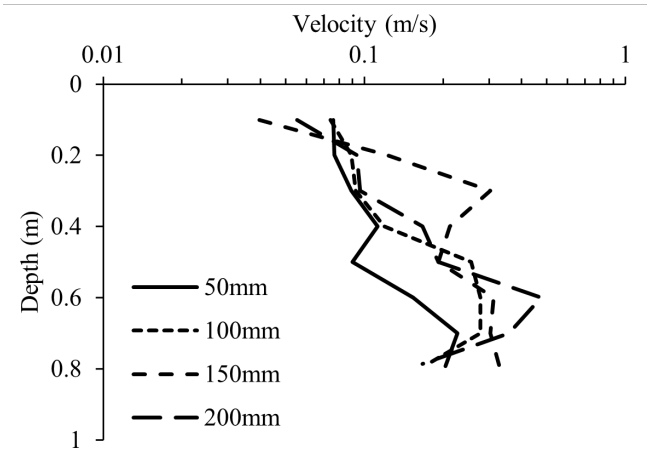


Figure 4.5: The velocities of balls dropped at heights of 50, 100, 150, and 200 mm as a function of depth for a polymer fluid using base case parameters Table (4.1).

4.3.5 Polymer dissolution

Further experiments were performed to verify that the observed phenomenon was not a result of the adopted mixing method, perhaps because it does not achieve full dissolution of the polymer granules. Figure 4.6 compares results with and without pre-wetting of the polymer granules with IPA coupled with the use of deionised water in place of Oxford tap water for solution preparation. It can be seen that the combination of pre-wetting and de-ionised water increased the viscosity of the fluid, greater than with de-ionised water alone, with some of the highest results recorded in the investigation. The exceptionally high viscosity throughout the entire column results from the absence of ions that typically induce polymer chain curling by

interacting with like charges along the polymer structure. Additionally, the use of IPA facilitates efficient low-shear dissolution, further contributing to the increased viscosity. However, alcohol wetting did not prevent the development of a heterogeneous fluid with structured regions of differing viscosity. This result indicates that the structuring is not a consequence of the mixing procedure, both bubbling and IPA wetting gave heterogeneous fluids.

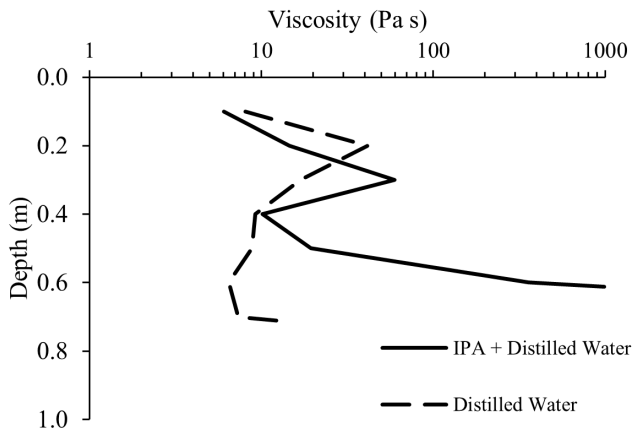


Figure 4.6: The viscosity as a function of depth for a polymer fluid wetted with isopropyl alcohol prior to mixing. For comparison, a plot of viscosity for a drop test conducted with polymer fluid prepared using distilled water only. N.B. the x-axis is on a log scale to accommodate the extremely high viscosities measured.

4.3.6 The effect of standing time on viscosity development

Figure 4.7 examines changes in polymer viscosity over 48 hours, focusing on the development of high-viscosity regions with time after mixing the polymer fluid. The results indicate that viscosity profiles remain relatively uniform immediately after mixing, but significant changes occur when the fluid is left undisturbed. Within 3 hours, the viscosity increased across the sample, with localised high-viscosity regions emerging. By 12 hours, these variations became more pronounced, showing substantial increases in viscosity; this trend continued up to at least 48 hours post-mixing. These findings suggest that the polymer fluid does not achieve a homogeneous state within the supplier's recommended 24-hour standing time after mixing. At 48 hours, the fluid maintained persistent inhomogeneity, but relatively similar viscosities to those measured at 24 hours, indicating a possible reduction in further network development processes but no trend to a homogeneous fluid. This raises concerns about the consistency of the fluid used in field applications, as contractors may be sampling and testing and then

deploying a non-uniform mix, potentially affecting performance during excavation. This is particularly problematic given the lack of insight into the underpinning mechanism(s).

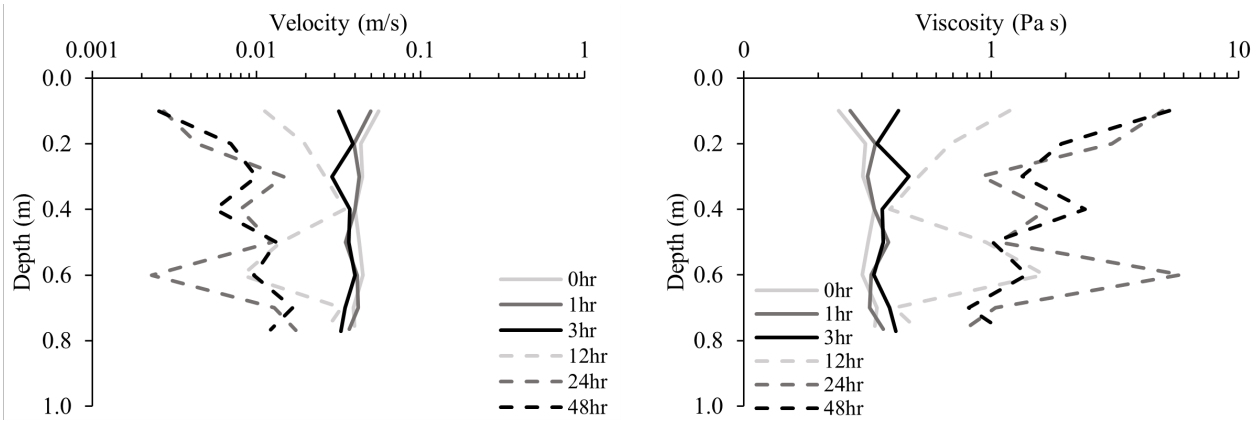


Figure 4.7: (a) Measured velocity and (b) inferred viscosity as a function of depth for a KB SlurryPRO CDP polymer fluid (1.2 kg/m^3) over a standing time of 0 to 48 hours.

4.3.7 Rotational viscometry

To further explore the progression of polymer viscosity over time, complementary rotational viscometer testing was conducted on matching polymer samples at a shear rate of 0.05 s^{-1}. This shear rate was chosen because it represents the lower end of the operational range of the viscometer, thereby providing data that are closest available to the shear rates experienced during soil permeation. This test was run continuously on a sample taken immediately after mixing and monitored over 48 hours. The results show a marked viscosity increase within the first hour, followed by a very minor increase over the remaining test duration (Figure 4.8). These findings provide a contrasting perspective to those presented in Figure 4.7, where the polymer fluid took approximately 24 hours to reach a viscosity suitable for use on-site. The viscometer test was performed on a 6.7 ml sample with continuous slow rotation, whereas the drop tests involved approximately 8 litres of static fluid. This raises questions about the testing of representative samples – specifically, whether a small-scale viscometer test adequately represents the behaviour of larger volumes of polymer fluid. The viscometer results suggest that at a more local level, polymer viscosity may appear fully developed shortly after mixing, indicating potential readiness for application. However, on a larger scale, a full 24-hour period may be necessary and the behaviour of undisturbed bulk fluid may continue to evolve beyond this time. These findings highlight the importance of using appropriate sampling and testing protocols on-site to ensure representative and repeatable

results for effective application. It is important to consider the nature of the shear to which the fluid is subjected in both the viscometer testing and the ball drop experiment. In a rotational viscometer, the fluid is subjected to continuous shear, which may break down polymer networks, whereas the fluid is static up to the arrival of the ball in the ball-drop test. Rotational viscometers can provide an accurate and appropriate characterisation of polymer fluids; however, they are often limited in the range of shear rate-shear stress combinations over which measurements can be made. The viscometer employed in this study had a shear rate range of 0.01 s^{-1} to 264 s^{-1}. While this range allowed useful characterisation of the fluid, it did not enable full measurement of the Newtonian plateaus at very low or high shear rates. In the context of polymer fluid application for bore stability, the zero-shear viscosity, the viscosity of the fluid as the shear rate approaches zero, is particularly important, as it governs the fluid behaviour around soil particles as it advances into the excavation face. Rotational viscometers struggle to directly investigate the approach to the zero-shear viscosity; instruments designed to apply extremely low shear rates often struggle to measure the associated low shear stress with sufficient accuracy. The ball drop test provides an alternative method, enabling the use of spheres of varying size and density to determine fluid properties such as zero-shear viscosity and yield stresses (Chhabra and De Kee, 2007). In this study, spheres of identical size and density were used to enable the identification of heterogeneities within the fluid. The mean shear rate around a falling sphere can be approximated by Equation 4.4 (Godínez et al., 2014):

$$\dot{\gamma} \approx \frac{2v_z}{d} \tag{4.4}$$

Based on this relationship, the shear rates imposed on the fluid during the drop ball test ranged from 0.0034 s^{-1} to 23.6 s^{-1}, applying a lower shear rate range than the rotational viscometer, with both its lowest and highest applied shear rates being lower. It is important to note that the shear rate is set by the fall velocity and can be changed only by changing the ball diameter and/or density. Another noteworthy distinction between the two tests is the sample volume. As noted above, the viscometer used in this study used a sample volume of 6.7 ml of fluid, although other models can accommodate volumes of up to 500 ml. By contrast, the drop ball test was conducted in approximately 8 litres of fluid to give local

apparent viscosities across a substantial volume. Given that polymer networks can span hundreds of millimetres within the test column, the cumulative effect of polymer chain interactions can be investigated. Therefore, the ball drop test effectively inspects the bulk rheological behaviour of the fluid along the fall path, while the small sample volume used in the viscometer limits the volume over which polymer networks can form and the continuous shearing may well disrupt their formation.

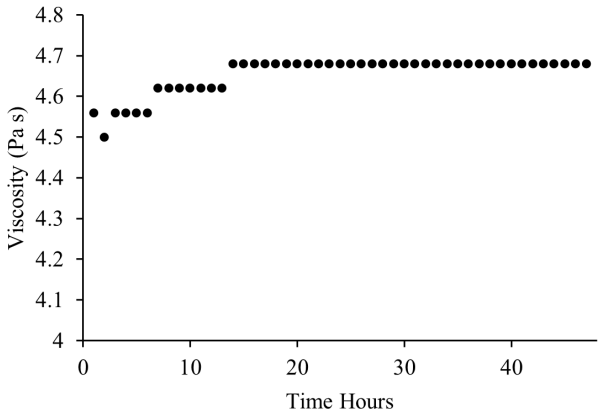


Figure 4.8: Variation of viscosity with time determined with a rotational rheometer at a shear rate of 0.05 s^{-1} for a KB SlurryPRO CDP polymer fluid (1.2 kg/m^3) from 0 to 48 hr from the time of mixing. Note y-axis starts at 4 Pa s.

4.3.8 Influence of de-airing on viscosity development

The drop tests consistently showed a pattern of a region of higher viscosity near the top of the column and lower viscosity toward the bottom. Careful observation of the fluid revealed small, trapped, air bubbles which it was hypothesised were buoying more viscous regions upward. To confirm this hypothesis, polymer fluids were again prepared using a standard bubbling procedure but then de-aired for one hour in a vacuum tank. Drop tests were conducted immediately after de-airing, 1 hour from mixing, and at 24 and 48 hours post-mixing to examine the formation of high-viscosity regions in the absence of trapped air (see Figure 4.9). The removal of the entrapped bubbles by the de-airing process results in the high-viscosity regions now being concentrated near the bottom of the column, suggesting that these regions were slightly denser than the surrounding fluid, causing them to sink. This finding supports the hypothesis that air bubbles significantly influence the vertical distribution of heterogeneity and hence viscosity variation within the polymer fluid.

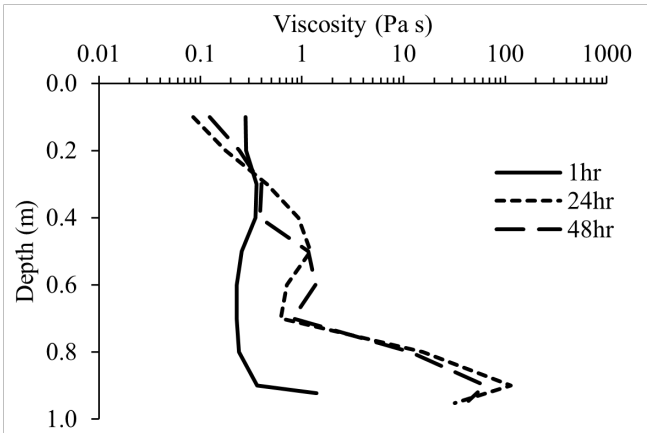


Figure 4.9: The viscosity as a function of depth for a deaired polymer fluid using base case parameters (Table 4.1) for a KB SlurryPRO CDP polymer fluid (1.2 kg/m^3). N.B. the high viscosity regions are now located exclusively at the base of the column. Note from this figure onwards in this investigation the base of the column is located at the 1.0 m mark.

These findings have important implications for the testing of polymer solutions mixed by bubbling on-site. Samples collected from the upper regions of a bubble-mixed tank may exhibit higher viscosities than those taken from a medium depth within the tank. This discrepancy could lead to a significant overestimation of the overall viscosity of the fluid. This also may occur in excavations or storage tanks if air bubbles remain trapped. In an undisturbed tank, higher viscosity regions are likely to form both at the top, due to trapped bubbles, and at the bottom as dissolving polymer granules tend to sink. This phenomenon may explain anecdotal observations of significantly higher viscosities in freshly mixed polymer compared to samples taken during excavation in the field. To ensure more representative viscosity measurements, samples should be inspected for air bubbles before testing. Additionally, bubbler bars in the mixing tanks should be set to induce fluid circulation, in addition to agitating the fluid, to help maintain a more uniform viscosity. On-site viscosity is typically assessed using a Marsh funnel with a 1.5 L sample, but it is not feasible to de-air the test samples in the field, though a double funnel test suggested in Bridges and Robinson (2020) may help – the test sample is passed through the funnel and then through the funnel again. Times may be recorded for each test to see if there is an effect. Attention to the mixing set-up and sampling procedure is crucial to minimising viscosity inconsistencies in the sampled fluid.

4.3.9 Effect of mechanical shear on polymer viscosity

To investigate whether high-viscosity regions in the polymer fluid can be disrupted and subsequently re-formed, a sample was prepared, de-aired, and left to stand in a column. A plate mixer (shown in Figure 4.10) made from a threaded steel bar and a series of three plastic plates with holes drilled through them out of phase with the alternating plate. This mixer allows the fluid to be remixed whilst exposing the fluid to a minimum of air entrainment. For each remix, the mixer was pushed up and down through the fluid column five times at 1-minute intervals.

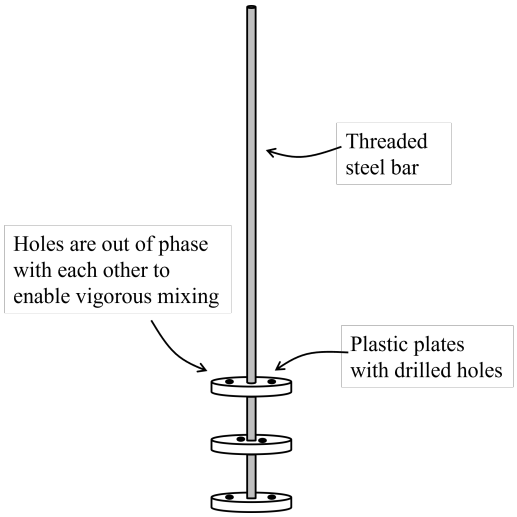


Figure 4.10: Diagram of plate mixer used to excite and mix polymer fluid without introducing air into the solution.

The first drop test was performed 1 hour after the mixing, following the deairing of the fluid. A further test was then conducted after the fluid had been left undisturbed for 24 hours. The fluid was then remixed with the plate mixer and tested immediately thereafter. This process was repeated at 48 hours and 192 hours (all times from initial mixing). Due to the time required for deairing, higher viscosity regions had already formed at the surface and 0.4 m depths at 1 hour after mixing (see Figure 4.11). The 24-hour test, before the first remixing, revealed further development of significant viscosity heterogeneity. Indeed, polymer networks developed to such high viscosities that the test could not be completed within the battery life of the camera. However, after remixing, the viscosity heterogeneity was much less pronounced, indicating that the high-viscosity structures had been broken down, resulting in a more homogeneous fluid. After the remixing at 24 hours, the viscosity of the fluid never returned to the same level achieved before remixing, possibly as a result of some damage to

the polymer chains from the shearing. The change in homogeneity is reflected in the CV for the 24-hour results: before remixing, the CV was 1.26, whereas after remixing, it dropped by 72% to 0.35. This difference demonstrates a substantial reduction in heterogeneity. To further analyse the structural changes, viscosity gain factors (η_x) were calculated by dividing the viscosity determined at each 100 mm interval (η_z) by the average viscosity (over the fluid depth) from the initial 1-hour test ($\eta_{t=1}$) as follows:

$$\eta_x = \frac{\eta_z}{\eta_{t=1}} \tag{4.5}$$

The viscosity gain factor provides insight into the extent to which the fluid viscosity changes in each region down the column over time. As shown in Figure 4.12, the viscosity gain in the quiescent fluid is relatively large throughout the column, with significantly greater gains in some regions. In contrast, the remixed fluid exhibits a much lower viscosity gain, with some regions previously showing a large gain now revealing a viscosity only marginally greater than that achieved just 1 hour after mixing. This shows that remixing disrupts the high-viscosity structures, resulting in a more uniform fluid. However, in the ball drop tests, there was no significant reduction in viscosity; equally, there was no further significant increase in viscosity. It seems that there is a tendency to a more homogeneous fluid with time and repeated mixing, possibly promoted by the remixing.

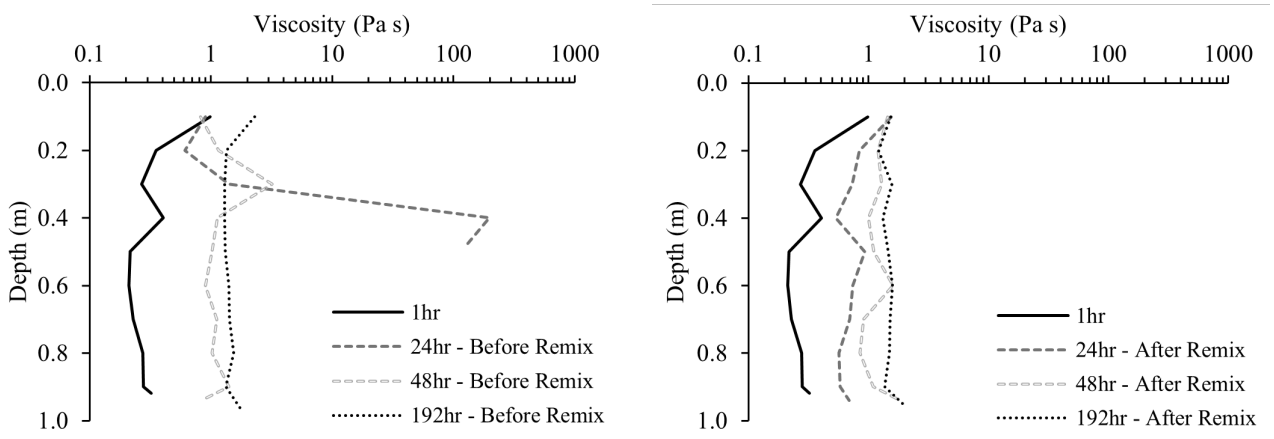


Figure 4.11: The viscosity as a function of depth for (a) a polymer fluid that has been left undisturbed for a period and (b) the same polymer after it has been remixed at each time step using base case parameters (see Table 4.1). A drop test was conducted immediately after mixing and deairing and then several more tests were conducted over several days on the fluid after periods of quiescence and then immediately after remixing.

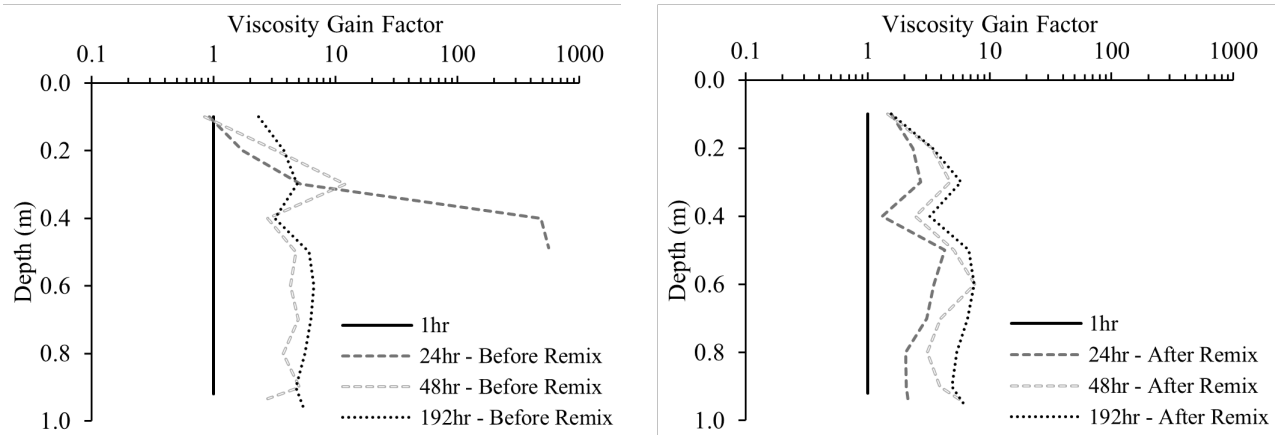


Figure 4.12: The viscosity gain factor as a function of depth for (a) a polymer fluid that has been left undisturbed for a period and (b) the same polymer after it has been remixed at each time step. The viscosity gain factor is calculated by dividing the viscosity in each region by the inferred viscosity immediately after mixing and de-airing. This parameter provides insight into the viscosity development in each region of the fluid.

To simulate possibly more realistic agitation of the polymer fluid by a piling rig, tests were conducted using an 80 mm diameter propeller spinning at 200 rpm at the base of the column. The propeller was run for 15-minutes, lifting to the surface every 5 minutes. Propeller mixing was performed after fluid standing times of 0, 12, 24, and 48 hours. A drop test was performed immediately after each mixing. Figure 4.13 shows that this mixing/agitation led to a more uniform fluid viscosity throughout the column. Comparing the results from Figure 4.11, the viscosities after propeller agitation were of a similar magnitude to those after the plate remixing, suggesting that the agitation effectively disrupted localised high-viscosity regions rather than damaged the polymer. The CV for these tests further illustrates that while some variation in viscosity remains, the fluid is significantly more homogeneous than when left undisturbed (see Table 4.3). This suggests that mechanical agitation, such as that provided by a piling rig, can be expected to maintain a more consistent viscosity in polymer fluids during excavation.

Table 4.3: Coefficient of variance of polymer fluid viscosity following exposure to propeller shear.

Fluid standing time (hr)	**CV**
0	0.25
12	0.65
24	0.31
48	0.33

These findings indicate that during active excavation, the polymer fluid can be expected to

maintain a relatively homogeneous viscosity due to the continuous agitation. However, when left to stand, the fluid is likely to form network structures, leading to heterogeneity and the development of regions with significantly higher viscosities compared to freshly agitated fluids. This tendency for viscosity variation highlights the importance of sampling practice, namely that a sample of fluid from a bore that has been standing overnight may not be representative of the fluid as a whole after work recommences and the fluid has been mixed by the passage of the excavation tool.

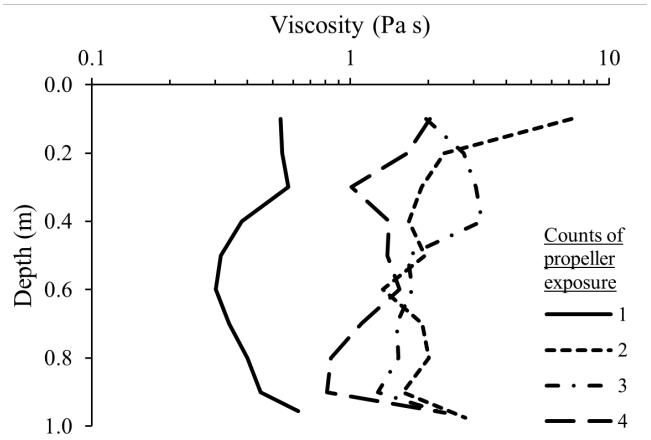


Figure 4.13: The influence of the use of propeller: viscosity as a function of depth for a polymer fluid immediately after 1, 2, 3, and 4 counts of propeller exposure after standing times of 0, 12, 24, and 48 hours, respectively.

4.3.10 Influence of polymer concentration

Batches of polymer fluid over a range of concentrations, as shown in Table 4.2, were prepared to investigate the effect of polymer concentration on viscosity development. As expected, drop tests conducted 24 hours after mixing showed a clear trend of increasing viscosity with higher concentrations (see Figure 4.14). To further analyse this effect, the results are presented in two plots based on the average viscosity recorded at 0 and 24 hours, as presented in Figure 4.15. The data reveal that viscosity increases supralinearly as polymer concentration increases, indicating that even small changes in concentration can lead to significant changes in fluid viscosity (note the viscosity axis of Figure 4.15 is logarithmic). Trend lines fitted to the data in Figure 14 show that viscosity follows an approximately exponential trend with concentration. This exponential relationship highlights the sensitivity of the polymer fluid viscosity to concentration and the need for careful control, especially if polymer is lost by sorption onto the soil, with an exponential reduction in viscosity. Note that the 24 hr results

in Figure 4.15 show more scatter than the immediately after mixing results, suggesting that network formation has a random component.

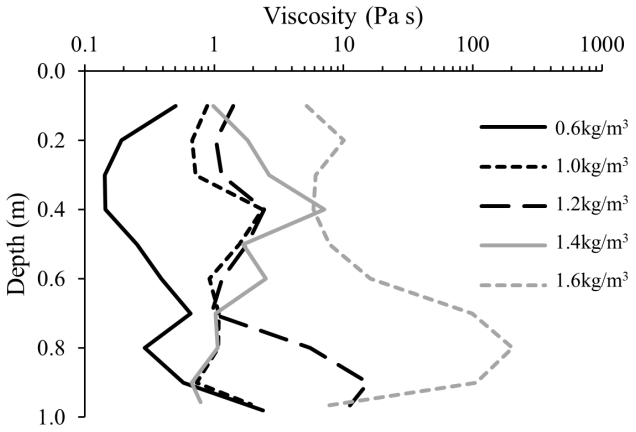


Figure 4.14: Influence of polymer concentration on the variation of viscosity with depth for a polymer fluid using base case parameters (Table 4.1).

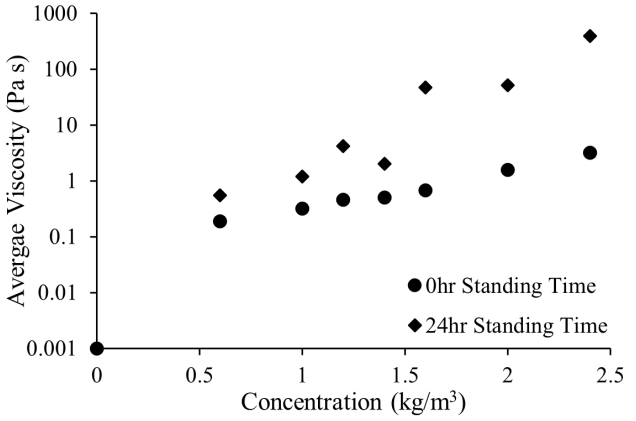


Figure 4.15: Variation of average viscosity of a given polymer mix as a function of the associated polymer concentration. One series of tests is conducted at 0 hours standing time and the other at 24 hours. A reference value for the water solvent (at 20 °C) has been included for reference (corresponding to c = 0 kg/m3).

4.3.11 Concentration and polymer molecular interaction

When considering molecular interactions, polymer solutions can be classified into three concentration regimes: dilute, semi-dilute, and concentrated. In the dilute regime, the rheological properties are primarily determined by the solvent, with minor influence from the dispersed polymer molecules. As the polymer concentration reaches a critical overlapping threshold, the fluid rheology changes significantly, as documented by Lizcano Niño et al. (2020) for hydrolysed polyacrylamides (HPAMs) in brine. The semi-dilute regime can be further subdivided into unentangled and entangled sub-regimes. In the unentangled

semi-dilute phase, polymer molecules are closely packed and in contact with each other, but there is no significant entanglement. In contrast, the entangled semi-dilute regime is characterised by substantial entanglements between polymer chains, leading to a marked increase in viscosity. In the concentrated regime, the fluid behaviour is dominated by the polymer molecules, which are highly overlapped and entangled; the ratio of solvent molecules to monomer units is low, resulting in limited solvent interaction (Agasty and Singh, 1998). Figure 4.16 provides an indicative plot of viscosity as a function of concentration, illustrating indicative trends along with sketches depicting the arrangement of polymer chains in each regime. For the application of HPAMs in civil engineering, the relevant concentration range falls within the semi-dilute regime. The adopted concentrations for support fluids exceed those of the dilute regime and likely straddle the semi-dilute and concentrated regimes.

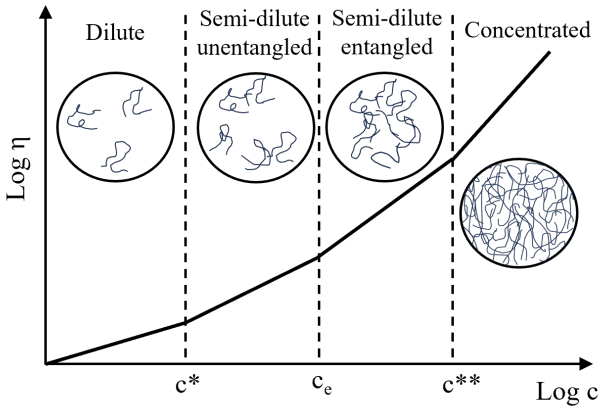


Figure 4.16: Indicative relationship between viscosity and concentration for polymer solutions on a log-log scale showing the transition points at overlap concentration (c), entanglement concentration (c^e), and the initial point of polymer chains interpenetration (c**) (Marani et al., 2015). Sketches have been added to indicate the arrangements of the polymer molecules in each regime. Adapted from Kol et al. (2020).*

4.4 Possible causes of heterogeneity

4.4.1 Phase separation investigation

Phase separation was initially suspected to be the cause of the observed inhomogeneity within the polymer fluid. Phase separation refers to the spontaneous division of a homogeneous liquid into two distinct phases, each characterised by different concentrations of components (Xu et al., 2023). To explore this possibility, a series of drop tests were again conducted on a column of fluid which was mixed, de-aired, and left quiescent for 24 hours. Lower viscosity

regions of the fluid identified by the drop tests were carefully siphoned off to isolate the denser, more viscous portion. A subsequent drop test confirmed the successful isolation of the more viscous fluid. This isolated fluid was then poured into a planetary mixer and remixed for 20 minutes at 235 rpm. The method implemented is presented in Figure 4.17 (N.B. the fluid was subjected to a remixing rate and geometry that were sufficient to ensure proper excitation but minimise molecular damage). If phase separation had occurred, one would expect a significantly higher concentration of polymer molecules in the isolated fluid, leading to little or no change in viscosity after remixing. However, the drop test results presented in Figure 4.18 show a marked decrease in viscosity in the remixed fluid, aligning closely with that of the previously siphoned-off fluid. This outcome suggests that the variation of viscosity within the fluid was not due to phase separation into concentrated and dilute regions.

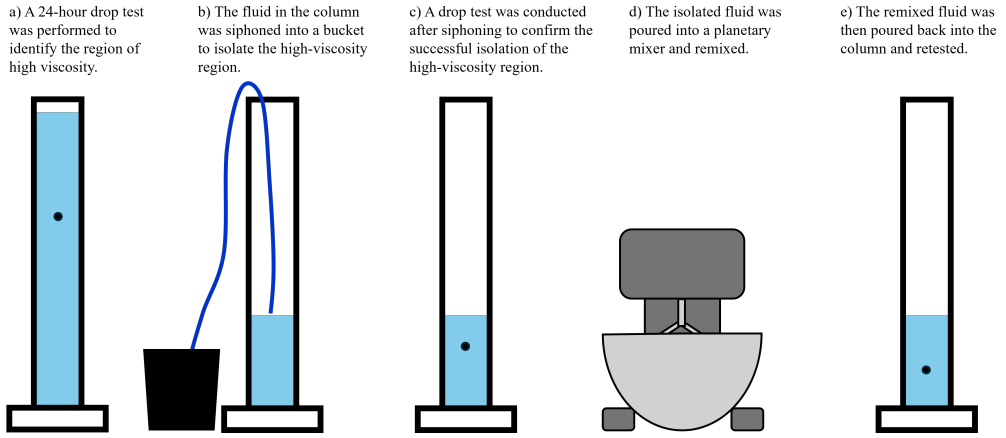


Figure 4.17: The method implemented in the phase separation investigation testing.

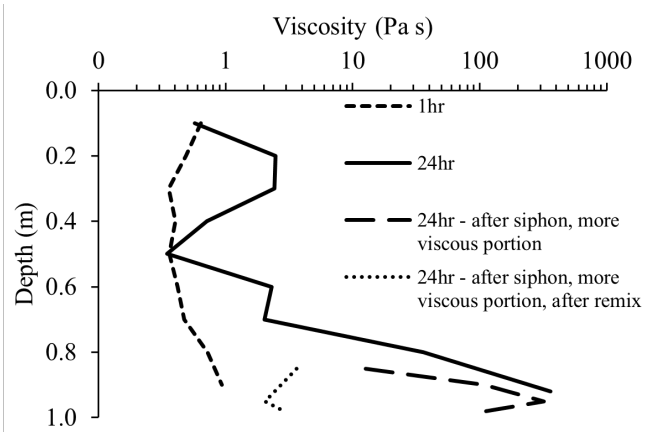


Figure 4.18: The viscosity as a function of depth for a polymer fluid over a series of drop tests conducted to investigate whether phase separation was the cause of the varying viscosities.

To further investigate the possibility of phase separation occurring, specific gravity tests were undertaken. Specific gravity differences would be expected between the more and less viscous

portions of the fluid if phase separation were occurring. To investigate this, testing was conducted using a density meter (Anton Paar, DMA 5001) with a precision of ±5E-06 g/cm^3. Polymer products from three suppliers were selected for testing: KB, Bauer, and Cetco (new product), which is understood to be a relatively pure HPAM product. To establish a baseline, polymer fluid samples were prepared at concentrations of 0.5, 1.0, 1.5, and 2.0 g/L and the specific gravity was measured for samples taken from a well-stirred volume. The results of this testing show that the increase of fluid specific gravity with polymer concentration is relatively modest (see Figure 4.19). The Bauer and Cetco polymers showed very similar specific gravities across the concentration range whereas the KB specific gravities were slightly higher.

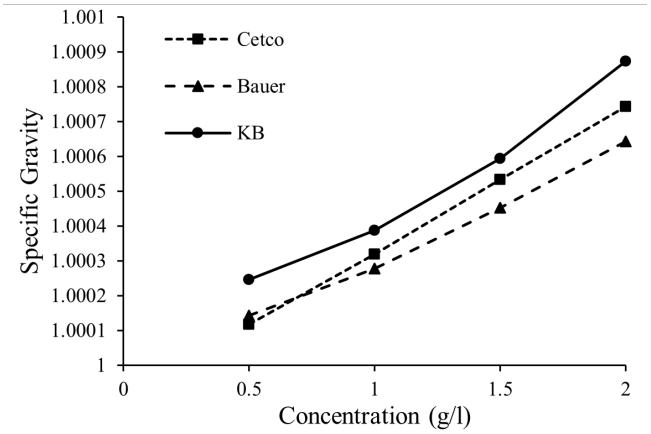


Figure 4.19: Variation of measured specific gravity of polymer samples as a function of concentration for three polymer products (tests at 20°C).

Samples of the high and low-viscosity polymer fluids, which had previously been tested in the viscometer, were also tested using the density meter. The viscosity at one of the measured points, in this case 1.32 s^{-1}, is plotted against specific gravity, as presented in Figure 4.20. This figure does not show the increase in specific gravity correlated with the increase in viscosity, as would be expected with phase separation. The data show that a decrease in viscosity can coincide with an increase in specific gravity, an unexpected outcome given that the high viscosity regions consistently occurred at the bottom of the fluid column. Importantly, the sample of the Cetco fluid that was identified as the higher viscosity region at the base of the column and consequently isolated and sampled (denoted as "Cetco Thick") had a lower viscosity at a shear rate of 1.32 s^{-1} but a higher viscosity at lower shear rates than the "Cetco Thin" sample. In essence, the sample from the base of the column exhibited a greater degree of shear-thinning (a phenomenon whereby fluids exhibit a reducing viscosity with an

increasing shear rate) than the siphoned sample. The higher degree of shear-thinning from the fluid at the base suggests a higher concentration of polymer molecules. However, since the viscosity curves for the two samples cross, the overall difference in viscosity between local zones is less significant than encountered in previous drop tests. It is clear, however, that localised zones of differing viscosity have occurred in the tested samples. These results provide further evidence that phase separation is not responsible for the observed phenomenon. If phase separation were occurring, there would be an increase in the specific gravity with increase in fluid viscosity, reflecting the increased concentration of polymer molecules in the denser regions.

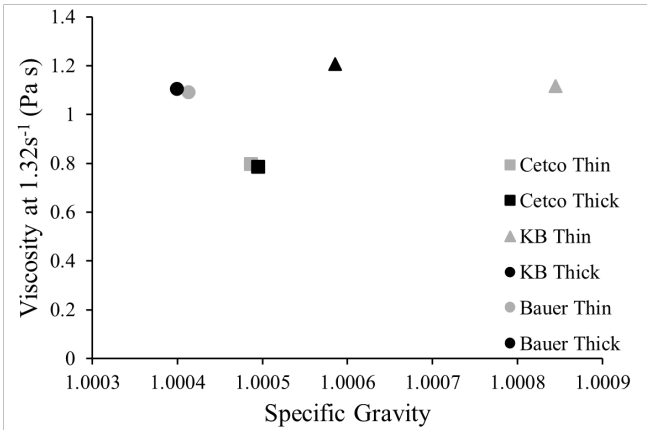


Figure 4.20: The viscosity at a shear rate of 1.32 s^{-1} as a function of specific gravity for three polymer products (measured at 20 °C).

The results of the mechanical shearing experiments and density testing rule out phase separation as the cause of the observed phenomenon, suggesting there must be alternative underlying factor(s). Given the behaviour of polymer molecules in varying concentration regimes, the likely explanation is the development of networks within the polymer solutions. Network formation occurs when polymer molecules form reversible physical crosslinks, creating a weak physical network within the solution. In the case of the HPAM solution, these crosslinks are temporary, with bonds that form and break over time (Rubinstein and Colby, 2003). This behaviour aligns well with the experimental findings. In the unentangled semi-dilute regime, crosslinking occurs at a lower rate, whereas in the entangled semi-dilute regime, crosslinking is more frequent, resulting in significant variations in viscosity. The observed reduction in viscosity following the remixing of high-viscosity polymer fluid suggests that remixing temporarily breaks the crosslinks in the polymer networks, further supporting

this hypothesis.

4.5 Parametric study on factors influencing viscosity and network development

4.5.1 Influence of polymer type

The proprietary nature of the chemical compositions of commercially available polymer fluids presents a significant challenge in explaining differences between products from a theoretical standpoint. Nevertheless, such differences may be significant when selecting the most appropriate product for particular applications. To investigate the differences between products, drop tests were performed on seven commonly used polymer products listed in Table 4.2. A selection of results is shown in Figure 4.21, where drop tests were conducted immediately after mixing, 0 hours, and 24 hours later. The polymer samples were mechanically mixed but tested without de-airing as these tests pre-dated the recognition of the effect of trapped air. The resulting viscosity profiles were again normalised by considering the viscosity gain factor, η_x, as presented in Figure 4.22. The results show significant differences between products. Bauer Slurry LTP709 and KB's HPAMs exhibit the highest η_x throughout, indicating significant viscosity development over time. In contrast, Cetco Shore Pac and KB's polyacrylate (PA) display large viscosities near the surface but maintain similar viscosity levels to the freshly mixed fluid in deeper regions. These findings illustrate how viscosity varies across polymer types and regions within samples, revealing complexities in predicting, testing and managing fluid behaviour in the field.

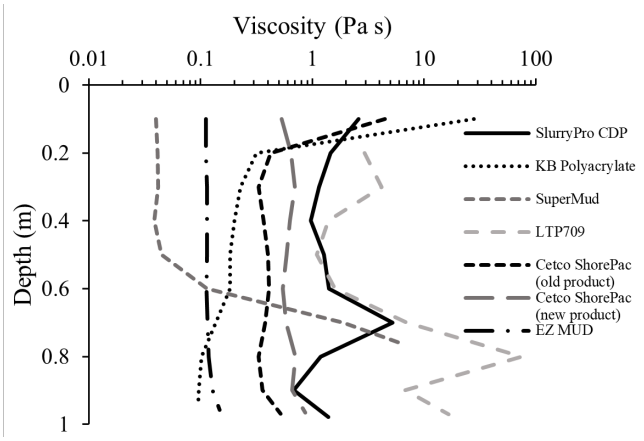


Figure 4.21: Influence of the polymer product on the viscosity as a function of depth using base case parameters (Table 4.1). N.B. the concentration for all products was 1.2 kg/m^3 apart from the EZ Mud which is an emulsion polymer and was prepared at a concentration of 5 l/m^3.

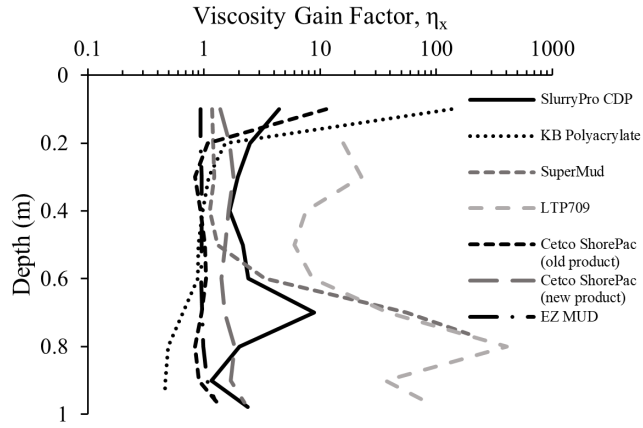


Figure 4.22: The viscosity gain factor as a function of depth for a polymer fluid using base case parameters (Table 4.1) for a series of polymer products.

4.5.2 Influence of site mixing method

The mixing method parameter was investigated to determine, firstly, whether it was a cause of the observed heterogeneity phenomena and, secondly, whether each method facilitated a greater viscosity. The investigation was conducted by comparing two identical polymer batches: one mixed by bubbling and the other mechanically mixed in a planetary mixer. Although bubbling is now used on many construction sites, mechanical mixing can often be used instead, so it is important to explore the influence of the chosen method on the resulting polymer viscosities. Figure 4.23 presents the results of drop tests conducted after a standing time of 24 hours. The findings indicate that the bubbling method produced a polymer fluid with higher viscosity compared to the mechanically mixed batch. This difference is further highlighted by the viscosity gain factor in Figure 4.24, which demonstrates that the bubbled

mix exhibited higher viscosity at most depths. These findings indicate that the selected mixing method impacts the viscosity development of the fluid. Mechanical mixing may result in some polymer molecules adhering to the mixing equipment instead of being dissolved into the bulk fluid; efforts were made to minimise this effect. Bubbling, by contrast, may provide a more effective means of homogenising the fluid, enhancing the integration of polymer molecules into the full fluid volume with less mechanical shear.

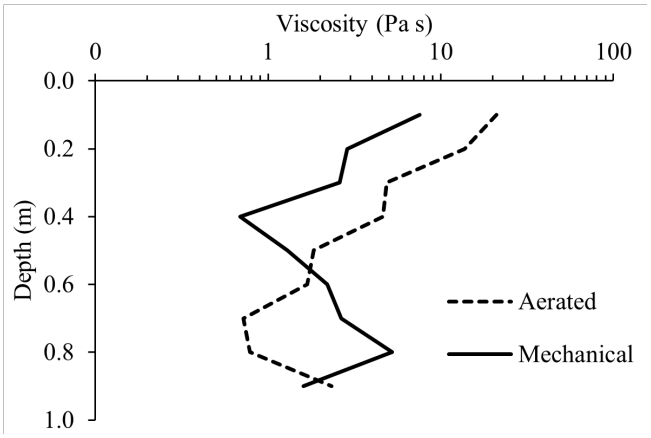


Figure 4.23: Influence of mixing method on the viscosity as a function of depth using base case parameters (Table 4.1) for two mixing methods: mixing by bubbling and mechanical mixing. N.B. Neither of these mixes was deaired.

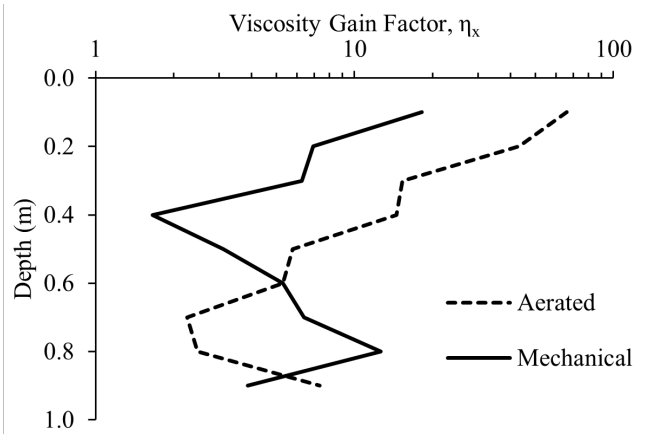


Figure 4.24: The viscosity gain factor as a function of depth for polymer fluids that have been mixed with bubbling and mechanically.

4.5.3 Influence of salt content

A key consideration for coastal sites and excavation in saline soils is the potential impact salts have on polymer fluid properties. To investigate this effect, a polymer fluid mix (of SlurryPRO CDP, at 1.2 kg/m^3 concentration, and no added sodium hydroxide for pH adjustment) was prepared with distilled water and then sodium chloride was added to achieve

a concentration (0.35 g/L) equivalent to one-hundredth of the total dissolved solids found in seawater (National Oceanic and Atmospheric Administration (NOAA), 2023). Two tests were conducted on the solution, one at 24 hours after mixing, which was followed by the sodium chloride addition, and the next an hour after the addition. The results show that the average viscosity decreased significantly from 42.2 Pa s to 1.7 Pa s, representing an almost 25-fold reduction, as shown in Figure 4.25, though it may be noted that the average viscosity was still 1,700 times that of water. The fluid heterogeneity also significantly reduced after salt addition, the CV dropping from approximately 1.6 to 0.7. This is a direct consequence of the salt causing the individual polymer molecules to coil, which reduces their radius of gyration and therefore their ability to form extensive networks. These findings highlight the substantial implications for the use of polymer fluids in environments with even slightly saline groundwaters, such as in regions of seawater intrusion.

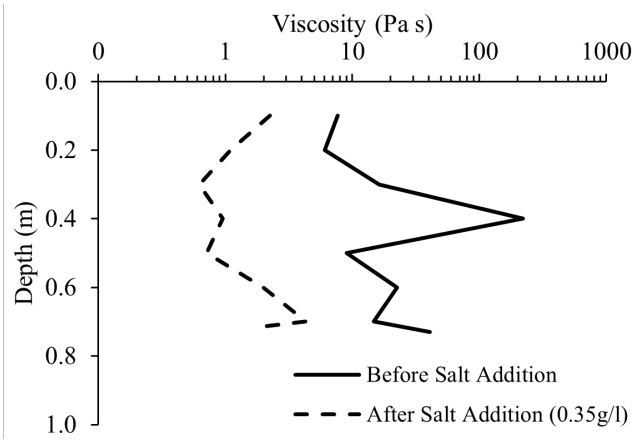


Figure 4.25: Influence of salt content on the viscosity as a function of depth for a polymer fluid mixed with distilled water. One test was conducted before and after salt addition.

4.5.4 Influence of temperature on the development of networks

A separate investigation examined the effect of temperature on polymer network development. A batch of polymer fluid was prepared and divided between two columns: one maintained at a constant 18.4 °C in a temperature-controlled room, and the other placed in an insulated, ice-cooled container, maintaining an average temperature of 10.4 °C. After mixing, the polymer was stored at these temperatures for 24 hours before a drop test was performed on each column (see Figure 4.26). Both mixes exhibited a high-viscosity region near the surface (these samples were not de-aired prior to testing, which contributed to the presence of polymer networks at the fluid surface); however, substantial variations in viscosity were

observed below this surface layer. In some regions, the viscosity in the colder column was found to be ten times greater than that in the warmer column. These findings suggest a strong influence of temperature on polymer network formation, likely because lower temperatures reduce Brownian motion of polymer molecules, allowing network links to persist for longer.

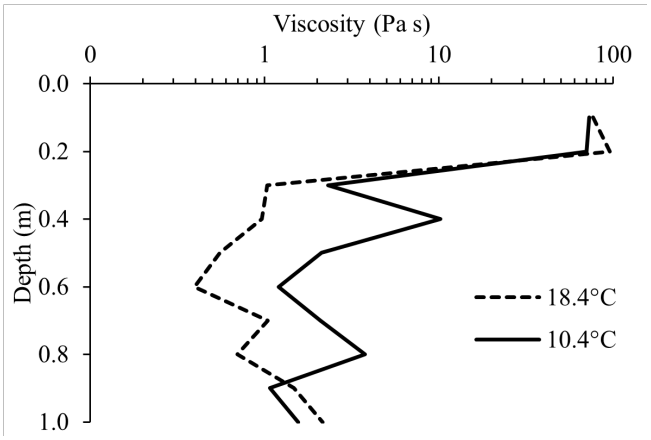


Figure 4.26: The viscosity as a function of depth for a polymer fluid using base case parameters (Table 1) for two columns held at different temperatures.

4.6 Parametric study of environmental factors

4.6.1 Influence of photodegradation

To investigate the influence of UV exposure and the damage it may cause to polymer molecules, the drop test method was employed. One column of polymer fluid was exposed to sunlight for 12 hours in open air, while an identical column was shielded from sunlight using an opaque black plastic cover for the same duration. After the exposure period, both fluid columns were re-mixed and allowed to stand quiescent for 24 hours. Subsequently, several drop tests were conducted over the following 12 hours to assess the rate of degradation. The UVA radiation levels measured during the 24-hour period are plotted as a function of Universal Time (UT) in Figure 4.27, with data sourced from the Reading weather station.

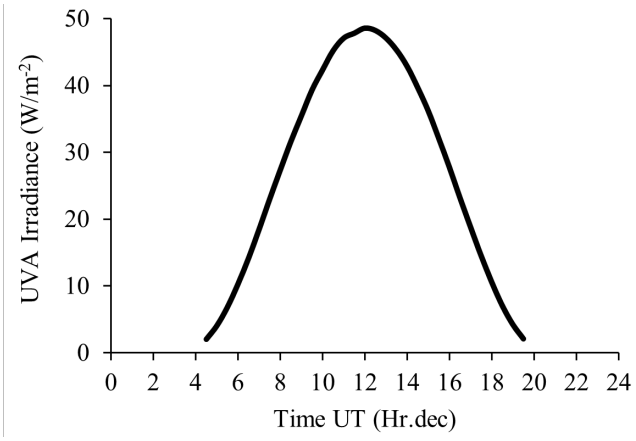


Figure 4.27: UVA radiation measured by the Reading weather station throughout the day of the photodegradation test. The clear weather conditions meant that the conditions were similar in Oxford.

The drop test results for 0 and 12 hours of exposure are presented in Figure 4.28. Before UV radiation exposure, both columns of polymer fluid had developed polymer networks. Following UV exposure in one column, viscosity decreased significantly, and the fluid exhibited a more homogeneous viscosity, indicating a loss of polymer network forming ability. In contrast, the non-exposed column continued to show network formation.

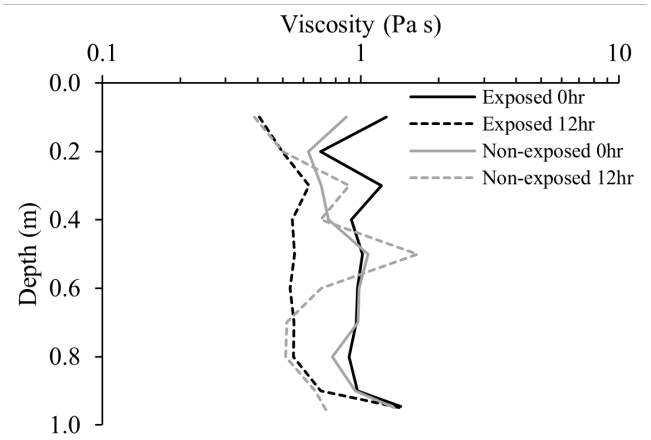


Figure 4.28: The influence of exposure to UV radiation on the viscosity as a function of depth using base case parameters (Table 4.1).

The viscosity gain factors for the UV-exposed and non-exposed columns are plotted as a function of time in Figure 4.22. This approach shows the extent of polymer viscosity degradation. The normalised viscosity of the unexposed fluid increased by 10.4% over 12 hours, whereas the viscosity of the exposed fluid decreased by 39.3% over the same period. These results suggest that polymer fluid stored in open tanks on-site will be degraded by sunlight. Although UV radiation penetrates the fluid, it will be attenuated as it penetrates leading to less degradation at depth. However, prolonged exposure can be expected to lead to

loss of fluid activity over significant volumes of polymer fluid. This will increase material consumption and project costs. To avoid wastage, stored fluid should be shielded from sunlight.

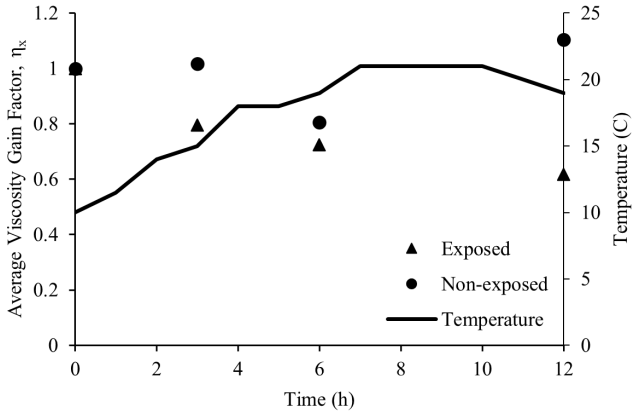


Figure 4.29: The viscosity gain factor as a function of time for exposed and protected columns of polymer fluid. Temperature as a function of time is plotted on the secondary axis.

4.6.2 Influence of temperature

The effect of temperature on the viscosity of polymer fluids was investigated using an IKA viscometer equipped with a water-jacketed test head. Tests were conducted over a temperature range from 0 to 50 °C, and the results are presented in Figure 4.30. There is a clear linear trend of a decreasing viscosity as the temperature increases. The plot shows a 19.5% reduction in viscosity as the temperature increased from 0 °C to 30 °C. These findings suggest that if large variations in temperature are expected, viscosity tests should be carried out at in-use temperatures. Adjustments may be necessary to the in-use polymer concentration in hot environments.

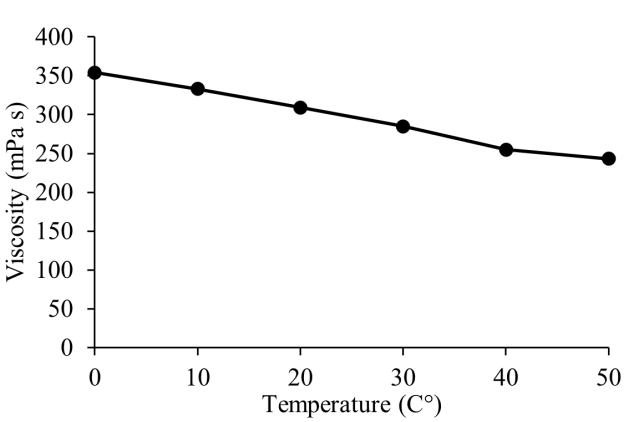


Figure 4.30: The viscosity as a function of depth for a polymer fluid using base case parameters (Table 1) for two columns held at different temperatures.

4.7 Summary

This study has identified and investigated a phenomenon previously unreported in the civil engineering literature, heterogeneity in polymer fluids. Using a novel investigative approach, the research suggests that this phenomenon arises not from phase separation as first suspected, but from the development of networks of weak, physical crosslinks developing between polymer molecules. High-viscosity networks evolve over time, when a fluid is quiescent significantly influencing the overall behaviour of the fluid. The findings have important implications for field practices, particularly in the mixing, sampling, storage, and testing of polymer fluids. Key findings can be summarised as follows:

- Time significantly influences network development with strongest network development occurring within the first 24 hours. Viscosity decreases upon pumping due to network disruption will partially recover when the fluid remains quiescent, for example, in a bore.
- Mixing methods directly affect fluid performance. Direct air bubbling lifts more viscous networks to the surface region buoyed by air bubbles. To reduce this effect bubbler bars in mixer tanks should be set so as to circulate as well as homogenise the fluid in the tanks. Early project tests are recommended to establish mixer arrangements capable of ensuring all polymer powder is dissolved and the in-tank fluid is homogenised.
- Testing various polymer types highlights their different behaviours under identical conditions. This chapter provides an initial performance assessment of some leading products used for excavation support. Consistent testing is essential to ensure individual products meet acceptable standards for on-site applications.
- Salts can substantially reduce the viscosity of polymer fluids.
- Polymer photodegradation should be a concern for site teams and those storing samples in the laboratory. The drop tests illustrate its impact. UV degradation leads to wasted polymer and higher costs. Contractors should implement protective measures against UV exposure to preserve polymer fluid performance and minimise wasted expenditure.
- Temperature variations markedly affect network development and so viscosity. Viscometer tests showed an almost 20% viscosity reduction from 0 °C to 30 °C while

drop tests revealed up to a tenfold viscosity difference across columns held at 10.4 and 18.4 C. Although in-situ ground temperatures are likely to be less variable, the impact of temperature should be considered for fluid management, preparation, and testing. Convection currents resulting from temperature variation may lift more viscous fluid to the top of containers, field tanks, and silos. Samples from surface regions may not be representative.

- The observed heterogeneity in polymer fluids requires careful consideration during sampling, both on-site and in the laboratory. Stirring and agitating the fluid before testing are recommended to ensure homogeneity to enable accurate comparison with established specifications.

Given the potential impact of heterogeneity, it is crucial to further explore its significance in real-world situations. Future research should focus on understanding how these networks affect flow behaviour in situ and their interactions with soil, ensuring that engineering practice accounts for these complexities to optimise performance and reliability.

5 Laboratory investigation of polymer fluid flow in sands

5.1 Introduction

A crucial consideration for polymer fluids used to support an excavation are the flow dynamics of the fluid as it penetrates into the excavation face. For a support fluid to be effective, it needs to exert a stabilising force at or very near to the excavation face (within a few centimetres) (EFFC/DFI Support Fluids Task Group, 2019). It is therefore vital that the fluid does not penetrate the excavation face too rapidly and too far from the face, otherwise there is an increasing risk that backward sloughing of the soil from the excavation face will occur.

This chapter presents an investigation into the penetration behaviour of polymer fluids. For this investigation, a permeameter apparatus was designed and built. This apparatus allows for the flow of polymer fluid through soil whilst simultaneously measuring the pore pressure at selected depths and the rate of fluid flow throughout the duration of the test. This testing enabled the study of water displacement within a sand bed and the development of flow over time. In this study, the mechanics of the flow itself were examined and then the mechanics of the flow in relation to parameters, including polymer concentration and sand grading. The findings from this testing will help to inform models describing polymer fluid flow in porous media and enhance understanding of the critical parameters which affect the penetration rate, and how these can be controlled for optimal on-site performance.

5.2 Materials and methods

5.2.1 Permeameter test apparatus

Figure 5.1 presents a schematic diagram of the laboratory permeameter apparatus constructed for this investigation. Air supplied from the laboratory system was channelled via flexible hosing into an air regulator. The chosen air regulator (from SMC) controlled the air

pressure in proportion to an electrical signal received from a power supply. A steel vessel that housed the fluid, was pressurised forcing flow through the sand bed. A direct line connected the pressurised vessel to the permeameter body.

The permeameter itself consisted of a 1 m long by 0.144 m diameter Perspex cylinder closed by two round steel flanges. Each flange had a circular channel bored into it, housing an o-ring to ensure the column remains fluid-tight. The top flange had a large opening, allowing the column to be filled with fluid and sand once confined between the flanges. This top flange also included a tapping for air release as the column fills with water, and a safety valve to automatically relieve pressure should it exceed safe limits. Along the side of the column, a series of tappings were fitted, each with a threaded and sealed steel fitting, to which flexible hosing was attached, leading to a pore pressure transducer (PPT). The tappings in the sand bed intruded 20 mm into the side of the bed; the first tapping was positioned in the fluid zone above the sand surface to provide a measurement of the applied pressure. The bottom flange had a hole bored into it that leads to the discharge pipe. A mesh covered the hole in the flange to prevent fines from clogging the discharge pipe. An additional PPT is located along the discharge pipe; this allowed for the measurement of the pressure difference along the pipe, thereby enabling a regular determination of apparent viscosity using the Hagen–Poiseuille equation:

$$\eta = \frac{\pi \Delta P r^4}{8QL} \tag{5.1}$$

Where η is the apparent viscosity, ΔP is the change in pressure, Q is the flow, r is the radius, and L is the length of the pipe.

A spigot is fitted to the end of the discharge line and set level at the top of the sand in the column. The discharged fluid is collected in bulk in bottles, with the mass of the fluid logged with a load cell situated beneath the platform on which the bottles rest. The spigot is set above the level of the fluid in the discharge bottle to prevent siphoning of the fluid. Both the PPTs and the load cell are connected to a data acquisition system, controlled by LabView programming running on a laptop connected to the setup. Figures 5.2 and 5.3 show the assembled permeameter apparatus along with the column and the position of the PPTs in relation to the sand surface.

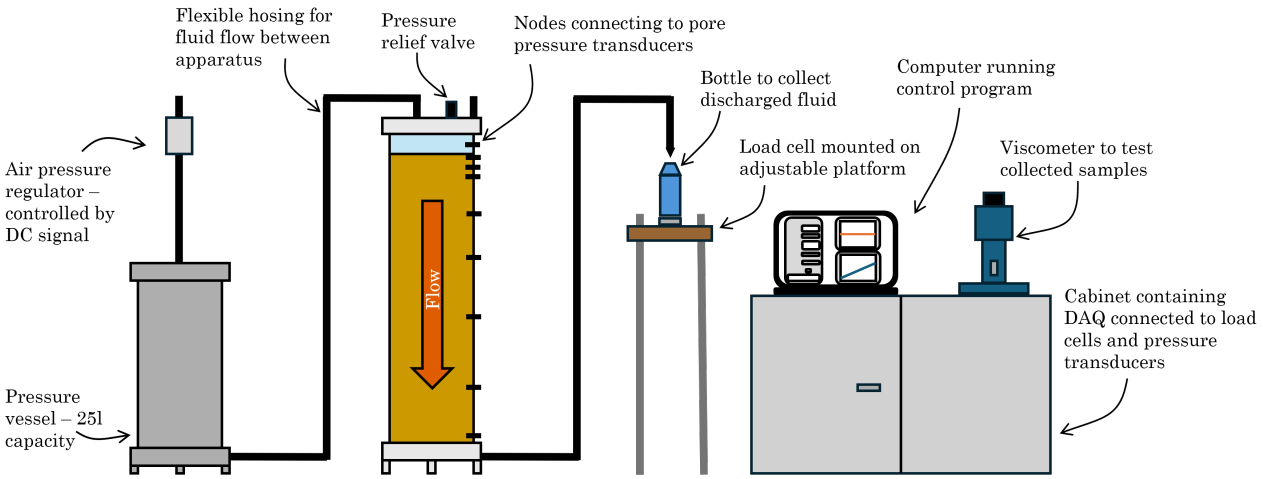


Figure 5.1: Schematic of the permeameter apparatus, including the instrumentation and the data acquisition system.

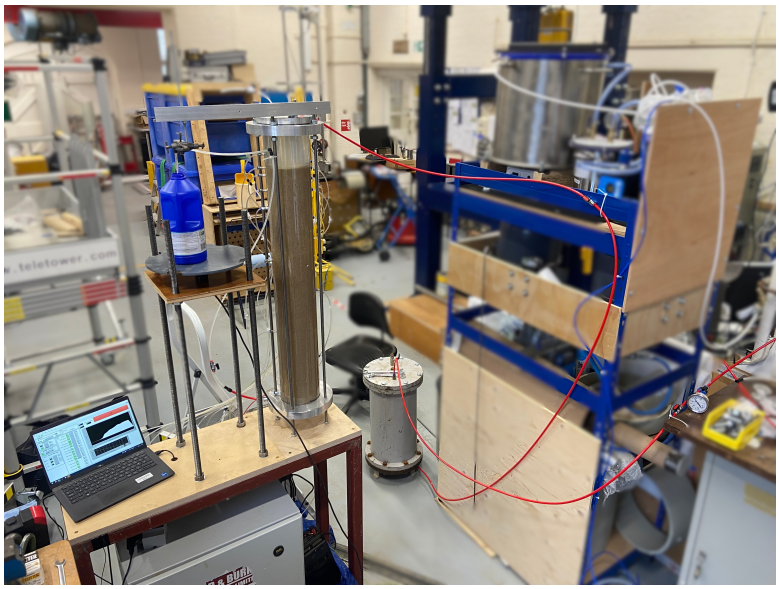


Figure 5.2: Image of the built permeameter within the lab.

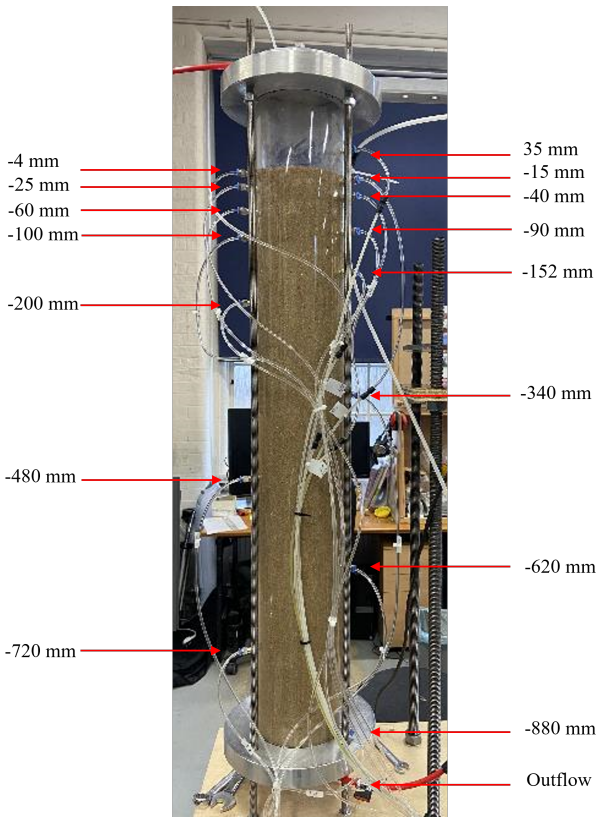


Figure 5.3: Permeameter column with the location of each PPT down its depth noted in relation to the sand surface.

5.2.2 Permeameter test procedure

To initiate the testing cycle, 6.5 litres of water are poured into the column. The mesh designed to prevent fines in the discharge pipe is then positioned at the bottom of the column. A predetermined mass of sand is subsequently pluviated into the column using a bespoke sand rainer. The sand descends through the water, forming the bed at a relatively slow and uniform rate, resulting in a loose, uniform sand bed. The average dry densities of the sand beds formed in this manner were 1539 kg/m^3 and 1518 kg/m^3 for the LB 16/30 and 14/25 sands, respectively. Any water remaining above the sand surface is syringed off and weighed to determine the total mass of water and sand within the column before testing.

The pressure vessel is filled with 10 litres of water and, along with the permeameter, is then sealed. The computer program is initiated to begin logging data, and pressure is applied to the pressure vessel. As water flows from the pressure vessel into the permeameter, the air at the top of the column is displaced until water exits the air release tapping in the top flange. Once all air has been expelled, the column is sealed. The air regulator ensures that a constant pressure is applied to the water, and the discharge rate is continuously monitored by the load

cell. From this tracked rate of discharge, the permeability of the sand can be determined using Darcy's law:

$$K = \frac{Q\eta L}{A\Delta P} \tag{5.2}$$

Where Q is the flow rate, K is the intrinsic permeability, A is the cross sectional area, ΔP is the pressure difference across the flow path, η is the viscosity, and L is the length of the flow path. ΔP can be expressed as:

$$\Delta P = \Delta h \rho_w g \tag{5.3}$$

Where Δh is the equivalent head difference of the permeating fluid, ρ_w is the density of water, and g is gravity. The hydraulic gradient, i_h, and hydraulic conductivity, k_w, can be expressed as below:

$$i_h = \frac{\Delta h}{L} \tag{5.4}$$

$$k_w = \frac{Q}{i_h A} \tag{5.5}$$

Substituting equations 5.4 and 5.5 into Equation 5.2 Darcy's Law can be expressed as the following:

$$K = \frac{k_w \eta}{\rho_w g} \tag{5.6}$$

Once the water permeability (hydraulic conductivity) test has been completed, tests on the samples of the discharged polymer fluid test can be undertaken. The polymer fluid is prepared following the same method outlined in Section 3.2.3, but with 25 litres of the fluid mixed to ensure the pressure vessel is completely filled. The fluid is pressurised, forcing it to flow through the sand bed and displace the water within the pores. Theoretically, all the water is displaced after 1 pore volume (PV) (Nijjer et al., 2019). The PV is defined as the total volume of the pores within the saturated sand bed, which is equivalent to the volume of water present at the start of the test. Typically, the PV in these tests was around 6 litres.

The PV parameter indicates the degree of polymer circulation. Later in the chapter, it can be seen that the PV, initially filled with water, is almost entirely displaced by the polymer fluid at 1 PV. However, due to the complex nature of the porous media and the readily soluble polymer, there may be some mixing between the polymer fluid and water, as well as trapped water that exits at a PV greater than 1. Throughout the test, samples are taken for analysis using the IKA ROTAVISC lo-vi viscometer, with testing conducted in the same manner as detailed in Section 3.2.5 for the IKA model. This viscometer testing serves as a surrogate to indicate the concentration of polymer molecules in the discharged fluid.

5.2.3 Additive mixing

Two additives frequently employed on sites using the KB International SlurryPRO polymer system are: EnhancIT 100 (E100) and EnhancIT 200 (E200). These are specifically designed as a "fluid loss additive" and a "solids control additive", respectively (KB International, 2025). Given the small recommended doses, these products require considerable care during mixing to ensure proper integration into the system. The standard doses of the additives for KB SlurryPRO are 10% E100 and 5% E200 by mass of the base polymer. Due to their reactive nature, the additives were individually pre-mixed with 100 ml of distilled water using a magnetic stirrer before being applied to the polymer fluid with a spray bottle. This method ensured reasonably uniform integration into the polymer fluid system.

5.2.4 Sand grading

Three sands were used in this testing: Leighton Buzzard Garside 16/30 sand, Leighton Buzzard Garside 14/25 sand, and Thanet Sand obtained from a CFA piling rig from the North Quay construction site in Canary Wharf, London, at a depth of -28 mOD. To characterise the sands used in this testing, 1 kg of Leighton Buzzard (LB) sand and 2.67 kg of Thanet Sand were sieved and their particle size distribution (PSD) was determined following the method set out in BS EN 933-1:2012 . Figure 5.4 presents the results of this sand sieving procedure, and Table 5.1 presents the d50 of the test sands, thereby providing a characterisation of each sand tested.

Table 5.1: The d50 of the sands used in the permeameter testing.

Sand	d50 (mm)
16/30 Leighton Buzzard	0.716
14/25 Leighton Buzzard	0.893
Thanet Sand	0.158

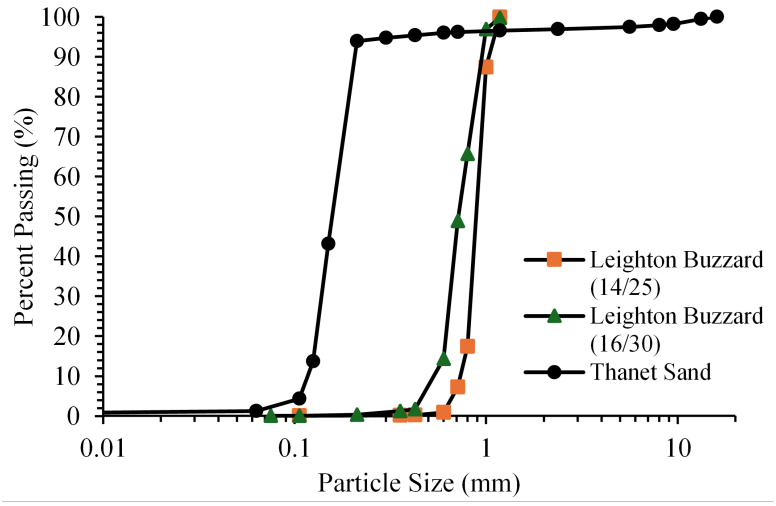


Figure 5.4: The percentage of the sand mass passing sieve sizes for sands used in the permeameter testing.

5.2.5 Scope of testing

The base case parameters adopted for the present investigation are presented in Table 5.2. The parameters used to explore the flow behaviour of polymer fluids in porous media are listed in Table 5.3. These particular parameters were selected because they offer valuable insight into important considerations for fluid system design and conditions encountered on site. Once again, this investigation examined a variety of common polymer systems used in the industry, which are typically sold as proprietary products rather than by their specific chemical formulae. The study provides initial insights into the differing performance of these systems. The investigation also looked at how applied pressure and concentration affect flow behaviour. Higher pressure increases fluid flow, which leads to greater polymer fluid consumption and more frequent refilling. While this provides enhanced security against sloughing at the excavation face, and bulk collapse of the excavation, it is a critical consideration that this testing provided insight into. Additionally, the polymer concentration is a crucial factor for engineers to consider. A concentration that is too high can result in wasted materials and higher project costs, while one that is too low can increase

replenishment costs and the risk of excessive fluid penetration, potentially leading to inadequate support pressure at the excavation face.

The investigation used sand beds with hydraulic conductivities that were at or even surpassed the typical permeability limits for which polymer fluids are normally considered suitable. To simulate conditions common on London construction sites, Thanet Sand sourced from the North Quay site was also tested. Furthermore, the study explored how including additives affects the polymer fluid flow behaviour. Additives are often mixed into a fresh polymer fluid despite being intended for use after the system has already been used at least once. This part of the testing sheds light on how these additives alter the fluid properties.

Table 5.2: Permeameter adopted base case parameters.

Parameter	**Type/Value**
Polymer product	SlurryPRO CDP
Polymer concentration, c (kg/m^3)	1.2
Polymer fluid age after mixing (hours)	24
Applied pressure (kPa)	30
Sand grade	LB sand 16/30

Table 5.3: Parameters and their ranges explored in the permeameter study.

Parameter	**Variation**
Polymer products	SlurryPRO CDP, Bauer Slurry LTP709, Cetco Shore Pac
Applied pressure (kPa)	5, 10, 20, 30
Concentration, c (kg/m^3)	0.6, 1.0, 1.2, 2.4
Sand grade	LB sand 16/30, LB sand 14/25, Thanet Sand
Additives	No additives, Additives (KB E100 and E200)

5.3 Results

Features of the flow mechanics that dictate the rate of the flow are explored in the following testing. These features are the viscosity of the fluid and the retention of polymer molecules within the porous media. Polymer molecules are retained by way of mechanical trapping,

adsorption to soil particles, and hydrodynamic retention (i.e. molecules being trapped in eddies that form within the porous media) (Sorbie, 1991). The following provides a list of the permeameter tests conducted, the reason for testing, and how they relate to the features of the flow mechanics:

1. **Hold periods** - A hold period is a set amount of time during which the flow was paused. This was tested to investigate whether the formation of localised, high-viscosity networks, similar to those observed in drop ball tests, would be seen in the permeameter. The test also allows for the investigation of polymer fluid behaviour during long-duration pauses in excavation, such as when a piling rig is unavailable. In such cases, the applied fluid head may be reduced to maintain the polymer fluid front as close as possible to the excavation face.

2. **Polymer product** - Due to their widespread use and a lack of clarity regarding the difference between them, three polymer products from different suppliers were tested. The investigation provides insight into how each product performs and the influence of differing formulations on the viscosity of the fluid and the uniformity with which the water in the sand bed is displaced. This highlights the importance of carefully considering product selection for specific jobs.

3. **Applied pressure** - This investigation explored the relationship between applied pressure and the rate of advancement of the polymer fluid front. A higher pressure provides short-term confidence by quickly establishing the fluid front, but it leads to long-term uncertainty as the fluid penetrates too far into the surrounding soil. Conversely, a lower pressure offers more long-term certainty by limiting the fluid penetration, but at the cost of a lower support pressure. This analysis is therefore crucial for engineers to determine the optimal fluid head needed for excavation stability and to predict when that head loses the capacity to prevent excavation failure.

4. **Concentration** - The concentration of the polymer fluid directly influences its viscosity, a key controlling parameter in flow behaviour. Understanding the link between fluid flow and concentration is crucial, as it allows engineers to determine the required amount of product and, consequently, the associated cost for supporting an excavation on-site.

5. **Sand grading** - The sand grading investigation explores how polymer fluids flow through beds with varying pore sizes and grain geometry. The testing will shed light on the influence of the nature of the porous media on mechanical trapping. The testing will also explore the limits of using polymer fluid with soils that have an excessively high hydraulic conductivity.

6. **Additive use** - The influence of additives on polymer fluid performance is a little-explored area of research, despite these substances being regularly added to fluids both when mixing and throughout their lifecycle on-site. The analysis will provide insight into their influence on the flow behaviours of polymer fluids.

5.3.1 Exemplar results

During a permeameter test, the discharge rate of fluid leaving the testing apparatus, the pressure profile down the depth of the sand bed, and the viscosity of samples taken throughout the test were all measured. The following presents exemplar results from the testing.

Discharge and flow rate

Figure 5.5(a) presents an exemplar result for the measured discharge of polymer fluid effluent over time for a test conducted with the base case parameters (Table 5.2). From these measurements, the flow of fluid over time can be determined as presented in Figure 5.5(b).

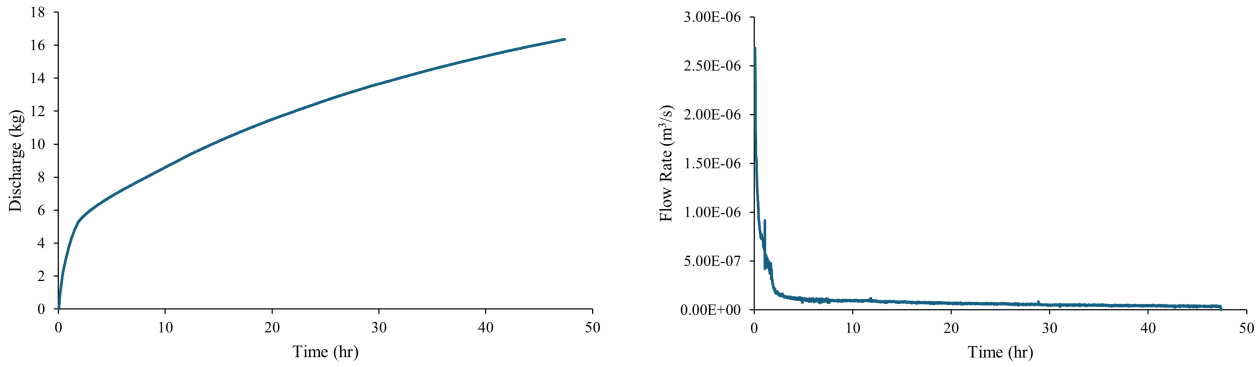


Figure 5.5: (a) Measured discharge as a function of time from a permeameter test conducted using the base case parameters (Table 5.2). (b) The inferred flow as a function of time, derived from the discharge data.

Flow in pore volumes is used to normalise the permeameter test results as it indicates the quantity of fluid that has passed through the bed at any given time relative to the volume of the bed.

Figure 5.6 shows flow as a function of the PV for the exemplar test. From this plot, it can be seen that the flow rate decreases as the polymer fluid displaces water from the sand bed to nominally full displacement at PV = 1. Between 0 and 1 PV the flow decreases rapidly. Thereafter, and unexpectedly, the flow rate continues to decrease but much more slowly. This trend was consistent across all tests.

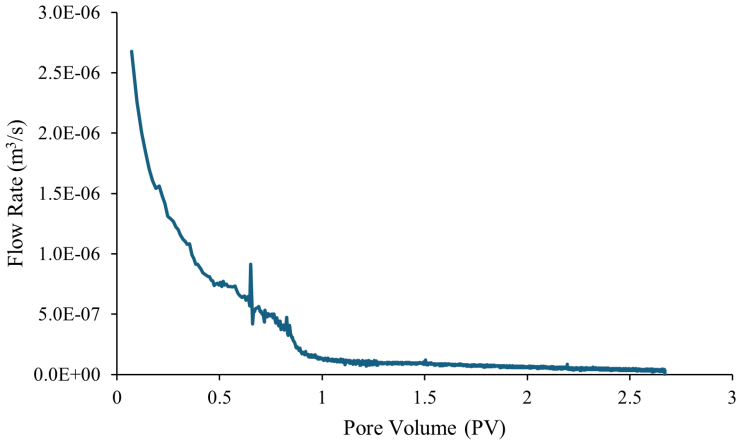


Figure 5.6: The flow as a function of the PV for the exemplar permeameter test conducted using base case parameters as noted in Table 5.2.

Pressure profile

Figure 5.7 presents the measured pore pressures down the depth of the column during an initial water permeability test. The plots are taken at two distinct moments during the test: one at 0.5 PVs and the other at 2.5 PVs. The results show that there is minimal change to the pressure profile during the test; these results serve as a reference for future plots for polymer permeation tests. Note that the pressure at the base of the column is relatively high due to the significant constraint in the pipe diameter. This is caused by the abrupt transition from the large-diameter column to the smaller 8 mm diameter discharge pipe, which restricts flow and limits pressure dissipation.

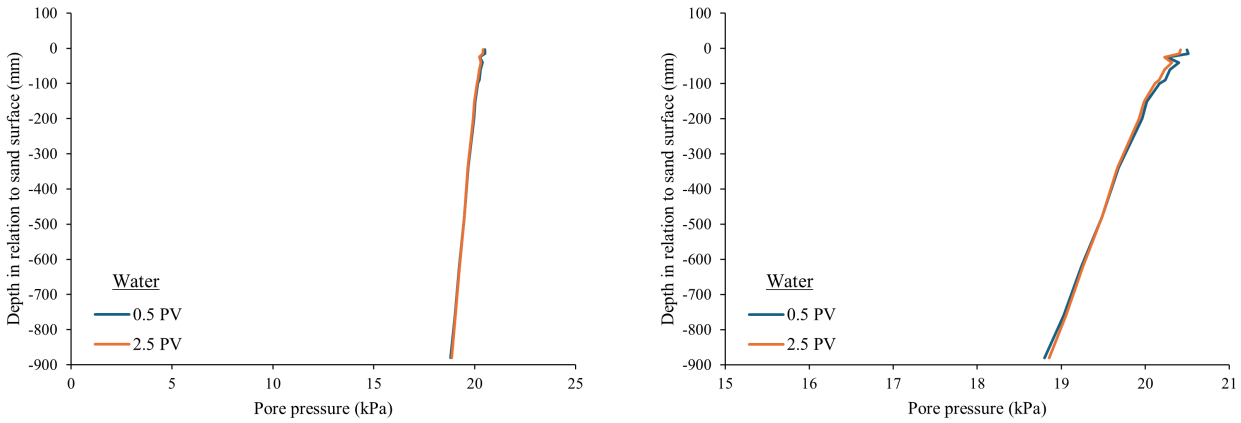


Figure 5.7: (a) The development of the pressure profile as a function of the column height during a water permeability test. Plots for PVs of 0.5 and 2.5 are presented to illustrate this progression. The applied pressure for this test was 20 kPa. (b) A magnified view of the same plots, with a restricted x-axis to more clearly highlight the two pressure profile plots. Note the pressure at the base of the column is not 0 owing to the narrow discharge pipe.

To help with the analysis and to expose behaviours of the fluid within the sand bed over the duration of the test the pressure fraction, P_f, is determined by Equation 5.7:

$$P_f = \frac{\Delta P_z}{\Delta P_T} \tag{5.7}$$

Where ΔP_z is the difference in pore pressure between the given height in the column and the bottom of the sand bed and ΔP_T is the difference in pressure over the full height of the sand bed. Figure 5.8 presents the pressure fraction as a function of the height of the column for the same test and results presented in Figure 5.7.

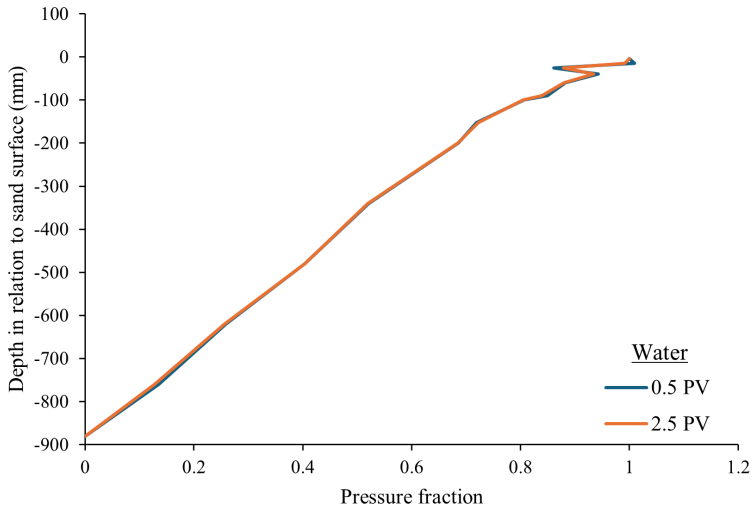


Figure 5.8: Pressure fraction, P_f, as a function of depth down the sand bed, showing the pressure drop as the fluid is pressurised to flow from top to bottom.

Figure 5.9 illustrates the pressure profile for a series of PVs for the base case polymer test. Each plot within the figure represents measurements taken at different PVs (and thus time intervals) during the test. This setup effectively facilitates tracking of the polymer front as it progresses down the depth of the sand bed. Figure 5.9 clearly demonstrates this polymer front tracking; when the pressure in each plot begins to rise past the pressure at the base of the bed, it indicates that the polymer fluid has reached that specific depth. For example, in the 0.5 PV - 0.72 hr plot, the pressure starts to rise at the 490 mm depth mark, indicating the polymer front has penetrated to the PPT located there. The consistent measurement of pore pressure also allows for the monitoring of fluid behaviour over time, which will be further expanded upon in the analysis. Note the back pressure rise once the polymer reaches the base of the column. This is caused by the increasing viscosity of the fluid at the exit, as the concentration of polymer molecules approaches its original entry concentration. As a pointer for the reader, the steeper decline in the pressure profile, or lower pressure drop, is indicative of a less viscous fluid.

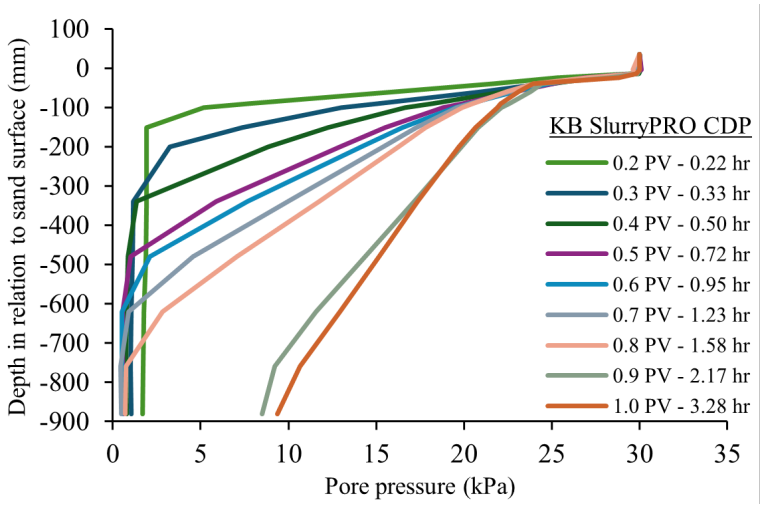


Figure 5.9: The evolution of the pressure profile as a function of depth for a pressurised polymer fluid flowing through a sand bed. Each plot represents the pressure profile at a specific moment within the first PV of the test. Note: the top of the sand bed is at 0 mm

Viscometer testing

Viscometer tests were undertaken throughout the permeameter testing to indirectly track the polymer concentration as a function of the PV. Figure 5.10 presents the complete set of viscometer tests conducted during the base case permeameter test (Table 5.2).

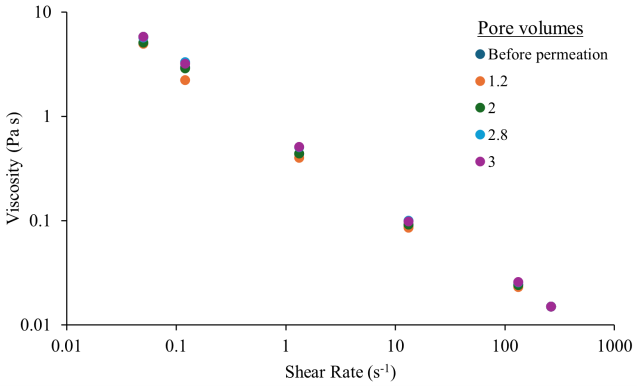


Figure 5.10: The viscosity as a function of the applied shear rate for a series of samples taken from the discharge pipe of the permeameter over the course of a test. The measurements were conducted using a rotational viscometer, and the test was performed using the base case parameters from Table 5.2.

To gain further insight into the viscosity of the exiting fluid, viscosities of the discharged fluid, at a single shear rate, have been selected and are plotted in Figure 5.11. Figure 5.11(a) presents the measured viscosity corresponding to a shear rate of 0.05 s^{-1}, demonstrating an increase in viscosity of the filtrate as the test progresses. Figure 5.11(b) presents the viscosity fraction, η_{frac} derived by equation:

$$\eta_{frac} = \frac{\eta_n}{\eta_{before}} \tag{5.8}$$

Where η_n is the viscosity at a specific shear rate at any given PV and η_{before} is the measured viscosity at the same shear rate of a sample of the fluid before permeation is initiated. The trend in these plots reflects the general behaviour of each permeameter test. As permeation progresses, the pockets of water that may become trapped during the initial permeation of polymer fluid are progressively flushed out. This results in a more concentrated polymer fluid solution, leading to a discharge with an increasing viscosity.

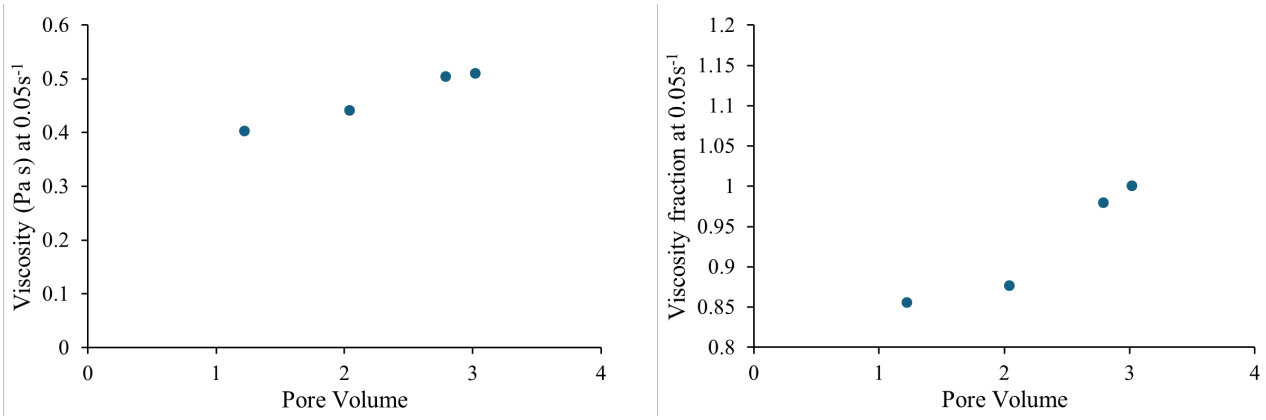


Figure 5.11: (a) The measured viscosity of samples taken during the base case permeameter test (Table 5.2) at a shear rate of 0.05 s^{-1} as a function of the PV at which the sample was taken. (b) The normalised viscosity fraction for the same test, also measured at a shear rate of 0.05 s^{-1} as a function of the PV. The normalisation is such that a viscosity fraction closer to 1 indicates that the fluid viscosity is closer to its original value before passing through the sand bed.

5.3.2 Hold periods

Whilst conducting the base case test, the opportunity was taken to investigate the effect of temporarily halting polymer fluid flow before restarting it to see if network formation could lead to a build-up of viscosity in soil pores and hence higher pressure drops. This is relevant to practice as periods of very low permeation may occur during excavation, if the head is allowed to drop to near the same level as the groundwater. It is therefore of interest to investigate whether the permeameter tests show a similar behaviour to the falling ball test, where undisturbed fluid forms networks, leading to a higher viscosity and consequently a lower permeation rate. These "hold periods" were established by removing the driving pressure for durations of 55 hours (just over 2 days), 17 hours (overnight), and 133 hours (4.5 days), respectively, for hold periods 1, 2, and 3. After each hold, the pressure was reinstated, and the discharge rate was measured.

Figure 5.12 presents the results from this test. Each re-pressurisation following a hold period is referred to as a "cycle". From Figure 5.12, it is evident that after pressure reinstatement, the difference in discharge rate is relatively negligible, suggesting that the static period does not significantly affect the subsequent flow behaviour.

This observation might seem to contradict findings detailed in Chapter 4, where it was observed that the polymer fluid structured and built viscosity after periods of quiescence. One might therefore expect that the hold periods would allow the polymer fluid to develop

increased viscosity, leading to a slower flow through the sand bed. A possible reason for not seeing a decreased discharge rate is that the networks may be disrupted as they pass between sand particles. However, one might still expect the intact networks at the surface of the sand bed to contribute to a reduced permeation rate if present. A volume of fluid resided at the top of the column, where polymer networks might have formed. The absence of the networks suggests one of two possibilities: either the void volume is too small for network formation, or any networks that do form are broken very rapidly by the shear forces as they enter the pores.

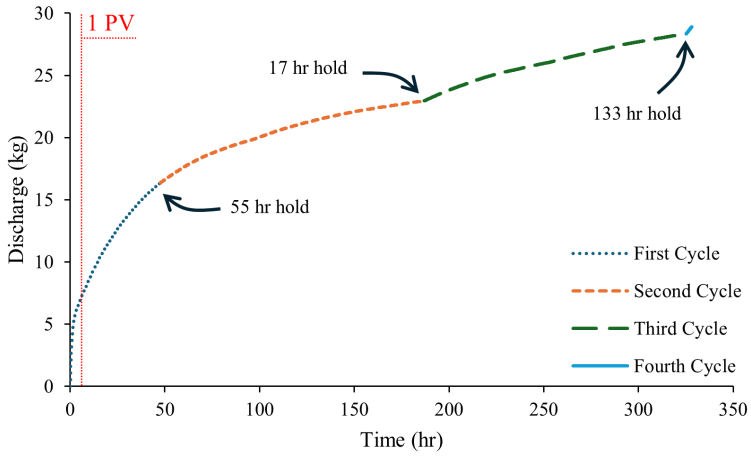


Figure 5.12: The effect of varying periods of fluid holding on the discharge is shown as a function of time for a base case permeameter test. The test was conducted using the parameters from Table 5.2, with the driving pressure removed for set periods to allow the polymer fluid to become stagnant.

5.3.3 Polymer product analysis

Given the differing measurements of viscosity between polymer products observed during API filter press and ball drop tests, coupled with the interest of industry in understanding various polymer products, an investigation was undertaken into the flow behaviour of different polymer products. Three polymer products were selected for this testing: Shore Pac (new product) (chosen for its assumed simpler chemical nature), KB SlurryPRO CDP, and Bauer Slurry LTP709 (given the capability of the latter two to develop a high viscosity, and their common use in industry).

Figure 5.13 presents the discharge time history for these three polymer products. In line with previous tests, the lesser ability of Cetco Shore Pac to develop viscosity at the same magnitude as the other two polymer products led to a greater discharge rate, with 3.5 PVs being discharged in just over 15 hours. The KB SlurryPRO CDP polymer product took 2 days

for just over 2.5 PVs, whereas the Bauer Slurry LTP709 product took 3 days for this volume.

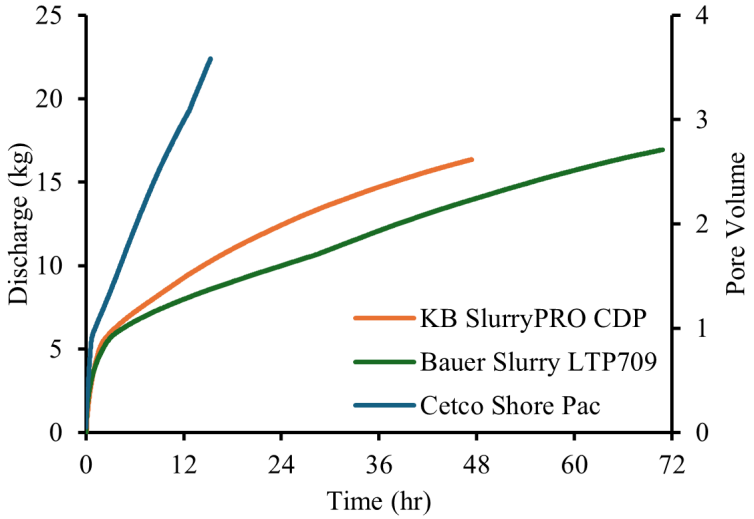


Figure 5.13: A comparison of the discharge performance for a series of different polymer products: Cetco Shore Pac, KB SlurryPRO, and Bauer Slurry LTP709, all mixed at 1.2 kg/m^3 concentration. The discharge is shown as a function of time for each product, with all fluids tested under base case conditions as outlined in Table 5.2. N.B. for the Cetco, KB, and Bauer products, 1 PV is located at 1.1, 3.3, and 4.3 hours respectively.

The flow, Q (m^3/s), as a function of the PV graph for the polymer products testing is presented in Figure 5.14. The graph shows the significant difference in the amount of flow at the same stages of polymer fluid displacing water from the sand bed for the varying polymer products. The Cetco product permeates into the sand bed at a rate 1.5 times greater than the other two products at the beginning of the test. At 0.8 PVs, the rate of flow of the Cetco product is roughly 3.5 times greater than that of the other products. Where the KB product initially has marginally lower flow than the Bauer Slurry LTP709 product, this is reversed after 40% of the water is displaced from the column. As the plot approaches 1 PV, the flow shows sudden decreases and increases. This indicates the polymer fluid exerting a higher resistance to the driving pressure, followed by a sudden release. After this release, the flow returns to a magnitude similar to its previous level.

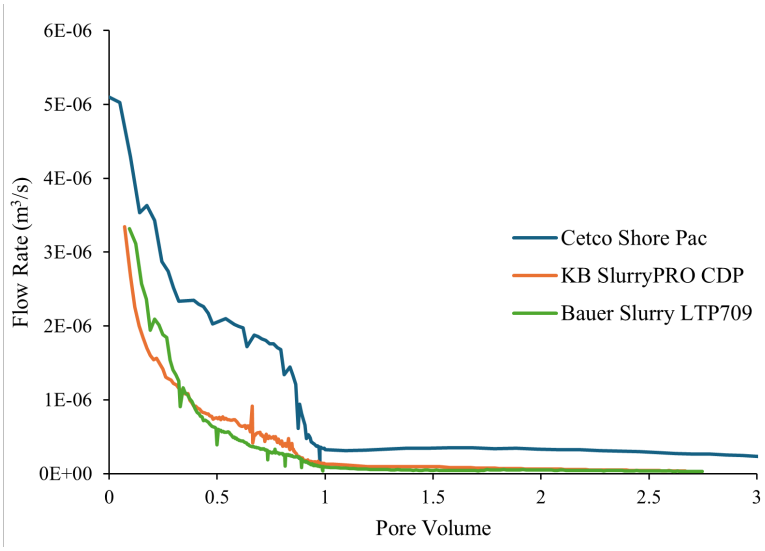


Figure 5.14: The influence of the polymer product on the fluid flow through the sand bed is shown as a function of the PV. The series of polymer products and their corresponding plots are identified in the legend.

Figure 5.15 presents the flow as a function of the PV for the polymer products test with a range limited to PV $>$ 2. This graph shows the relationship between flow and PV after the water in the sand bed has been displaced. The figure indicates that the relationship between flow and PV becomes approximately linear once the polymer fluid has displaced the water in the pores.

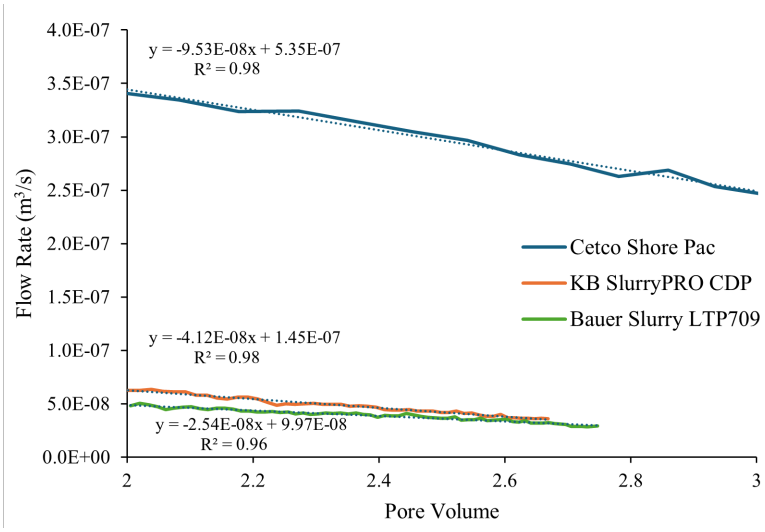


Figure 5.15: The influence of the polymer product on the fluid flow through the sand bed is shown as a function of the PV. The plots cover a range from 2 PVs to 3 PVs, representing the flow after the initial water pore volume has been displaced, and it is now polymer fluid displacing polymer fluid.

A two-part function was fitted to the data from all three tests. An exponential function was first fitted to each dataset for $0 \leq$ PV $<$ 1, leading to an average R-squared value of 0.93. For PV $>$ 1, a linear function was fitted to the data, resulting in an average R-squared of 0.80

across the three tests. In most tests, for PVs greater than 1, a linear function adequately describes the observed decline in flow. This suggests a transition in the dominant mechanism controlling flow reduction. Initially, mechanical entrapment of polymer molecules within soil particles likely caused the flow reduction. However, beyond 1 PV, the primary factor shifted to a cyclic relationship between increasing viscosity and decreasing shear rate, leading to a steady decline in flow. Conversely, an exponential relationship is appropriate when considering the displacement of water by the polymer fluid. In this scenario, the flow is expected to decrease at an accelerating rate as the polymer fluid progressively displaces the water within the porous medium. The function fitted to the data is as follows:

$$Q = a \cdot e^{-B_{pw} \cdot PV} \tag{5.9}$$

Where a is the flow rate difference, and B_{pw} is the flow decay rate for the flow as polymer displaces water. The a parameter is highly dependent on the initial flow. Given that the initial flow is controlled by the water that occupies the entire PV, it could be considered that the difference between the a exponent in the fitted function from test to test is a feature of sand bed formation. The B_{pw} parameter controls the rate of decline in the flow as the polymer fluid displaces the water and is therefore a crucial indicator of the performance of a polymer fluid. A larger value of B_{pw} indicates a greater flow decay rate over an equal volume displacement. The fitted linear function for the data where PV>1 is presented below:

$$Q = -B_{pp} + w \tag{5.10}$$

Where B_{pp} is the flow decay rate for the idealistic period of polymer displacing polymer and w is a constant reliant on the outcome of the initial flow behaviour described by Equation 5.9. The results from the trend fitting functions are presented in Tables 5.4 and 5.5. The R-squared value for the linear fits (where PV $>$ 1) reveals the influence of trapped water as the fluid is in a transitional stage around PV=1, resulting in a weaker fit. Conversely, the R-squared is very strong when PV $>$ 2, indicating the completion of this transition, as shown in Figure 5.15:

Table 5.4: The flow decay rate and the R-squared of the exponential function for each polymer product test from a PV of 0 to 1.

Polymer product	**Flow rate difference, a**	**Flow decay rate (polymer-water),** B_{pw}	**R-squared**
Bauer Slurry LTP709	4.5E-06	3.85	0.98
Cetco Shore Pac	7.7E-06	3.09	0.76
KB SlurryPRO CDP	3.7E-06	3.22	0.93

Table 5.5: The factors for the best fit linear trend and the R-squared of the linear function for each polymer product test from a PV of 1 to 3.

Polymer product	**Flow decay rate (polymer-polymer),** B_{pp}	**Polymer-polymer flow constant, w**	**R-squared**
Bauer Slurry LTP709	1.79E-08	8.06E-08	0.69
Cetco Shore Pac	4.09E-08	3.97E-07	0.61
KB SlurryPRO CDP	4.84E-08	1.62E-07	0.98

By combining exponential and linear functions fitted to the datasets, the performance of the polymer products can be analysed with greater ease. The Bauer Slurry LTP709 product exhibits the greatest flow decay rate up to a PV of 1, indicating that it may perform best in supporting a bore in the short term. Conversely, beyond a PV of 1, the KB product has the greatest flow decay rate, suggesting that it may reduce the flow most successfully over extended periods. The Cetco product does not appear to be as effective as the other two products in reducing the flow rate through the soil, a behaviour that may be attributable to its purer chemical formula which inhibits its ability to form a clogging mechanism.
The different behaviours exhibited between the various polymer products are further demonstrated by the pressure profiles throughout the duration of the tests, presented in Figures 5.16, 5.17, and 5.18. Over these pore volumes, we can observe distinct behaviours for each product. The Cetco Shore Pac fluid starts and finishes with a fairly linear loss of pressure down its depth, with the pressure loss increasing over the change in PV, which indicates the previously discussed slowing of the fluid. The KB fluid shows a contrasting

behaviour, forming a significant pressure drop roughly 25 mm deep into the sand bed at 1 PV. By 2.5 PVs, this pressure drop has increased significantly, indicating that the polymer molecules are clogging the pore space, leading to a greater pressure drop over this zone. In fact, at 2.5 PVs, 40% of the total pressure drop over the sand bed occurs in this region. This clogging is likely caused by partially dissolved polymer, or perhaps by clogging agents deliberately integrated into the product by the supplier. The Bauer Slurry LTP709 fluid also establishes a large pressure drop at approximately 25 mm deep at 1 PV. However, as shown in Figure 5.18, while the Bauer Slurry LTP709 forms a clogging mechanism quickly, it begins to degrade by 2.5 PVs. There is a possibility that if left long enough the clogging mechanism may re-form following degradation, but there was no evidence of this within the testing time frame. Conversely, the clogging mechanism formed by the KB fluid continues to develop at 25 mm depth and also closer to the surface.

While these results clearly indicate a clogging mechanism, this phenomenon was not apparent in other testing methods. For instance, API filter press tests showed no evidence of polymer molecule build-up on the filter paper, and the observed facilitation of higher shear strength and continued flow under pressurisation in industry also contradicted a simple clogging behaviour. Notably, the absence of evidence of a clogging behaviour in the API filter press test underscores that the clogging development of polymer fluid is less effective than that of bentonite. Figure 5.19 presents a diagram demonstrating the proposed behaviour. As the fluid permeates the sand, the flow rate decreases, making it more likely for the polymer molecules to adsorb onto the sand surface within the pore throats. The subsequent adsorption of additional molecules leads to the progressive filling of the pore space, which reduces the ability of molecules to pass through. The slowing of flow within the sand is what enables this clogging, causing it to form at depth.

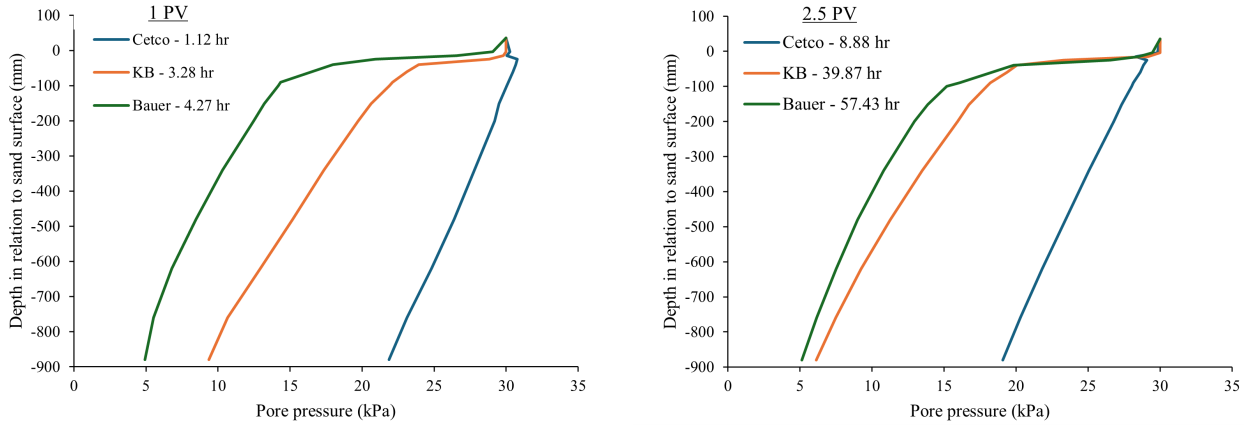


Figure 5.16: (a) A comparison of the pressure profiles for different polymer products (Cetco Shore Pac, KB SlurryPRO CDP, and Bauer LTP709) at 1 PV, the point at which the entire bed is theoretically saturated with the polymer fluid. (b) The pressure profiles for the same polymer products are presented at 2.5 PVs.

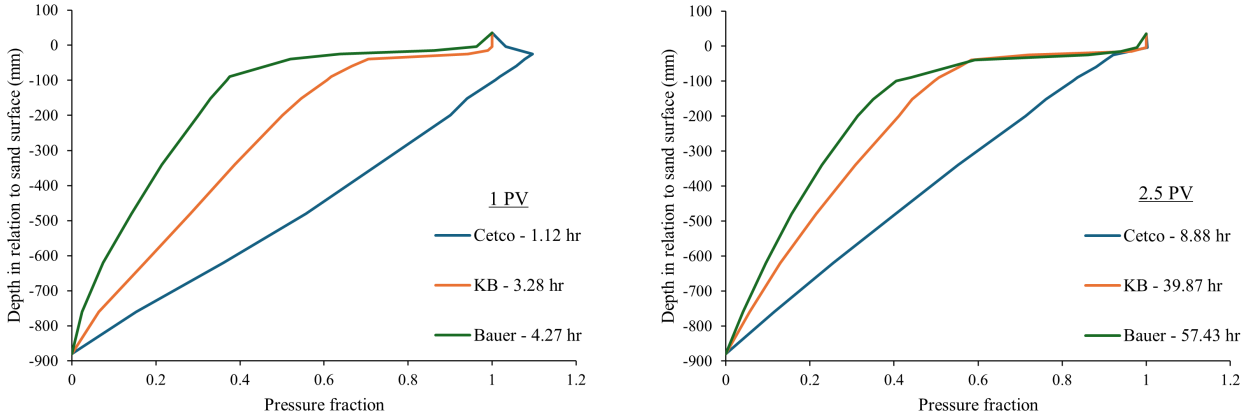


Figure 5.17: (a) A comparison of the pressure fraction profiles for different polymer products at 1 PV. (b) The pressure fraction profiles for the same polymer products are presented at 2.5 PVs.

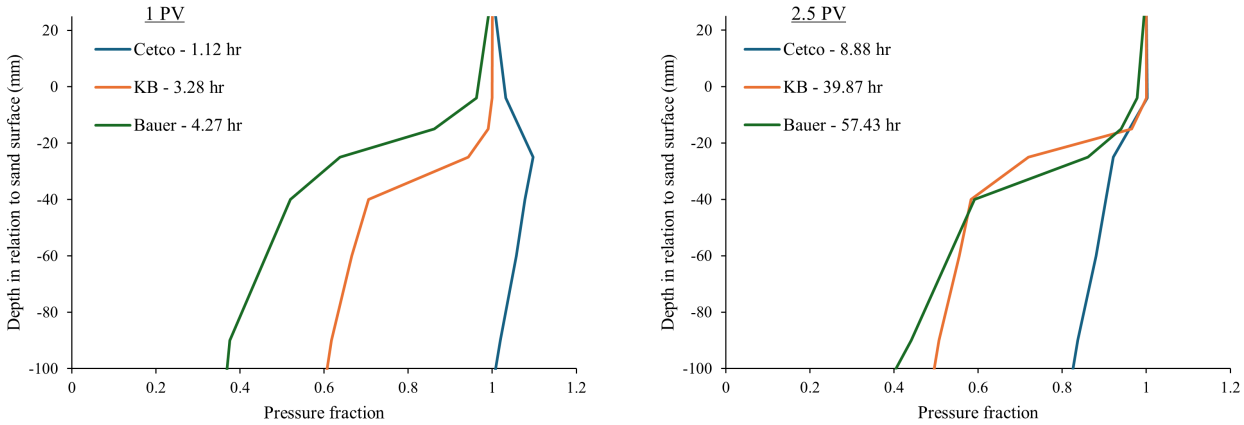


Figure 5.18: (a) The pressure fraction profile for varying polymer products at 1 PV. The y-axis is limited to the first 100 mm of depth into the sand bed to allow a closer inspection of surface behaviour. (b) The pressure fraction profiles for the same polymer products are presented at 2.5 PVs.

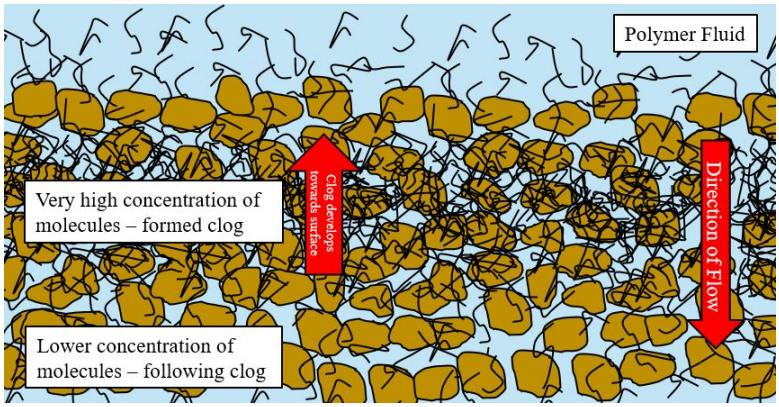


Figure 5.19: Diagram describing the formation of a polymer molecule clog within a sand bed during permeation.

Figure 5.20(a) presents the viscosity measured at 0.05 s^{-1} as a function of the PV over the course of permeation and Figure 5.20(b) presents the viscosity fraction as a function of the PV based on viscometer testing of discharge samples. These viscosity measurements are used as a proxy for polymer concentration here.

The plots for the Bauer Slurry LTP709 and Cetco Shore Pac products suggest that there may be a larger volume of trapped water pockets influencing the viscosity during the initial flow period. After 3 PVs, the discharged Bauer Slurry LTP709 polymer has the same viscosity as the fluid before it is permeated through the sand bed. At the same PV of 3, the Cetco product concentration is reduced to 60%, suggesting a higher degree of water pocket trapping and polymer molecule loss as it permeates the sand bed. The KB product, on the other hand, seemingly has quite a high concentration (85% of that before it is permeated) when it is first discharged from the sand bed, and slowly rises to a similar viscosity as it approaches 3 PV. In combination with the flow and pressure results, these results indicate that the Cetco product loses significant polymer molecules and is significantly diluted as it flows through the sand bed. If the mechanism is indeed entrapment, the molecules are doing little to clog the pore space, suggesting the lower viscosity is more likely to be a result of a non-uniform displacement of the water. The Bauer Slurry LTP709 polymer sees a similar reduction of viscosity, but its molecules are much more effective at clogging the pore space and slowing the flow. The KB product exhibits less viscosity reduction as it permeates the sand bed compared to the other two products. Indicating a uniform displacement of water and effective clogging from the molecules that are trapped.

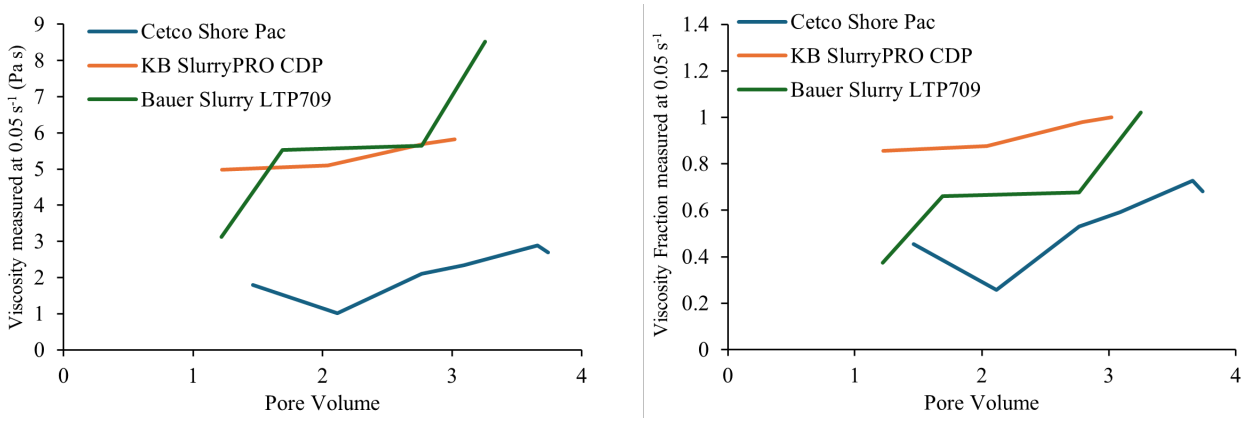


Figure 5.20: (a) A comparison of the measured viscosity of the discharged fluid as a function of the PV for a series of different polymer products. The viscosity was measured at a shear rate of 0.05 s^{-1}. (b) The viscosity fraction of the discharged fluid over the duration of the test.

A notable feature following some tests, but most notably with the Bauer Slurry LTP709, was the formation of small 'craters' on the surface of the sand once the test was completed. The formation of these craters suggests the development of preferential paths within the sand as the polymer permeates. This might occur as the clogging mechanism develops, where the applied pressure forces the formation of certain main arteries. However, further testing is warranted to investigate whether this cratering is purely a surficial phenomenon or if it continues with depth. During the continuous observation of the sand bed up to 1 PV there was no clear evidence of the cratering forming, suggesting that this effect is not associated with rapid flow.



Figure 5.21: A photograph of the sand surface within the column following a permeation test with Bauer Slurry LTP709, showing the final condition of the surface after the test.

5.3.4 Applied pressure analysis

When conducting a permeation test using the base case parameters (Table 5.2), the driving pressure was manipulated to push the polymer fluid through the sand at varying rates. The pressures applied corresponded to those commonly experienced within an excavation. Figure 5.22 presents the discharge as a function of time for this testing. The initial three hours of the test have been excluded because water was present in the sand bed during this period; thus, the presented results reflect pure polymer fluid flow through a sand bed. Whilst it could be argued that there might still be an influence from the initially water-saturated sand bed, the general trend of the discharge as a function of time persists beyond 2 PVs, when the PV has been replaced twice over.

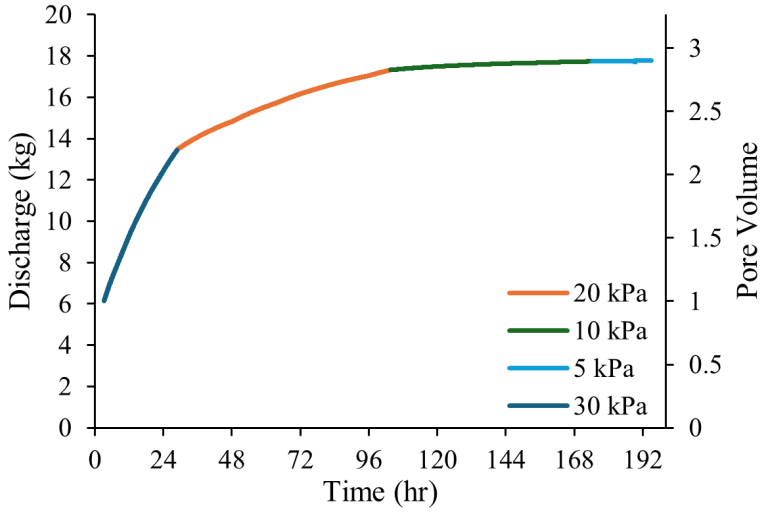


Figure 5.22: The effect of a series of applied pressure heads on the discharge of the KB SlurryPRO CDP polymer fluid. The discharge is shown as a function of time, and the fluid had a concentration of 1.2 kg/m^3.

As the flow rate through the sand column is a function of the combined resistance of the clogged and unclogged regions, these two regions have been considered separately. Figure 5.23 presents the pressure gradients across these two regions of the sand column as a function of flow rate. The flow rates were obtained from the best-fit linear trendlines over the dataset for the duration for which each pressure was applied. By reference to Figures 5.16 and 5.17, for the unclogged region of the sand column, the depth range 70 to 490 mm was selected. For the clogged region, the range 25 to 50 mm was selected. For the unclogged region, Figure 5.23 shows a linear relationship between applied pressure and the fluid flow rate. This is unexpected, as the relationship as detailed in Equation 3.3 (from Chhabra and Richardson

(1999)), the flow should scale with pressure to the power of 1/n. It would seem that the shear rate in the pores was sufficiently high for the fluid viscosity to be at the lower Newtonian threshold, that is, constant viscosity. The relationship highlights that an increased fluid head within the bore will lead to a more rapid progression of the polymer front into the surrounding soil, consequently reducing the support fluid capacity to prevent excavation failure, in particular, sloughing at the excavation face. The applied fluid head, therefore, must be chosen to balance maintaining a sufficient head factor for stability against preventing excessive penetration of the fluid and thus a reduction in stability with time. Also, of course, higher penetration results in higher fluid wastage. Figure 5.23 also presents the flow against the gradient for the clogged region. In this plot, the relationship is once again linear. However, it can be seen that, at the same flow rates, the pressure gradient in the clogged region is much greater than in the unclogged region. These results demonstrate the very significant impact that clogging can have.

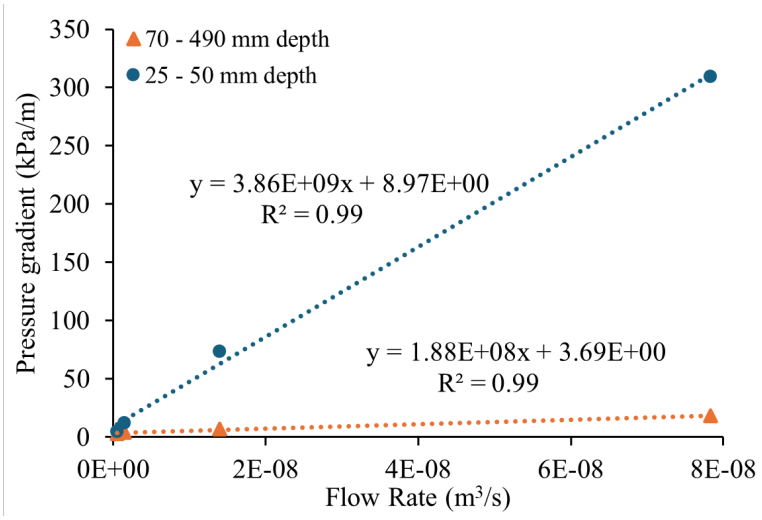


Figure 5.23: Gradients across largely unclogged region and largely clogged region of bed for a series of flow rates. The flow was derived from the best-fit trendline of volume over time. The fluid was KB SlurryPRO CDP at a concentration of 1.2 kg/m^3.

5.3.5 Concentration analysis

Determining the optimal concentration of polymer to be used in a support fluid system is an important consideration for sites employing such fluids. A concentration that is too high can result in a solution that is difficult to handle, potentially leading to problems with pumping, concrete casting, and excessive material usage. Conversely, a concentration that is too low can cause the fluid to permeate too rapidly into the surrounding soil, thereby losing its capacity

to adequately support an excavation. To address this, an investigation was undertaken to enhance the understanding of the relationship between polymer concentration and permeation behaviour, and to begin to quantify this relationship.

Figure 5.24(a) presents the results of the measured discharge over time for each concentration tested. The figure emphasises the stark difference between the flow rates, or gradients, of each concentration plot. This difference in flow rate is quantified in Figure 5.24(b), where each data point was taken as the gradient of the best-fit linear trendline for each concentration plot after 1 PV of permeation.

The data suggest that the relationship between the concentration and flow rate is exponential. This aligns with the known exponential relationship between concentration and viscosity, fortifying the idea that the viscosity of the fluid is the major contributing parameter to its flow behaviour.

In practical terms, these results reveal a crucial relationship for polymer fluid system design. The difference in performance between the 1.0 kg/m^3 and the 1.2 kg/m^3 fluids is quite large, considering the small adjustment in the quantity of added materials. Conversely, the difference in performance between a fluid with a concentration of 1.5 kg/m^3 and 2.5 kg/m^3 may be quite small in relation to the additional materials required by such a concentration increase.

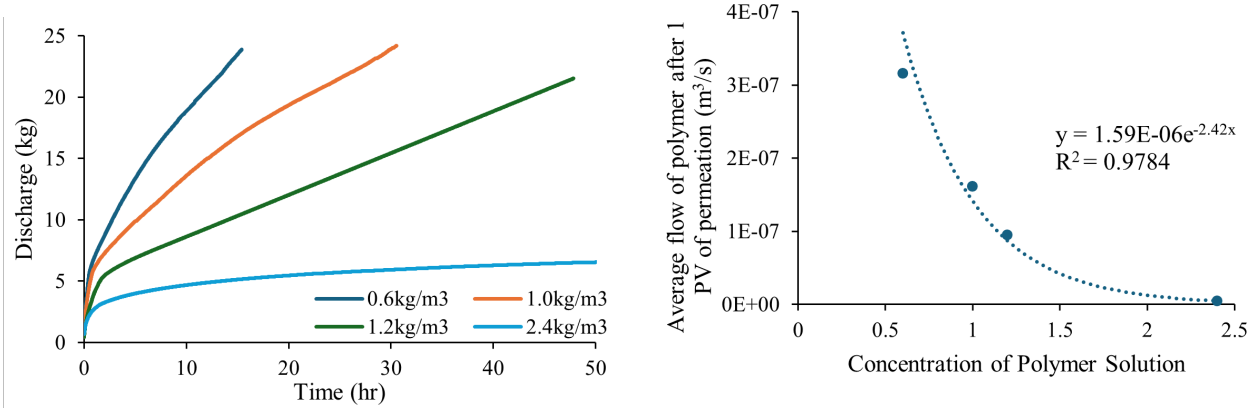


Figure 5.24: (a) The influence of varying polymer fluid concentrations on the discharge is shown as a function of time. The tests were conducted with a KB SlurryPRO CDP fluid with concentrations ranging from 0.6 kg/m^3 to 2.4 kg/m^3 and an applied pressure of 30 kPa (equivalent to a 3 m head). (b) The flow is derived from a linear best-fit line to the discharge data after 1 PV of permeation.

Figure 5.25 presents the calculated flow as a function of the PV for the series of polymer concentrations tested. N.B. the y-axis in Figure 5.25 is logarithmic. The figure demonstrates the relationship between increasing concentration and decreasing flow rate. For PV $>$ 1, the

rate of reduction in the flow increases as the concentration decreases. However, as the PV increases, this rate decreases, indicating that the flow will plateau as the viscosity reaches its zero-shear viscosity and the clogging mechanism has developed to its full extent.

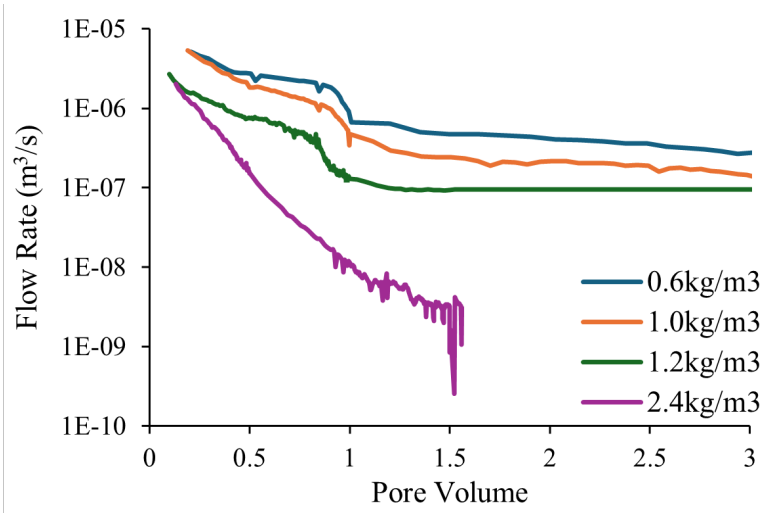


Figure 5.25: The influence of varying polymer fluid concentrations on the flow through the sand bed is shown as a function of the PV.

Figures 5.26 and 5.27 present the pressure profiles and pressure fractions with depth for the permeation tests with varying polymer fluid concentrations. At 1 PV, the results are as expected: higher concentrations lead to a greater pressure loss within the clogging region and across the entire sample depth. However, an unexpected reversal is observed at 1.5 PVs, where the overall pressure loss is reduced. Furthermore, the highest concentration fluid exhibits a pressure loss over the formed clog that is lower than that of the fluid with half its concentration. The precise cause of this phenomenon remains unknown and will necessitate further experimental investigation. It seems, however, that the observed behaviour is potentially driven by a rapid initial clogging mechanism attributed to the high concentration of polymer molecules.

As the polymer molecules permeate the sand bed, they become mechanically trapped within its porous structure. This initial trapping, and the associated increase in flow resistance, contribute to the immediate low flow rate and the substantial pressure drop observed across the entire column depth, particularly within the 0-70 mm region near the surface of the sand bed.

As the test progresses and polymer molecules continue to flow into the sand bed, the processes of trapping and coating the sand particles may reach a critical point. Beyond this

point, the viscous drag exerted by individual polymer molecules could diminish as they primarily interact with each other rather than directly with the sand particles, potentially beginning to act as a lubricant. This, combined with the possible establishment of preferential flow paths (capillaries) within the sand bed, which may widen in diameter as flow progresses, could lead to the observed reduction in the clogging mechanism.

The continued decrease in flow rate, as illustrated in Figure 5.25, is then assumed to be a consequence of this reduced flow. A decreasing flow rate leads to a corresponding decrease in the shear rate experienced by the fluid. For a shear-thinning fluid such as this, a reduction in shear rate results in an increased apparent viscosity. This establishes a reciprocating relationship between the shear rate and apparent viscosity, consistent with observations from other tests (e.g. those performed with Cetco), where escalating viscous resistance ultimately leads to further reduced flow, and consequently, an even greater apparent viscosity.

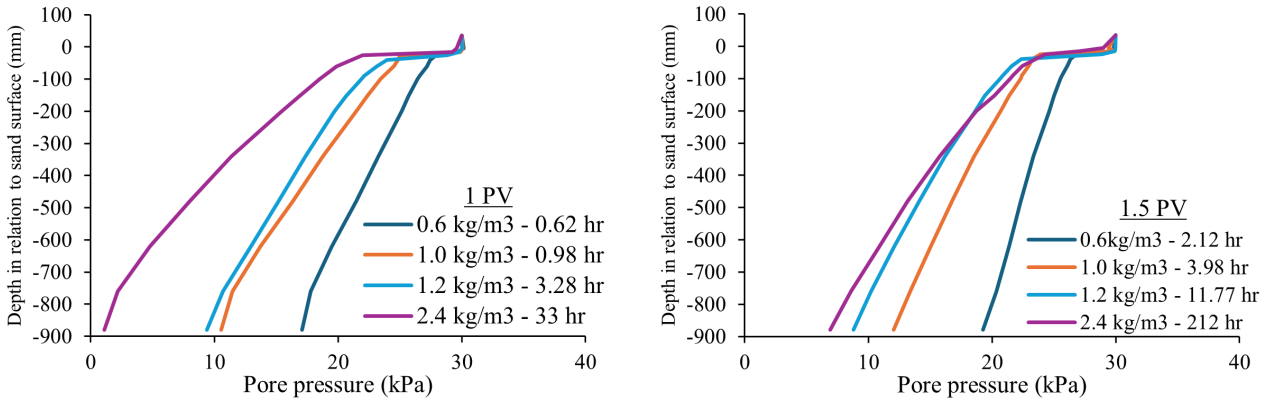


Figure 5.26: (a) The influence of a series of polymer concentrations of a KB SlurryPRO CDP fluid on the pore pressure profile down the column, presented at 1 PV. (b) The pore pressure profiles for the same permeation tests are presented at 1.5 PVs.

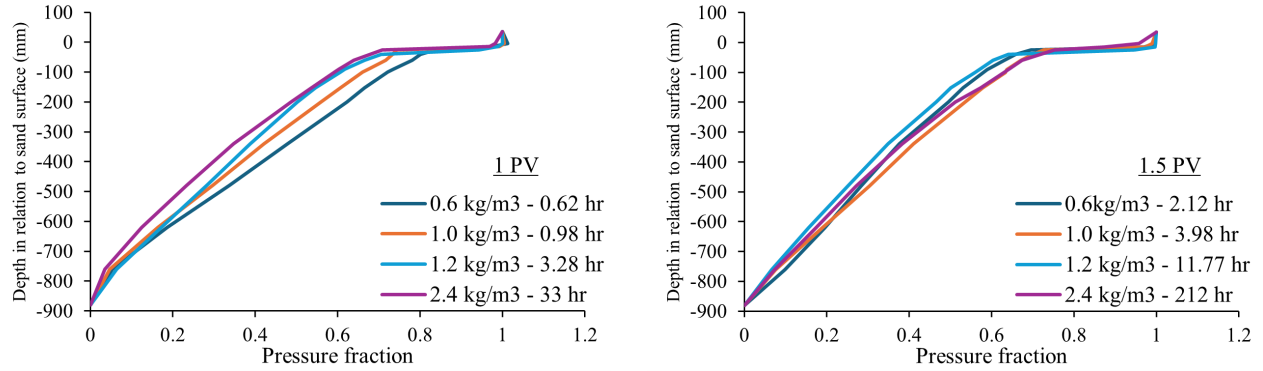


Figure 5.27: (a) The influence of varying polymer fluid concentrations on the pressure fraction profile down the depth of the sand bed, presented at 1 PV. (b) The pressure fraction profiles for the same polymer fluid permeations are presented at 2.5 PVs.

Figure 5.28 provides a close-up inspection of the pressure fraction losses occurring within the first 100 mm depth of the sand bed. At all concentrations tested, the fluids developed a clogging mechanism, indicated by the sudden pressure drop over a short change in depth. However, the graphs show that the effect of clogging on overall pressure loss is more pronounced at lower polymer concentrations than at higher ones. The graphs suggest that the clogging primarily occurs at a depth of approximately 25 mm into the sand bed. However, in higher concentrations of the solution, the clogging mechanism appears to develop and occur at shallower depths as permeation progresses. In the test with a concentration of 2.4 kg/m^3, for instance, the clogging occurs right up to the sand bed surface.

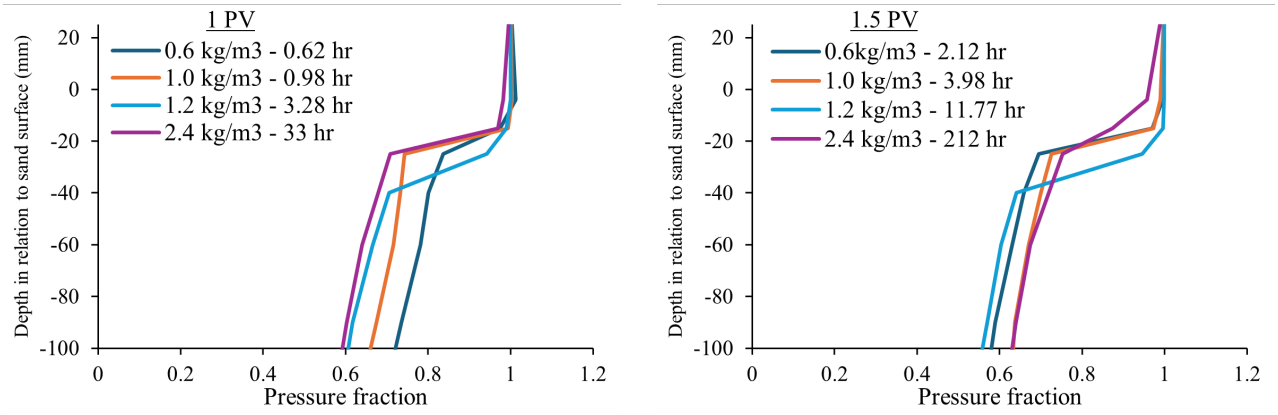


Figure 5.28: (a) The fraction of the applied pressure down the first 100 mm of sand bed depth for a series of polymer fluid permeations, presented at 1 PV. This limited view enables a closer inspection of surface mechanisms. (b) The pressure fraction profiles for the same permeations are presented at 2.5 PVs.

Figure 5.29 presents the difference in pressure fraction between 1 PV and 1.5 PVs down to a depth of 100 mm, which facilitates the inspection of the clogging mechanism's development for each polymer fluid concentration.

The figure reveals a depth-dependent development of the clogging mechanism. At a depth of 25 mm, the clogging mechanism in lower concentration fluids develops at a greater rate relative to the PV. Conversely, at this same depth, the highest concentration fluid shows evidence of clog degradation. However, at the shallower depth of 15 mm, the clogging mechanism has significantly developed in the 2.4 kg/m^3 fluid. The combination of deterioration at a deeper point and development at a shallower point suggests that the clogging mechanism has a depth limitation. This finding may indicate a limiting factor for the performance of polymer fluids in soils with unusually high groundwater pressure.

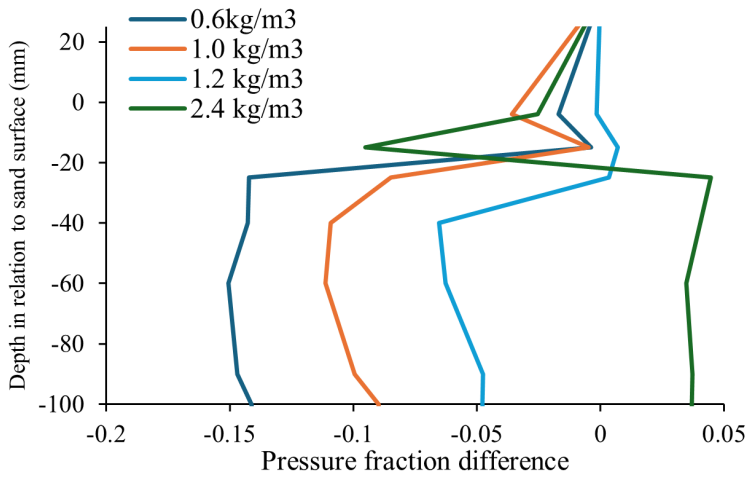


Figure 5.29: The difference in pressure fraction between 1 and 1.5 PVs is shown as a function of depth for a series of polymer concentrations. The y-axis is limited to a depth of 100 mm to facilitate the inspection of clogging behaviour at the sand bed surface.

Figure 5.30 presents the viscosity testing undertaken during the permeation of the polymers of varying concentrations. Figure 5.30(a) demonstrates the difference in the viscosity of the concentrations after they have passed through the sand bed. A noticeable feature from the testing is the much lower viscosity measured in the sample taken at 0.99 PVs during the permeation of the 1.0 kg/m^3 polymer fluid. The result emphasises the uniformity of the polymer front; whilst the polymer has some influence on the sample taken at 0.99 PVs (given the ability to measure the viscosity at 0.05 s^{-1} and the presence of "stringing" from the discharged fluid as the molecules interact with one another when subjected to shear), the main polymer front tends to come through abruptly at 1 PV. This behaviour is difficult to observe in other tests due to the challenges of isolating and conducting a high volume of viscometer tests, which are needed to expose this sudden jump in viscosity.

Another noticeable feature of the results is the dip in the measured viscosity at 2.1 PVs in the permeation of the 0.6 kg/m^3 polymer concentration fluid. The reduction in viscosity for this test sample may be caused by the lower viscosity not being able to displace the water present in the sand bed so effectively; and therefore water, that may still be present in some pore spaces, may still be influencing the viscosity of the discharged fluid.

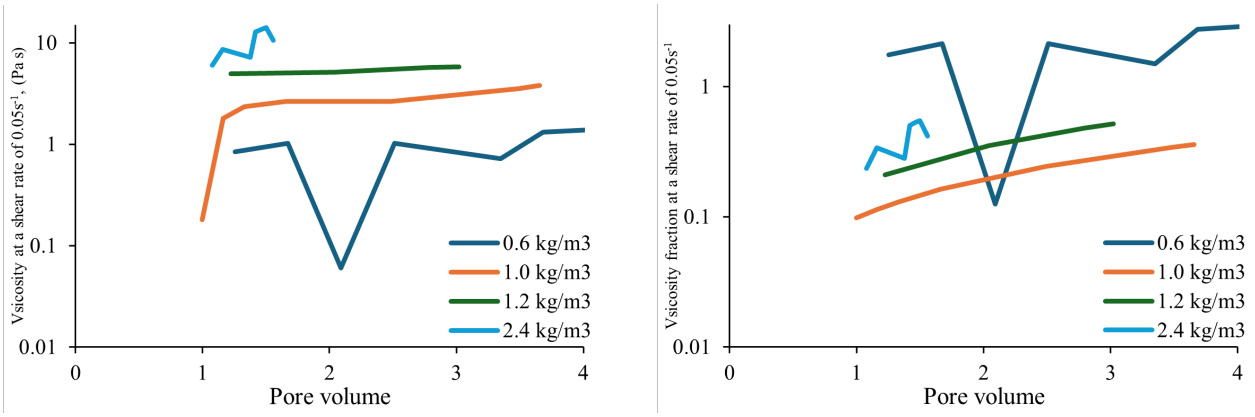


Figure 5.30: (a) The measured viscosity of samples taken from the discharge pipe during permeation tests as a function of the PV. All measurements were taken at a shear rate of 0.05 s^{-1} (b) The viscosity fraction, η_{frac}, is shown as a function of the PV. This fraction represents the proportion of the viscosity of the sample to the viscosity before it was permeated. Note that the y-axis for both graphs is logarithmic.

5.3.6 Sand grading analysis

The hydraulic conductivity of the LB 16/30 sand, used for the base case, was in the order of 10^{-4} m/s. The limiting hydraulic conductivity was explored in the testing with a coarser LB 14/25 sand, which had a hydraulic conductivity on the order of 10^{-3} m/s. This value is considered to be the practical limit for which polymer fluids are suitable for excavation support. Tests were also conducted with Thanet Sand from South East England, a relatively low-permeability sand and therefore, theoretically, more suitable for polymer fluid use. The formation of sand beds with the finer 16/30 sand was relatively repeatable, with a CV of 19.7% for the hydraulic conductivity. In contrast, the 14/25 sand beds exhibited much higher variability, with a CV of 83.3%. Despite this variance, the tests still provided valuable insights into flow behaviour in coarser sands.

Figure 5.31 clearly illustrates the stark difference in flow behaviour between finer and coarser sands. As expected, the polymer fluids flow much more quickly through the coarser soil. The greater pore volume and lower surface area in the coarser sand create a less-facilitating environment for polymer molecules to become trapped, bridge, or adsorb onto the sand surface and cause a build-up of molecules. This is evident in the discharge rate of KB SlurryPRO CDP in the 14/25 sand, which is much more linear past 1 PV than in the 16/30 sand, demonstrating less clogging. The lower surface area also reduces the frictional drag exerted by the polymer molecules on the sand particles, which in turn reduces the resistance to flow. Notably, a large decrease in flow rate was observed at different PVs across the tests,

for example, at 0.75 PVs in the coarser 14/25 sand versus 0.85 PVs in the finer 16/30 sand. These substantial reductions indicate that the polymer fluid is beginning to have a significant effect on the bulk flow. The Thanet Sand testing demonstrated exceptionally slow permeation, with the fluid almost reaching stagnation; the first sign of polymer discharge was after 0.58 PVs, indicating that the polymer was not displacing the water but was instead flowing between the sand bed and the wall of the permeameter.

The sudden reduction in flow appears to be largely absent in certain tests, specifically permeations into Thanet Sand and those involving high-viscosity, high-concentration solutions. The substantial flow reductions indicate faster advancement of certain portions of the polymer fluid. As the polymer fluid displaces the water, the two fluids interact to varying degrees. Where the viscosity is not as great or the flow is more turbulent, the interaction is more pronounced. This interaction and mixing can cause pockets of a transitional viscous fluid that may advance more quickly than the bulk polymer fluid, but not as a uniform front. These pockets reach the base of the sand bed quicker and thus significantly impact the flow behaviour before 1 PV is reached. Conversely, the fluids with a very high viscosity or those that form a clogging mechanism early prevent this mixing and advancement of a transitional fluid due to their limited interaction with the water.

When considering flow after 1 PV, the Cetco product exhibits a relatively stable flow in the 16/30 sand, whereas in the 14/25 sand, the flow actually slightly increases. This suggests that both the clogging mechanism and viscous drag resistance are failing to slow the fluid in this coarser sand bed. Conversely, the flow rate of the KB product in the 14/25 sand reduces at a very similar rate to the same product in the 16/30 sand, although the flow rate is consistently almost fourfold greater in the coarser sand.

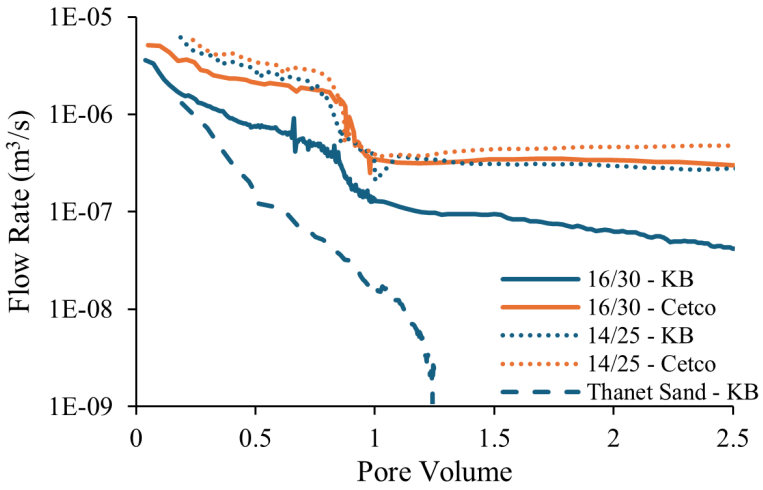


Figure 5.31: The influence of a series of sand grades on the flow of polymer fluids is shown as a function of the PV.

Figure 5.32 presents the pressure profile of the tests conducted with LB sand at 0.85 PVs, allowing for further inspection of the sudden drop in flow around this fraction of volumetric displacement. The figure shows that the polymer front in the 14/25 LB sand has already reached the base of the column. This is notable because a significant proportion of the initial water, approximately 15% (or roughly 0.9 litres), still remains. This indicates that in the coarser sand, the polymer front becomes much less uniform. These results indicate that there is some mixing between the polymer and water as it progresses through the sand bed, resulting in a transitional front of varying viscosity. This may lead to fingering in the polymer front, where fluid of a lower viscosity progresses quicker, causing the development of preferential capillaries and the presence of the pressurised fluid at the base of the column before the main polymer front reaches it.

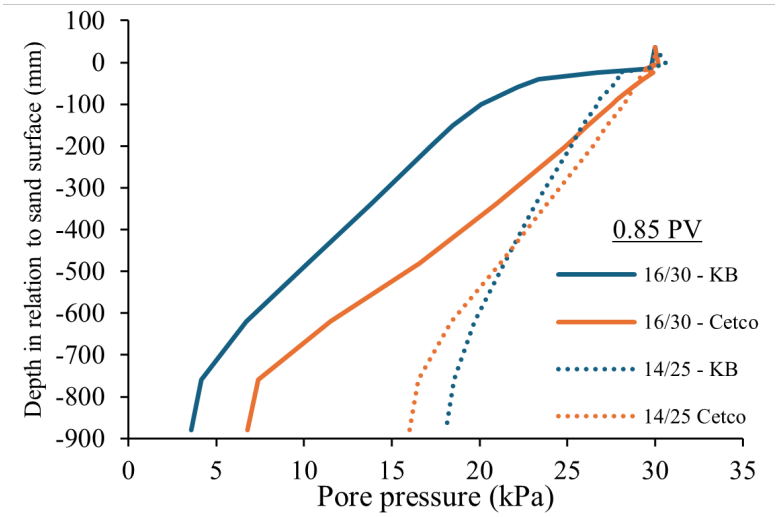


Figure 5.32: The pressure profiles for permeations of KB SlurryPRO CDP and Cetco Shore Pac at a concentration of 1.2 kg/m^3 are compared. The tests were conducted in 16/30 and 14/25 Leighton Buzzard sands, with the profiles presented at 0.85 PVs.

Figure 5.33 presents the viscosity fraction, η_{frac} at 0.05 s^{-1}, of the samples taken over the course of the permeation. The figure demonstrates the effect of sand grading on the rate of intermixing between water and the polymer fluid. Fluids discharged from coarser sands show lower initial viscosities than those from finer sands, but they exhibit a greater rate of viscosity increase with PV. This suggests that while intermixing initially reduces viscosity at the polymer front, the larger pore space in coarser sand results in less trapped water and more uniform displacement. This allows the flow to transition more rapidly to polymer displacing polymer, thereby reducing the influence of residual water.

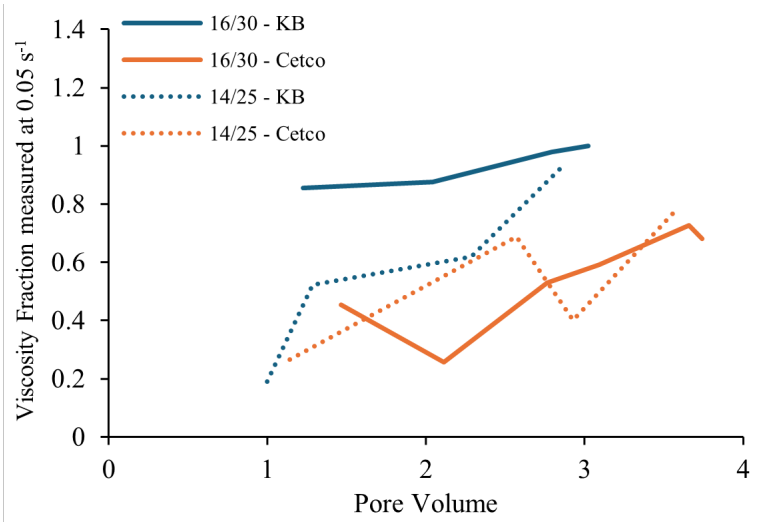


Figure 5.33: The viscosity fraction of samples taken throughout the permeation of polymer fluids into a series of different sand grades. The viscosity fraction is shown as a function of the PV.

Figure 5.34 presents the pressure profiles at selected PVs throughout the permeation of the

polymer products in the LB sands. Alongside this, Figure 5.35 presents the fraction of total pressure lost throughout the depth of the column for the same series of PVs. At a depth of 50 mm for the permeation of the Cetco product into both 16/30 and 14/25 LB sands, there was an 11% difference from 1 PV to 2.5 PVs for both tests, suggesting that the clogging behaviour with the Cetco product is limited, even in the finer sand. The difference at the same height for the KB product in the 16/30 and 14/25 LB sands was 12% and 6% respectively, demonstrating the importance of grain size for the clogging ability of the polymer fluid. Figure 5.36 presents the pressure profile of the Thanet Sand for a series of PVs over the course of the permeation. There is no discernible form to the pressure profile and no developing trends, indicating that the test apparatus was unable to accurately capture the pore pressure behaviour due to the very low permeability of the sand. These results demonstrate that a fixed wall permeameter is unsuitable to investigate the flow behaviours of polymer fluids in fine soils.

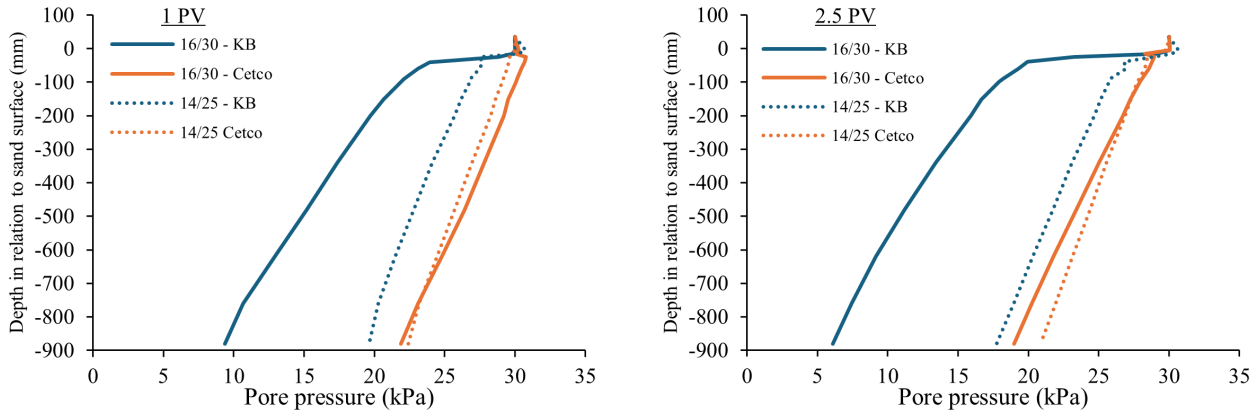


Figure 5.34: (a) The influence of a series of different sand grades on the pore pressure profile down the sand bed depth, presented at 1 PV. (b) The pore pressure profiles for the same permeations are presented at 2.5 PVs.

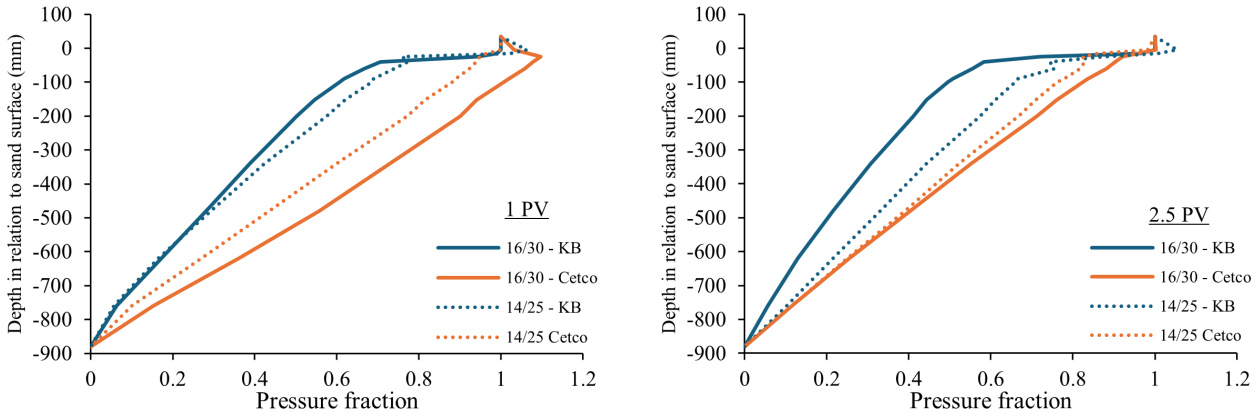


Figure 5.35: (a) The influence of a series of sand grades on the pressure fraction profile for polymer fluid permeations, presented at 1 PV. (b) The pressure fraction profiles for the same permeations are presented at 2.5 PVs.

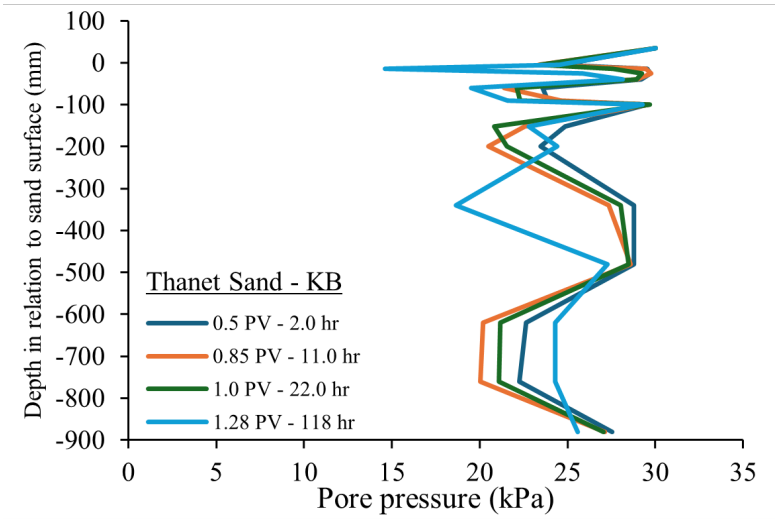


Figure 5.36: The evolution of the pressure profile for a series of PVs during the Thanet Sand test. The pressure profile is shown as a function of depth.

5.3.7 Additive analysis

On-site, additives are typically introduced as a dry powder directly to the polymer fluid using a hopper system. Although designed to clean recycled fluid, the author has often observed them being added to fresh fluid as well. These additives attract the charges of the HPAMs, polymerising them, whilst also attracting dispersed, negatively charged soil particles. To explore how these additives influence the flow behaviour of polymer fluid in sand, a series of tests were conducted. Figure 5.37 presents the flow as a function of PV, comparing the fluid with and without additives. Note that the graph uses a logarithmic y-axis.

The presence of additives clearly influences the fluid behaviour. The charges from the additives cause the polymer molecules to form gelled globules, which reduces the overall bulk

viscosity of the fluid. The measured viscosity of the polymer mixed with additives was 3.84 Pa s, compared to 5.82 Pa s for the fluid without, representing a nearly 35% decrease. This reduction in viscosity causes the fluid to permeate at a greater initial rate. The graph shows that during the initial displacement of water, the fluid with additives has a flow rate that is three to four times greater than the fluid without. Further into the test, a significant slowing of permeation is observed once these gelled globules have interacted with the sand bed. The flow occurring after PV $>$ 3.9 takes place over 119 hours, accounting for 80% of the total permeation duration. In this range, the flow approaches a near-stagnation point, becoming negligible.

Although additives are sometimes necessary for the recycling process to reduce solids content, their use requires careful consideration as they reduce the viscosity. The greatest slowing of fluid flow over the entire investigation occurred in the fluid containing additives. To achieve this benefit, it is crucial to ensure the resulting globules are as small as possible to facilitate greater dispersion. These behaviours offer the possibility of optimising fluid use for tunnelling, pipe-jacking, and caisson sinking, where the formation of these globules might allow the fluid to remain more effectively in the annuluses formed during these processes.

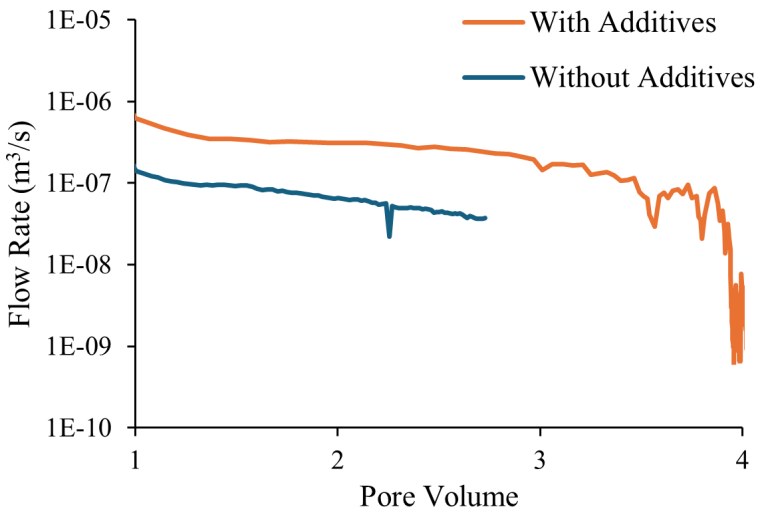


Figure 5.37: A comparison of the flow performance of two KB SlurryPRO CDP polymer solutions is shown as a function of the PV. The tests were conducted in LB 16/30 sand with a polymer concentration of 1.2 *kg/m^3. One solution contained E100 and E200 additives, while the other did not. Note that the y-axis is logarithmic.*

Figure 5.38 presents the pressure profile of the column for a series of PVs and times for the two permeations of polymer fluid, both with and without additives. This figure demonstrates the clogging behaviour that occurs as a consequence of using the additives. The extent of the

pressure drop caused by the clogging is so significant that by 4 PVs, the pressure at the base of the column is around 0.7 kPa, leading to the near-stagnation observed in the flow and discharge graphs.

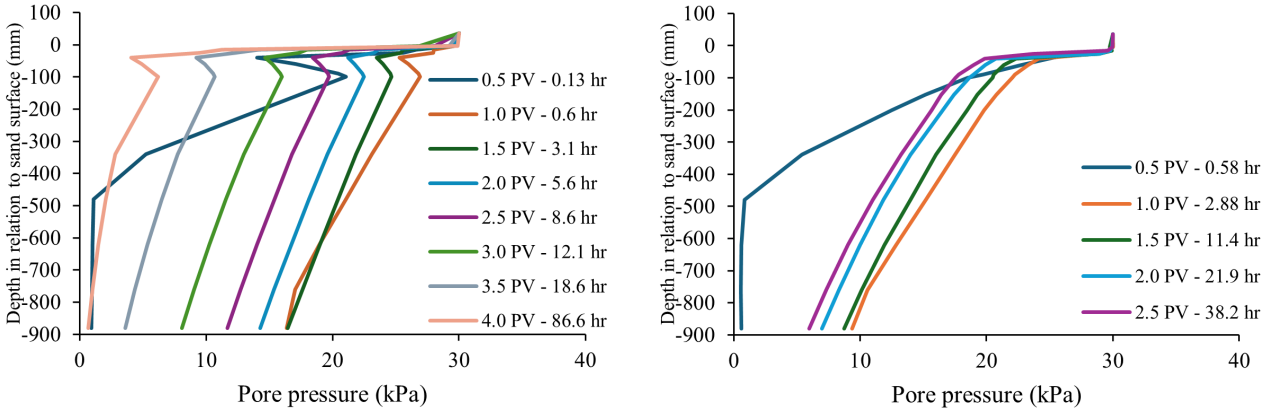


Figure 5.38: A comparison of the pore pressure profile evolution for a KB SlurryPRO CDP polymer solution with and without E100 and E200 additives is presented. The permeations were conducted in LB 16/30 sand with a polymer concentration of 1.2 *kg/m^3. (a) The pore pressure profiles for the solution with additives. (b) The pore pressure profiles for the solution without additives.*

To gain further insight into the flow behaviour and the extent of the clogging that is taking place, the fraction of total pressure drop over the depth of the column can be inspected, as presented for a series of PVs and times in Figure 5.39. For the polymer fluid without additives, the clogging mechanism that forms near the surface at roughly 25 mm depth contributes around 40% of the total pressure loss over the column depth. For the polymer fluid with additives, the clogging mechanism contributes 55% of the total pressure loss at the same PV and, by the end of the test, the clogging mechanism is contributing to almost 90% of the total pressure loss over the column depth; a vast difference in behaviour and capability to stagnate flow.

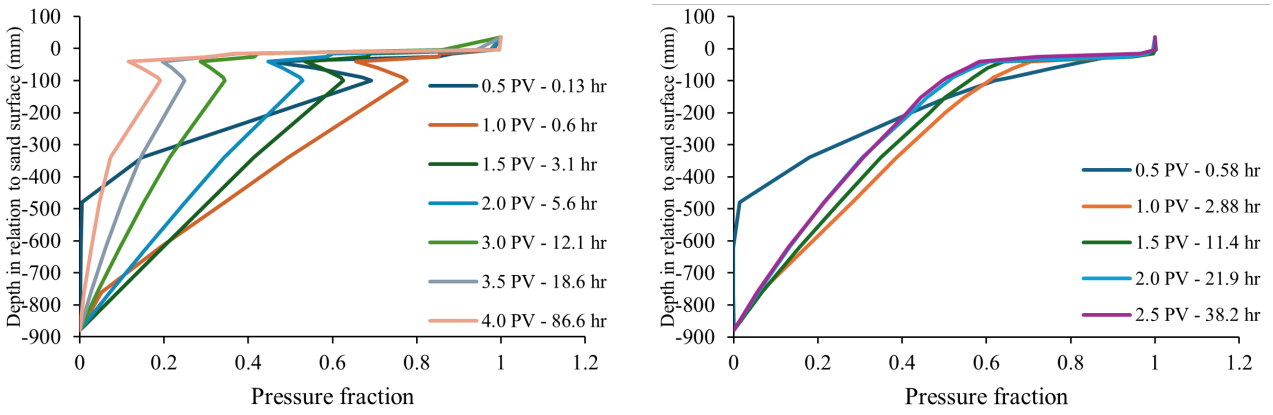


Figure 5.39: A comparison of the fraction of the total lost pressure down the depth of the sand bed for a polymer solution with and without E100 and E200 additives is presented. The permeations were conducted in LB 16/30 sand with a KB SlurryPRO CDP polymer solution at a concentration of 1.2 *kg/m^3. (a) The profile for the solution with additives. (b) The profile for the solution without additives.*

Figure 5.40 presents two images of the latter stage of the permeation of the KB SlurryPRO CDP treated with E100 and E200. The images clearly show gelled globules formed when additives were introduced. The right-hand image distinctly illustrates how these globules permeate and clog the sandbed.

Two points merit mention here. The mixing of the additives was careful and exact, as detailed in Section 5.2.3. On site, in the author's experience, these additives are often added in bulk without due regard for their reactivity, resulting in much larger than necessary gelled globules, 10s of centimetres in scale sometimes, that are unlikely to contribute to the desired bulk clogging ability of the polymer fluid. These larger, visible gelled globules became very apparent towards the latter part of the permeation, in the 3.5 - 3.8 PV region. These globules generally have a lower specific gravity than the bulk polymer fluid, causing them to float or be located near the top of the bulk fluid. In practice, this may be problematic: if the gelled globules are not present throughout the depth of the fluid, then their contribution to the clogging of pore spaces throughout the depth of the excavation may be limited. The only reason these additives contributed to the almost stagnation of the polymer fluid was due to their being pressurised through a predetermined route; whether they would have the same effect on site when not forced into the pore space remains a point for debate. With both of these points in mind, the author highlights the importance of adding these alternatively charged additives carefully and finely, or the benefits reaped from their addition to the fluid may be limited to purely a cleaning agent for recycled fluid.

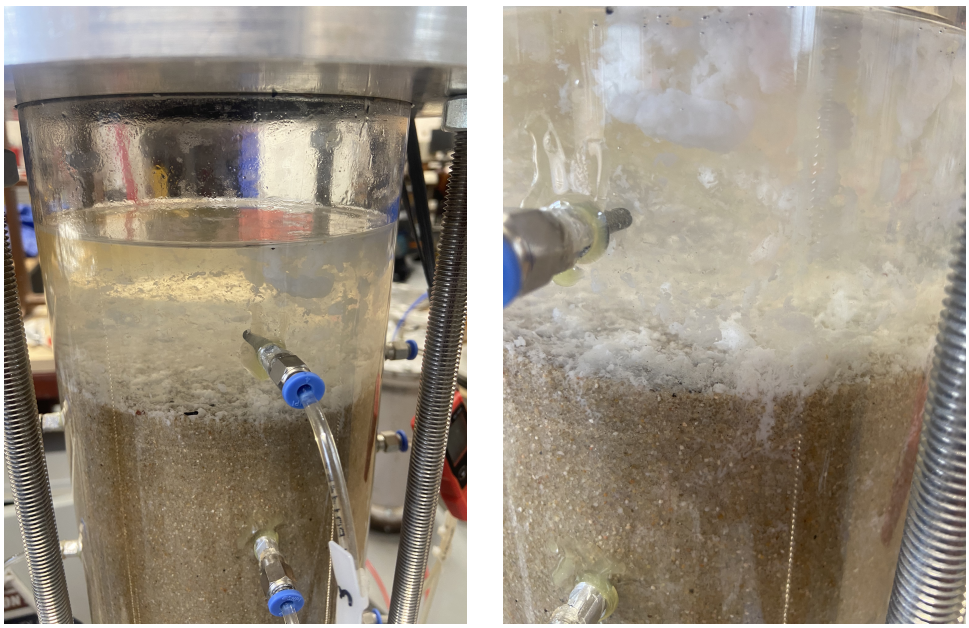


Figure 5.40: A photograph of the sand bed surface at the end of a permeation test with a KB SlurryPRO CDP polymer solution containing E100 and E200 additives. The image shows visual evidence of clogging, with polymer gels having made their way into the permeameter and consequently the sandbed.

Figure 5.41 presents the plots for the viscosity measured at 0.05 s^{-1} as a function of PV for the permeations of the polymer fluids both with and without additives. The plot demonstrates the reduction in viscosity that the fluid encounters when exposed to the additives. At 1.2 PVs, the fluid without additives has a viscosity 2.5 times greater than the fluid with additives. The rapid increase in viscosity observed in the fluid with additives between 1.2 and 1.35 PVs demonstrates the quick transition from water flow to polymer flow.

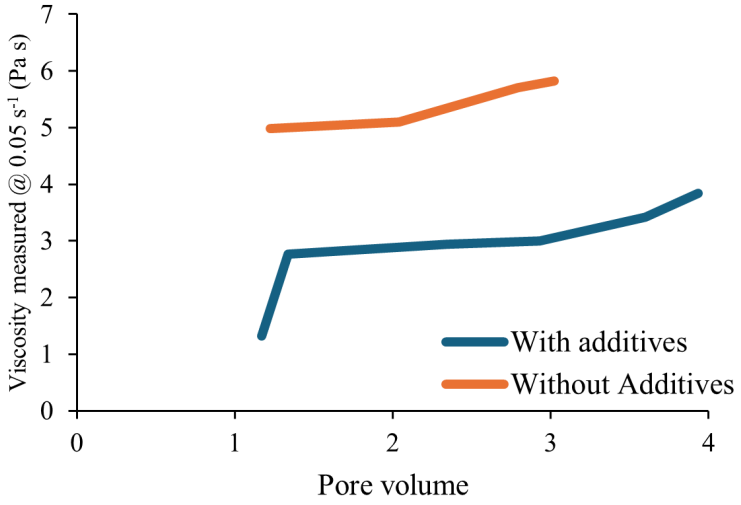


Figure 5.41: A comparison of the viscosity of two KB SlurryPRO CDP polymer solutions is shown as a function of the PV. The tests were conducted in LB 16/30 sand with a polymer concentration of 1.2 *kg/m^3. One solution contained E100 and E200 additives, while the other did not. The viscosity was measured at 0.05 s^{-1}.*

5.4 Summary

The study focusing on the flow of polymer fluids through sands has advanced from previous permeameter testing. The tests investigated the displacement of water initially present in the sand bed by the permeating polymer fluid. This testing spanned varying parameters to understand their influence on flow behaviour in sands, aiming to develop a deeper understanding of the phenomena and to help inform practical applications. The testing has provided a significant database to aid in developing theoretical models for flow and to assist with the numerical modelling necessary to expand the understanding of flow behaviour at a rate fast enough to meet the increasing uptake of the fluid in industry. Key findings are summarised as follows:

- The testing found evidence of the presence of a clogging mechanism, the existence of which has, until now, been a debated phenomenon. This significantly impacts the understanding of the flow behaviour of polymer fluids and will need to be taken into account for models describing flow. This mechanism offers longer-term support pressure and a greatly decreased fluid penetration rate, potentially enabling the use of the fluid near protected sites, such as aquifers and rivers.

- Visual and numerical evidence from this testing indicates that the polymer fluid develops partially preferential paths during permeation, adding weight to the use of capillary modelling to describe its flow behaviour.

- The performance of the polymer fluid varies greatly from supplier to supplier. Some polymer products are less able to develop the same viscosity as others, and some are less effective at developing the clogging mechanism discussed. These results indicate that great care needs to be taken when choosing polymer suppliers. Until the formulation, molecular weight, and degree of hydrolysis are known and can be optimised by all suppliers, the performance of these different products will continue to vary, affecting both cost and excavation stability when using polymer products.

- The applied pressure to a polymer fluid has an exponential relationship with the flow. This finding means that contractors should be diligent in determining the necessary

pressure for excavation stability. This may need to be higher for soils with higher groundwater pressures, and then kept as low as possible (taking into account a safety factor) in order to prevent unnecessary wastage of the polymer product and unnecessary penetration depth.

- The polymer concentration has a negative exponential relationship with the flow rate through sands, though this will be limited by the pure solution flow rate. This means that in the concentration range that contractors are generally advised to use, they will likely experience quite large performance increases and decreases depending on the increase or decrease in concentration applied. This highlights the importance of diligent monitoring of fluid loss records and adapting concentration levels to optimise performance and cost depending on the soil being supported by the fluid.

- The results from the sand testing offer guidance on the limit of hydraulic conductivity where polymer fluids become no longer capable of supporting an excavation. The coarser sands that were tested formed beds with hydraulic conductivities in the order of magnitude of 10^{-3} m/s. In this order, the polymer fluid exhibited a much greater flow rate and stopped showing signs of forming an effective clogging mechanism to assist the viscous resistance in slowing the flow of the fluid.

- The additive testing offers promise of an effective material that could lead to improved performance, especially in circumstances where limiting flow to a certain depth is crucial for the environmental context. However, the results and the author's experience with the fluids in the lab indicate that their use must be carefully considered and implemented to reap potential benefits and not to instead detract from the performance of polymer fluids.

Given these findings, there is still more work to be done to achieve a comprehensive understanding of the flow behaviour of polymer fluids in sands, though the results provided offer good guidance for optimising their use and open the door for numerical modelling that can explore different features of the flow.

6 Investigation of polymer fluid-soil interaction

6.1 Introduction

Previous studies on the influence of polymer fluid on the shear resistance of soils (Lam et al., 2014, 2015a; Verst et al., 2022a) have indicated that they may facilitate a higher shear resistance than alternative support fluids at excavation walls. However, where previous testing focused on sands and field tests, this investigation specifically examines the influence of polymer fluids on clay behaviour. The testing was split into two components: oedometer testing and direct shear testing. The oedometer testing enabled a closer examination of clay softening when exposed to polymer fluids. The shear testing examined how different support fluids affect the shear resistance of an excavation face against a concrete interface.

An area of concern with respect to the use of polymer fluids in excavation support is the rate and extent to which they affect soil swelling and softening. As soils are subjected to loading and unloading, they undergo compression and swelling, respectively. In saturated clays, these volume changes involve the rearrangement of grains, along with the compression or swelling of the clay particles themselves, and the seepage of fluid (Atkinson, 2007). Terzaghi's (1936) effective stress principle is presented below:

$$\sigma' = \sigma + u \tag{6.1}$$

Where σ' is the effective stress (the stress carried by the soil solid skeleton), σ is the total stress (the total stress applied to the bulk soil), and u is the pore water pressure. Excavations in overconsolidated clays can result in negative pore pressures. Consequently, when excavations are made in these clays, they tend to absorb water, leading to softening and a reduction in their undrained shear strength over time (Powrie, 2018).

The rate of this softening in practice, as detailed by Powrie (2018), is dependent on the bulk permeability of the soil, the soil stiffness, and the availability of water. The availability of water is the parameter of particular interest in this investigation, as it represents the

differentiating factor between established methods and the use of polymer fluids. In London Clay, the effects of softening are sometimes accounted for by applying a factor of 0.6-0.8 (usually referred to as the α value in pile design) to the undrained shear strength, S_u (Powrie, 2018). Therefore, being able to accurately quantify the extent of swelling with alternative fluids could have a significant impact on the final design of a foundation.

Another key area of interest when using polymer support fluids is their effect on the shear resistance of the excavation face. Initial tests by Lam et al. (2014) and Verst et al. (2022a) suggest that polymer fluids are less detrimental to shear resistance of piles in sands than bentonite slurry, and facilitate a shear resistance comparable to, or even higher than, that achieved with water. The polymer fluids achieve this due to the lack of a filter cake developing at the sand face, which facilitates more direct contact between the sand and the final installed foundation element. However, the investigations conducted by both Lam and Verst focused on a sand-concrete interface. There remains a lack of laboratory research on the influence of polymer fluids on the shear resistance generated by piles on clays.

In this section of the project, a novel method and apparatus were devised to investigate the swelling behaviour of clays when exposed to polymer fluids. An existing oedometer apparatus was modified to enable a clay sample to swell directly under polymer fluid. The findings from this testing offer insights into the swelling and softening behaviour of clay in response to polymer fluids when exposed in deep foundation excavations.

To examine the influence of support fluids on clay-concrete interfaces, a modified direct shear methodology was devised for this investigation. Tests were conducted on laboratory kaolin clay, which is an extensively researched and well-understood soil. Further tests were conducted on Lambeth Clay (predominantly the Reading Formation) from the Lambeth Group samples to provide test results for a regularly encountered soil in London. For this investigation, a direct shear box was chosen. Given the time and resource constraints of the project, the direct shear apparatus was deemed the most suitable for examining the effect of polymer fluid on interface strength.

6.2 Materials and methods

6.2.1 Clay preparation

The kaolin was mixed in a 110 litre ribbon blade mixer, as depicted in Figure 6.1. Dry kaolin powder was weighed and added to the drum, followed by water in a ratio of 5 parts water to 4 parts kaolin. A vacuum of -0.8 bar was then applied to the drum throughout the two-hour mixing period to ensure the removal of most air bubbles.



Figure 6.1: The ribbon mixer used to mix kaolin clay. The dry kaolin powder was measured into the drum, water was then added in a prescribed volume, and the mixer was sealed and a vacuum applied whilst mixing.

Once mixing was complete, the slurry was pumped out of the mixer and into the consolidation apparatus, pictured in Figure 6.2. The consolidometer itself comprises a hydraulic ram mounted onto a loading frame. The mixed slurry was pumped into two drums, which were bolted together and sealed with silicone sealant. Filter papers were positioned at both the base and top of the drums to allow for water drainage into channels as the ram applied pressure and the slurry consolidated.

The clay was consolidated in steps, up to 200 kPa, and then fully unloaded in one step. The distance between the loading frame and the top of the clay sample was measured to determine the extent of consolidation. After consolidation was complete, the sample was removed from the consolidometer, cut into manageable pieces, and wrapped in several layers of cling film to maintain its moisture content. The test clay specimens were then cut from each block of

kaolin.



Figure 6.2: On the left is the consolidation apparatus used to consolidate the kaolin clay into a workable mass from which good-quality, homogeneous test samples can be obtained. On the right is the ribbon mixer used to mix the dry kaolin powder and water into a deaired slurry.

6.2.2 Polymer preparation

The polymer was prepared in the same manner as detailed in Section 3.2.3. Given the small quantity of polymer fluid required for each test, a single batch of polymer fluid was mixed and sufficed for the entire suite of testing. Figure 6.3 presents the viscosity test results conducted for the batch of fluid used in this investigation.

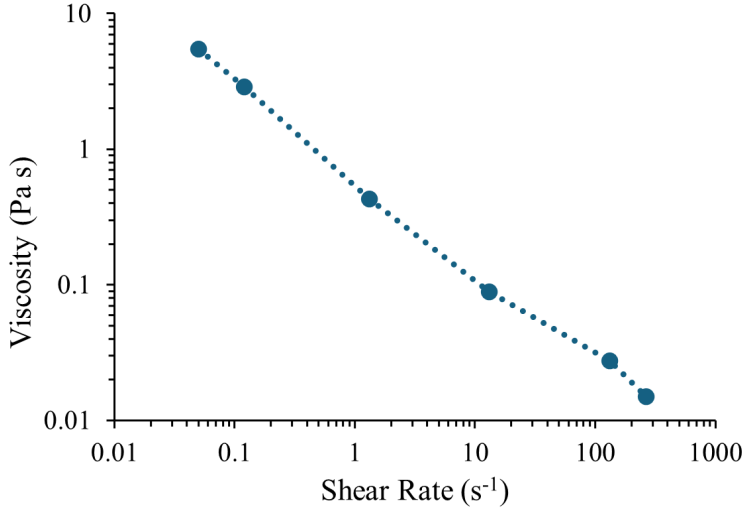


Figure 6.3: The viscosity against shear rate for the polymer fluid used in the oedometer testing. The polymer fluid consisted of SlurryPRO CDP (KB) mixed at 1.2 kg/m^3 concentration in treated tap water.

6.2.3 Oedometer test apparatus

Figure 6.4 provides an illustration of a standard oedometer testing apparatus, used to investigate the 1-dimensional consolidation and swelling behaviour of soils. In this setup, the soil sample, contained within a confining ring, is fully submerged in water. As loads are either applied or removed via the loading element, the sample consolidates or swells, respectively. During these volumetric changes, the water within and around the sample follows drainage paths through the porous stone and the soil sample itself. Concurrently, a displacement transducer tracks the volumetric changes of the sample.

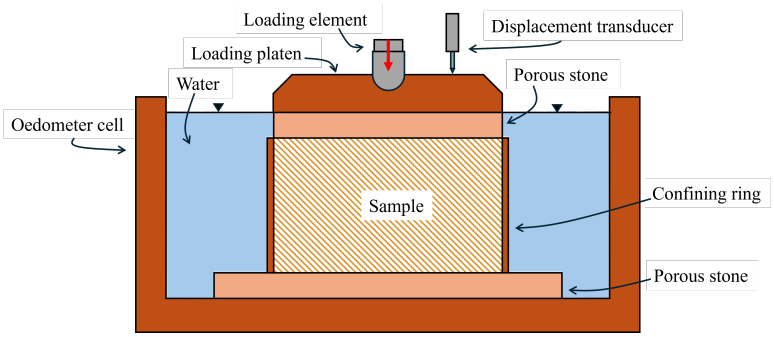


Figure 6.4: A diagram of a standard oedometer cell apparatus used for investigating the swelling of soils.

The primary challenge in investigating the swelling behaviour of a clay sample under polymer fluid using a classical oedometer apparatus lies with the placement of porous stones at the top and bottom of the soil sample. As the soil sample consolidates, the expelled water flows into these porous stones. However, given the relatively low volume of water expelled, this water was likely to remain within these porous stones. Consequently, when the load was removed for the swelling stages, the fluid taken on by the sample would be the water that had been dispelled during consolidation.

To address this, the porous stones needed to be adapted. Initial considerations included sintered bronze discs with larger pore volumes than used in the standard apparatus to facilitate fluid exchange, but this consideration proved to be both costly and protracted. Figure 6.5 presents the final apparatus configuration. Two Perspex discs, each featuring channels connecting the side to the midpoint of its base, replaced the traditional sintered bronze porous discs. Reservoirs of polymer fluid were connected via hosing to the side of these discs. At the soil face of each disc, a coarse mesh with a 4.18 mm aperture was placed,

followed by a fine mesh of 0.026 mm. This configuration allowed a head of polymer fluid to be applied to the interface side of the Perspex dish, effectively displacing the water expelled during consolidation with polymer fluid. This ensured a pure clay-polymer fluid interface for the subsequent swelling stages.

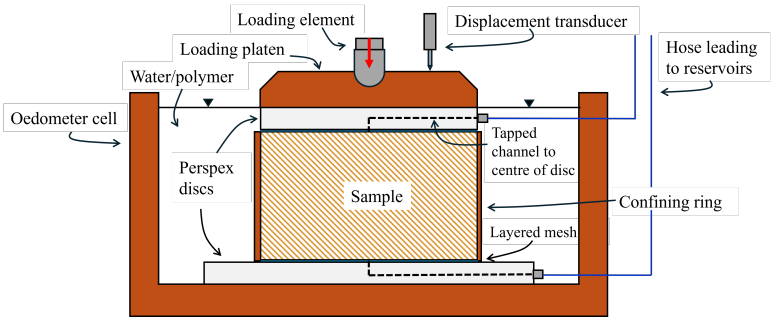


Figure 6.5: A diagram of the adapted oedometer apparatus used to investigate the swelling behaviour of kaolin when exposed to polymer fluid.

6.2.4 Clay mass loss during tests

Although the assembled apparatus performed well, the use of a coarser mesh meant that the clay face at the edge of the sample became slightly eroded during testing. The finer mesh placed between the coarse mesh and the clay performed well in mitigating this deterioration, but not perfectly. The erosion of the clay sample and the ability of the apparatus to exchange fluids are, unfortunately, strongly related and would require more time and money to prevent than was feasible in this project.

Figure 6.6 presents the estimation of clay mass lost during the testing sequence against the maximum normal stress applied to the sample. The clay mass lost was estimated by determining the estimated dry mass of the clay in the test sample before the test and the measured dry mass of the clay afterwards. Given the consistency of the moisture content for the clay samples measured, this estimation would seem to be a reliable one.

From these results, it can be seen that the test samples exposed to water regularly lost more clay mass than the samples exposed to polymer fluid. This is a clear demonstration of the dispersion-inhibiting properties of the polymer fluid. The test with treated water appeared to lead to a greater mass loss over the testing, perhaps a consequence of the high pH environment eroding the clay slightly more than if it were a neutral environment, though between the two, there is a 0.5% difference in material loss. If there was a deteriorating effect of the high pH

environment, it was outweighed by the dispersion-inhibiting properties of the polymer fluid. Despite the observation that with each increment of load, the evidence of clay loss became more apparent, there was no trend of clay loss with increased mass, indicating that the erosion that occurs in the sample occurs to a certain depth determined by the apparatus configuration and was not cumulative over the sequence. The increasing evidence of erosion must therefore be caused by the displacement of the eroded clay by the dispelled fluid after each added load. Overall, the quantity of clay mass loss in these tests must be considered for analysis, but it was not so great that it invalidates test results and shows that the adapted testing configuration was suitable for the investigation.

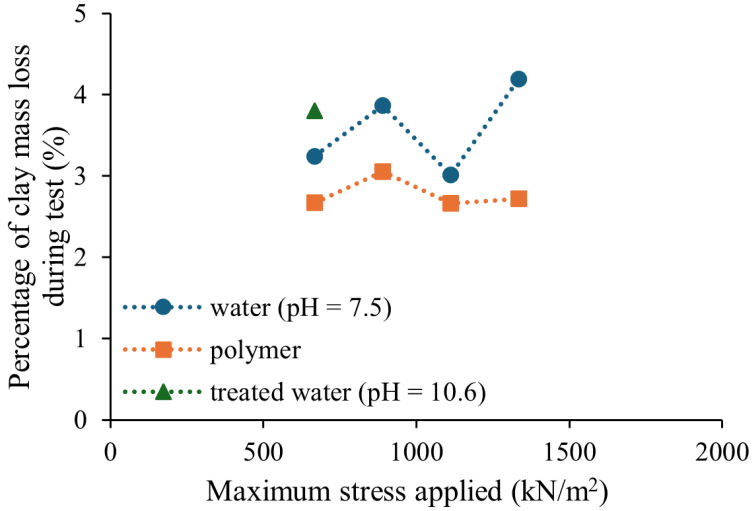


Figure 6.6: The percentage of mass lost from the total mass of the clay sample for each oedometer test conducted.

Figure 6.7 shows the complete oedometer set-up. Once the oedometer cell has been assembled, it can be positioned within the lever-arm rig. Masses are placed on the lever-arm, which, in turn, exerts a tenfold force of the weight onto the soil sample. The displacements occurring within the soil sample are measured and recorded by a displacement transducer connected to a computer running a control program for the test. At the necessary moment during the test, valves on the reservoir line can be opened to displace the water at the clay surface on both the top and bottom of the soil sample.

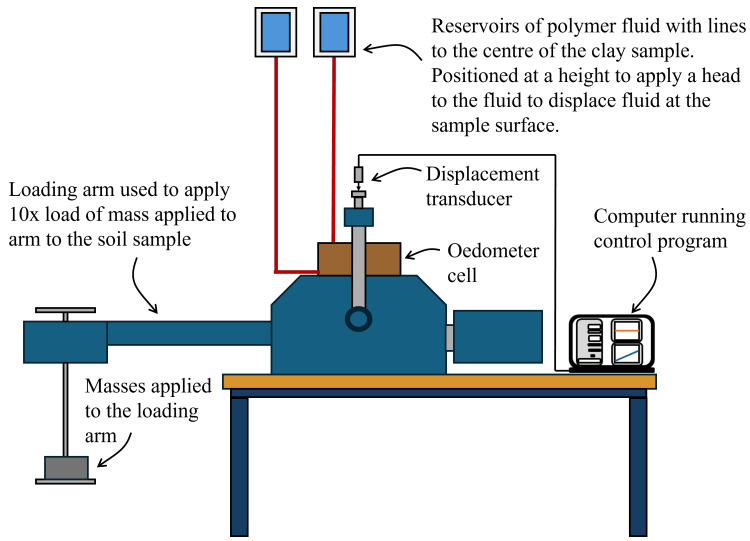


Figure 6.7: A diagram of the full oedometer set up used in the laboratory investigation of clay swelling under polymer fluid.

6.2.5 Oedometer test procedure

The procedure adopted for this investigation closely follows the classical oedometer test, with only a couple of minor differences. Initially, each component of the apparatus was weighed for reference. The confining ring was then inserted into the kaolin block and cut out; this method offers the best chance of producing a homogeneous and consistent clay sample across tests. Excess clay was trimmed from the confining ring and placed into sample trays to make 3 samples for each test. These excess cuttings were then oven-dried at 105°C, with their mass recorded both before and after drying to determine the moisture content of the clay. The prepared test sample and confining ring were subsequently placed into the oedometer, and the apparatus was set up as depicted in Figure 6.7.

Prescribed, cumulative masses were then loaded in stages onto the lever arm. Each subsequent mass was applied once the rate of change in displacement was less than 0.01 mm/hr. If the test involved polymer, the reservoirs were opened, allowing the polymer fluid to completely replace the water sitting on the clay surface. Once the greatest prescribed mass had been applied and the soil had fully consolidated under the exerted force, the majority of the mass, apart from a nominal 0.2 kg (5.4 kN/m^2), was removed from the lever arm. This residual force ensured the loading element remained in contact with the specimen, allowing all swelling to be accurately recorded. Once the swelling had stabilised, the test was terminated, the sample removed, and a moisture content measurement was made for the test sample.

6.2.6 Direct shear apparatus

Figure 6.8 illustrates a standard direct shear box apparatus. The box was formed by two halves held together by screws, compelling the sample to shear at the joint between the top and bottom sections. A normal stress, σ_n, was applied throughout the process by an actuator acting upon a loading frame positioned atop the sample. Simultaneously, a shear stress, τ_n, was applied by an actuator acting on the side of the bottom half, forcing it across the clamped top half. The box was displaced by this actuator at a predetermined rate. The displacements and applied stresses were measured by displacement transducers and load cells around the apparatus, with data recorded by a computer program.

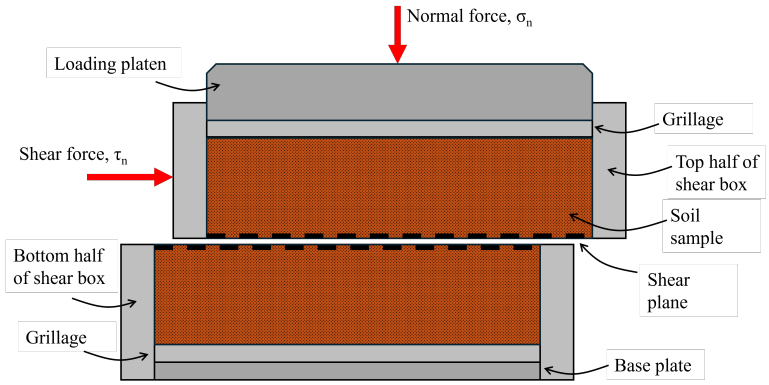


Figure 6.8: Diagram of direct shear test apparatus.

The machine utilised for the shear testing was a VJ Tech ShearSCAN Pro, shown in Figure 6.9. This machine supports fully submerged direct shear testing and comes equipped with a computer program that manages test execution, data logging, and results processing. The shear box itself had an internal space of 60 x 60 mm, with a combined depth of 50 mm when its two halves were assembled.

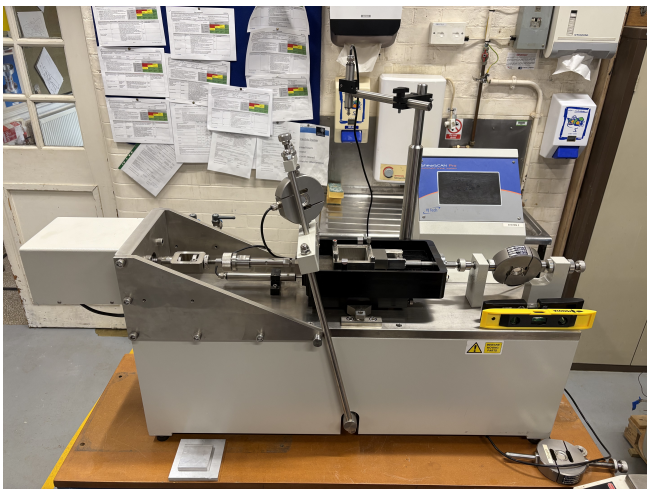


Figure 6.9: The VJTech Automatic Direct and Residual Shear System (ShearSCAN Pro) machine utilised for the interface shear testing conducted.

6.2.7 Concrete

The dry concrete mix used in the test was a Heidelberg Materials 40 N Concrete (C32/40). The dry-mix contained coarser aggregate that was excessively large for the apparatus. To address this, the mix was sieved to remove the oversized particles. Subsequently, pea shingle, no larger than 4 mm, was mixed into the concrete prior to water addition. The final composition of the concrete mix is presented in Table 6.1.

Table 6.1: Materials, their quantity, and notes regarding them used in the investigation into the effect of polymer fluid on the shear interface of clays.

Material	Proportion of mix (%)	Notes
CEM I 52, 5N	7.8	BS EN 197
Regen GGBS	7.8	BS EN 15167
Fine aggregate (0/4 mm)	23.5	BS EN 12620
Pea shingle (0/4 mm)	47.9	
Water	13.0	

6.2.8 Direct shear test procedure

The polymer fluid used in this testing was drawn from the same batch as the oedometer testing; for further details on the polymer fluid mix, refer to section 6.2.2. The bentonite slurry used in the testing was mixed as per the method outlined in Section 3.2.4.
Figure 6.10 outlines the testing method for direct shear tests. Clay samples were cut with wire for the kaolin tests, whilst the harder Lambeth Clay samples were cut with a bandsaw.

The shear box was assembled as shown in Figure 6.10(a). The carrier was flooded with the test fluid, and a normal stress of 250 kPa was applied to the top of the soil sample. The density of the kaolin was determined to be 1692.2 kg/m^3 through repeated measurements of soil samples; this density means 15 m of the soil exerts a pressure of 249 kPa, which informed the selection of the 250 kPa normal stress. The sample was consolidated under the normal stress for 24 hours. The normal stress was then relieved, allowing the sample to swell for 24 hours whilst exposed to the test fluid. The 24 hours for each process were sufficient to allow the soil to reach a relatively steady state, as measured by the displacement transducer located on the top of the sample.

Next, the sample was pushed up in the box so that the surface that had been in contact with the test fluid was now at the midpoint of the assembled shear box. Concrete was mixed and placed in the bottom half of the shear box. A pressure equivalent to a 15 m depth of concrete (345 kPa), based on theory and field measurements (McNamara et al., 2014), was then applied to the top of the shear box. The concrete was allowed to cure under this normal stress for 7 days. After 7 days, the shear test was conducted under the 345 kPa normal stress, at a progression rate of 0.6 mm/min for the kaolin testing and 0.0125 mm/min for the Lambeth Clay testing.

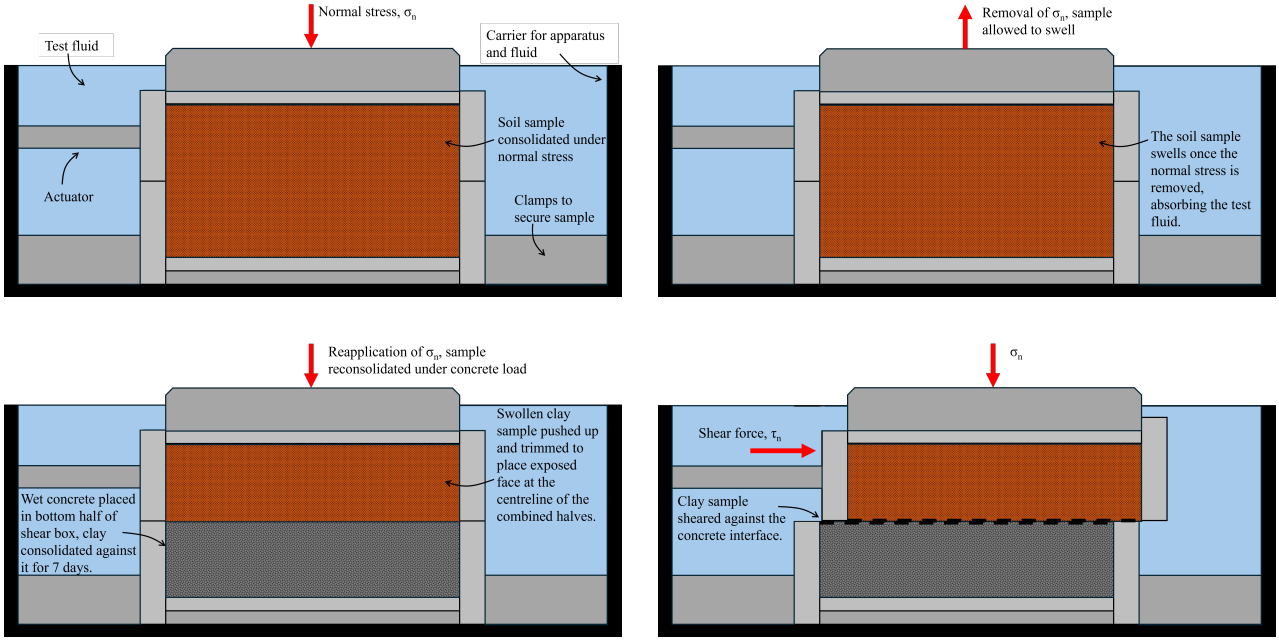


Figure 6.10: Procedural steps for the direct shear test: (a) Establishment of the direct shear apparatus and initial sample consolidation. (b) Release of confining pressure, allowing the soil sample to swell and absorb the test fluid. (c) Repositioning of the clay sample into the upper box half, followed by the placement of wet concrete in the lower half and subsequent consolidation of the clay against the concrete for seven days. (d) Commencement of the direct shear test.

An area of focus during testing was the location of the shear plane. A limitation of the shear box test is that it forces the shearing to occur at a specific location. By separating the top and bottom halves of the box using the lifting screws, a few millimetres of depth are provided for the shear plane to form. In this testing, it was crucial to place the concrete in the bottom half with careful precision to ensure the desired shear plane location.

Figure 6.11(a) illustrates the successful outcome of this careful concrete placement: the concrete level was just above the surface of the bottom shear box half, but not so high as to interfere with the top half as it was displaced. Figure 6.11(b) shows the two halves of the shear box, split at the shear plane with the shear plane facing upwards. This figure indicates how the method allowed for shearing at the interface. The box on the right of the picture displays areas of darker colouring, signifying concrete at the surface, whilst lighter areas suggest the embedment of aggregate into the clay sample.

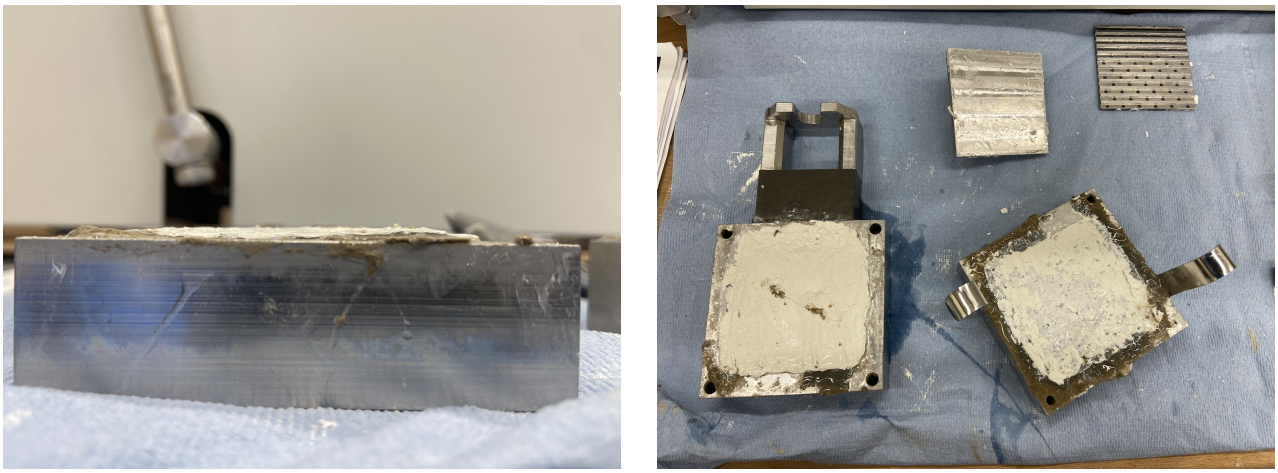


Figure 6.11: (a) The profile of the bottom half of the shear box after a completed kaolin-concrete interface test, exposed to polymer fluid. N.B. The concrete level was just above the surface of the box. (b) The full sample after the shearing has been completed. N.B. The varying shades in the sample on the right of the image indicate a reasonable locating of the shear plane.

Figure 6.12 displays the shear box after the sample has been sheared. To verify that the concrete interface was indeed the location of the shear plane for the Lambeth Clay tests, a pin was used to check the depth of material resting on top of the concrete. This was not as immediately obvious as it had been with the kaolin clay; given the much darker appearance of the Lambeth Clay, differentiating between shallow and deeper deposits of clay on the concrete surface proved challenging.

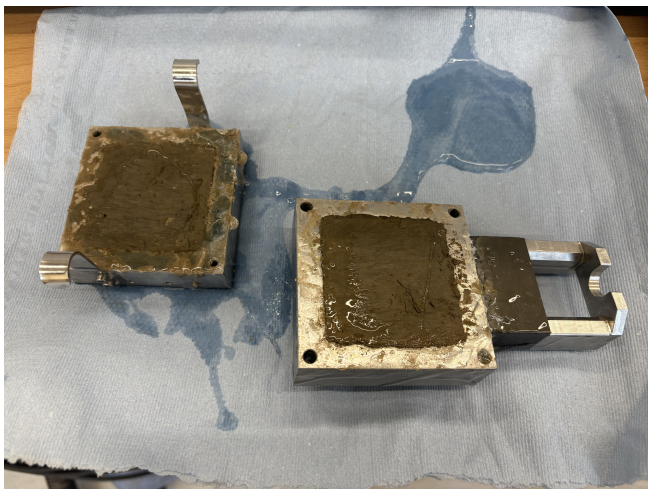


Figure 6.12: The full sample of Lambeth Clay and concrete following the exposure to polymer fluid and then shearing.

6.2.9 Scope of testing

The base case parameters for the oedometer testing are presented in Table 6.2. This investigation specifically focused on the mechanical differences in swelling behaviour between samples exposed to water and those exposed to polymer fluids. To explore the influence of water chemistry, an additional oedometer test was conducted using water treated with sodium hydroxide to increase its pH to 10.8. This was to examine whether such treatment had any adverse effect on the swelling behaviour. Tests were conducted with water, polymer, and the treated water across a range of maximum masses applied to the lever arm. Table 6.3 outlines the fluids tested, the maximum masses applied in the completed tests, and the resulting stress exerted on the sample.

Table 6.2: The adopted base case parameters for oedometer testing.

Parameter	Type/Value
Polymer type	SlurryPRO CDP
Polymer concentration, c (kg/m^3)	1.2
Clay type	Kaolin
Area of clay sample (m^2)	0.0044
Height of confining ring (mm)	20

The base case parameters for the shear interface testing are outlined in Table 6.4. This investigation focused on clays and how their exposure to various test fluids affected their shear resistance. Two types of clay were selected for testing: a laboratory kaolin and a real-world example of clays encountered in the field, a Lambeth Clay obtained from a construction site.

Table 6.3: Test fluids and stresses applied in the oedometer study.

Test fluid	**Maximum mass applied to lever arm (kg)**	**Maximum stress applied to clay(kN/m^2)**
Water	30, 40, 50, 60	667, 890, 1112, 1335
Polymer	30, 40, 50, 60	667, 890, 1112, 1335
Treated water	30	667

Shear tests were conducted on both clays without a concrete interface to establish the inherent properties of the clay. Additionally, each clay was exposed to water, polymer fluid, and bentonite slurry before the shear test was performed. This indicated the effects these test fluids have on the soil-concrete interface. Table 6.5 outlines the specific tests undertaken in this investigation.

Table 6.4: Shear box testing adopted base case parameters.

Parameter	**Type/Value**
Polymer type	SlurryPRO CDP
Polymer concentration, c (kg/m^3)	1.2
Area of clay sample (m^2)	0.0036
First consolidation stress (kPa)	250
Consolidation pressure for curing and normal stress for test (kPa)	345

Table 6.5: Tests conducted in the shear box soil-concrete interface testing.

Clay	**Test**
Kaolin	No interface, water, polymer, bentonite slurry
Lambeth Clay	No interface, water, polymer, bentonite slurry

6.3 Results

6.3.1 Moisture content tests

Over the 27 samples taken from the prepared test samples and subjected to a moisture content test, the average moisture content for the test clay before consolidation was 33%. These samples had a coefficient of variation (CV) of 0.03, demonstrating the consistency

between samples. Figure 6.13 presents the moisture content values of the oedometer samples after they have been consolidated and allowed to swell again under the same nominal load in the oedometer test procedure.

There is a clear relationship between the maximum normal stress applied and the moisture content of the sample. As the maximum pressure increases, the moisture content decreases; this is an expected relationship given that the hysteresis of the soil sample makes it less capable of taking on the fluid in swelling immediately after loading due to the rearrangement of clay particles that has taken place. Notably, however, for each maximum stress applied, the samples exposed to polymer fluid had a greater moisture content than those exposed to water. The clay sample exposed to the treated water had an even lower moisture content. A key feature of polymer fluid flow behaviour is the tendency for it to self-siphon. This is characterised when a small volume of the fluid is spilt from a container, and the polymer molecules exert a drag force on neighbouring molecules. Consequently, a volume larger than the initial spill is drawn out of the container. One possible explanation for the results is that the suction from the negative pore pressures, coupled with the self-siphoning mechanism that occurs when polymer molecules in the fluid interact with one another, may have enabled a greater volume of fluid to be taken in by the clay. Another factor to consider is the chemical interaction between the clay and the polymer fluid. The much lower moisture content in the clay following the treated water test suggests a deterioration of the clay clusters, which results in less pore space. This is caused by the tendency for the clay particles to disperse owing to repulsive charges present when exposed to alkaline solutions (Lambe and Whitman, 1969). While the high pH of the polymer fluid may also cause the dispersion, the coating of the clusters by polymer molecules may facilitate the clay maintaining its moisture content.

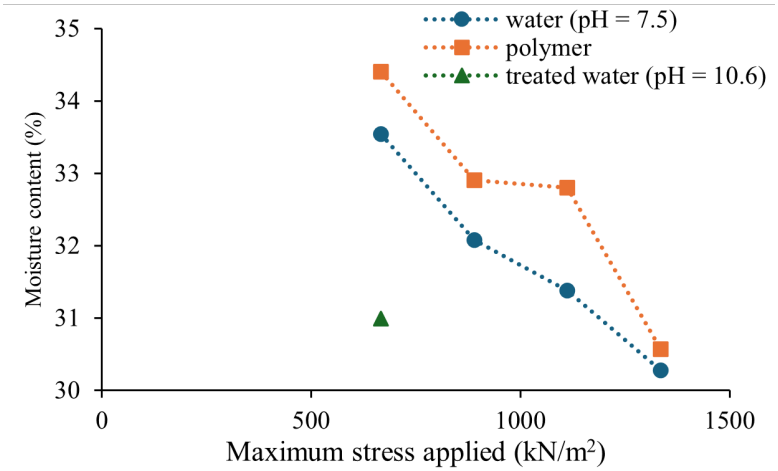


Figure 6.13: Moisture content loss against the maximum load applied to the clay test samples for the series of oedometer tests conducted with water, polymer, and treated water.

6.3.2 Oedometer testing - void ratio and fluid type

A standard analysis of oedometer test results involves determining the change in void ratio against the changing applied normal stress. Upon completion, a number of characteristics can be determined, including the coefficient of consolidation for 1-dimensional consolidation, c_v, the compression index, C_c, and the swelling index, C_s, among others. These characteristics are used to determine the rate at which soils respond to manipulated loads.

Figure 6.14 presents the void ratio against the applied normal stress for tests conducted with varying maximum applied stresses and fluid types. As can be observed from these figures, the void ratios over the course of testing were similar to one another over the consolidation cycle, indicating a reasonable reliability of the testing apparatus.

Between exposures to different fluid types during the swelling stage, the swelling of the soil was relatively similar, although there were some slight differences in the final void ratio.

Figure 6.15 presents the swelling index, C_s, against the maximum stress applied for the various fluid exposures. The C_s is determined by the gradient of the line between the unloading steps for the void ratio against the natural logarithm of the applied normal stress. As per the figure, the sample exposed to polymer fluid seemingly routinely has a higher swelling index and, therefore, a slightly higher void ratio each time the clay swells. There was not a great difference between the samples exposed to the different fluids, but there does seem to be a pattern, indicating that exposure to the different fluids does affect the final characteristics of the soil when it takes on the fluid. This may again point to the siphoning

behaviour of the polymer fluid, causing a higher volume of fluid to be taken on when swelling. Another possible reason for the slightly greater volume of fluid absorbed is the chemical interactions between the clay and the fluid. The high pH of the polymer fluid may deteriorate the clay clusters into smaller fragments, increasing their surface area and potentially allowing for a greater intake of fluid during the swelling stages.

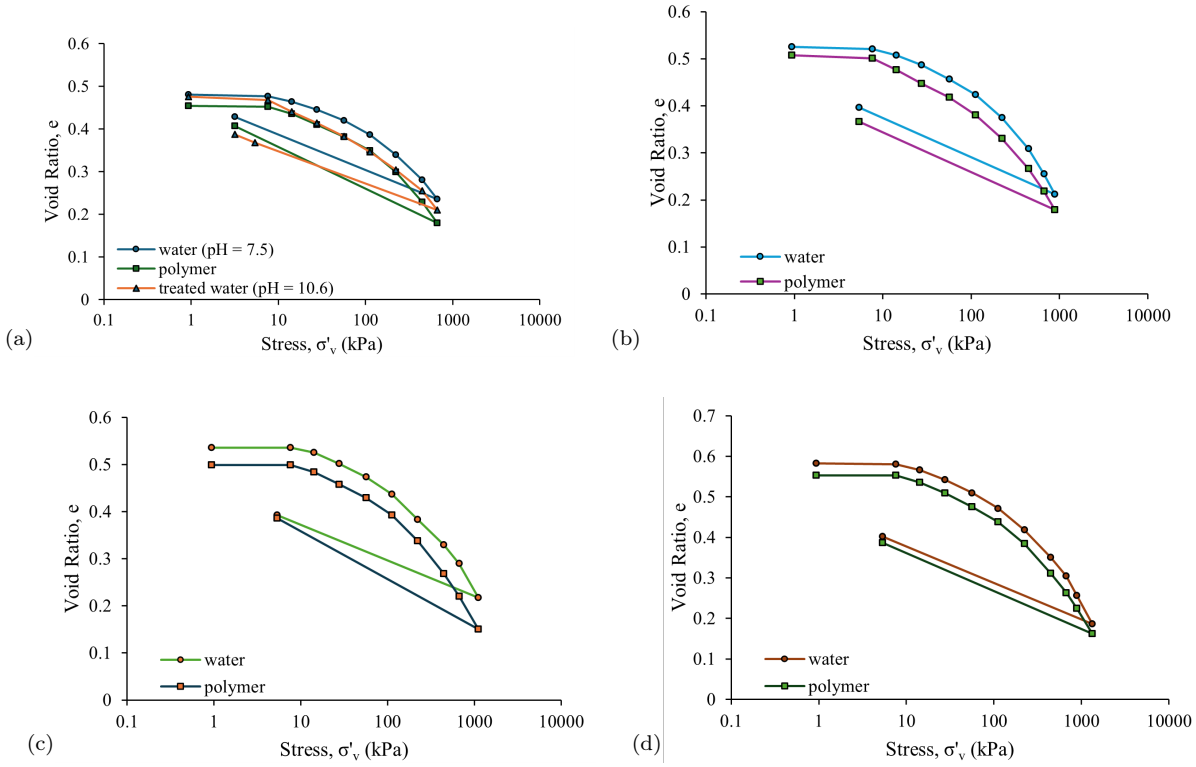


Figure 6.14: The void ratio against stress for a series of fluid types (a combination of water, polymer fluid, and treated water) where a maximum normal stress applied to the sample was (a) 670 kPa (b) 890 kPa (c) 1110 kPa (d) 1340 kPa.

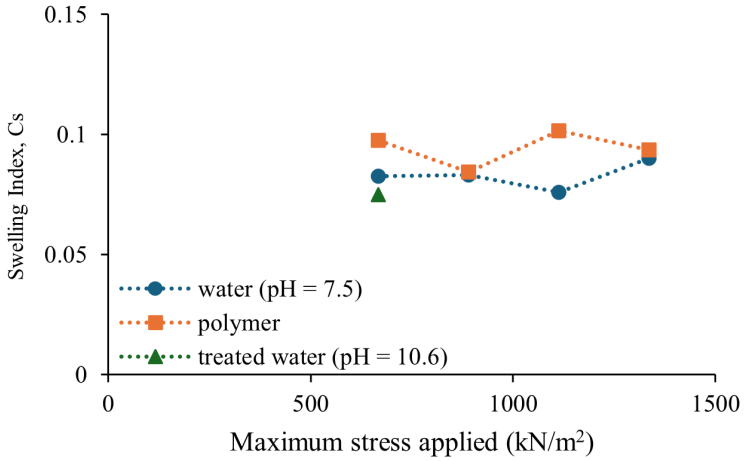


Figure 6.15: The swelling index against the maximum applied normal stress to the test clay sample. The swelling index is determined from the gradient of the void ratio against the natural log of the applied normal stress.

6.3.3 Oedometer testing - influence of fluid type on swelling rate

Figure 6.16 presents the zeroed swell strain against time for the unloading stage of the oedometer test. These plots enable the inspection of the swelling mechanics when the soil was drawing in water or polymer fluid. The zero strain was taken at the point in the last consolidation step where the soil sample had settled under the maximum applied stress. Figure 6.17 presents the swell strain per dry clay mass against the square root of time. The swell strain per dry clay mass uses the final dry clay mass to account for the variable factor of clay mass loss discussed in Section 6.2.4; in other words, it might be expected that with a higher clay content there would be more swell, potentially leading to skewed results. The figure is plotted with a square root time x-axis to provide more clarity to the earlier stages of the swelling, where the majority of the strain occurs. For these plots, a Python code was used to determine the best-fitting hyperbolic model for the data as follows:

$$y = \frac{jx}{s + x} \tag{6.2}$$

Where j is the swell limit coefficient and s is the swelling rate coefficient. The fitting was successful in all cases with an average R^2 of 0.965 across all fitted functions. In the function, the j coefficient controls the plateau of the swelling strain as the x approaches infinity, where the s function controls the rate at which this plateau is approached. Figure 6.18 presents the determined s coefficients from the function fitting against the maximum test so that the swelling rate for the soils exposed to each fluid type can be assessed. For each unloading, bar one, of maximum stress applied, the polymer fluid had a greater swelling rate than the water. Between the treated water and the more neutral water, the clay exposed to treated water exhibited a lower swelling rate. This indicates that the observed consistently higher swelling rate of the polymer was not attributable to the higher pH of the fluid. These are curious results given on-site observations, which suggest that clays become very soft when exposed to water, less so when exposed to bentonite slurry, and even less so when exposed to polymer fluids. One might expect that with a greater swelling rate, the clay pores would have a higher void ratio in less time, causing the soil to soften and break up more rapidly. These results contradict this. It may be the case that polymer molecules act as a binder in the soils, meaning that even though they may infiltrate at a greater rate, they may also prevent

softening and consequently the breaking up of the soil.

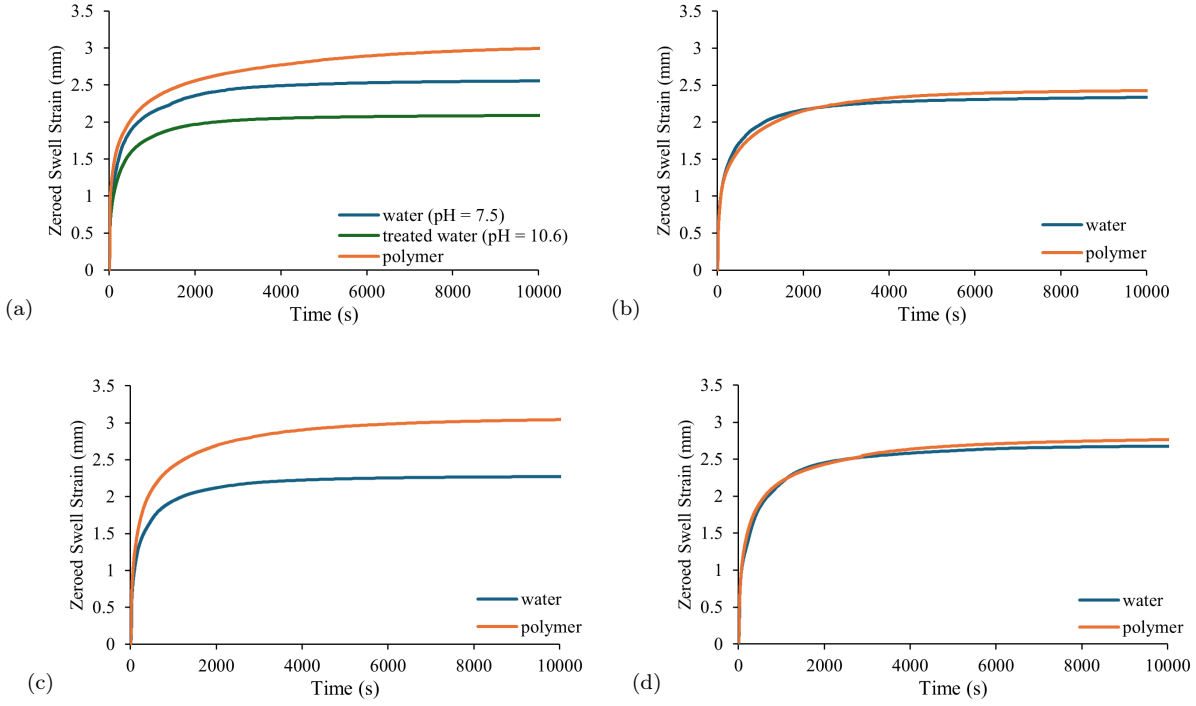


Figure 6.16: The swelling strain against time for clay samples exposed to and drawing in water and polymer fluid. The graphs present the results where the maximum load applied to the clay sample was (a) 667 kPa, (b) 890 kPa, (c) 1112 kPa, (d) 1335 kPa.

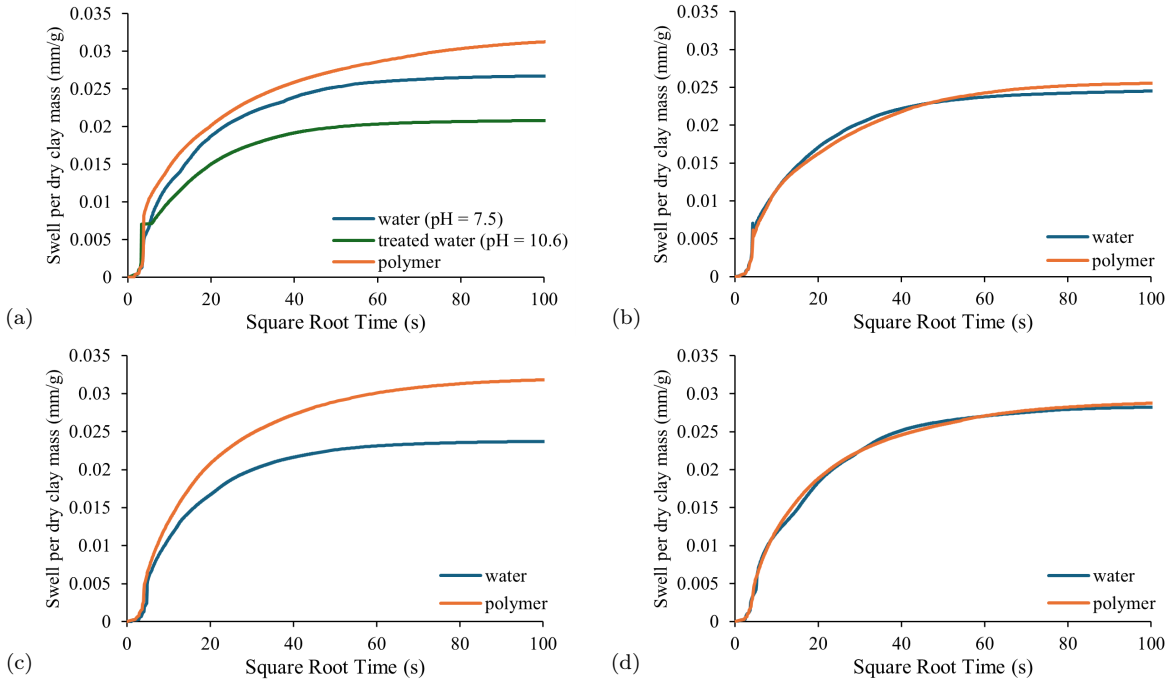


Figure 6.17: The swelling strain per dry clay (kaolin) mass against the square root time for clay samples exposed to varying fluids in the oedometer testing. The graphs present the results where the maximum load applied to the clay sample was (a) 667 kPa, (b) 890 kPa, (c) 1112 kPa, (d) 1335 kPa.

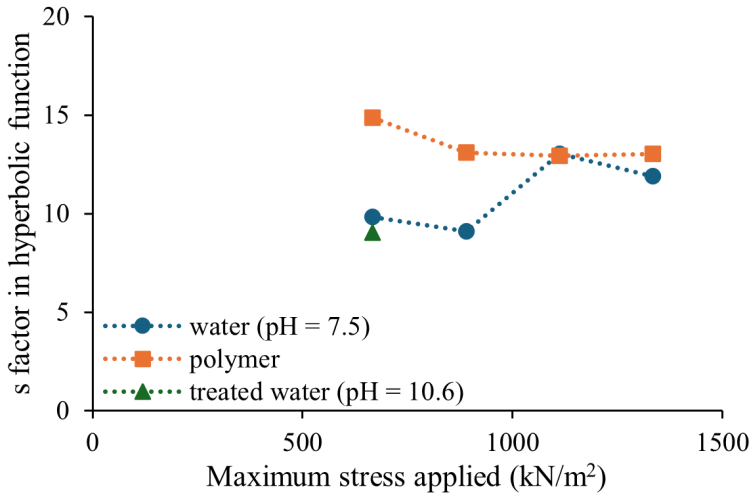


Figure 6.18: The best fitting b factor for the hyperbolic function against the maximum normal stress applied for the different fluids tested during the swelling stage of the oedometer test.

6.3.4 Shear testing - kaolin clay tests

The first half of this investigation focused on the shear interface between laboratory-mixed kaolin clay and concrete. To understand the inherent shear behaviour of the soil and what to expect if the shear occurred purely within the soil itself (referred to as the control test), a kaolin test sample was sheared without a concrete interface, as depicted in Figure 6.8.

One clay sample was sheared at a rate of 0.6 mm/min, which was consistent with the rate used for other kaolin interface tests. The second sample was subjected to a significantly slower shear rate of 0.0125 mm/min. While this lower rate may still be too fast for the complete dissipation of pore pressures during shearing, it should allow for a substantial portion of the pore pressure to dissipate. Figure 6.19 presents the shear stress (kPa) generated in the soil against the strain (%) as the top half of the shear box is forced over the bottom half.

The faster kaolin clay shear test generated approximately 35% more shear stress than the slower test, indicating the significant effect of pore pressures on shear resistance at the higher rate. The slower test showed a shear rate that peaked at around 5% strain (or 3 mm shear), whilst the faster test peaked at approximately 8.5% strain (or 5.1 mm shear).

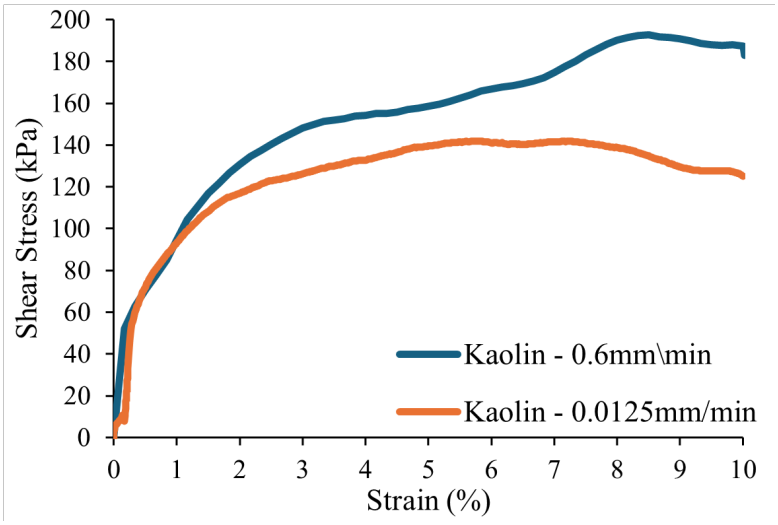


Figure 6.19: Shear box testing results of laboratory mixed kaolin to enable characterisation of the soil. The tests were conducted under 345 kPa normal stress.

Figure 6.20 presents all the results from the shear box testing of kaolin clay conducted at a rate of 0.6 mm/min. The maximum shear stress required to maintain the rate of displacement was 144 kPa for water, 172 kPa for bentonite slurry, and 196 kPa for polymer. Figure 6.21 shows the shear fraction, τ_{frac}, results for these tests, with τ_{frac} calculated using Equation 6.3:

$$\tau_{frac} = \frac{\tau_n}{\tau_{control\ peak}} \tag{6.3}$$

Here, τ_n is the shear stress at any given moment in the shear test, and $\tau_{control\ peak}$ is the peak shear stress measured during the control test. N.B. The closer τ_{frac} is to 1, the closer it is to the peak shear stress generated purely by the soil when shearing.

From these results, it can be seen that the interface that has swollen under water exposure exhibits 75% of the shear resistance of the pure clay. The bentonite slurry interface generates 89% of the pure clay shear resistance, whilst the soil face that has swollen under polymer has a shear resistance equivalent to the shear resistance of the pure clay sample with no interface. A possible explanation for these results relates to the swelling behaviour of the clay under different fluids. The swelling of clay when exposed to water has no limiting factors, the pores take on water that permeates easily and offers no solid resistance when there. The swelling under bentonite slurry was influenced by drawing in both water and possibly the formation of a thin bentonite filter cake, causing a lesser reduction in the effective stress of the clay. The oedometer tests showed that the volume and rate of clay swelling under polymer fluid were

only marginally different to those under water. The comparable shear strength between the polymer-exposed interface to that of a kaolin control sample tested without an interface indicates the polymer molecules may have been acting as a binder as they were absorbed. This binding property may counteract the increase in pore pressure and preserve the shear strength of the clay.

This is greatly encouraging for polymer use in industry, as it suggests that its use is, at the very least, not detrimental to shear resistance; at best, it is the support fluid that facilitates the greatest shear resistance.

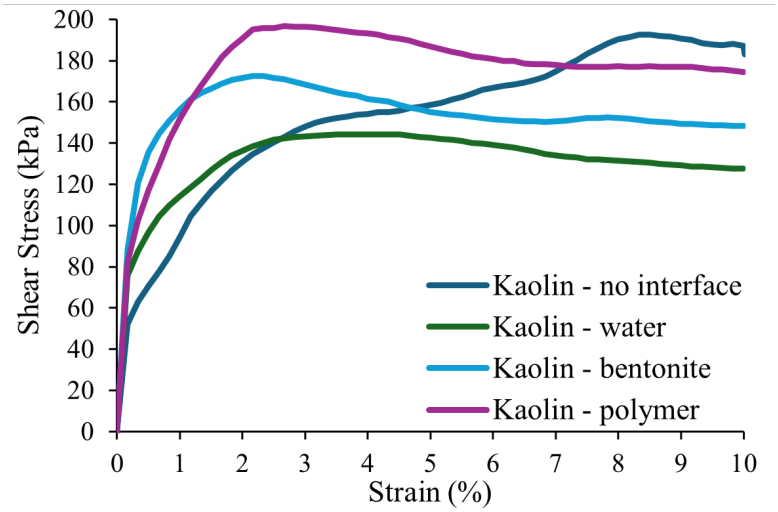


Figure 6.20: Shear box test results for kaolin clay, comparing the shear stress for samples exposed to different fluids before concrete was cured against them. The legend identifies each fluid type exposure, and a benchmark test on kaolin with no interface is also presented. The applied normal stress was 345 kPa.

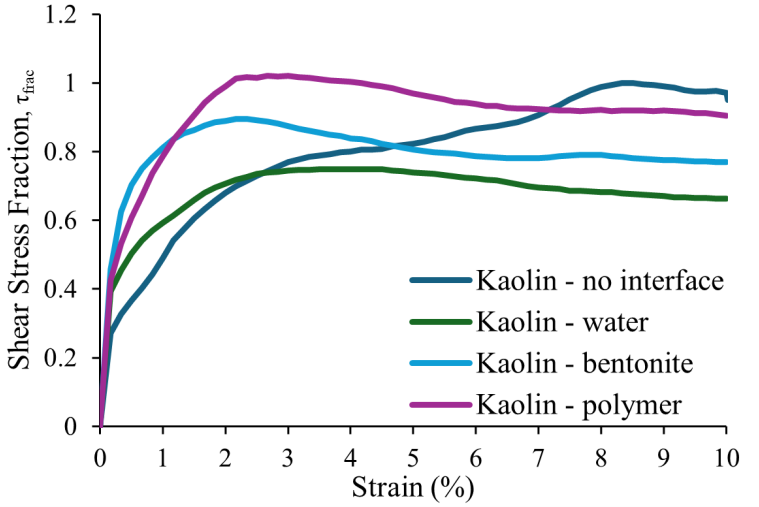


Figure 6.21: The shear stress fraction against the shear strain for a series of clay-concrete interface strength tests conducted with clay samples exposed to a series of support fluids and one test with no concrete interface, i.e. a shear test of purely kaolin clay.

6.3.5 Shear testing - Lambeth Clay tests

The Lambeth Clay was obtained from the One North Quay, Canary Wharf, London site. The clay was obtained by a CFA piling rig at a depth of -11 mOD. The clay was then wrapped in layers of cling film and stored in a dark, temperature-controlled room. The Lambeth Clay tests offer insight into how natural soils encountered on a construction project might respond to the use of different support fluids.

All Lambeth Clay samples were sheared at 0.0125 mm/min to allow full dissipation of the pore pressures. The results from the Lambeth Clay testing are presented in Figure 6.22. From initial inspection, the maximum stress required to maintain the shear rate appears similar amongst all support fluids used. Figure 6.23 presents the τ_{frac} against strain graph, which allows the differences between support fluids to be quantified more easily. The repeated similarity in results with the adjusted direct shear method for the interface test indicates both the good repeatability and the reliability of the test method and its results.

The maximum shear stresses generated by the water, bentonite slurry, and polymer against concrete were 100.7%, 98.6%, and 98.0%, respectively, of the maximum shear stress generated in the test of the soil alone, with no interface. Given the negligible difference, it suggests that when in soils that are less susceptible to softening and have such a low permeability (such as overconsolidated clays), the fluid used to support them will have a negligible effect. Rather, for optimum shear resistance for the permanent foundation element that displaces the support fluid, the main concern would be how effectively the support fluid can be displaced by the rising concrete to prevent inclusions and allow a properly formed foundation element.

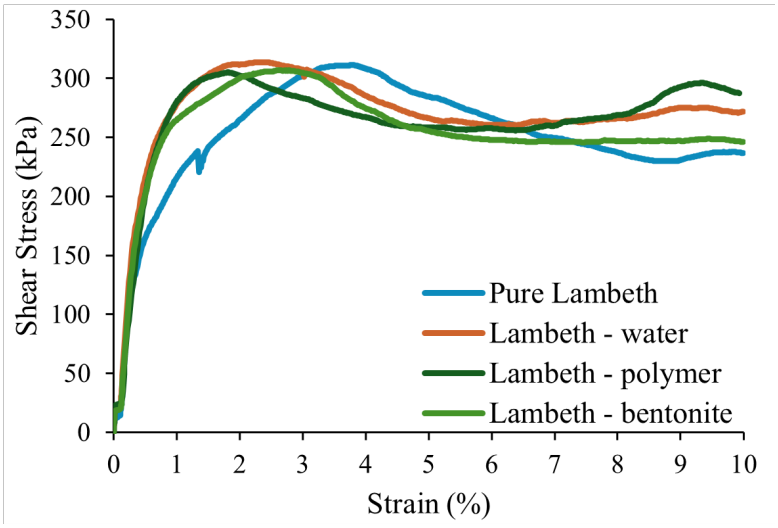


Figure 6.22: Shear stress against strain for a series of soil-concrete interface shear box tests conducted with Lambeth Clay samples and a series of support fluids

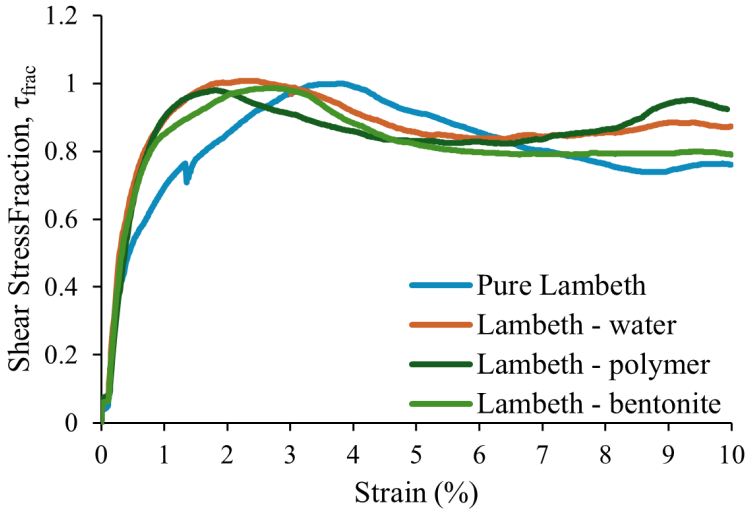


Figure 6.23: The shear stress fraction against shear strain for the Lambeth Clay soil-concrete interface tests after the clay sample had been exposed to a series of support fluids, and one test conducted with no interface.

6.4 Summary

The study into clay swelling when exposed to various fluids was prompted by observations on site that soil faces exposed to water and bentonite slurry were softer compared to those exposed to polymer fluids. Initially, it was hypothesised that the presence of polymer molecules in the fluid would slow down clay swelling, thereby delaying softening and the breakdown of the soil at the excavation face. However, the testing revealed some unexpected behaviours.

Adapting the design and setting up the testing apparatus proved to be a challenging task.

Evidence of soil sample erosion when using the adapted apparatus jeopardised the reliability of the results. Yet, after processing, it appeared that the quantity of clay lost in each test was at a similar level, and to an extent, this erosion could be accounted for. During this process, the dispersion-inhibiting properties of the polymer fluids were exemplified, with consistently lower clay loss in samples exposed to polymer fluid. Furthermore, the erosion of clay in water produced dispersed clay particles, whilst the erosion in polymer fluid produced small lumps of clay. If the testing were to be repeated with more time and funding, the Perspex plates could be replaced by coarsely sintered bronze discs with a similar channel running through, to provide a less abrasive surface for applying normal force.

Although the test results were not substantially different, the testing found that the change in the swelling index was slightly different between clay samples exposed to different fluids, and was consistently higher in samples exposed to polymer fluid. This indicates that clays exposed to polymer fluid were taking on slightly more fluid than those exposed to water. The comparison of swelling rates also indicates that, whilst the difference was not huge, clays take on polymer fluid at a greater rate than water when swelling, perhaps accelerated by the self-siphoning behaviour that polymer fluids exhibit.

These results suggest that the observed greater softening in clays exposed to water and bentonite slurry on site may not necessarily be due to a slower swelling rate, but rather a different mechanism. Perhaps the polymer molecules were behaving as a binder to maintain the excavation face hardness.

To build on this investigation, a range of polymer fluids could be tested, as well as naturally derived polymer fluids that behave similarly to bentonite slurry and may offer insight into the differing mechanics between these commonly used fluids. Future investigations may also focus on the coating behaviours of polymers to examine whether this is indeed the feature that maintains hardness, and to what extent this binding mechanism may maintain the hardness of an excavation face when considering how the strength of an excavation face, left supported by the fluid for a prolonged period, may be affected.

The study into how polymer fluid use as a support fluid influences the shear strength of clay excavation faces was inspired by the work of Lam and Verst (2014 & 2022). Their results suggested that polymer fluid use in sands facilitates higher shear resistance in excavations

than bentonite slurry. This study aimed to investigate whether similar results would be observed for a clay interface.

A novel method was devised to utilise a common direct shear box apparatus, allowing for exposure to varying support fluids (water, bentonite slurry, polymer fluid), the curing of concrete against the sample, and subsequent shearing. Two clays were tested: laboratory-prepared kaolin clay, serving as a well-researched benchmark, and Lambeth Clay sourced from a construction site, reflecting actual on-site conditions.

The testing using kaolin clay indicated that exposure to water led to the least shear strength at the interface, with a peak shear stress reaching 75% of that measured in the shear test conducted on a kaolin sample with no concrete interface. In turn, bentonite slurry exposure led to an interface resistance of 89% of the peak shear stress measured in the shear test conducted on a kaolin sample with no concrete interface. Notably, the face exposed to polymer fluid facilitated a shear resistance at the interface on parity, if not slightly greater than, the shear resistance generated in the test conducted through the clay sample with no interface.

The interface shear testing conducted with Lambeth Clay produced results with a very different narrative. After exposure to all support fluid types, the shear resistance generated by each Lambeth Clay sample was on parity with the sample sheared with no interface. These results indicate that overconsolidated clays, often encountered on site in London, will not be adversely influenced by the choice of support fluid to which they are exposed. However, if softer clays that may be more susceptible to further softening are encountered on site, the support fluid choice may greatly impact the shear resistance.

To build on the shear testing, it is encouraged to widen the investigation with a variation of applied normal stresses, along with a wider range of clays tested, such as a normally consolidated clay sourced from a site, to investigate whether the behaviour observed in the tests conducted with kaolin is reflected. A study into a variation of exposure times would also improve confidence in the stability of foundation elements installed following prolonged excavation periods.

Overall, the key takeaways from this investigation are that excavations in softer clays may require direct shear testing, as detailed in the investigation, to quickly and effectively determine whether the support fluid choice will adversely affect the shear resistance and

therefore the final foundation design. In overconsolidated clays, the support fluid choice is less likely to affect the final foundation design, and therefore other considerations may be the commanding factors in support fluid choice, such as site constraints, budget, or environmental constraints.

7 Conclusions and recommendations for further research

7.1 Introduction

This thesis has presented the findings from a series of investigations aimed at developing the understanding of polymer support fluids in civil engineering, to further their viability as a tool in making construction cheaper, more practical, and more sustainable. The research was conducted experimentally and focused on enhancing industry practice, the management of the fluids, developing the understanding of polymer fluid flow processes, and advancing the understanding of polymer-soil interactions. With a series of bespoke tests and novel methodologies, the research uncovered previously unrecognised behaviours, facilitated better management of the fluid, and improved the ability of engineers to design foundations excavated with polymer fluids. This chapter summarises the key contributions of this research and proposes the direction of future testing.

7.2 Key contributions

In this section, the key contributions are detailed for each piece of experimental work completed.

7.2.1 Qualitative testing of polymer fluids on site

- The well-established apparatus for bentonite slurry testing, the American Petroleum Institute filter press, was adapted to investigate its suitability for qualitative polymer fluid assessment and to explore the ability of the polymer fluid to develop a 'filter cake' on the surface of porous media. The testing revealed and emphasised that synthetically derived polymer fluids, such as HPAM, do not develop a filter cake. The absence of a cake means that the chosen filter paper becomes the sole controlling factor in the test, whereas for bentonite slurries, the test result is much less dependent on the paper and almost entirely dependent on the filter cake formed. The results show that the filter

press test is not a reliable test for on-site use for polymer fluids.

- Following in-depth analysis of the results, it was discovered that the polymer fluid was exhibiting Newtonian behaviour when flowing through the filter paper at high shear rates. This is significant as it means that the flow of the fluid through the paper should be treated as flow in a porous medium, rather than through a bundle of capillaries. This finding shows that the API filter press, with a careful methodology and robust filter papers, can be used to provide a rapid indication of the lower bound of apparent viscosity in porous media and therefore an indicator of flow behaviour in coarser soils.

7.2.2 Polymer fluid heterogeneity

- Following observations of the fluid behaviour in the laboratory, a simple apparatus and method were devised to investigate an apparent variation of viscosity within a body of bulk polymer fluid. The testing rapidly identified that the heterogeneity in the viscosity of polymer fluid does occur, but the cause of it was unknown. After a significant desk study and regime of laboratory testing, the cause of the heterogeneity was determined to be the polymer molecules forming a network. These high-viscosity networks greatly influence the behaviour of the polymer fluid under static conditions and have a significant effect on how the polymer fluids should be treated in the laboratory and on-site. The findings also open the door to the use of the falling ball procedure to characterise polymer fluids and investigate the influence of external factors.

- The polymer networks are time-dependent; if the fluid is left undisturbed, the networks develop significantly over the first 24 hours after mixing. By 48 hours, although the average viscosity does not show a significant increase in 24 hours, the fluid remains heterogeneous. The results from the testing highlight how important it is to allow a freshly batched mix of polymer fluid to stand for 24 hours before use. This is due to the network development and the time taken for the HPAM to fully dissolve, and achieve its greatest possible viscosity.

- The testing conducted on the different commercial polymer systems showed that the viscosity, at constant concentration, can vary greatly between polymer products. As the

product formulations are proprietary, this means the only attributing factor to the performance is the brand name, rather than the industrial process used to create it or a specific component of its chemical formulation. This can be problematic for engineers deciding on which product is the most suitable for their project and may hinder progress in determining the most effective formulations for different civil engineering applications.

- To address the issue of heterogeneity on site, all characterisation testing (for example, quality control testing) either in the laboratory or on site should be on samples agitated or stirred to ensure the fluid is homogenous so that the results can be compared to those from other samples.

- The impact that photodegradation has on the viscosity of the polymer fluids was stark. The testing highlighted this as an issue for site work. Given the impact of photodegradation contractors are strongly recommended to put in place measures to protect the polymer fluid on site.

- Testing to investigate the influence of temperature on the viscosity of the fluid revealed a 20% difference in viscosity from 0°C to 30°C. This difference in viscosity may not have too great an effect on the performance of the fluid, given the fairly constant ground temperature. However, it may raise concerns that a polymer is over- or under-performing if there are significant differences in temperature between tests.

7.2.3 Polymer fluid flow in sands

- The bespoke permeameter, designed and built to investigate the flow behaviours of polymer fluids in sands (one of the most challenging soil types for which support fluids will be used), was employed to expand upon previously completed testing and explore different mechanisms in greater detail. The testing provides a larger database for researchers using numerical modelling to hone in on building models that will accurately describe polymer fluid flow through porous media. This, in turn, will help of engineers to predict the behaviour of polymer fluids under varying site conditions.

- Most significantly, the testing found evidence of clogging being developed by the polymer fluids as they flowed into the sand. The tendency for polymer systems to clog

has long been debated in the civil engineering field, but these results allow researchers to move past this discussion. The clogging mechanism appears to be the formation of a partially clogged region relatively close to the entry surface during permeation. The clogged region then develops in different ways and at different rates depending on external applied parameters and the grading of the soil. The demonstration of this mechanism also opens the door to developing polymer systems where the flow becomes so low that it does not risk the excavation stability or endanger any environmental receptors of concern, such as a river or aquifer.

- Indeed, the permeameter tests indicate that the polymer product suppliers currently may be adding clogging agents to their products.

- The testing of a selection of polymer fluid products echoes the previous comments in Section 7.2.2, highlighting the starkly different flow behaviours from product to product. The testing emphasises the need for engineers to have a better insight into the chemistry of the polymers and to be able to understand how their formulations impact their flow behaviours. This would, in turn, allow engineers to select the polymer product with the formulation most suited to their intended purpose.

- The permeation tests with varying applied pressures demonstrated a linear relationship between flow rate and pressure gradient over the largely unclogged region of the column. This suggests that at these flow rates, the fluid was Newtonian at the lower viscosity threshold. However, this linear relationship differs between the clogged region and the zone below it. Notably, for a given flow rate, there was obviously a much greater pressure drop across the clogged region. This relationship means that for contractors, the applied polymer head should be as low as reasonably possible. The engineer must decide on an applied head that is not so great that it causes unnecessary waste of polymer into the surrounding soil, but is great enough to counteract the soil pressure and groundwater pressure with a factor of safety to ensure the stability of the excavation.

- The testing conducted to investigate the influence of polymer concentration on flow behaviour found a negative exponential relationship between the two parameters. As

the concentration is increased, the flow rate of the polymer fluid falls at a decreasing rate. This relationship implies that an engineer should consider the most problematic ground conditions within an excavation and tailor the concentration accordingly. It should be high enough to amply exploit this relationship between the two parameters, but not so high that the cost of the additional polymer concentration exceeds the benefits provided, such as a decreased flow rate and a more easily managed fluid.

- The permeation tests using different sand gradings provides supplementary data for modelling polymer fluid flow in coarser soils, which have a hydraulic conductivity that would currently be considered too high for their use. The testing emphasised the greater flow of the fluids in coarser sands and the limited clogging ability of the currently available polymer systems in coarse soils.

- The testing conducted in Thanet Sand was inconclusive in obtaining comprehensive data during permeation. However, this was partly due to the lack of flow into the sand, indicating that when sands with fines are encountered on site, they are unlikely to be problematic from the standpoint of fluid loss and the inability to provide support due to a pressure front acting too great a distance into the surrounding soil.

- The results from the additive testing were particularly noteworthy, demonstrating the impact of a product that is regularly added to the bulk polymer mix throughout its lifecycle. These additives are often included in fresh fluid yet are designed to clean recycled fluid. The results indicated that the additives reduce the bulk viscosity of a polymer fluid quite dramatically, although towards the end of each test , they provided significant clogging. The use of the additives should be subject to a management plan and be monitored by the engineers on-site. The main point of contention from this work would be how quickly, if at all, they can provide useful clogging. In the testing, the globules that formed as a result of the additives did not develop effective clogging until the end of the test due to their low specific gravity, meaning they did not reach the sand surface until the end of the test. If these globules are not drawn into the excavation face because of their poor dispersion in the bulk fluid, the benefits they provide may be limited, in which case their addition may need to be limited to the cleaning stages of the

lifecycle of the polymer fluid.

7.2.4 The influence of polymer fluid on clay swelling

- In the testing conducted to explore the influence of polymer fluid on the swelling behaviour of clay, a standard oedometer apparatus was modified and a novel methodology was devised to facilitate the exchange of fluids within the apparatus and ensure swelling with the intended fluid. Despite some limitations of the testing apparatus, it was possible to complete the desired operation successfully.

- It had been repeatedly observed on site that soils exposed to bentonite become softer than those exposed to polymer fluid, and soils exposed to water softer still. Originally, a hypothesis was formed that, due to the polymer molecules, as the clay swells and takes on the fluid, the molecules would act in much the same way as in the permeation tests: exerting a viscous drag and greatly slowing the swelling stage. However, what was actually observed in the testing was that the slight difference in swelling rate indicated that the clay exposed to the polymer was swelling at a slightly greater rate than with water, and in the process, actually tended to take on more fluid than the clay samples exposed to water. This may be caused by the self-siphoning mechanism exhibited by the polymer, drawing the fluid in at a greater rate and encouraging further ingression into the clay sample. It may also be a consequence of chemical reactions between the fluid and clay, allowing a greater volume of fluid to be drawn in. The observations made on-site of clay samples softening more when exposed to water and bentonite slurry than polymer fluid exposure may, in turn, be due to the polymer molecules acting as a binder within the soil, rather than a resistance to flow into a swelling soil.

7.2.5 The influence of polymer fluid on clay shear strength

- A direct shear box apparatus was adapted to investigate the effect that exposure to different support fluids has on the shear strength of clay. Two different clays were tested: kaolin and Lambeth Clay. The laboratory-prepared kaolin clay provided a benchmark clay that is well-researched and understood, while the site-sourced Lambeth Clay provided a real clay experienced regularly on sites in London.

- For each clay-concrete interface test conducted, a control sample of the clay itself was sheared to provide a benchmark. As a percentage of the shear resistance generated in the pure clay sample, the samples exposed to water, bentonite, and polymer fluid produced 75%, 89%, and 102%, respectively. For all three support fluids, the Lambeth Clay samples showed a shear resistance that was equivalent to that of the control sample.

- The results suggest that in some clays that are more permeable and more susceptible to softening, the chosen support fluid may greatly influence the shear strength of the soil and, therefore, the final foundation design. Conversely, in overconsolidated clays that are less susceptible to softening, the chosen support fluid is less likely to be a concern for the final shear strength, and other factors such as practicality and cost will be the deciding factors in the choice of support fluid.

7.3 Recommendations for future research

7.3.1 Chemistry

- **Polymer characterisation** - The development of the understanding of the chemical formulations and how they relate to the performance of polymer fluids would allow systems to be tailored to specific applications and would give engineers more agency to decide what product best suits the purpose. Investigating the relationship between the degree of hydrolysis, molecular weight, added chemicals, and the viscosity and ability to develop a clog could enable more optimised systems.

- **Mix water chemistry** - There has been some work carried out to investigate the relationship between polymer fluid viscosity and the concentration of ions present in the mix water, both in this research and by others. However, this could be taken further with a controlled investigation into the impact of principal ions found in most waters: calcium, magnesium, and sodium on fluid viscosity, to allow polymer systems to be adapted to the mineral content of the site mix water.

- **Rebar interactions** - The interactions between the polymer, the rebar cage, and the concrete should be examined. The HPAM molecules quite readily adsorb to the surface

of rusted iron. A research area would be to understand whether the pouring of concrete displaces the coating of polymer or whether it struggles to, resulting in a space being left between the placed concrete and the rebar, which in turn could reduce the tension capacity of the foundation element. If this is the case, control measures may need to be adopted to prevent or work around this.

- **Polymer networks** - The formation of a polymer network is a phenomenon that warrants further investigation, given its potential as a highly potent mechanism for the management of fluid behaviour. This study highlights unresolved questions, for example, the density of these networks, where an inconsistency was found between laboratory density measurements and observed tendency of the zones of viscous (networked) fluid to sink (after de-airing). If network formation can be promoted within an excavation, it could potentially increase the viability of using polymer fluids in even coarser soils and enhance the ability of the fluid to support excavations for prolonged periods.

- **Additives** - The testing demonstrates the clear potential of the additives to clog and reduce fluid flow in permeable soils with minimal filter cake formation - provided the fluid is managed to keep its soil solids content low. Building on these findings, further research is warranted to characterise the macromolecules formed by the additives based on their size and clogging efficacy. For example, while larger macromolecules may be effective for coarser sands with a higher hydraulic conductivity, they could be economically inefficient in finer sands. This customisation would allow for the fluid management to be tailored to specific site requirements, optimising both performance and cost.

7.3.2 Mixing procedure

- The mixing procedures for polymer fluids vary greatly from site to site, from technician to technician, and even between laboratories. Over the course of the research, a more exact method to develop repeatability in small-scale samples was developed in the Permeation Of Polymer Fluids in Soils (POPFS) project, using isopropyl alcohol to first wet the dry powder. There is opportunity for optimisation of polymer fluid mixing on site. Currently there are conflicting practices concerning the stages and procedures

carried out in water treatment, polymer fluid mixing, additive mixing, and cleaning procedures. If the optimum process can be developed, it will reduce polymer wastage and improve polymer fluid quality and reliability, and allow engineers to easily check whether the polymer fluid operations on site are being conducted optimally.

7.3.3 Influence on shear resistance

- Work has been conducted in this and several other research projects focused on the influence of polymer fluid on the shear strength of soils, with promising results in all investigations. These results have indicated that polymer fluid is no more detrimental than any other support fluid to the shear strength of a soil and, in fact, suggest that the use of polymer fluid will enable the reduction in length of bored piles owing to the lesser, if any, reduction in shear strength seen in the soil from polymer fluid use. Conducting a comprehensive shear strength investigation with bespoke equipment and access to medium or full-scale field testing will enable the quantification of the possible pile length reduction to realise these benefits.

7.3.4 Embodied carbon

- Arguably the biggest challenge facing humanity currently is climate change, so having an understanding that the development of anything novel will be beneficial for the environment is crucial. On the surface, the use of polymer fluids seems more sustainable than bentonite. They tend to be used at a fortieth of the concentration of bentonite, the bulk mix is theoretically able to be reused over the entire length of the project though regular topping up with fresh polymer is required, and they offer the possibility of a reduction in pile length. However, a formal embodied carbon or sustainability analysis has not yet been conducted. An investigation to comprehensively determine the environmental impact of using bentonite, synthetic polymers, and natural polymers would be greatly welcomed to provide clarity and confidence in this field.

7.3.5 Naturally derived polymers

- Research is ongoing into the viability of naturally derived polymers, such as Carboxy Methyl Cellulose and Xanthan, as support fluids. The use of natural polymers has been

problematic due to their rapid biodegradation in the field, which necessitates the use of biocides. Furthermore, they lack the ability to inhibit soil dispersion, meaning soil-slurry separation plant is still required. Future work would be beneficial if it is viable to formulate a product that is both more microbially resistant, capable of inhibiting the dispersion of solids, and importantly, more sustainable than the use of synthetic polymers.

7.3.6 Suitability for other applications

- This work has focused on the use of polymer fluids to support excavations. However, work has been and is being conducted to understand their viability in other civil engineering applications, such as caisson sinking or pipe jacking. In these cases, the fluid is used as a lubricant rather than a support fluid. Using the same polymer fluids for these purposes as for excavation support is a limited endeavour, as it is in the nature of these fluids to permeate slowly into the surrounding soil rather than form a barrier to completely prevent permeation. It therefore makes sense that for these purposes, the polymer systems should be adapted. On the face of it, a mix with a higher polymer content might be advised; this would make the pumping of the fluid more difficult, but the lubricant would likely remain in the annulus, providing a more reliable source of lubrication than a thinner fluid mix. It may be viable to mix a polymer fluid with additives designed to form larger globules, such as Kobbleblok (KB), or even polymerise in-situ to create a less permeable gel-like material. Investigations into adapting the fluid for these sorts of purposes may be key to optimising other civil engineering processes.

7.4 Concluding remarks

The development of infrastructure is a great contributor to human progress and is crucial to the success of equitable and effective societal advancement. However, construction is extremely expensive and one of the largest contributors to global emissions. The research conducted across the globe to advance construction, so that its environmental impact is limited while enabling the necessary progress to support and allow the global population to thrive, is invaluable.

The work conducted for this thesis aims to make a contribution to this goal. The investigations have shed light on and developed the understanding of a fluid that may contribute to reducing the cost, both monetarily and environmentally, of construction projects. The work revolved around physical testing, exploring how to optimise the management of the fluid, how it works to support an excavation, and its interactions with soil. All of this was done so that the civil engineering sector can build its trust in the use of a promising advancement in construction.

A Site Guide to Polymer Support Fluids

A Guide to the Preparation and Use and Re-use of Polymer Support Fluids for The Site Team



UNIVERSITY OF OXFORD

ARUP

EPSRC
Engineering and Physical Sciences Research Council

Environmental Geotechnics Ltd

February 2024 – Revision 3

1 Background

Polymer fluids are an alternative support fluid to the more traditional bentonite slurries for excavation support. Importantly, polymer fluids rely on a different mechanism to achieve support of excavations. Where bentonite relies on building a filter cake at the excavation face to stop flow into the soil and maintain a positive head difference on the excavation, polymer fluids rely on their viscosity to slow the flow through the soil and maintain a positive head.

Polymers are sorbed onto soil as it is excavated, and some are designed to prevent soil from dispersing into the fluid so that there is no need for a soil-fluid separation plant. Solids should not disperse into the fluid and raise its density as happens with bentonite. With bentonite slurries the soil does disperse to small particles, so a soil-slurry separation plant is necessary. This note relates only to polymer fluids which inhibit soil dispersion.

However, as a consequence of sorption of polymer onto the soil, polymer molecules are removed from the fluid so that the polymer concentration drops with use. After each use it is necessary to add fresh polymer to maintain the concentration of polymer in the fluid.

Another significant difference between polymer and bentonite support fluids is that soil particles in polymer fluid are not held in suspension like they are in bentonite. In polymer fluids soil particles readily descend under gravity to the base of the pile and can accumulate.

There are currently few dedicated polymer technicians in the industry and there is no formal training scheme to become one. The use, testing, maintenance and piling methodology are fundamentally different for bentonite and polymer fluids and when the fluids are treated alike quality issues arise.

The following is an introductory guide for those involved with polymer fluids on site. In particular, when setting up the polymer farm, managing and using the polymer fluid, sampling the polymer fluid in the excavation and polymer fluid testing.

2 Polymer Fluid Head in the Excavation

For all types of support fluid there must be a positive head of fluid in the excavation against the external groundwater for stability. It is recommended that for polymer fluids the fluid level in the excavation is at least 3 m. above the groundwater level at all times plus an allowance for the drop in fluid level in the bore as each bite of soil is excavated. The extraction rate of the auger or bucket must also be controlled to allow fluid above to pass the dig tool to avoid creating suction below and reducing stability. The fluid level must be controlled in a similar manner to bentonite except that a greater positive head is recommended (3 m or more).

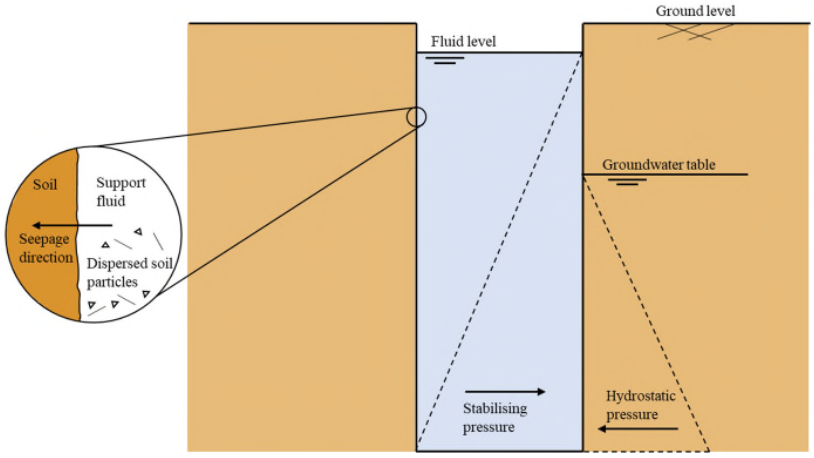


Figure 1. Schematic of fluid supported excavation, adapted from Lam & Jefferis (2018).

3 Polymer Fluid Preparation and Management

There are four key stages for polymer fluid production and management:

1) Treating the mix water prior to polymer addition
2) Preparation of polymer fluid and fluid storage
3) Use of polymer fluid in the excavation
4) Boosting polymer fluid after use in an excavation

3.1 Treatment of the mix water

a) There should be a tank dedicated to water treatment. This tank should be fitted with air bubbler lines to mix and homogenise the contents.

b) The water should be treated with sodium hydroxide (caustic soda). Sodium hydroxide should be added to achieve a pH in the range 10.6 to 11.0. This is the optimum pH range for precipitation of calcium and magnesium ions and the performance of the polymer molecules.

c) A properly calibrated electronic pH meter will be needed for the pH measurement. pH papers are not sufficiently accurate.

d) Note the quantity of sodium hydroxide necessary to treat each tank of water. The same amount of sodium hydroxide should be required each time a tankful of water is treated unless there has been a major change in the chemistry of the water supplied to the site. If such a change occurs record it on the site data sheets.

e) Strictly adhere to safety guidance and wear PPE when handling sodium hydroxide – it can burn and blind.

f) The water treatment tank will accumulate precipitated crystals. There is no need to remove these crystals. Indeed, it is best to leave them in the tank as they act as seed crystals for later precipitates to grow on. In this way, they encourage rapid precipitation and so is a good water treatment practice. When possible, the water should be treated at least a day before use to allow precipitation of calcium and magnesium ions in the water. This should allow sufficient time for the ions within the water to completely precipitate.

3.2 Mixing of the polymer fluid

g) There should be a separate tank dedicated to the mixing of polymer fluid. This tank should be fitted with air bubbler lines to mix and homogenise the contents.

h) The recommended method on site for adding polymer powder to the mixing tank is with a venturi eductor system, such as the one shown below which should discharge directly in the mixing tank. To achieve good mixing the water in the educator must flow as a jet and small amounts of polymer powder should be mixed into a large volume of water. Mixing a lot of polymer into a small volume of water wastes polymer product and leads to clumps of unhydrolysed polymer known as ‘fish eyes’ which are an indicator or poor mixing. If these are present they will be seen on the screen of the Marsh funnel when a funnel test is done on the fresh polymer fluid.



Figure 2. Example of hopper used in venturi eductor system employed to mix polymer fluid.

i) During the blending of the polymer into water, the mixing tank should be bubbled using the bubbler mounted in the tank. The bubblers should continuously agitate the full volume of the tank fluid to ensure that the polymer is fully integrated into the fluid. The bubblers should be aimed to prevent the build-up of undissolved polymer at the base of the tank. The bubbling need not be continued after all the polymer has dissolved.

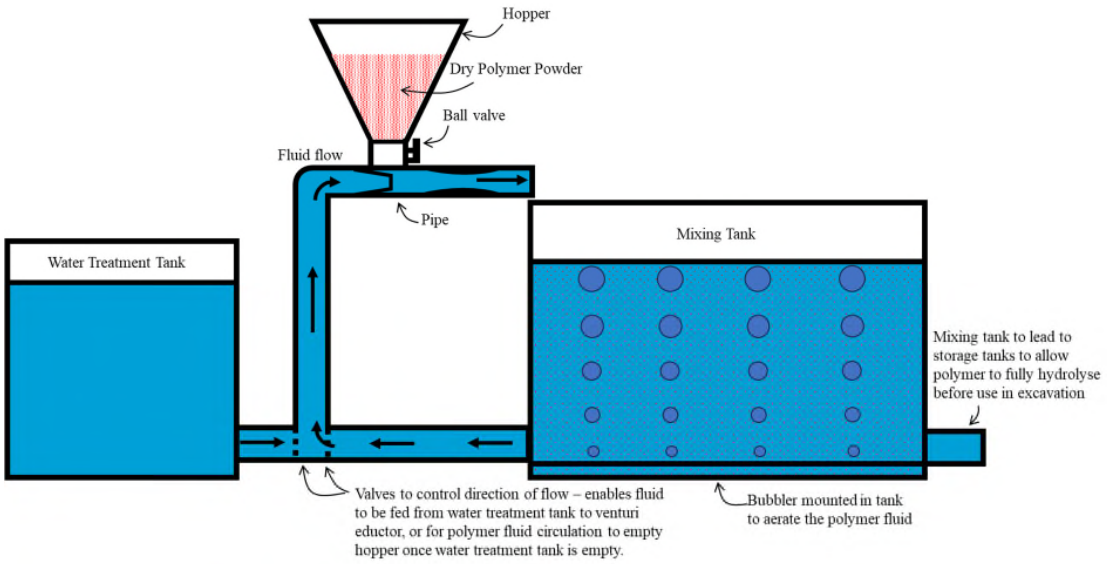


Figure 3. A diagram of a venturi eductor used to introduce dry polymer powder to solvent at a controlled rate.

j) The mixing of additives (such as KB's E100 and E200) should be undertaken by fully dissolving the additive in a separate volume of water (for example, a bucket of water) then slowly distributing this mix along the mixing tank while it is agitated by bubbling.

k) It is recommended that the mixing tank is open topped as it allows for visual inspection of fluid during mixing. As sunlight degrades polymer the mixed fluid should be pumped to closed/covered tankage once mixing is complete and all polymer is dissolved.

l) The base of the mixing tank should be inspected at intervals to check that there is no build-up of undissolved polymer. If there is a build-up, then the mixing process should be reviewed, and the bubbler lines may need to be adjusted – note they should aim generally downwards to lift material from the base of the tank.

3.3 Storage of the fresh polymer fluid

There should be a series of tanks used for storage of the fluid prior to use and for the return of the fluid after use. The number and capacity of the storage tanks should be managed according to the total amount of fluid needed for excavations at any given time on site.

It may seem simple to account for the total necessary storage capacity, but this is not always done. The largest volume necessary at any given time should be calculated and the storage capacity should be sufficient to take all the returned polymer fluid as completed excavations are concreted, boost this returned fluid and add any new polymer fluid required to supplement the volume, with a reserve to make up for any sudden fluid loss should this occur. NB: on some sites, it is specified that the support fluid in the excavation should be completely exchanged for fresh fluid or boosted fluid before concreting, this needs to be accounted for when calculating total storage volume.

Polymer degrades when exposed to sunlight. It is therefore important to store the polymer in closed tankage and to cover open topped tanks with a sheet when possible.

3.4 Use of polymer fluid

The maintenance of the polymer support fluid plays a vital role in the construction of foundations. If a polymer support fluid is not properly maintained the quality of the finished product will greatly suffer. The team managing the fluid are key to ensuring good construction practice. Below are some general points for good practice:

- Take sufficient time when mixing polymer, the powder should be added methodically, rather than mixed in a hurry, for example, by dumping powder into water.
- Anticipate the needs for the next day. Preparing and maintaining the fluid a day in advance will ensure that the excavation and concreting processes are unhindered.
- Keep a sufficient stock of materials necessary for the fluid, i.e. the polymer powder, any additives and caustic soda. If the stocks are not maintained, then construction will stop.
- Keep a check on the amounts used and question any major changes in consumption.
- The materials should be stored appropriately. Prevent chemicals from exposure to atmosphere, i.e. keeping lids on containers and storing caustic soda in a safe manner according to COSHH specifications.
- Keep work areas as clean as possible. Wet polymer powder will begin to hydrolyse and stick to surfaces making then slippery. It is therefore important to clean and prevent build-up of polymer on the mixing equipment, such as venturi eductors. Keep testing areas clean to ensure reliable results.
- Maintain supplies for test equipment, for example, breaker for the polymer fluid in the sand content test.

- Be sure to keep good record of test results. Unexpected test results are useful for the engineers and site team to determine issues in the construction that need addressing.

If unsure about anything with the polymer fluid, then consult engineers on the project and consult the EFFC/DFI guide on support fluids, the link to which is given at the end of this guide.

3.5 Boosting of polymer fluid

When boosting the polymer fluid the in-use fluid should be pumped back to open topped storage tanks where solids can settle from the fluid. If cleaning additives are to be used, they should be blended into polymer fluid while it is entering the storage tank to encourage the suspended solids to settle to the bottom of the tank. The cleaned fluid should then be tested against the site specification to determine the amount of boosting needed. From the testing the quantity of polymer to add and sodium hydroxide required to treat should be determined following advice from the polymer supplier or from site experience. Boost materials may be added as the fluid is returned from the excavation or in a mixing tank. The boost materials may be added to the fluid in the same manner as was conducted in initial mixing.

Note some boosting will result from the addition of make-up fluid to make up for volume losses during the excavation.

4 Sampling fluid in the excavation

To sample the fluid in an excavation, a 3-part sampler is preferred. This ensures that the sample is taken at the desired depth without leakage and is easy to control.

> *Samplers like a flap sampler or trapdoor sampler are commonplace but be aware that the flaps will not open unless the sampler is moving at speed so small adjustments of depth when the sampler is already submerged are futile.*

The fluid should be sampled for testing regularly to understand how the fluid is performing in the bore and as required by the works specification. Sampling and testing may be done every 3-4 hours during excavation and can be done opportunistically, i.e. when the piling rig is emptying excavated soil or just before/after scheduled breaks in the work. If an excavation is left supported by fluid overnight samples and tests should be undertaken before leaving site and first thing before recommencing work to determine the effect of the standing time on the quality and level of the fluid. The fluid level should be as high as practicable before leaving site; this level should be recorded. The fluid level should be checked and recorded when work recommences to confirm that there has been no unacceptable drop in level. If there has been a significant drop in level this should be recorded and action taken, for example, topping-up during the night.

5 Testing the polymer fluid

5.1 Viscosity

The Marsh funnel test will give an indication of the fluid viscosity and hence the polymer concentration in the fluid. However, it is important to understand that the ‘dirtiness' of a used polymer also increases the Marsh funnel test time and therefore the viscosity test result should be interpreted together with the density test result (see below).

Control values should be provided to the site team. Marsh funnel times should be provided for freshly mixed polymer, and polymer fluid of acceptable quality for re-use.

> *Care needs to be taken to wash the funnel out after each use and clean the spigot of the Marsh funnel with a small bottle brush prior to and after each use to ensure reliable results.*

A Marsh funnel test should be carried out on the used polymer fluid returned after use in an excavation to assess how much polymer needs to be added to make it suitable for re-use.

5.2 Density

A density bottle should be used to measure the fluid density. A mud-balance is not preferred for density measurement, being of insufficient volume and accuracy. The bottle should be used with an electronic scale accurate to $\pm$0.1g and the bottle should have a volume 700 ml or greater. For preference a spring-top bottle should be used.

The procedure is:

1. *Weigh the bottle when dry and empty, W_1.*
2. *Weigh the bottle full of water (carefully dry the outside of the bottle before weighing), W_2.*
3. *Weigh the bottle full of polymer fluid, W_3.*
4. *As the density of water is 1.0 the density of the polymer fluid is:*
5. *Density of polymer fluid = $(W_3-W_1)/(W_2-W_1)$*
6. *There is no need to repeat weighing W1 and W2 each time a polymer fluid density is measured but they should be checked weekly.*

The polymer fluid should have a density of less than 1.02 kg/litre and preferably no more than 1.01 kg/litre.

> *Although the mud balance is widely used for bentonite slurry, it should not be used to determine the density of polymer fluids. It has insufficient precision for polymer fluids and cannot give useful results.*

5.3 Sand content

The sand content thimble should be filled with polymer fluid to the ‘mud to here’ line. Bleach or another polymer breaker can then be added to the thimble which should be shaken to mix the polymer and the breaker. Only a small amount of breaker is needed. The full volume of fluid must be poured onto the screen any remaining solids in the thimble washed out onto the screen. The solids on the screen then should be gently washed with breaker solution to ensure that all material finer than the screen is washed through it. The solids remaining on the screen then should be washed back into the thimble, and the sand content read off from the scale. The sand content should not be higher than SPERWall limits i.e. 2% for re-use, 5% during digging and 1% prior to concreting, after the polymer has been fully broken and washed through the screen.

Note wear goggles and PPE appropriate to the breaker used.

5.4 pH

The pH should be measured with an electronic pH meter that is accurate to $\pm$0.1pH. The pH meter should be calibrated regularly and replaced when necessary to ensure accurate results. The pH of the treated water should be in the range of 10.6 to 11.0. This pH range is optimum for precipitation of calcium and magnesium and the performance of the polymer molecules. However, for the polymer fluid in use, a somewhat lower pH may be acceptable – refer to the Works specification.

Test papers are not acceptable as an alternative to pH meter as they are not sufficiently precise, and colours can be difficult to interpret.

5.5 Fluid Loss

Fluid loss tests are not specified in SPERWall but may be requested in the Works specification to investigate polymer fluid filtration. If fluid loss tests are conducted on site

then a hardened filter paper should be used and the pressure should be 3 bar or lower to ensure the filter papers are not punctured/damaged.

Tests should be done on fresh polymer fluid for comparison as results will depend on the paper used; significant variability in the results should be expected even for filter papers taken from the same packet.

5.6 Interpreting test results

For all test results refer to the Works specification for compliance values. The works specification may follow Table C20.2 of SPERW (2017) which shows typical test and compliance values and is included below as Table 1.

Table 1 Typical test and compliance values for support fluid prepared from polyacrylamide polymers used in bored piles (Table C20.2, SPERW, 2017).

Property to be measured	Test method and apparatus	Compliance values			
		Freshly mixed	Ready for reuse	During digging	Prior to concreting
Density: g/ml	Electronic balance or similar	1.01 g/ml	<1.02	<1.05	<1.02
Fluid loss: ml at 30 minutes	Low temperature fluid loss test	n/a	n/a	n/a	n/a
Filter cake thickness: mm at 30 minutes	Low temperature fluid loss test	*	*	*	*
Marsh funnel flow time: seconds	Marsh cone	>90	60-120	60-120	90-120
Shear strength (10 min gel strength): N/m2	Fann viscometer	n/a	n/a	n/a	n/a
Sand content, per cent by bulk volume	Sand content set	0	<2%	<5%	<1%
pH	Electrical pH meter to BS 3445; range pH 7 to 14	9-11	9-11.5	9-11.5	9-11.5

Notes:
* If filter cake thickness is specified it should be for a fixed volume of fluid (400 ml) as all fluid may drain from the cell during the test.
For polymer fluids with low solids contents Marsh funnel time is an indicator of the active polymer concentration in the fluid (polymer sorbed onto soil in suspension will not contribute to solution viscosity). The maximum of Marsh funnel time of 120 s for 'ready for re-use fluid' is a typical value. It may be revised if appropriate experience exists or if the polymer supplier recommends other values. The minimum Marsh funnel time of 60 s for digging fluid is again a typical value. A higher value may be used if recommended.

Specifications are evolving as new polymer systems are developed. From experience garnered since SPERW (2017) some revised values are suggested. It is important to note that compliance values will depend on the particular polymer system used.

Viscosity, prior to use or re-use – 80 – 120s Marsh funnel time is a common range for in use fluids. Somewhat lower values may be permissible in an excavation but values less than 45s are unlikely to be acceptable.

Density – The density of the fluid prior to use or re-use should be <1.02 kg/litre and for preference no greater than 1.01 kg/litre. The polymer concentration in the fluid should be maintained at a value sufficient to prevent density build-up during excavation. The <1.05 (during digging) figure in Table 1 now seems high.

Sand Content – The fluid should have a sand content of <2% for re-use. If it exceeds this the fluid will need cleaning and boosting.

pH, mix water and polymer fluid prior to use or re-use – The pH should be between 10.6 and 11.0.

6 General Procedures

Spillage – Care should be taken to keep the polymer fluid contained in the excavations and in the storage tanks. Spillage of the powders or fluid can create a slip hazard and should be cleaned-up promptly. Spilled material also can get into the environment outside of the project and so, again, should be cleaned as soon as possible.

Pumping – The viscosity of polymer fluids has been observed to reduce following centrifugal pumping (Lam et al, 2010). This is caused by the high pumping rate and sharp geometry of the equipment. Positive displacement and diaphragm pumps should be used where possible to limit this degradation. Consistent sampling and testing after pumping

should be performed to record the effect on performance. More information on pumping of support fluids is presented in the EFFC/DFI guide.

Base cleaning – Base cleaning practice will greatly affect the performance of the pile. Good practice entails ensuring that all sediment in the excavation is at the base of the pile and the subsequent removal. To ensure all the sediment has settled the fluid should be replenished with new polymer fluid completely or cleaned. To clean the polymer fluid manufacturers will often supply cleaning products, the applied dosage may be mixed into the excavation by using the excavating tool to turn over the fluid in the pile a few times. NB: the dosages recommended by the supplier need to be adhered to, too low or high may have no affect or damage the polymer respectively. After the recommended wait time the base can be cleaned with a cleaning bucket or pumped out into a sedimentation tank and dealt with separately. For a more comprehensive guide on base cleaning the EFFC/DFI Support Fluids Guide should be consulted.

Adding Flocculants – When adding any additives to the polymer fluid it is suggested to seek advice from manufacturer/supplier before use. As a general rule the flocculants are potent chemicals for the purpose and so should be diluted in a water solution before adding to polymer fluid in the mixing tank. The flocculants may then be added by carefully and slowly pouring into a moving flow of the mixed polymer fluid.

Disposal – If it is proposed to dispose of the fluid to sewer the water utility should be contacted and a plan developed. Typically, this will require that a sample of fluid is broken down with the breaker to be used prior to the bulk fluid disposal. Any solids in the fluid should be allowed to settle (to the level that could be achieved in a bulk tank) and a sample of broken fluid then sent to a laboratory for environmental testing as required by the water utility company. If the broken fluid complies with the water utility company's disposal

standards, then the company may agree to accept the fluid subject to agreed disposal procedures and payment of appropriate fees. The full volume of polymer fluid can then be broken down in the tanks on site. Care should be taken to keep any settled solids in the tanks for separate disposal.

For further information on support fluids see:

Guide to Support Fluids for Deep Foundations by the joint EFFC/DFI Support Fluids Task Group, at:
https://www.effc.org/content/uploads/2019/04/EFFC_Support_Fluids_Guide_FINAL.pdf

7 Contact

As this guide is circulated and used the authors would like to add to it and take onboard comments. If you have any feedback to help improve the knowledge and practices in the industry or questions regarding the guide, please contact:

daniel.mcnamara@hertford.ox.ac.uk

Oxford, January 2024.

8 Acknowledgements

The authors gratefully acknowledge the financial and technical support from Arup for this research. This work was supported by the EPSRC under the Industrial Cooperative Awards in Science & Technology scheme, under voucher number 210165.

7 Site Images



Figure 4. Aerial view of a site using polymer fluid. The polymer "farms" can be seen bottom and to the left of the image. This was an effective layout and well-designed storage system to supply the needs of the site.



Figure 5. Well mixed polymer fluid. Upon visual inspection well-mixed polymer fluid should be fairly indescernible from water excepting its viscoity and lubricity. In this figure, there is evidence of larger unhydrolysed polymer masses, these are likely where a flocculant has been added in or where polymer has been added to the solution a bit too quickly.



Figure 6. Poorly mixed polymer fluid. The caking of polymer is evident on the splash plate. The fluid itself shows lots of unhydrolysed clumps. This mix has been made up in haste and no care has been given to how the powders were added.



Figure 7. Covered storage tanks used for polymer fluid. Covering prevents photodegradation (from sunlight)– when left standing. There are hatches on the tanks that allow visual inspection.



Figure 8. An example of a flushed through sand content test. The sand content is at a reasonable level.



Figure 9. Marsh funnel test being conducted. The equipment is dirtier than it should be before performing the test.

9 References

EFFC/DFI Support Fluids Task Group. (2019). *Guide to Support Fluids for Deep Foundations*. 1st Edition. European Federation of Foundation Contractors and Deep Foundations Institute.

Lam, C., Jefferis, S. A., & Goodhue, K. G. (2010). Observations on viscosity reduction of PHPA polymer support fluids. In Geotechnical Special Publication|Geotech Spec Publ (pp. 184-191). American Society of Civil Engineers. https://doi.org/10.1061/41106(379)23

Lam, C. & Jefferis, S. (2018). *Polymer Support Fluids in Civil Engineering.* London: ICE Publishing.

References

Agasty, S. and Singh, R. P. (1998). Scaling equation for viscosity of polydimethylsiloxane in ethyl acetate: From dilute to concentrated solutions. *Journal of Applied Polymer Science*, 67(8):1435–1442.

American Petroleum Institute (2009). *Recommended Practice for Field Testing Water-based Drilling Fluids*. ANSI/API Recommended practice 13B-1, 4th edition.

Atkinson, J. H. (2007). *The mechanics of soils and foundations*. Taylor & Francis, London, 2nd ed. edition.

Attard, G. and Barnes, C. (1998). *Surfaces*. Oxford University Press.

Barnes, H. A., Hutton, J. F., and Walters, K. (1989). *An introduction to rheology*, volume 3. Elsevier.

Bridges, S. and Robinson, L. (2020). *A Practical Handbook for Drilling Fluids Processing*. Gulf Professional Publishing, Houston, TX, USA.

British Standards Institute (2012). BS EN 933-1:2012: Tests for geometrical properties of aggregates. determination of particle size distribution. sieving method. Technical report, British Standards Institute.

Charp, P. A. (2017). UV-C penetration through acrylic plastic. `https://hps.org/publicinformation/ate/q12178.html`. Accessed: 27 May 2025.

Chhabra, R. P. and De Kee, D. (2007). *Bubbles, Drops, and Particles in Non-Newtonian Fluids*. CRC Press, Boca Raton, FL.

Chhabra, R. P. and Richardson, J. F. (1999). *Non-Newtonian Flow in the Process Industries: Fundamentals and Engineering Applications*. Butterworth-Heinemann, Oxford.

EFFC/DFI Support Fluids Task Group (2019). *Guide to Support Fluids for Deep Foundations*. European Federation of Foundation Contractors and Deep Foundations Institute, 1st edition.

Ejezie, J. O. (2018). *Flow and Filtration Behaviour of Polymer Based Excavation Support Fluids in Coarse Soils*. PhD thesis, University of Manchester.

Ejezie, J. O., Jefferis, S. A., Lam, C., Sedighi, M., and Ahmad, S. M. (2021). Permeation behaviour of PHPA polymer fluids in sand. *Géotechnique*, 71(7):561–570.

Glossop, M. (1964). *Grouts and Drilling Muds in Engineering Practice*. Butterworths.

Godínez, F. A., de la Calleja, E., Lauga, E., and Zenit, R. (2014). Sedimentation of a rotating sphere in a power-law fluid. *Journal of Non-Newtonian Fluid Mechanics*, 213:27–30.

Gregory, J. and Barany, S. (2011). Adsorption and flocculation by polymers and polymer mixtures. *Advances in colloid and interface science*, 169(1):1–12.

Institution of Civil Engineers (2016). *ICE Specification for Piling and Embedded Retaining Walls*. ICE Publishing, third edition edition.

KB International (2025). Polymer products. https://www.kbtech.com/products.

Kol, R., Nachtergaele, P., De Somer, T., D'hooge, D. R., Achilias, D. S., and De Meester, S. (2020). Toward more universal prediction of polymer solution viscosity for solvent-based recycling. *Industrial & Engineering Chemistry Research*, 59(43):19163–19172.

Lam, C. and Jefferis, S. (2018). *Polymer Support Fluids in Civil Engineering*. ICE Publishing, London.

Lam, C., Jefferis, S. A., and Martin, C. M. (2014). Effects of polymer and bentonite support fluids on concrete–sand interface shear strength. *Géotechnique*, 64(1):28–39.

Lam, C., Jefferis, S. A., Suckling, T. P., and Troughton, V. M. (2015a). Effects of polymer and bentonite support fluids on the performance of bored piles. *Géotechnique*, 65(3):209–218.

Lam, C., Martin, P. J., and Jefferis, S. A. (2015b). Rheological properties of PHPA polymer support fluids. *Journal of Materials in Civil Engineering*, 27(11):04015021.

Lambe, T. W. and Whitman, R. V. (1969). *Soil mechanics*. Wiley, New York ;.

Lizcano Niño, J. C., de Sousa Ferreira, V. H., and Moreno, R. B. Z. L. (2020). Less-concentrated hpam solutions as a polymer retention reduction method in ceor. *Fuentes: El reventón energético*, 18(1):75–92.

Lukežič, A., Vojíř, T., Čehovin, L., Matas, J., and Kristan, M. (2018). Discriminative correlation filter tracker with channel and spatial reliability. In *Proceedings of the IEEE Conference on Computer Vision and Pattern Recognition (CVPR)*, pages 5740–5749, Salt Lake City, UT, USA. IEEE Computer Society.

Marani, D., Gadea, C., Hjelm, J., Hjalmarsson, P., Wandel, M., and Kiebach, R. (2015). Influence of hydroxyl content of binders on rheological properties of cerium–gadolinium oxide (cgo) screen printing inks. *Journal of the European Ceramic Society*, 35(5):1495–1504.

Martin, F. (1975). The effect of hyrolysis of polyacrylamide on solution viscosity, polymer retention and flow resistance properties. In *SPE Rocky Mountain Petroleum Technology Conference/Low-Permeability Reservoirs Symposium*, pages SPE–5339. SPE.

McCash, E. M. (2023). *Surface Chemistry*. Oxford University Press.

McNamara, A. M., Suckling, T. P., McKinley, B., and Stallebrass, S. E. (2014). A field trial of a reusable, hollow, cast-in-situ pile. *Proceedings of the Institution of Civil Engineers - Geotechnical Engineering*, 167(4):390–401.

McNamara, D., Sheil, B., Jefferis, S., and Barker, C. (2024a). Analysing the suitability of the american petroleum institute filter press test for polymer support fluids. In Duc Long, P. and Dung, N. T., editors, *Proceedings of the 5th International Conference on Geotechnics for Sustainable Infrastructure Development*, pages 477–486, Singapore. Springer Nature Singapore.

McNamara, D. P., Sheil, B. B., Jefferis, S. A., Barker, C., and Nicholson, D. (2024b). An investigation of the behaviour of polymer fluids in the american petroleum institute filter press. *Géotechnique*, 75(7):953–963.

Mohanan, N., Montazer, Z., Sharma, P. K., and Levin, D. B. (2020). Microbial and enzymatic degradation of synthetic plastics. *Frontiers in Microbiology*, Volume 11 - 2020.

National Oceanic and Atmospheric Administration (NOAA) (2023). Sea water. https://www.noaa.gov/jetstream/ocean/sea-water. Last updated: 28 March 2023; Accessed: 27 May 2025.

NEOM Newsroom (2024). NEOM establishes SAR 700 million concrete factory for THE LINE. https://www.neom.com/en-us/newsroom/neom-establishes-sar-700-million-concrete-factory-for-the-line. Accessed: 23 May 2025.

Newton, I. (1833). *Philosophiae naturalis principia mathematica*, volume 1. G. Brookman.

Nijjer, J. S., Hewitt, D. R., and Neufeld, J. A. (2019). Stable and unstable miscible displacements in layered porous media. *Journal of Fluid Mechanics*, 869:468–499.

Ostwald, W. and Auerbach, R. (1926). Ueber die viskosität kolloider lösungen im struktur-, laminar-und turbulenzgebiet: Ueber die geschwindigkeitsfunktion der viskosität disperser systeme, v. *Kolloid-Zeitschrift*, 38:261–280.

Painter, P. and Coleman, M. (1997). *Fundamentals of Polymer Science*. Lancaster: Technomic Publishing Company, Inc.

Powrie, W. (2018). *Soil Mechanics: Concepts and Applications, Third Edition*. CRC Press, Boca Raton, FL, 3rd ed. edition.

Rubinstein, M. and Colby, R. H. (2003). *Polymer Physics*. Oxford University Press, Oxford, UK.

Sigurdsson, H., Houghton, B., McNutt, S., Rymer, H., and Stix, J. (2015). *The Encyclopedia of Volcanoes*. Academic Press.

Sims, H. (2020). Fluid loss and adsorption of polymer support fluids used in deep foundations. *Cambridge Press*.

Sorbie, K. S. (1991). *Polymer-improved oil recovery*. Blackie and Son Ltd, Glasgow and London.

Thasnanipan, N., Aye, Z. Z., Submaneewong, C., and Teparaksa, W. (2002). Performance of wet-process bored piles constructed with polymer-based slurry in bangkok subsoil. In *Deep Foundations 2002: An International Perspective on Theory, Design, Construction, and Performance*, pages 143–157. ASCE.

Uchiyama, N. and Horiuchi, S. (1994). In-situ utilization of waste bentonite slurry. In Goumans, J., van der Sloot, H., and Aalbers, T., editors, *Environmental Aspects of Construction with Waste Materials*, volume 60 of *Studies in Environmental Science*, pages 217–226. Elsevier.

Verst, R. (2021). *Stabilisation mechanisms of polymer solutions in the context of temporary earth-wall support - Stabilisierungswirkung von Polymerlösungen bei der Stützung von Erdwänden - Dissertation*. Lehr- und Forschungsgebiet Geotechnik, Bergische Universität Wuppertal.

Verst, R., Blumenthal, A. v., Du, J., König, D., Pulsfort, M., and Wichtmann, T. (2022a). Systematic laboratory and field study on the shear resistance of the soil-concrete interface of diaphragm walls and bored piles. In *DFI-EFFC International Conference on Deep Foundations and Ground Improvement: Smart Construction for the Future*.

Verst, V. A., Lieske, W., Baille, W., Pulsfort, M., and Wichtmann, T. (2022b). On the applicability of viscosity-based capillary bundle concepts to predict the penetration behaviour of polymer solutions into sand. *Acta Geotechnica*.

Waele, A. (1923). *Viscometry and Plastometry*. Journal of the Oil and Colour Chemists' Association. Oil and Colour Chemists' Association.

Xanthakos, P. P. (1979). *Slurry Walls*. McGraw-Hill, New York, NY.

Xu, Z., Wang, W., Cao, Y., and Xue, B. (2023). Liquid-liquid phase separation: Fundamental physical principles, biological implications, and applications in supramolecular materials engineering. *Applied Physics Reviews*, 10(1).

Yang, S. T., Lo, Y. M., and Chattopadhyay, D. (1998). Production of cell-free xanthan fermentation broth by cell adsorption on fibers. *Journal of Chemical Technology and Biotechnology*, 73(4):317–320.